Advanced Thermal Analysis of Microelectronics Using Spreading Resistance Models

by

©S. Masood Razavi

A Thesis submitted to the School of Graduate Studies in partial fulfillment of the requirements for the degree of

Doctor of Philosophy

Department of Mechanical Engineering

Memorial University of Newfoundland

May 2016

St. John's Newfoundland

Abstract

Thermal analysis of electronic devices is one of the most important steps for designing of modern devices. Precise thermal analysis is essential for designing an effective thermal management system of modern electronic devices such as batteries, LEDs, microelectronics, ICs, circuit boards, semiconductors and heat spreaders. For having a precise thermal analysis, the temperature profile and thermal spreading resistance of the device should be calculated by considering the geometry, property and boundary conditions. Thermal spreading resistance occurs when heat enters through a portion of a surface and flows by conduction. It is the primary source of thermal resistance when heat flows from a tiny heat source to a thin and wide heat spreader. In this thesis, analytical models for modeling the temperature behavior and thermal resistance in some common geometries of microelectronic devices such as heat channels and heat tubes are investigated. Different boundary conditions for the system are considered. Along the source plane, a combination of discretely specified heat flux, specified temperatures and adiabatic condition are studied. Along the walls of the system, adiabatic or convective cooling boundary conditions are assumed. Along the sink plane, convective cooling with constant or variable heat transfer coefficient are considered. Also, the effect of orthotropic properties is discussed. This thesis contains nine chapters. Chapter one is the introduction and shows the concepts of thermal spreading resistance besides the originality and importance of the work. Chapter two reviews the literatures on the thermal spreading resistance in the past fifty years with

a focus on the recent advances. In chapters three and four, thermal resistance of a two-dimensional flux channel with non-uniform convection coefficient in the heat sink plane is studied. The non-uniform convection is modeled by using two functions than can simulate a wide variety of different heat sink configurations. In chapter five, a non-symmetrical flux channel with different heat transfer coefficient along the right and left edges and sink plane is analytically modeled. Due to the edge cooling and non-symmetry, the eigenvalues of the system are defined using the heat transfer coefficient on both edges and for satisfying the orthogonality condition, a normalized function is calculated. In chapter six, thermal behavior of two-dimensional rectangular flux channel with arbitrary boundary conditions on the source plane is presented. The boundary condition along the source plane can be a combination of the first kind boundary condition (Dirichlet or prescribed temperature) and the second kind boundary condition (Neumann or prescribed heat flux). The proposed solution can be used for modeling the flux channels with numerous different source plane boundary conditions without any limitations in the number and position of heat sources. In chapter seven, temperature profile of a circular flux tube with discretely specified boundary conditions along the source plane is presented. Also, the effect of orthotropic properties are discussed. In chapter 8, a three-dimensional rectangular flux channel with a non-uniform heat convection along the heat sink plane is analytically modeled. In chapter nine, a summary of the achievements is presented and some systems are proposed for the future studies. It is worth mentioning that all the models and case studies in the thesis are compared with the Finite Element Method (FEM).

Acknowledgements

I would like to express the deepest appreciation to my supervisor, Dr. Yuri S. Muzychka, who has the attitude and the substance of a great mentor.

I would also like to express my gratitude to Dr. Serpil Kocabiyik, the co-supervisor of this thesis, for her useful comments, remarks and engagement.

Last but not the least, I would like to thank my lovely wife, Sama, and my family. This work could not have been possible without their continuous support and encouragement.

Table of Contents

List of Tables

List of Figures

Nomenclature

A	Area, m^2
	Constant for linear dependence of thermal conductivity on temperature
	Solution coefficients
A_0	Fourier coefficient
A_b	Baseplate area, m^2
A_i	Fourier coefficients
A_{jm}	Coefficients in algebraic equations
A_m	Fourier coefficients
A_{mn}	Fourier coefficients
A_n	Fourier coefficients
A_s	Heat source area, m^2
a	Linear dimensions, m
B	Constant for linear dependence of thermal conductivity on temperature
	Solution coefficients
B_0	Modified Fourier coefficient
B_i	Fourier coefficients
Bi	Biot number, $\equiv \frac{ha}{k}$

Bi_{avg}	Biot number based on mean heat transfer coefficient, $\equiv \overline{h}c/k$
Bi_e	Biot number based on right edge heat transfer coefficient, $\equiv h_e c/k$
Bi_o	Biot number based on maximum heat transfer coefficient, $\equiv h_o c/k$
$Bi(x)$	Biot number based on variable conductance, $\equiv h(x)c/k$
B_m	Modified Fourier coefficients
B_{mn}	Modified Fourier coefficients
B_n	Modified Fourier coefficients
b	Linear dimensions, m
b_j	Coefficients in algebraic equations
C	Solution coefficients
C_n	Fourier coefficient
c	Linear dimensions, m
D	Unknown constant of separation of variables
D_n	Fourier coefficient
d	Linear dimensions, m
f	Influence coefficient, K/W
$f(x)$	Least squares function represent the exact value
$g(x)$	Least squares function represent the exact value
H	Plate thickness, m
h	Convection heat transfer coefficient, W/m^2K
h_1	Heat transfer coefficient along the left edge, W/m^2K
h_2	Heat transfer coefficient along the right edge, W/m^2K
h_c	Interfacial contact conductance, W/m^2K
h_e	Heat transfer coefficient along the edges, W/m^2K
h_o	Maximum heat transfer coefficient of coolant, W/m^2K
h_s	Sink plane conductance, W/m^2K
h_s	Sink plane conductance, W/m^2K

J	Bessel function of the first kind
K	Kirchhoff transform
k	Thermal conductivity, W/mK
k_{eff}	Effective thermal conductivity, W/mK
k_{xy}	In-plane thermal conductivity, W/mK
k_z	Through-plane thermal conductivity, W/mK
k_1, k_2	Effective layer conductivities, W/mK
L	Plate length, m
I_N	Least squares integral
i	Index denoting layers 1 and 2
m	Indices for summation
	Heat sink distribution parameter
N	Weight function
	Maximum number of terms in summation
N_s	Number of heat sources
n	Indices for summation
	Unit normal vector, positive in the outward direction
$p(x)$	Least squares function represent the exact value
Q	Total heat flow, W
Q_{ref}	Reference heat flow, W
q	Heat flux, W/m^2
R	Thermal resistance, K/W
R_t	Total thermal resistance, K/W
R_t^*	Dimensionless thermal resistance, $\equiv k\left(x_2 - x_1\right) R_t$
	Dimensionless thermal resistance, $\equiv kaR_t$
r	Cylindrical coordinate

s	Fourier series coefficient
T	Temperature, K
T_0	Reference temperature, K
T_f	Film temperature, K
$\overline{T}_s$	Mean source temperature, K
t	Thickness, m
t_1, t_2	Layer thickness, m
$\bar{t}_1$, $\bar{t}_2$	Effective layer thickness, m
t_{eff}	Effective thickness, m
W	Plate width, m
X	x coordinate of source/sink center, m
	Eigenfunction
X_c	Heat source centroid, m
x	Cartesian coordinate
x_1	Position of the left edge of the source, m
x_2	Position of the right edge of the source, m
Y	Bessel function of the second kind
	y coordinate of source/sink center, m
Y_c	Heat source centroid, m
y	Cartesian coordinate
z	Cartesian coordinate

Greek Symbols

β	Eigenvalue
δ	Eigenvalue
δ_n	Eigenvalue
ϵ	Width to length aspect ratio of plate
ϵ_H	Height to length aspect ratio of plate
ϕ	Spreading function
γ	Dummy variable, m^{-1}
κ	Dimensionless thermal conductivity
κ_m	Arbitrary coefficient
λ	Eigenvalue
ρ_m	Arbitrary coefficient
ψ_m	Arbitrary coefficient
τ	Dimensionless thickness, $\equiv t/a$
θ	Apparent temperature, K
	Temperature excess, K
$\overline{\theta}_s$	Mean source temperature excess, K
φ_m	Arbitrary coefficient
ς	Orthotropic transform variable
ϑ_m	Arbitrary coefficient
ξ	Orthotropic transform variable
ζ	Orthotropic transform variable
	Transformed z coordinate

Subscripts

avg	Average
0	The reference values for the Kirchhoff transform
1, 2	Layers 1 and 2, respectively
$1D$	One dimensional
$3D$	Three dimensional
$base$	Base surface or sink plane of the substrate
c	Contact
cp	Contact plane
e	Edge
	Effective
eff	Effective value
f	Film
i	Number of sources/sinks on each surface
	ith source
j	jth source
	Index for summation
∞	Denotes a property of the ambient
m	Index for summations
mn	Indexes for summations
N	Maximum number of terms in summation
n	Index for summations
r	In the r-direction
ref	The reference values for the temperature-dependent thermal conductivity relation

s	Sink plane of the substrate when referring to the heat transfer coefficient
	Sink, source or spreading
T	Total
t	Total
x	In the x-direction
xy	In the xy-plane
xz	In the xz-plane
yz	In the yz-plane
z	In the z-direction

Superscripts

b	Bottom surface
t	Top surface
*	Specific dimensionless parameter
’	Pertaining to bottom surface
$\overline{(.)}$	Mean value

Chapter 1

Introduction

1.1 Overview

Thermal management is a key factor that determines the capability, life, and safety of the product. For designing an effective thermal management system, thermal characteristics of the device such as spreading resistance should be considered, Fig. 1.1. Thermal spreading resistance occurs when heat flows through different layers with different areas and even in some cases is the main source of thermal resistance. Thermal spreading resistance should be analyzed in different electronic industries such as batteries [1], micro processors [2], LEDs [3-5], semiconductors like Gallium Nitride (GaN) devices [6], ICs [7], circuit boards [8-10], and heat spreaders [11-13], Fig. 1.2.

1.1.1 Spreading Resistances

Spreading resistance is a type of thermal resistance which occurs in heat conduction through different cross sections. Spreading resistance or constriction resistance have the same general meaning and are often used interchangeably. However, the term of spreading resistance is mostly used when heat flows from a narrower region to a wider region and constriction

Figure 1.1: A schematic view of the relationship between thermal spreading resistance, thermal analysis, and thermal management.

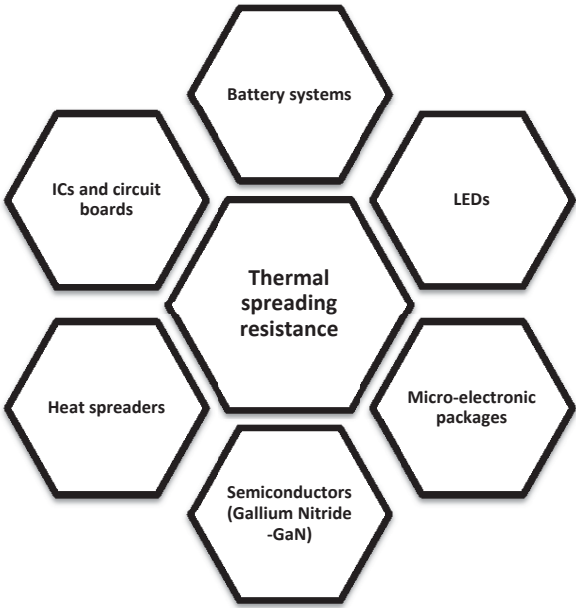

Figure 1.2: A schematic view of different industries which are actively involved with thermal analysis and spreading resistance.

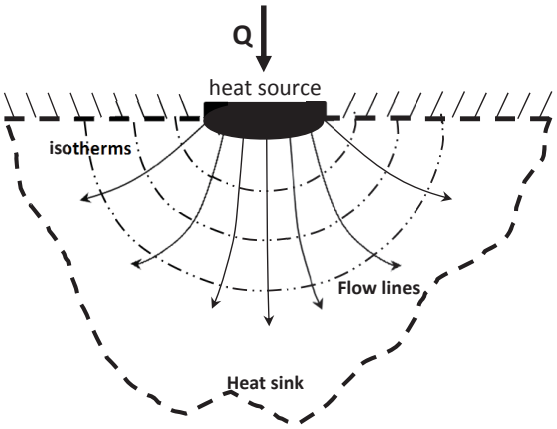

Figure 1.3: Arbitrary shape heat source on a half space.

resistance is used when heat flows from a wider region to a narrower one [14]. For steady state problems, Laplace's equation is used to obtain temperature distribution:

$$\nabla^2 T = 0. \tag{1.1}$$

In the following section, thermal spreading resistance for semi-infinite regions and finite regions will be discussed.

1.1.1.1 Spreading Resistance in Semi-infinite Regions

In semi-infinite regions, heat enters through a finite region and spreads over the semi-infinite region without any spatial boundaries, as shown in Fig. 1.3. For the case of steady state heat transfer, Laplace's equation should be satisfied, $\nabla^2 T = 0$.

In these systems, spreading resistance is calculated using mean temperature over the heat source area $(\overline{T_s})$, temperature far from the heat source as a heat sink $(T_{z\to\infty})$, and total heat flow rate (Q)[15, 16]. Therefore, the equation of thermal spreading resistance has the following form [17]:

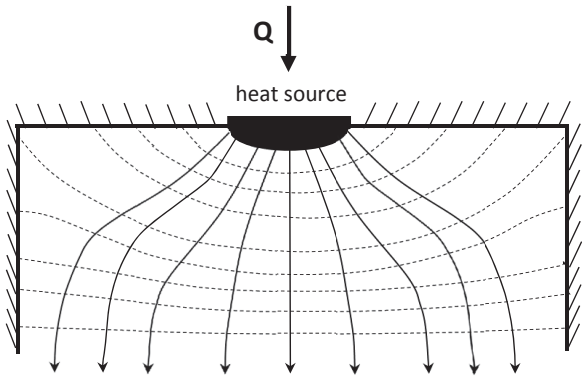

Figure 1.4: Arbitrary shape heat source on a flux tube or channel.

$$R_T = \frac{\overline{T_s} - T_{z\to\infty}}{Q} = \frac{\overline{\theta}}{Q}. \tag{1.2}$$

For defining the mean heat source temperature, the following integration is used,

$$\overline{T}_s = \frac{1}{A_s}\int\int_{A_s} T(x, y, 0)\mathrm{d}A_s. \tag{1.3}$$

1.1.1.2 Spreading Resistance in Finite Regions

For finite regions, thermal spreading resistance depends on all boundary conditions of the system. For example, if a circular heat source is mounted on top of a circular flux tube with adiabatic edges, heat flux lines are bent and constrained because of adiabatic edges and after some distance, become parallel to the axis of the flux tube. The temperature near the heat source is multi-dimensional, while the temperature far from the source becomes one dimensional [18]. This system is shown in Fig. 1.4. As shown, the heat flux lines are orthogonal with isotherm lines. Temperature distribution can be obtained solving Laplace's equation and applying the boundary conditions.

For the case of flux tube or channel with adiabatic edges, the total thermal resistance is

composed of the one dimensional thermal resistance and thermal spreading resistance.

$$R_T = R_{1D} + R_s. \tag{1.4}$$

Also, one dimensional thermal resistance for multilayered devices can be obtained from the following equation,

$$R_{1D} = \sum_{i=1}^{N} \frac{t_i}{k_i A} + \frac{1}{hA}. \tag{1.5}$$

The total thermal resistance for steady heat transfer can be calculated by mean source temperature $(\overline{T}_s)$, temperature far from the source $(T_{z\to\infty})$, and total heat transfer rate from the source into the flux (Q),

$$R_{total} = \frac{\overline{T}_s - T_{z\to\infty}}{Q}. \tag{1.6}$$

The one dimensional thermal resistance is,

$$R_{1D} = \frac{\overline{T}_{z=0} - T_{z\to\infty}}{Q} \tag{1.7}$$

and the total thermal resistance is,

$$R_{total} = R_{1D} + R_s. \tag{1.8}$$

After some algebra, the spreading resistance equation that was proposed by Mikic and Rohsenow [19] is defined as follows,

$$R_s = R_{total} - R_{1D} = \frac{\overline{T}_s - T_{z\to\infty}}{Q} - \frac{\overline{T}_{z=0} - T_{z\to\infty}}{Q}, \tag{1.9}$$

$$R_s = \frac{\overline{T}_s - \overline{T}_{z=0}}{Q}. \tag{1.10}$$

It is worth mentioning that the thermal spreading resistance will disappear when heat source area is equal to the area of the channel or tube. However, for many devices which have both types of thermal resistances, thermal spreading resistance can be the major part of thermal resistance and should be considered as the main factor for designing the thermal management system of the device [14].

Semi-conductor micro-electronic devices can be assumed as a finite region which is in contact with heat sources and heat sinks. For finding the temperature distribution for this finite region, Laplace's equation should be satisfied by considering specified boundary conditions. For isotropic systems, thermal conductivity is constant in all of directions and Laplace's equation has the following form:

$$\nabla^2 T = 0. \tag{1.11}$$

However, for orthotropic systems, thermal conductivity varies in different directions and Laplace's equation becomes,

$$\nabla \cdot (k \nabla T) = 0. \tag{1.12}$$

1.1.2 Parameters Involved in Spreading Resistance Solution

Different parameters are involved in spreading resistance solutions. The most important parameters are definition of characteristic length scale which is used for solving process, shape effects of different systems, imposed boundary conditions, and the reference temperature that is assumed for heat sources, Fig. 1.5.

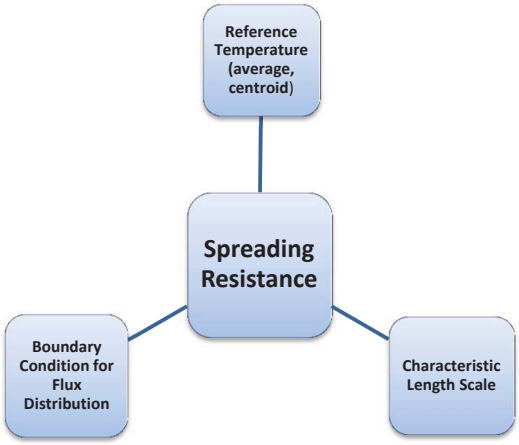

Figure 1.5: Some parameters that involved in spreading resistance solution.

1.1.2.1 Characteristic Length Scale

Defining the proper characteristic length scale is very important for considering thermal spreading resistance in different devices with different geometries. As was shown in different research [18, 20, 21, 22], the best characteristic length scale is the square root of heat source area, $\ell = \sqrt{A}$.

1.1.2.2 Shape Effects

The effects of shape and geometries of a system are negligible when the square root of heat source area, $\sqrt{A}$, is used as the characteristic length scale. For example, spreading resistance for different shape of heat sources including rectangular and elliptical sources with similar areas, aspect ratios, and boundary conditions are approximately identical when square root of source area is used as the characteristic length scale.

1.1.2.3 Boundary Condition of Flux Distribution

Different types of heat flux distributions can be applied to the systems as heat sources. Therefore, considering different models for heat flux distributions and considering its effect

on thermal spreading resistance is essential. However; in most of the systems with different heat sources, the heat flux distribution for each individual source is not known. In these cases, a constant heat flux can be assumed for the heat source without loss of accuracy. Considering isoflux heat source instead of isothermal boundary conditions for circular and elliptical sources cause a 8% greater thermal spreading resistance. This result is 4.1% less for parabolic heat source condition. Also, for other geometries like regular polygonal areas and semicircles, the spreading resistance has small difference for different heat source boundaries. Therefore, it is noticeable that the isoflux boundary condition can be assumed as the heat source boundary condition without causing any major error when the boundary condition of the heat source is not precisely known [23].

1.1.2.4 Reference Temperature

As has been shown earlier, for calculating thermal spreading resistance, mean temperature of the heat source should be used. Due to the different types of heat sources, an error approximation is required for the case of using maximum source temperature as the mean temperature. For instance, if the maximum source temperature is used for a circular source on a half space, the spreading resistance is -21.4% less for the case of uniform heat flux. Also, for the case of parabolic heat flux, thermal spreading resistance based on maximum temperature is 17.9% greater than exact value.

1.1.3 Dimensionless Thermal Resistance

To compare thermal spreading resistance in different systems with different parameters and boundary conditions, it is better to define dimensionless thermal spreading resistance. Dimensionless thermal spreading resistance can be defined as follows using thermal spreading resistance (R), thermal conductivity (k), and characteristic length scale (ℓ),

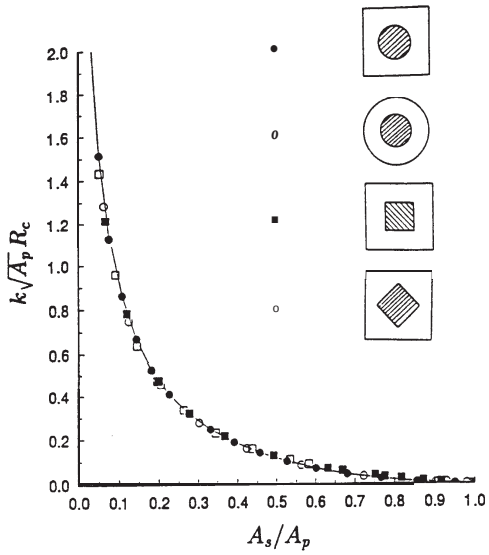

Figure 1.6: Dimensionless resistance versus dimensionless source area for different source contours and flux tubes [24].

$$R^* = Rk\ell. \tag{1.13}$$

As mentioned before, the characteristic length scale is assumed as $\ell = \sqrt{A_s}$.

Dimensionless spreading resistance is a weak function of shape of heat source and flux tube, if the area ratio of source on flux tubes does not change [14, 20, 21, 22], Fig. 1.6.

1.2 Thermal Analysis

In this thesis, the thermal spreading resistance is studied in the flux tubes and channels which are the basic geometries that are practically used in different industries. In this section, some industrial applications of this problem is mentioned and the problem statement is clarified.

1.2.1 Industrial Applications

As discussed earlier, the thermal spreading resistance is a key factor for designing the thermal management system of different applications such as batteries [1], micro processors [2], LEDs [3-5], semiconductors like Gallium Nitride (GaN) devices [6], ICs [7], circuit boards [8-10] and heat spreaders [11-13]. In the following, a schematic view of batteries, LED and micro electronic devise are shown.

In the battery cooling industry, battery cells are heat sources which are in contact with cooling plate which can be considered as a flux channel and the cooling plate contains cooling channels which can be modeled as discrete heat sink lines, Fig. 1.7.

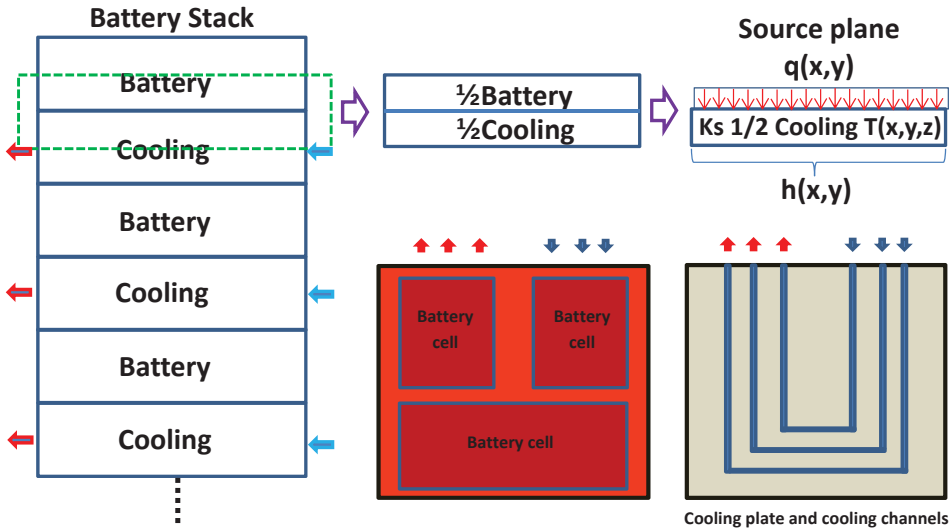

Figure 1.7: A schematic view of a battery stack which consist of several battery cells and cooling channels.

Thermal management in the LEDs industry is crucial in the life time and lighting design, Fig. 1.8. Therefore, the designer should have accurate information about the accurate temperature over time in order to conclude the life time of the system [4].

Microelectronic industry which is one of the fastest growing industry [25] need a capable thermal management system to keep the micro-electronic device operating at optimum

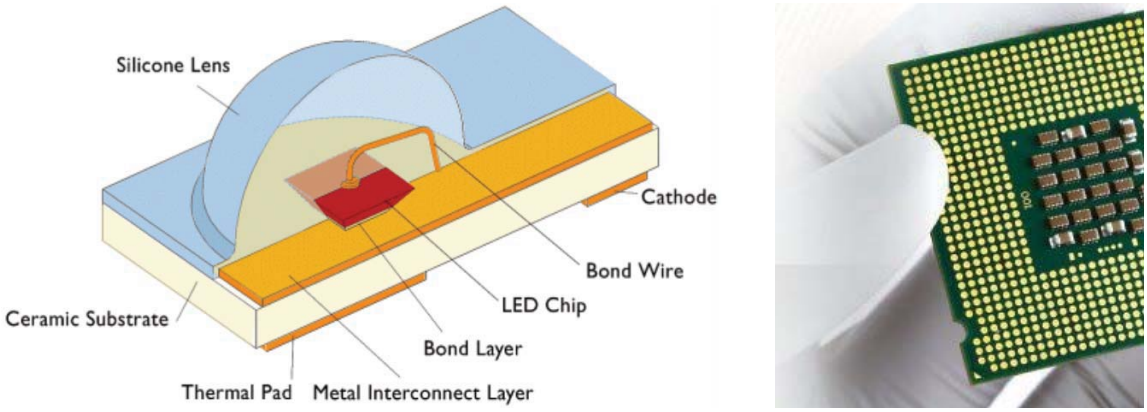

Figure 1.8: Left) Sketch of Luxeon Rebel LEDs [5] Right) A sample of micro-electronic device [25].

temperature. By using the novel micro-fabrication technologies, the size of microelectronic devices are decreasing. However, because of high density of circuits in micro fabrication and the resulting heat generation, thermal management and heat removal systems of these devices should be more precise and reliable than previous models.

1.2.2 Problem Statement

Thermal spreading resistance occurs in semi-conductor devices which is in contact with heat sources and heat sinks and varies by changing the geometry, boundary conditions, properties and specifications of the device. In this thesis, a number of new applications of thermal spreading resistance theory for flux channels and circular disks are addressed such as the effect of variable heat transfer coefficient, convective cooling along the edges, and different heat source types along the source plane. Both isotropic and orthotropic systems are considered.

For finding the temperature profile, Laplace equation should be satisfied by considering

the specified boundary conditions. Laplace equation have the following form for the orthotropic flux channel and tube:

$$k_x \frac{\partial^2 \theta}{\partial x^2} + k_y \frac{\partial^2 \theta}{\partial y^2} + k_z \frac{\partial^2 \theta}{\partial z^2} = 0, \qquad 0 < z < t \qquad \text{Flux channel,} \tag{1.14}$$
$$k_r \left(\frac{\partial^2 \theta}{\partial r^2} + \frac{1}{r} \frac{\partial \theta}{\partial r} \right) + k_z \frac{\partial^2 \theta}{\partial z^2} = 0, \qquad 0 < z < t \qquad \text{Flux tube.}$$

In the case of isotropic system, thermal conductivity , k, is constant in different directions. However, in the orthotropic problems, different thermal conductivity in different directions should be considered. For this purpose, the method of stretched coordinates is used and the orthotropic system is converted to the isotropic system with effective isotropic properties. For solving the Laplace equation, the method of separation of variables is used and the constants are specified by considering different boundary conditions. The boundary conditions along the walls of the system specify the eigenvalues of the system. Due to the complexity of the boundary conditions in the source and sink plane, the orthogonality property cannot be used and the least squares techniques is applied. Different methods will be used for simplification of the Least squares technique and a computational efficient method is presented.

In the following, some of the specifications of the studied problems are shown:

- Different geometries
  - Two-dimensional flux channel
  - Three-dimensional flux channel
  - Flux tube
- Boundary conditions in the source plane:

  - Different sources such as isothermal and isoflux
  - Adiabatic surfaces outside of the heat source regions
  - Single or multiple heat sources
  - Concentric and eccentric heat sources

- Boundary conditions along the edges:
  - Adiabatic surface
  - Convective cooling

- Boundary conditions in the sink plane:
  - Uniform heat transfer coefficient
  - Variable heat transfer coefficient, $h(x)$

- Different Properties:
  - Isotropic
  - Orthotropic

1.3 Methodology

1.3.1 Separation of Variables

The method of separation of variables is widely used for solving the conduction heat transfer problems. This method can be used for solving non-homogeneous problems. A system is considered non-homogeneous if more than one boundary or initial condition is non-zero and/or the governing differential equation contains constant or variable terms which are not differentials. Non-homogeneous problems are characterized by either non-homogeneous

boundary condition and/or non-homogeneous differential equations. Many problems with non-homogeneous boundary conditions can be solved using the principle of superposition, by alternately solving auxiliary homogeneous problems. For multi-dimensional steady-state heat conduction problems with no source; if more than one boundary condition is non-homogeneous, the problem can be split up to simpler problems with one non-homogeneous boundary condition [26].

As the method of separation of variables is widely used through the thesis, an example of solving procedure is presented in this section. If the problem characterized by the following mathematical statement:

$$\frac{\partial^2 T}{\partial x^2} + \frac{\partial^2 T}{\partial y^2} = 0, \tag{1.15}$$

and the following boundary conditions:

$$\begin{aligned} x = -a \qquad & T(-a, y) = T_s, \\ x = +a \qquad & T(+a, y) = T_s, \\ y = -b \qquad & T(x, -b) = T_s, \\ y = +b \qquad & T(x, +b) = T_o. \end{aligned} \tag{1.16}$$

This problem is characterized by a homogenous problem and four non-homogenous boundary conditions. In order to apply separation of variables, we most have at most one non-homogenous boundary condition. Since the system is linear, we may systematically set all but one boundary condition to zero and solve the system. The final solution is then a superposition of four solutions. Alternatively, we may homogenize the system by defining

a temperature excess:

$$\theta(x, y) = T(x, y) - T_s, \tag{1.17}$$

such that the following system results:

$$\frac{\partial^2 \theta}{\partial x^2} + \frac{\partial^2 \theta}{\partial y^2} = 0, \tag{1.18}$$

and the following boundary conditions:

$$\begin{aligned} x = -a \qquad & \theta(-a, y) = 0, \\ x = +a \qquad & \theta(+a, y) = 0, \\ y = -b \qquad & \theta(x, -b) = 0, \\ y = +b \qquad & \theta(x, +b) = T_o - T_s = \theta_o. \end{aligned} \tag{1.19}$$

Further, for convenience we will redefine the placement of the co-ordinate axes, and take advantage of symmetry by applying the following equivalent boundary conditions:

$$\begin{aligned} x = 0 \qquad & \frac{\partial \theta}{\partial x} = 0, \\ x = a \qquad & \theta(a, y) = 0, \\ y = 0 \qquad & \theta(x, 0) = 0, \\ y = 2b \qquad & \theta(x, 2b) = T_o - T_s = \theta_o. \end{aligned} \tag{1.20}$$

The benefits of these changes will be apparent later as we proceed through the solution. The method of separation of variables may now be applied by assuming that a product solution of the form:

$$\theta(x, y) = X(x) * Y(y). \tag{1.21}$$

Substituting this solution into the governing differential equation yields the following expression after dividing by the assumed solution form:

$$\frac{\frac{\partial^2 X}{\partial x^2}}{X(x)} = -\frac{\frac{\partial^2 Y}{\partial y^2}}{Y(y)} \tag{1.22}$$

This relationship can only be satisfied if the left hand side and right hand side equal a constant which may be equal to zero, a negative number or a positive number. In other words:

$$\frac{\frac{\partial^2 X}{\partial x^2}}{X(x)} = -\frac{\frac{\partial^2 Y}{\partial y^2}}{Y(y)} = 0, -\lambda^2, +\lambda^2 \tag{1.23}$$

This yields the following three cases for solutions to the separated equations:

Case A - 0

$$\begin{aligned} \frac{\partial^2 X}{\partial x^2} &= 0, \qquad X(x) = Ax + B, \\ \frac{\partial^2 Y}{\partial y^2} &= 0, \qquad Y(y) = Cy + D. \end{aligned} \tag{1.24}$$

Case B - $-\lambda^2$

$$\frac{\partial^2 X}{\partial x^2} + \lambda^2 X(x) = 0, \qquad X(x) = A\cos(\lambda x) + B\sin(\lambda x), \tag{1.25}$$
$$\frac{\partial^2 Y}{\partial y^2} - \lambda^2 Y(y) = 0, \qquad Y(y) = C\cosh(\lambda y) + D\sinh(\lambda y).$$

Case C - $+\lambda^2$

$$\frac{\partial^2 X}{\partial x^2} - \lambda^2 X(x) = 0, \qquad X(x) = A\cosh(\lambda x) + B\sinh(\lambda x), \tag{1.26}$$
$$\frac{\partial^2 Y}{\partial y^2} + \lambda^2 Y(y) = 0, \qquad Y(y) = C\cos(\lambda y) + D\sin(\lambda y).$$

Each of these solutions is admissible and a linear combination of each may be assumed. However, it is easier to examine each separately and determined which solutions contribute to the final solution.

Examination of the boundary conditions at $x = 0$ and $x = a$ reveals that the Case (A) and case (C) solutions for $X(x)$ vanish since these conditions yield $A = 0$ and $B = 0$. However, for case (B) we obtain the following:

$$\left.\frac{\partial X}{\partial x}\right|_{x=0} = -A\lambda\sin(\lambda.0) + B\lambda\cos(\lambda.0) = 0, \tag{1.27}$$

or

$$B = 0, \tag{1.28}$$

and

$$X(a) = A\cos(\lambda a) = 0. \tag{1.29}$$

Since $A \neq 0$, otherwise we would have no solution, we must choose,

$$\lambda a = \frac{n\pi}{2}, \qquad n = 1, 3, 5, \cdots, \tag{1.30}$$

or,

$$\lambda_n = \frac{(2n-1)\pi}{2a}, \qquad n = 1, 2, 3, \cdots. \tag{1.31}$$

Thus there are an infinite number of values of λ which satisfy the solution for $X(x)$. In applied mathematics, the system defined by,

$$\frac{\partial^2 X}{\partial x^2} + \lambda^2 X(x) = 0, \tag{1.32}$$

and,

$$\begin{aligned} x = 0, \qquad & \frac{\partial \theta}{\partial x} = 0, \\ x = a, \qquad & \theta(a, y) = 0, \end{aligned} \tag{1.33}$$

is referred to as a boundary value problem or more appropriately as a Sturm-Liouville problem. The solution to the problem up to this point may be written as,

$$\theta(x, y) = \sum_{n=1}^{\infty} [C_n \cosh(\lambda_n y) + D_n \sinh(\lambda_n y)] \cos(\lambda_n x), \tag{1.34}$$

which is a superposition of all possible solutions. The remaining constants referred to as Fourier coefficients may now be solved by applying the final boundary conditions along $y = 0$ and $y = 2b$.

Application of the boundary condition along $y = 0$ yields,

$$C_n = 0. \tag{1.35}$$

Thus the solution becomes:

$$\theta(x, y) = \sum_{n=1}^{\infty} D_n \sinh(\lambda_n y) \cos(\lambda_n x), \tag{1.36}$$

The final constant may now be evaluated from the following expression:

$$\theta_o = \sum_{n=1}^{\infty} D_n \sinh(\lambda_n 2b) \cos(\lambda_n x). \tag{1.37}$$

We will evaluate the constants by means of a Fourier expression, by multiplying each side of the expression by the eigenfunction such that,

$$\theta_o \cos(\lambda_m x) = \sum_{n=1}^{\infty} D_n \sinh(\lambda_n 2b) \cos(\lambda_n x) \cos(\lambda_m x), \tag{1.38}$$

and integrating over the interval $[0, a]$,

$$\int_0^a \theta_o \cos(\lambda_m x) dx = \sum_{n=1}^{\infty} \int_0^a D_n \sinh(\lambda_n 2b) \cos(\lambda_n x) \cos(\lambda_m x) dx, \tag{1.39}$$

The trigonometric functions of sine and cosine exhibit a property of orthogonality such that,

$$\int_0^l \cos(\lambda_n x)\cos(\lambda_m x)dx = 0, \qquad n \neq m, \tag{1.40}$$
$$\int_0^l \cos(\lambda_n x)\cos(\lambda_m x)dx \neq 0, \qquad n = m.$$

Thus, using this property, we may write Eq. (1.39) in the following manner, since all terms in the series vanish except for when $n = m$:

$$\int_0^a \theta_o \cos(\lambda_n x)dx = \int_0^a D_n \sinh(\lambda_n 2b)\cos^2(\lambda_n x)dx. \tag{1.41}$$

This may now be solved for the constant D_n to give:

$$D_n = \frac{\int_0^a \theta_0 \cos(\lambda_n x)dx}{\sinh(\lambda_n 2b)\int_0^a \cos^2(\lambda_n x)dx}. \tag{1.42}$$

Evaluation of the integrals yields the following expression:

$$D_n = \frac{2\theta_o \sin(\lambda_n a)}{\lambda_n a \sinh(\lambda_n 2b)}. \tag{1.43}$$

The final solution now becomes:

$$\theta(x,y) = \sum_{n=1}^{\infty} \frac{2\theta_o \sin(\lambda_n a)}{\lambda_n a \sinh(\lambda_n 2b)} \sinh(\lambda_n y)\cos(\lambda_n x). \tag{1.44}$$

The method of separation of variables is widely used through the thesis.

1.3.2 Least Squares

The method of least squares is an approximate analytic solution technique which is applied to linear and non-linear problems. Accuracy of this method is usually determined by com-

paring the method with known solutions to gauge the level of approximation, otherwise, when solving problems which no known solutions exist, the only indicator is whether or not there is convergence in successive approximations. The terminology applied in this method is that the first approximation is the solution obtained using a trial function with one undetermined coefficient, while the successive approximations using two or more undetermined coefficients are denoted as the second, third approximations, and so on. Given a differential equation which governs some quantity say ϕ, we denote the differential operator as $L(\phi)$. We may define:

$$\int_v wL(\phi)dv = 0, \tag{1.45}$$

where w is a weight function. If we approximate a solution for ϕ denoted as $\widetilde{\phi}$, where,

$$\widetilde{\phi} = \sum_{i=1}^{N} a_i\phi_i(x_1, x_2, x_3) = a_1\phi_1 + a_2\phi_2 + a_3\phi_3 \cdots . \tag{1.46}$$

Assuming that $\widetilde{\phi}$ is chosen such that the end conditions are all satisfied, then we define the residual:

$$R = L(\widetilde{\phi}). \tag{1.47}$$

The residual will change as the coefficients of the trial solution are varied. Thus we strive to minimize the residual R for N constraints. We have:

$$\int_v w_i L(\widetilde{\phi})dv = \int_v w_i R dv = 0, \qquad i = 1..N. \tag{1.48}$$

In the least squares method we choose:

$$w_i = \frac{\partial R}{\partial a_i}, \tag{1.49}$$

such that,

$$\int_x \frac{\partial R}{\partial a_i} R dx = \frac{\partial}{\partial a_i} \int_x R^2 dx = 0. \tag{1.50}$$

1.4 Organization of the Thesis

This thesis contains nine chapters including seven papers that are published, accepted, or submitted to international journals and conferences. The first chapter is an introduction about the thermal spreading resistance. The second chapter is a review paper that is submitted to the Journal of Thermophysics and Heat Transfer. This chapter is a review of literature about different spreading resistance problems in the past fifty years with a detailed discussion about the recent advances in analytical modeling of these problems. Chapter three is published in the Journal of Heat Transfer and chapter four is presented in the ASME IMECE 2014 conference. In these chapters, the effect of variable conductance on the thermal resistance of flux channels with different properties and configurations is discussed, Fig. 1.9 and Fig. 1.10. Furthermore, different symmetrical and non-symmetrical systems with different thicknesses and different heat sinks configurations are studied.

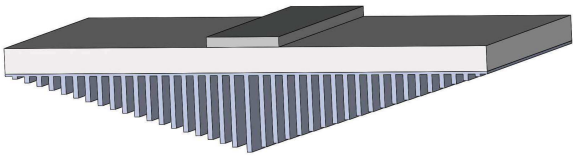

Figure 1.9: 3D view of symmetrical flux channel with variable conductance.

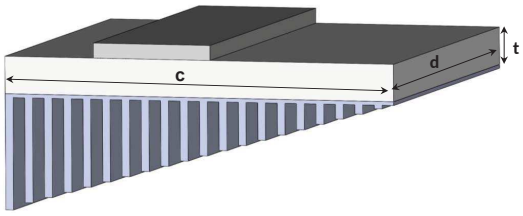

Figure 1.10: 3D view of non-symmetrical flux channel with variable conductance.

Chapter five is submitted to the Journal of Advances in Applied Mathematics and Mechanics and discussed the thermal resistance of eccentric flux channels with different edge

cooling boundary conditions along the edges. Due to the non-symmetry of the channel, the eigenvalues of the system are more complex and the orthogonality property is not satisfied. Therefore, a proper weight function is defined to satisfy the orthogonality property. Also, the effect of directional orthotropic properties is discussed. Some case studies for different orthotropic systems are modeled and the results are compared with numerical commercial software, Fig. 1.11.

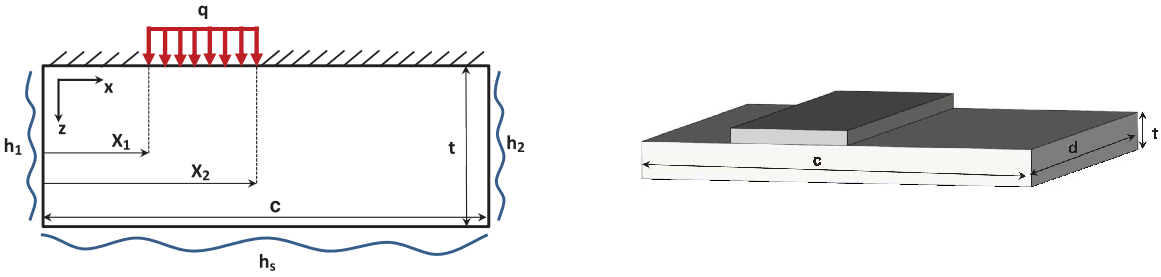

Figure 1.11: 2D flux channel with eccentric heat source and edge cooling.

Chapter six was presented in the ASME InterPACKICNMM 2015 conference. This chapter is about the thermal behavior of flux channels with discretely specified boundary conditions along the source plane. An analytical approach for modeling the temperature profile along the system is discussed, Fig. 1.12. In the proposed model, the source plane boundary condition can consist of a combination of first kind (Dirichlet or prescribe heat flux) and the second kind (Neumann or prescribed heat flux). The time efficiency of the presented analytical method versus numerical commercial software is shown.

Chapter seven is submitted to the ITHERM 2016 conference. In this chapter, the temperature profile in circular disks with different specified boundary conditions along the source plane is modeled, Fig. 1.13. In the presented method, there is no limitation in the number of heat sources. Also, the effect of prescribed temperature and heat fluxes are considered simultaneously.

Chapter eight is submitted to the Journal of Thermophysics and Heat Transfer. In this chapter, a three-dimensional flux channel with non-uniform heat conductance along the

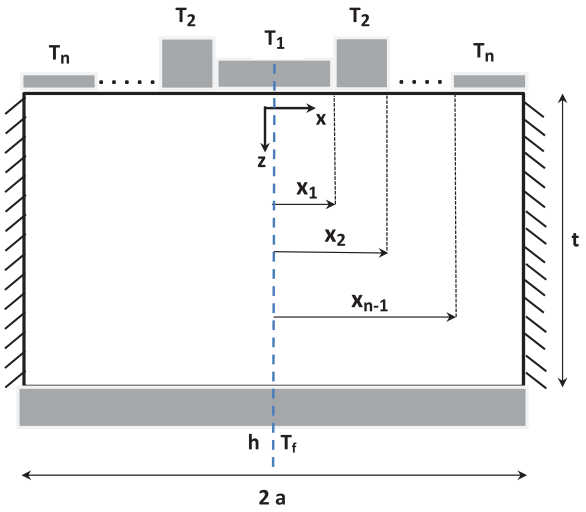

(a) Discretely specified contact temperatures along the source plane.

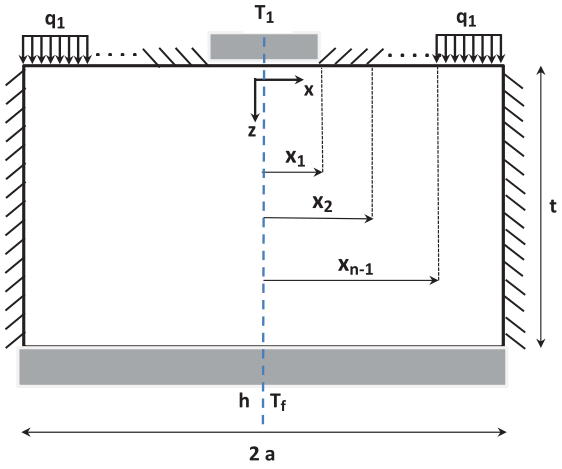

(b) Discretely specified temperature, heat flux, and adiabatic conditions along the source plane.

Figure 1.12: 2D symmetrical flux channel.

heat sink plane is modeled, Fig. 1.14. For modeling the system, the problem was divided to three simpler problems and the superposition method is used.

Chapter nine is a summary of advantages of the presented models throughout the thesis. Several suggestions to continue further investigations are presented in this chapter as well.

1.5 References

[1] Pesaran, A. A., and Keyser, M., "Thermal Characteristics of Selected EV and HEV Batteries," *Annual Battery Conference: Advances and Applications*, California, Jan. 2001.

[2] Guan, D., Marz, M., and Liang, J., "Analytical Solution of Thermal Spreading Resistance in Power Electronics," *IEEE Transactions on Components, Packaging and Manufacturing Technology*, pp. 278-285, 2012.

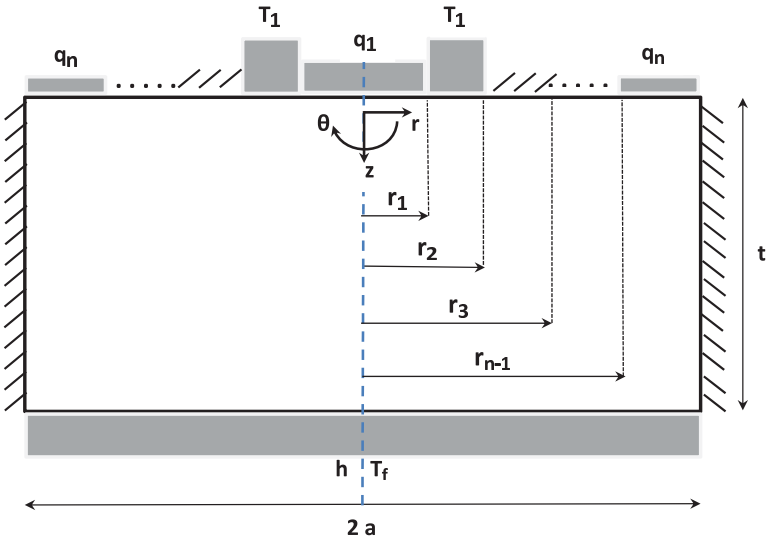

Figure 1.13: Flux tube with arbitrary boundary condition along the source plane.

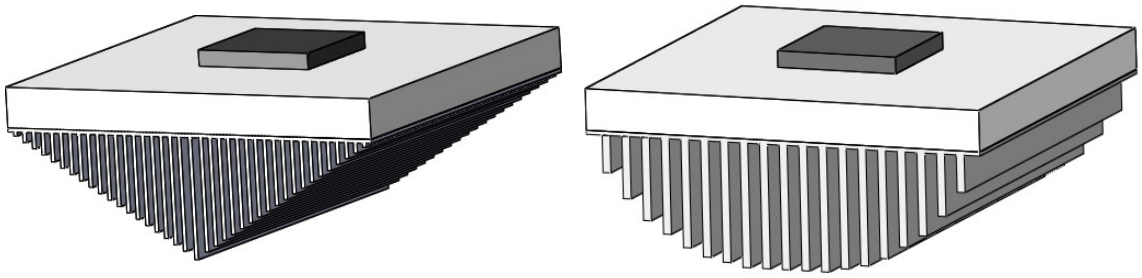

Figure 1.14: Flux channel with non-uniform conductance.

[3] Lasance, C. J. M., and Poppe, A., "Challenges in LED Thermal Characterization," *10th Int. Conf. on Thermal, Mechanical and Multiphysics Simulation and Experiments in Micro-Electronics and Micro-Systems*, 2009.

[4] Poppe, A., and Lasance, C. J. M., "On the Standardization of Thermal Characterization of LEDs, Part 2: Problem Definition and Potential solutions," *Therminic 2008*, Rome, Italy, Sep. 2008.

[5] Poppe, A., and Lasance, C. J. M., "On the Standardization of Thermal Characterization of LEDs," *25th IEEE Semi-Therm Symposium*, pp. 151-158, 2009.

[6] Qi, Q., and Monthei, D., "An Analytical Thermal and Stress Analysis Tool for Die Attach Optimization in GaN Power Amplifier (PA) Applications," *IEEE 14th Electronics Packaging Technology Conf.*, pp. 136-141, Mar. 2012.

[7] Karmalkar, S., Mohan, P. V., Nair, H. P., and Yeluri, R., "Compact Models of Spreading Resistances for Electrical/Thermal Design of Devices and ICs," *IEEE Transactions on Electron Devices*, vol. 54, no. 7, July 2007.

[8] Ellison, G., "Extensions of a Closed Form Method for Substrate Thermal Analyzers to Include Thermal Resistances From Source-to-Substrate and Source-to-Ambient," *Seventh IEEE Semi-Therm Symposium*, pp. 140-148, 1991.

[9] Ellison, G., "Thermal Analysis of Microelectric Packages and Printed Circuit Boards Using an Analytic Solution to the Heat Conduction Equation," *Advances in Engineering Software*, pp. 99-111, 1994.

[10] Ellison, G., "Thermal Analysis of Circuit Boards and Microelectronic Components Using an Analytical Solution to the Heat Conduction Equation," *Twelfth IEEE Semi-Therm Symposium*, pp. 144-150, 1996.

[11] Lam, T. T., and Fischer, W. D., "Thermal Resistance in Rectangular Orthotropic Heat Spreaders," *ASME Advances in Electronic Packaging*, vol. 26-1, American Society of Mechanical Engineers, Fairfield, NJ, pp. 891-898, 1999.

[12] Yovanovich, M. M., Culham, J. R. and Teertstra, P. M., "Modeling Thermal Resistances of Diamond Spreaders on Copper Heat Sinks," *Int. Electronics Packaging Conf.*, Austin, TX, September 29 - October 2, 1996.

[13] Yovanovich, M. M., Culham, J. R., and Teertstra, P. M., "Analytical Modeling of Spreading Resistance in Flux Tubes, Half Spaces, and Compound Disks," *IEEE*

Transactions on Components, Packaging, and Manufacturing Technology-Part A, vol. 21, no. 1, pp. 168-176, 1998.

[14] Lee, S., Song, S., Au., V., and Moran, K. P., "Constriction/Spreading Resistance Model for Electronics Packaging," *in Proc. 4th ASME/JSME Thermal Eng. Joint Conf.*, Maui, HI, pp. 199-206, Mar. 1995.

[15] Sadeghi, E., Bahrami, M., and Djilali, N., "Analytic Solution of Thermal Spreading Resistance: Generalization to Arbitrary-Shape Heat Sources on a Half-Space," *ASME 2008 Summer Heat transfer Conf.*, Jacksonville, FL., USA, August 10-14, 2008.

[16] Carslaw, H. S., and Jaeger, J. C., "Conduction of Heat in Solids," London, UK: *Oxford University Press*, second ed., 1959.

[17] Muzychka, Y. S., Yovanovich, M. M, and Culham, J. R., "Thermal Spreading Resistance in Compound and Orthotropic Systems," *Journal of Thermophysics and Heat Transfer*, vol. 18, no. 1, January-March 2004.

[18] Yovanovich, M. M., and Marotta, E. E., "Thermal Spreading and Contact Resistances," in *Heat Transfer Handbook*, A. Bejan, and A. D. Kraus, Eds. New York: Wiley, ch. 4, pp. 261-393, 2003.

[19] Mikic, B. B., and Rohsenow, W. M., "Thermal Contact Resistance," *M.I.T. Heat Transfer Lab Report No. 4542-41*, Sep. 1966.

[20] Yovanovich, M. M., "Thermal Constriction Resistance of Contacts on a Half-Space: Integral Formulation," *AIAA Progress in Astronautics and Aeronautics, Radiative Transfer and Thermal Control*, vol. 49, edited by A. M. Smith, New York, pp. 397-418, 1976.

[21] Yovanovich, M. M., and Burde, S. S., "Centroidal and Area Average Resistances of Nonsymmetric, Singly Connected Contacts," *AIAA Journal*, vol. 15, no. 10, pp. 1523-1525, 1977.

[22] Yovanovich, M. M., Burde, S. S., and Thompson, J. C., "Thermal Constriction Resistance of Arbitrary Planar Contacts With Constant Flux," *AIAA Progress in Astronautics and Aeronautics, Thermophysics of Spacecraft and Outer Planet Entry Probes*, vol. 56, edited by A. M. Smith, New York, pp. 127-139, 1977.

[23] Muzychka, Y. S. and Yovanovich, M. M., "Thermal Resistance Models for Non-Circular Moving Heat Sources on a Half Space," *Journal of Heat Transfer*, vol. 123, pp. 624-632, August 2001.

[24] Naraghi, M. H. N., and Antonetti, V. W., "Macro-Constriction Resistance of Distributed Contact Contour Areas in a Vacuum Environment," *ASME HTD, Enhanced Cooling Techniques for Electronics Applications*, vol. 263, pp. 107-114, 1993.

[25] http://www.freiberginstruments.com/branches/microelectronic-industry.html

[26] Ozisik, M. N., "Heat Conduction," A Wiley-Interscience publication,1980.

Chapter 2

A Review on Recent Advances in Thermal Spreading Resistance Problems

M. Razavi
Y.S. Muzychka

Department of Mechanical Engineering, Memorial University of Newfoundland, St. John's, NL, Canada, A1B 3X5

S. Kocabiyik

Department of Mathematics and Statistics, Memorial University of Newfoundland, St. John's, NL, Canada, A1C 5S7

Abstract

Thermal spreading resistance problems were studied by different researchers for fifty years. Some reviews were written on different models of thermal spreading resistance problems in 1986 [1], 2003 [2], and 2005 [3]. After 2005, some advanced analytical models were presented for thermal spreading resistance in three dimensional compound flux channels and compound cylindrical flux tubes. In this paper, the literature on thermal spreading resistance in the past fifty years is chronologically presented and the past decade advances are specifically described. The spreading resistance of compound rectangular flux channel and circular flux tube with and without contact resistance are presented. The sink boundary condition is assumed as isothermal and convective cooling with constant and variable heat

[1]Submitted to the Journal of Thermophysics and Heat Transfer

transfer coefficient. Furthermore, the effects of discrete sinking, orthotropic property and temperature dependent thermal conductivity are presented.

Keywords: Electronics Cooling, Heat Conduction, Thermal Resistance, Orthotropic Property, Temperature Dependent Thermal Conductivity

2.1 Introduction

Thermal engineers are interested to obtain the thermal spreading resistance for modeling the thermal behavior of electronic devices. The spreading resistance occurs when heat enters the system through a small region and flows by conduction. Thermal spreading resistance becomes the main source of the thermal resistance in the electronic devices with small contact ratios of source to the cross-section of the system. For the analytical modeling, the geometry of the system usually was simplified to the flux channel (rectangle) or flux tube (cylinder). The electronic devices with multi-layers were modeled as compound flux channels and flux tubes. Due to different boundary conditions and properties, different approaches were used to model the systems. Different factors were involved in the thermal spreading resistance problems including the modeling approach, geometry, property and boundary conditions of the system. A schematic diagram that shows some of the important factors for modeling the thermal spreading resistance problems is shown in Fig. 2.1.

Thermal spreading resistance problems have been considered since 1960 [4]. Different analytical models [4-6], numerical models [7-10] and experimental studies [11, 12] were proposed on thermal spreading resistance problems. Different configurations of the system such as systems with single layer [6, 13] and compound systems [10, 14, 15, 16], axisymmetric systems [17-19] and non-axisymmetric systems [6, 16, 20, 21, 22] were investigated. The compound systems were assumed with perfect contact [14] and interfacial contact resistance [16]. The main studied geometries were rectangular flux channels [20] and cylin-

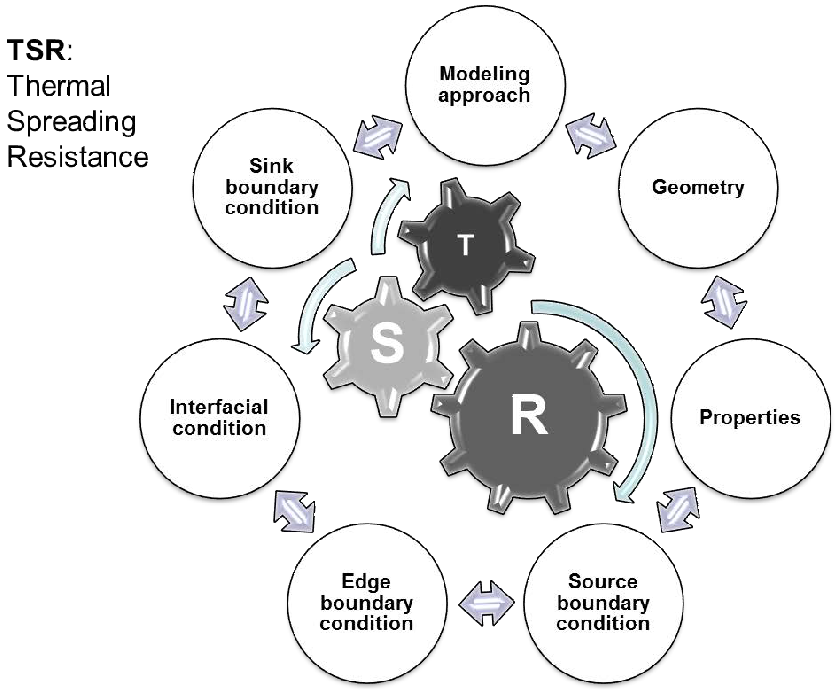

Figure 2.1: Important factors for modeling the thermal spreading resistance problems.

drical flux tubes [23]. Further, the systems with isotropic properties [6, 7, 13, 20, 24, 25] and orthotropic properties [16, 26, 27] were studied. The temperature dependent thermal conductivity was also considered [10, 28, 29, 30, 31]. Different source boundary conditions were studied including systems with one heat source [6, 20, 32, 33, 34] and multiple heat sources [16, 21]. The concentric heat source [35] and eccentric heat source [6, 9, 16, 20] were discussed by different researchers. The boundary conditions along the walls were considered as adiabatic [14] or convective cooling [6, 13]. The sink boundary condition was assumed as isothermal sink [4, 36] or convective cooling [16, 32, 37, 38, 39]. The heat transfer coefficient along the sink plane was assumed constant in most of the literature [13, 16, 20, 34]. Recently, a flux channel with variable heat transfer coefficient along the sink plane was studied [6]. In the following, some of the research studies on thermal spreading/constriction resistance chronologically ordered and briefly described.

2.1.1 Thermal Spreading Resistance Research Before 1980

Kennedy [4] started the research on thermal spreading resistance problems in semiconductor devices in 1960. He obtained an analytical solution for a finite cylinder with uniform-axisymmetric heat source and isothermal sink. Mikic [40] considered thermal contact resistance in semi-infinite regions. Mikic and Rohsenow [5] investigated thermal constriction resistance of symmetric, coaxial cylindrical contacts and obtained an infinite series expression to model the isothermal contact for the boundary condition over the contact area. Cooper et al. [41] presented the thermal contact resistance and introduced the thermal constriction parameter based on the isothermal contacts spots. Yovanovich [42] obtained a theoretical model for the overall contact resistance of a smooth sphere in contact with a rough flat in the vacuum by using linear superposition of micro and macro constriction resistances. He also proposed a correlation for the minimum thermal resistance of soldered joints [43].

After 1970, many research studies were done on analytical modeling of transient and steady spreading/constriction resistance in isotropic semi-infinite regions, flux channels and flux tubes [3, 44, 45, 46, 47, 48, 49, 50, 51, 52, 53].

Yovanovich et al. [54] considered the thermal constriction resistance between contacting paraboloids and developed a general expression for thermal constriction resistance of circular contact flux on right circular cylinders [51] and on a half-space [55]. Then single arbitrary shape with constant flux on insulated half-spaces [46], annular contacts on circular flux tubes [50], and constriction resistance due to a circular annular contact [55] were investigated.

Schneider et al. [49, 52] considered transient thermal behavior of a thin circular disk on a half-space and transient behavior for two semi-infinite bodies in contact through a small circular contact area. Burde et al. [56] theoretically obtained a model of steady thermal constriction resistance between smooth spheres and rough flats in contact. Ellison [11]

used theoretical and empirical methods for obtaining thermal characteristics of a forced-convection cooled ceramic package with an extruded aluminum heat sink.

Yovanovich et al. [53] examined steady state thermal constriction resistance of doubly-connected, planar, contact areas with constant heat flux bounded by coaxial circles, squares and equilateral triangles. They presented a general solution for the thermal constriction resistance of a compound disk due to a heat flux over a circular portion of the upper surface [15].

2.1.2 Thermal Spreading Resistance Research 1980-1990

In this decade, different aspects of thermal spreading resistance problems were investigated. Transient spreading resistance problems [57, 58] and steady and transient constriction were considered [17]. Some analytical and numerical methods were proposed for the thermal resistance of arbitrary contacts on half-spaces [7, 37, 38, 59, 60, 61, 62]. Further, spreading resistance problems were considered for flux tubes and channels [1, 3, 8, 35, 60, 61, 62, 63, 64]. Finally, thermal constriction affected by surface layers [12] and the effect of contact boundary condition on thermal constriction resistance for circular contacts [65] were investigated. The main concepts of some of them are mentioned in the following paragraphs.

Yovanovich et al. [59] developed an analytical-numerical solution for the constriction resistance of arbitrary single or multiple areas subjected to uniform or distributed heat flux. Also, the thermal constriction resistance of an ellipsoidal contact model [64] and transient heat conduction from an arbitrary uniform heat source into a semi-infinite solid [57] were studied. Moreover, a transient constriction resistance for isoflux heat source on semi-infinite flux channels was considered [58].

Martin et al. [7] numerically obtained the spreading resistance of arbitrary shaped planar contacts on isotropic half-spaces. Further, Rozon et al. [8] numerically investigated the geometry effect between material interfaces. Negus and Yovanovich [35, 60] presented an

analytical-numerical method for spreading resistance in concentric circular flux tube with uniform contact flux and calculated the thermal constriction resistance for circular flux tube with an isothermal contact. Furthermore, Negus et al. [61, 65] considered the problem of thermal constriction resistance for anisotropic rough surfaces and developed the thermal constriction resistance of a circular isoflux and isothermal heat source on a half-space.

Dryden et al. [17] analyzed the effect of coating on steady-state and transient thermal spreading resistance for an arbitrary axisymmetric contact spot flux on half-spaces. Saabas and Yovanovich [62] proposed an analytical-numerical solution for the thermal spreading resistance of circular micro-contacts distributed over elliptical contours on circular flux tubes and half-spaces.

Yovanovich [1] reviewed thermal contact, gap and joint conductance for point and line contacts and conforming rough surfaces. Lemczyk and Yovanovich [37] conducted a research on thermal constriction resistance for circular heat source on a half-space and its variation with variable Biot number. Also, they modeled the same problem for more general layered problems [38]. Fisher and Yovanovich [12] analytically and experimentally investigated the thermal constriction of a sphere in elastic contact with a flat surface coated with a layer. Negus et al. [63] used the square root of heat source area to non-dimensionalize thermal constriction resistance of three different configurations on insulated semi-infinite cylinders and observed similar results for all configurations at any given relative contact size.

2.1.3 Thermal Spreading Resistance Research 1990-2000

In this time period, many analytical and numerical research studies were published about different thermal spreading resistance problems. Industrial applications of thermal spreading resistance problems were studied by Muzychka et al. [66, 67], Yovanovich et al. [36, 39], and Mantelli and Yovanovich [68]. Further, thermal spreading resistance in the compound systems were considered by Yovanovich et al. [36, 39, 69, 70] and Muzychka et

al. [66, 67].

Lee et al. [71] developed an analytical model for the thermal resistance of bolted joints. Mantelli and Yovanovich [68] considered the same problem for satellite application. Lee et al. [32] and Song et al. [72] developed an analytical solution for constriction/spreading resistance for electronic components with different types of heat sinks. Das and Sadhal [73] modeled the thermal constriction resistance between two solids for random distribution of contacts by using a square region contains randomly placed contacts. Lam and Fisher [26] presented a solution for the thermal resistance of rectangular orthotropic heat spreaders. They demonstrated the result for several values of the vertical-to-horizontal thermal conductivity ratio, the Biot number, and the full range of the nondimensional width of the applied heat flux.

Ellison [33, 74, 75] analytically considered the thermal behavior of printed circuit boards and microelectronic packages like a rectangular, multi-layer structure with discrete heat sources. Muzychka et al. [66, 67] presented a solution for the thermal constriction resistance of an isoflux or isothermal planar heat source in contact with multilayered semi-infinite flux tube with application in conductive coating.

Yovanovich and Teertstra [76] presented a numerical solution for thermal constriction resistance of isothermal circular disks. Yovanovich [77] obtained the constriction resistance of planar isoflux heat sources within semi-infinite conductors. He considered the transient spreading resistance of arbitrary isoflux contact areas such as regular polygons and the hyperellipse [78]. Furthermore, Yovanovich et al. [36, 39] reviewed the previously published analytical modeling of spreading resistance in flux tubes, half spaces, and compound disks which were relevant to diamond spreader on copper heat sink. Finally, a general expression for the spreading resistance of isoflux rectangles and strips on the surface of a finite compound rectangular flux channel with convective or conductive heat sinks were presented [69, 70].

2.1.4 Thermal Spreading Resistance Research After 2000

After 2000, different aspects of thermal spreading resistance were analytically and numerically investigated. Some of these aspects are as follows: different types of flux tubes [22, 27, 79, 80, 84], channels [20, 22, 27, 79, 80], annular sectors [34], and half space [81, 82, 83, 84, 85]; isotropic materials [14, 20, 79], anisotropic materials [86], orthotropic materials [14, 27, 79, 87], and materials with temperature dependent conductivities [84]; single and multiple heat sources [21]; concentric and eccentric heat sources [9, 20, 22, 27]; isoflux [20, 34, 83], isothermal [81, 85], inverse parabolic [34], and parabolic [34] heat flux distribution; centroidal and mean temperature of each heat source [14]; elliptic or hyperellipse [81, 82, 83, 85], strip and circular [22], rectangular [22, 82], and equilateral triangular heat sources [9]; side and end cooling [18], edge cooling [27, 80] and convection in the source plane [14]; single and multilayer systems [14, 19, 20, 27, 34, 87, 88].

Numerical studies on the thermal spreading resistance were done by Ying and Toh [86], Wang and Yan [9] and Rahmani and Shokouhmand [84]. Ying and Toh [86] studied the thermal spreading resistance for the materials with anisotropic properties. Wang and Yan [9] numerically studied the eccentric circular, square and equilateral triangular heat sources on circular heat flux tubes and investigated the influence of eccentricities, shapes and fractal boundary of the heat source on the thermal spreading resistance. Rahmani and Shokouhmand [84] numerically investigated the thermal spreading resistance of isotropic half-space and heat flux tube which have temperature-dependent conductivity.

Ellison [25] examined the thermal spreading resistance for a rectangular source centered on a rectangular plate. Vermeersch and Mey [89] studied the thermal spreading resistance of a rectangular flux channel as a function of the convective heat transfer coefficient at the bottom of the flux channel. Sadeghi et al. [81, 85] obtained a general model based on an elliptical source on a half-space which can be used for calculating the spreading resistance for different geometries for isoflux and isothermal conditions.

Thermal spreading resistance for different industrial applications were considered [19, 22, 86, 21, 24]. Ying and Toh [86] analytically and numerically studied the thermal spreading resistance for electronic packaging with anisotropic properties. Kim et al. [21] established a correlation to predict spreading resistance of multi-electronic components with multiple heat sources. Karmalkar et al. [22] proposed curve-fit models for quick estimation of the thermal spreading resistance for some geometry applicable for designing of ICs. Culham et al. [88, 90] considered the role of the thermal spreading resistance and material properties for designing of plate fin heat sinks and multilayer printed circuit boards. Lasance [91, 92] studied different approaches for obtaining the spreading resistance in LEDs. Dong et al. [24] analyzed the influence of the thermal spreading resistance in high power LED package. Guan et al. [19] proposed an approximate model to solve the spreading resistance in a pyramidal structure for multilayer substrates which has application in power electronics.

Muzychka et al. [14, 16, 20, 23, 27, 34, 79, 80, 82, 87] solved the thermal spreading resistance problems for different systems with different geometries, boundaries and properties. They analyzed the circular and rectangular systems with isotropic and orthotropic properties and concentric and eccentric arbitrary heat sources [13, 18, 20, 79, 80, 87]. They obtained a general solution for the thermal spreading resistance in a compound annular sector for uniform, parabolic, and inverse parabolic heat flux distribution [34]. Also, they reviewed the thermal spreading resistance in compound and orthotropic systems and proposed simple transformations for orthotropic and isotropic systems [87]. They considered the solution of stationary and moving rectangular and elliptic heat sources on a half space and showed if the square root of the heat source area is used to non-dimensionalize the thermal spreading resistance, it is a weak function of shape for stationary and moving heat sources [82]. Further, they obtained thermal spreading resistance of circular flux tubes and rectangular flux channels for isotropic and compound system and modeled the rectangular flux channel by the circular flux tube's solution with using the suitable geometric equiva-

lence [13, 79]. They considered the effect of edge cooling on the thermal spreading resistance in circular flux tubes and rectangular flux channels [80]. They proposed a solution for the thermal spreading resistance of eccentric isoflux rectangular heat sources on finite rectangular compound flux channels [20]. They presented the solution of the thermal spreading resistance for flux tubes and channels by considering compound and orthotropic systems. They also considered the system with or without edge cooling and considered the effects of eccentric heat sources and different heat flux distributions [27]. Furthermore, Muzychka [14] presented an influence coefficient method for calculating the mean and centroidal temperature of discrete heat sources on a finite convectively cooled substrate by considering isotropic, orthotropic, and compound systems. Also, the convection in the source plane which causes heat dissipation through the source plane was considered. Recently, Muzychka et al. [16, 23] modeled the thermal spreading resistance in compound orthotropic systems with interfacial resistance.

Yovanovich [18] presented a solution for the thermal spreading resistance of a circular source on a finite circular cylinder with uniform side and end cooling. The thermal spreading resistance models were summarized in a heat transfer handbook by Yovanovich and Marrota [2]. Furthermore, Yovanovich wrote a review paper about his forty years of research in contact, gap and joint resistance [3].

Gholami and Bahrami [93] studied the thermal spreading resistance in a rectangular slab with different thermal conductivity in different directions, $k_x \neq k_y \neq k_z$, and discretely specified inward and outward heat flux along the source and sink plane, respectively. Recently, Razavi et al. [6] studied the effect of variable heat transfer coefficient along the sink plane to consider the effect of variable heat sinking in electronic devices.

2.2 Problem Statement

For analytical modeling of the electronic devices, the geometry of the system is usually simplified as the rectangular flux channel or circular flux tube. Due to the existence of different layers in the electronic devices, the simplified geometries are assumed as compound flux channel or compound flux tube. The material of each layer can be orthotropic with different in-plane and through-plane thermal conductivities. Further, a contact thermal resistance may exist between different layers. The geometries of the discussed systems are shown in Figs. 2.2- 2.3.

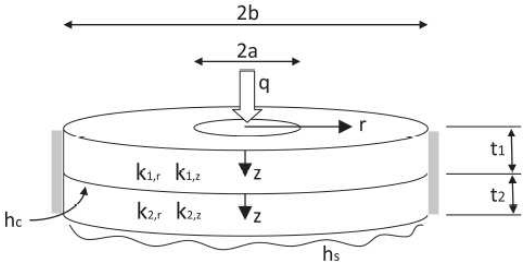

Figure 2.2: Compound flux tube with interfacial contact resistance, h_c, and orthotropic properties.

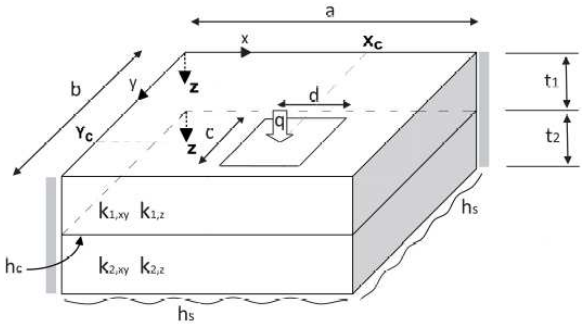

Figure 2.3: Compound flux channel with interfacial contact resistance, h_c, and orthotropic properties.

The interfacial contact resistance is presented in the form of a contact conductance, h_c, that also may represents as equivalent resistance by considering the nominal thickness of contact region and its thermal conductivity,

$$R_t = \frac{t_i}{k_i A_b} = \frac{1}{h_c A_b} \qquad \Rightarrow \qquad h_c = \frac{k_i}{t_i}. \tag{2.1}$$

The coordinate system for both geometries is localized and each layer has dependent coordinate system to model different thermal conductivity in plane and through plane of each layers. The governing equation of both systems is Laplace's equation. The variable θ is de-

fined as the temperature excess relative to the film temperature in the sink plane, $\theta = T - T_f$. The Laplace equation based on the Cartesian coordinate system for the rectangular flux channel is,

$$\begin{aligned} k_{1,xy}\left(\frac{\partial^2\theta_1}{\partial x^2}+\frac{\partial^2\theta_1}{\partial y^2}\right)+k_{1,z}\frac{\partial^2\theta_1}{\partial z^2}=0, \qquad 0<z<t_1, \\ k_{2,xy}\left(\frac{\partial^2\theta_2}{\partial x^2}+\frac{\partial^2\theta_2}{\partial y^2}\right)+k_{2,z}\frac{\partial^2\theta_2}{\partial z^2}=0, \qquad 0<z<t_2. \end{aligned} \tag{2.2}$$

The Laplace's equation for the circular flux tubes using the cylindrical coordinate system is,

$$\begin{aligned} k_{1,r}\left(\frac{\partial^2\theta_1}{\partial r^2}+\frac{1}{r}\frac{\partial\theta_1}{\partial r}\right)+k_{1,z}\frac{\partial^2\theta_1}{\partial z^2}=0, \qquad 0<z<t_1, \\ k_{2,r}\left(\frac{\partial^2\theta_2}{\partial r^2}+\frac{1}{r}\frac{\partial\theta_2}{\partial r}\right)+k_{2,z}\frac{\partial^2\theta_2}{\partial z^2}=0, \qquad 0<z<t_2, \end{aligned} \tag{2.3}$$

where $k_{1,xy}, k_{2,xy}, k_{1,r}, k_{2,r}$ are in plane thermal conductivities and $k_{1,z}, k_{2,z}$ are through plane thermal conductivities.

Regarding the boundary conditions of the system along the source plane, a constant heat flux, q, exists over the source region and an adiabatic condition specified out of the source region,

$$\begin{aligned} -k_{1,z}\left.\frac{\partial\theta_1}{\partial z}\right|_{z=0}=q, \qquad \text{Over source region}, \\ -k_{1,z}\left.\frac{\partial\theta_1}{\partial z}\right|_{z=0}=0, \qquad \text{Outside source region}. \end{aligned} \tag{2.4}$$

Along the interfacial contact region of the flux channel and the flux tube, the condition

represents the equality of flux exists,

$$k_{1,z}\left.\frac{\partial\theta_1}{\partial z}\right|_{z=t_1} = k_{2,z}\left.\frac{\partial\theta_2}{\partial z}\right|_{z=0}. \tag{2.5}$$

Further, a condition for the temperature drop due to the thermal contact resistance is defined as follows,

$$-k_{1,z}\left.\frac{\partial\theta_1}{\partial z}\right|_{z=t_1} = h_c[\theta_1(x,y,t_1) - \theta_2(x,y,0)], \qquad \text{Flux channel}, \tag{2.6}$$

$$-k_{1,z}\left.\frac{\partial\theta_1}{\partial z}\right|_{z=t_1} = h_c[\theta_1(r,t_1) - \theta_2(r,0)], \qquad \text{Flux tube}. \tag{2.7}$$

The boundary conditions along the sink planes of the flux channel and the flux tube are,

$$-k_{2,z}\left.\frac{\partial\theta_2}{\partial z}\right|_{z=t_2} = h_s\theta_2(x,y,t_2), \qquad \text{Flux channel}, \tag{2.8}$$

$$-k_{2,z}\left.\frac{\partial\theta_2}{\partial z}\right|_{z=t_2} = h_s\theta_2(r,t_2), \qquad \text{Flux tube}. \tag{2.9}$$

The adiabatic boundary conditions exist along the edges of the system. For the rectangular flux channel,

$$\left.\frac{\partial\theta_i}{\partial x}\right|_{x=0,c} = 0, \qquad i = 1,2; \tag{2.10}$$

$$\left.\frac{\partial\theta_i}{\partial y}\right|_{y=0,d} = 0, \qquad i = 1,2. \tag{2.11}$$

and for the flux tube,

$$\left.\frac{\partial \theta_i}{\partial r}\right|_{r=0} = 0, \qquad i = 1, 2; \tag{2.12}$$

$$\left.\frac{\partial \theta_i}{\partial r}\right|_{r=b} = 0, \qquad i = 1, 2. \tag{2.13}$$

2.2.1 Transformation of Orthotropic System to Isotropic System

To facilitate the solution, the orthotropic system is transformed to the isotropic system using the method of stretched coordinates [16, 27]. The effective isotropic properties for each layer of the flux channel is obtained by defining the following variables for each layer,

$$\zeta = \frac{z}{\sqrt{\frac{k_{1,z}}{k_{1,xy}}}}, \qquad \text{Top layer of the flux channel,} \tag{2.14}$$

$$\varsigma = \frac{z}{\sqrt{\frac{k_{2,z}}{k_{2,xy}}}}, \qquad \text{Bottom layer of the flux channel.} \tag{2.15}$$

and for the flux tube,

$$\zeta = \frac{z}{\sqrt{\frac{k_{1,z}}{k_{1,r}}}}, \qquad \text{Top layer of the flux tube,} \tag{2.16}$$

$$\varsigma = \frac{z}{\sqrt{\frac{k_{2,z}}{k_{2,r}}}}, \qquad \text{Bottom layer of the flux tube.} \tag{2.17}$$

Using the variables ζ and ς, the effective isotropic layer properties for the flux channel are defined as,

$$k_1 = \sqrt{k_{1,xy}k_{1,z}}, \qquad \bar{t}_1 = \frac{t_1}{\sqrt{\frac{k_{1,z}}{k_{1,xy}}}}, \qquad \text{Top layer of the flux channel,} \tag{2.18}$$
$$k_2 = \sqrt{k_{2,xy}k_{2,z}}, \qquad \bar{t}_2 = \frac{t_2}{\sqrt{\frac{k_{2,z}}{k_{2,xy}}}}, \qquad \text{Bottom layer of the flux channel,}$$

and for the flux tube,

$$k_1 = \sqrt{k_{1,r}k_{1,z}}, \qquad \bar{t}_1 = \frac{t_1}{\sqrt{\frac{k_{1,z}}{k_{1,r}}}}, \qquad \text{Top layer of the flux tube,} \tag{2.19}$$
$$k_2 = \sqrt{k_{2,r}k_{2,z}}, \qquad \bar{t}_2 = \frac{t_2}{\sqrt{\frac{k_{2,z}}{k_{2,r}}}}, \qquad \text{Bottom layer of the flux tube.}$$

By using the definition of k_1 and k_2, the orthotropic Laplace's equations are transformed to the isotropic form. The transformed Laplace's equations for the flux channel are,

$$\frac{\partial^2\theta_1}{\partial x^2} + \frac{\partial^2\theta_1}{\partial y^2} + \frac{\partial^2\theta_1}{\partial \zeta^2} = 0, \qquad 0 < \zeta < \bar{t}_1, \tag{2.20}$$
$$\frac{\partial^2\theta_2}{\partial x^2} + \frac{\partial^2\theta_2}{\partial y^2} + \frac{\partial^2\theta_2}{\partial \varsigma^2} = 0, \qquad 0 < \varsigma < \bar{t}_2,$$

and for the flux tube,

$$\left(\frac{\partial^2\theta_1}{\partial r^2} + \frac{1}{r}\frac{\partial\theta_1}{\partial r}\right) + \frac{\partial^2\theta_1}{\partial \zeta^2} = 0, \qquad 0 < \zeta < \bar{t}_1, \tag{2.21}$$
$$\left(\frac{\partial^2\theta_2}{\partial r^2} + \frac{1}{r}\frac{\partial\theta_2}{\partial r}\right) + \frac{\partial^2\theta_2}{\partial \varsigma^2} = 0, \qquad 0 < \varsigma < \bar{t}_2.$$

The boundary conditions should also be transformed. Along the source plane,

$$\begin{aligned} -k_1 \left.\frac{\partial \theta_1}{\partial \zeta}\right|_{\zeta=0} &= q, \qquad \text{Over source region,} \\ -k_1 \left.\frac{\partial \theta_1}{\partial \zeta}\right|_{\zeta=0} &= 0, \qquad \text{Outside source region.} \end{aligned} \tag{2.22}$$

Along the contact plane,

$$\begin{aligned} k_1 \left.\frac{\partial \theta_1}{\partial \zeta}\right|_{\zeta=\bar{t}_1} &= k_2 \left.\frac{\partial \theta_2}{\partial \varsigma}\right|_{\varsigma=0}, \qquad \text{Condition of equality of flux,} \\ -k_1 \left.\frac{\partial \theta_1}{\partial \zeta}\right|_{\zeta=\bar{t}_1} &= h_c[\theta_1(x,y,\bar{t}_1) - \theta_2(x,y,0)], \qquad \text{Temperature drop for flux channel,} \\ -k_1 \left.\frac{\partial \theta_1}{\partial \zeta}\right|_{\zeta=\bar{t}_1} &= h_c[\theta_1(r,\bar{t}_1) - \theta_2(r,0)], \qquad \text{Temperature drop for flux tube,} \end{aligned} \tag{2.23}$$

and along the sink plane,

$$\begin{aligned} -k_2 \left.\frac{\partial \theta_2}{\partial \varsigma}\right|_{\varsigma=\bar{t}_2} &= h_s \theta_2(x,y,\bar{t}_2), \qquad \text{Flux channel,} \\ -k_2 \left.\frac{\partial \theta_2}{\partial \varsigma}\right|_{\varsigma=\bar{t}_2} &= h_s \theta_2(r,\bar{t}_2), \qquad \text{Flux tube.} \end{aligned} \tag{2.24}$$

The other boundary conditions remain unchanged, Eqs. (2.10- 2.13).

2.2.2 Solution of the Flux Tube

In this section, the general solution of isotropic flux tube is briefly described. The solution is extended to the compound system later. The Laplace's equation for the isotropic flux

tube is,

$$\frac{\partial^2\theta}{\partial r^2} + \frac{1}{r}\frac{\partial\theta}{\partial r} + \frac{\partial^2\theta}{\partial z^2} = 0. \tag{2.25}$$

The general form of the solution using the method of separation of variables is,

$$\theta(r,z) = A_0 + B_0 z + [A_1 J_0(\lambda r) + B_1 Y_0(\lambda r)][A_2\cosh(\lambda z) + B_2\sinh(\lambda z)]. \tag{2.26}$$

The first two terms represent uniform heat flow. To consider the spreading resistance portion of the solution, first two terms are discarded. The thermal resistance based on uniform heat flow can be added to the thermal spreading resistance to obtain the total thermal resistance, $R_t = R_{1D} + R_s$. Applying the center line condition of the flux tube, Eq. (2.12), results in $B_1 = 0$. The eigenvalues of the system are obtained using Eq. (2.13),

$$\frac{d}{dr}(J_0(\lambda r))\bigg|_{r=b} = -\lambda J_1(\lambda r)\bigg|_{r=b} = J_1(\lambda b) = 0, \tag{2.27}$$

and the eigenvalues are,

$$\delta_n = \lambda_n b = 3.8317, 7.0156, 10.1735.13.2327, \cdots . \tag{2.28}$$

To obtain more eigenvalues, the constant π can be added to the previous eigenvalue, $\delta_i - \delta_{i-1} = \pi$. The general solution at this point is,

$$\theta(r,z) = \sum_{n=1}^{\infty} J_0(\lambda_n r)\Big(A_n\cosh(\lambda_n z) + B_n\sinh(\lambda_n z)\Big). \tag{2.29}$$

Using the boundary condition at $z = t$ relates the unknown coefficients A_n and B_n by

spreading function, ϕ,

$$B_n = -A_n \left(\frac{\lambda_n \tanh(\lambda_n \bar{t}_1) + \frac{h_s}{k_1}}{\lambda_n + \frac{h_s}{k_1} \tanh(\lambda_n \bar{t}_1)} \right) = -A_n \phi. \tag{2.30}$$

The solution becomes,

$$\theta(r,z) = \sum_{n=1}^{\infty} A_n J_0(\lambda_n r) \Big(\cosh(\lambda z) - \phi \sinh(\lambda_n z) \Big). \tag{2.31}$$

The final boundary condition is along the source plane. Applying this boundary condition and using the orthogonality property results,

$$A_n = \frac{\frac{q}{k_1} \int_0^a J_0(\lambda_n r) r dr}{\lambda_n \phi \int_0^b J_0^2(\lambda_n r) r dr} = \frac{2qa}{\phi k_1} \frac{J_1(\delta_n \frac{a}{b})}{\delta_n^2 J_0^2(\delta_n)} \tag{2.32}$$

Substituting the A_n in the solution gives the final solution,

$$\theta(r,z) = \sum_{n=1}^{\infty} \left(\frac{2qa}{\phi k_1} \frac{J_1(\delta_n \frac{a}{b})}{\delta_n^2 J_0^2(\delta_n)} \right) J_0\left(\delta_n \frac{r}{b}\right) \left(\cosh\left(\delta_n \frac{z}{b}\right) - \phi_n \sinh\left(\delta_n \frac{z}{b}\right) \right). \tag{2.33}$$

The temperature distribution along the source plane, $z = 0$, is,

$$\theta(r,0) = \sum_{n=1}^{\infty} \left(\frac{2qa}{\phi k_1} \frac{J_1(\delta_n \frac{a}{b})}{\delta_n^2 J_0^2(\delta_n)} \right) J_0\left(\delta_n \frac{r}{b}\right). \tag{2.34}$$

The mean temperature in the source region is,

$$\overline{\theta}_s = \frac{1}{\pi a^2} \int_0^a \theta(r,0) 2\pi r dr = \frac{4qb}{k_1} \sum_{n=1}^{\infty} \frac{J_1^2(\delta_n \frac{a}{b})}{\phi \delta_n^3 J_0^2(\delta_n)}. \tag{2.35}$$

The thermal spreading resistance is defined as [5],

$$R_s = \frac{\overline{\theta}_s - \overline{\theta}_{cp}}{Q} = \frac{4b}{k_1 \pi a^2} \sum_{n=1}^{\infty} \frac{J_1^2(\delta_n \frac{a}{b})}{\phi \delta_n^3 J_0^2(\delta_n)}, \tag{2.36}$$

and the total thermal resistance is,

$$R_t = R_{1D} + R_s = \frac{t_1}{k_1 \pi b^2} + \frac{1}{h_s \pi b^2} + \frac{4b}{k_1 \pi a^2} \sum_{n=1}^{\infty} \frac{J_1^2(\delta_n \frac{a}{b})}{\phi \delta_n^3 J_0^2(\delta_n)}. \tag{2.37}$$

To extend the solution to the case of compound system with interfacial resistance, the only required change is defining an appropriate spreading function, ϕ.

2.2.3 Rectangular Flux Channel with Eccentric Heat Source

The general form of the solution for the isotropic rectangular flux channel may be obtained using the method of separation of variables. The general procedure is similar to the approach that is discussed in the previous section. The eigenvalues of the system, λ_m, δ_n and β_{mn}, are defined as,

$$\lambda_m = \frac{m\pi}{a}, \qquad \delta_n = \frac{n\pi}{b}, \qquad \beta_{mn} = \sqrt{\lambda_m^2 + \delta_n^2}. \tag{2.38}$$

The general form of the solution is,

$$\begin{aligned} \theta(x,y,z) = {} & A_0 + B_0 z \\ & + \sum_{m=1}^{\infty} \cos(\lambda_m x)[A_1 \cosh(\lambda_m z) + B_1 \sinh(\lambda_m z)] \\ & + \sum_{n=1}^{\infty} \cos(\delta_n y)[A_2 \cosh(\delta_n z) + B_2 \sinh(\delta_n z)] \\ & + \sum_{m=1}^{\infty} \sum_{n=1}^{\infty} \cos(\lambda_m x) \cos(\delta_n y)[A_3 \cosh(\beta_{mn} z) + B_3 \sinh(\beta_{mn} z)] \end{aligned} \tag{2.39}$$

where $A_0 + B_0 z$ represents the uniform flow solution and three spreading resistance solutions in the form of Fourier series expansions [20]. By using the boundary condition along the sink plane, the Fourier coefficients relate to each other by the spreading function, ϕ, as

follows,

$$B_i = -\phi(\gamma_n)A_i, \qquad i = 1, 2, 3. \tag{2.40}$$

The spreading function, ϕ, for the convective cooling boundary condition along the sink plane is,

$$\phi(\gamma_n) = \frac{\gamma_n \tanh(\gamma_n \bar{t}_1) + \frac{h_s}{k_1}}{\gamma_n + \frac{h_s}{k_1}\tanh(\gamma_n \bar{t}_1)}, \tag{2.41}$$

where γ_n is replaced by λ_m, δ_n and β_{mn}. The spreading function for the ideal heat sink, $h_s \to \infty$, that represents the constant sink temperature is,

$$\phi(\gamma_n) = coth(\gamma_n \bar{t}_1). \tag{2.42}$$

The final coefficients are obtained by using the boundary conditions along the source plane. Applying the boundary conditions at $z = 0$ and using the orthogonality property result,

$$A_m = \frac{Q}{bck_1\lambda_m\phi(\lambda_m)} \frac{\int_{X_c-\frac{c}{2}}^{X_c+\frac{c}{2}} \cos(\lambda_m x)dx}{\int_0^a \cos^2(\lambda_m x)dx} = \frac{2Q\left[\sin\left(\frac{(2X_c+c)}{2}\lambda_m\right) - \sin\left(\frac{(2X_c-c)}{2}\lambda_m\right)\right]}{abck_1\lambda_m^2\phi(\lambda_m)}, \tag{2.43}$$

$$A_n = \frac{Q}{adk_1\delta_n\phi(\delta_n)} \frac{\int_{Y_c-\frac{d}{2}}^{Y_c+\frac{d}{2}} \cos(\delta_n y)dy}{\int_0^b \cos^2(\delta_n y)dy} = \frac{2Q\left[\sin\left(\frac{(2Y_c+d)}{2}\delta_n\right) - \sin\left(\frac{(2Y_c-d)}{2}\delta_n\right)\right]}{abdk_1\delta_n^2\phi(\delta_n)}, \tag{2.44}$$

$$A_{mn} = \frac{Q}{cdk_1\beta_{mn}\phi(\beta_{mn})} \frac{\int_{Y_c-\frac{d}{2}}^{Y_c+\frac{d}{2}} \int_{X_c-\frac{c}{2}}^{X_c+\frac{c}{2}} \cos(\lambda_m x)\cos(\delta_n y)dxdy}{\int_0^b \int_0^a \cos^2(\lambda_m x)\cos^2(\delta_n y)dxdy}, \tag{2.45}$$

$$A_{mn} = \frac{16Q\cos(\lambda_m X_c)\sin\left(\frac{1}{2}\lambda_m c\right)\cos(\delta_n Y_c)\sin\left(\frac{1}{2}\delta_n d\right)}{abcdk_1\beta_{mn}\lambda_m\delta_n\phi(\beta_{mn})}.$$

The coefficients of the uniform flow solution are,

$$A_0 = \frac{Q}{ab}\left(\frac{\bar{t}_1}{k_1} + \frac{1}{h_s}\right), \qquad B_0 = -\frac{Q}{k_1 ab}. \tag{2.46}$$

To calculate the thermal resistance, the mean source temperature should be obtained. For this purpose, temperature profile along the source plane, $z = 0$, is written using general form of the solution, Eq. (2.39), as follows [16],

$$\theta(x,y,0) = A_0 + \sum_{m=1}^{\infty} A_m\cos(\lambda_m x) + \sum_{n=1}^{\infty} A_n\cos(\delta_n y) + \sum_{m=1}^{\infty}\sum_{n=1}^{\infty} A_{mn}\cos(\lambda_m x)\cos(\delta_n y), \tag{2.47}$$

where,

$$A_m = \frac{4Q\cos(\lambda_m X_c)\sin\left(\lambda_m\frac{c}{2}\right)}{abck_1\lambda_m^2\phi(\lambda_m)}, \tag{2.48}$$

$$A_n = \frac{4Q\cos(\delta_n Y_c)\sin\left(\delta_n\frac{d}{2}\right)}{abdk_1\delta_n^2\phi(\delta_n)}, \tag{2.49}$$

$$A_{mn} = \frac{16Q\cos(\lambda_m X_c)\sin\left(\frac{1}{2}\lambda_m c\right)\cos(\delta_n Y_c)\sin\left(\frac{1}{2}\delta_n d\right)}{abcdk_1\beta_{mn}\lambda_m\delta_n\phi(\beta_{mn})}. \tag{2.50}$$

The mean temperature excess along the source plane is calculated by integration of Eq. (2.47),

$$\begin{aligned}\overline{\theta}_s = A_0 &+ 2\sum_{m=1}^{\infty} A_m \frac{\cos(\lambda_m X_c)\sin\left(\frac{1}{2}\lambda_m c\right)}{\lambda_m c} \\ &+ 2\sum_{n=1}^{\infty} A_n \frac{\cos(\delta_n Y_c)\sin\left(\frac{1}{2}\delta_n d\right)}{\delta_n d} \\ &+ 4\sum_{m=1}^{\infty}\sum_{n=1}^{\infty} A_{mn} \frac{\cos(\delta_n Y_c)\sin\left(\frac{1}{2}\delta_n d\right)\cos(\lambda_m X_c)\sin\left(\frac{1}{2}\lambda_m c\right)}{\lambda_m c \delta_n d}\end{aligned} \tag{2.51}$$

where X_c and Y_c are the position of the heat source's central point.

The total thermal resistance of the flux channel may be obtained using the mean source temperature excess over the source area,

$$R_t = \frac{\overline{\theta}_s}{Q} = R_{1D} + R_s, \tag{2.52}$$

where one dimensional resistance is,

$$R_{1D} = \frac{1}{ab}\left(\frac{\bar{t}_1}{k_1} + \frac{1}{h_s}\right), \tag{2.53}$$

and the thermal spreading resistance is,

$$\begin{aligned}R_s = &\frac{2}{Q}\sum_{m=1}^{\infty} A_m \frac{\cos(\lambda_m X_c)\sin(\frac{1}{2}\lambda_m c)}{\lambda_m c} \\ &+ \frac{2}{Q}\sum_{n=1}^{\infty} A_n \frac{\cos(\delta_n Y_c)\sin(\frac{1}{2}\delta_n d)}{\delta_n d} \\ &+ \frac{4}{Q}\sum_{m=1}^{\infty}\sum_{n=1}^{\infty} A_{mn} \frac{\cos(\delta_n Y_c)\sin(\frac{1}{2}\delta_n d)\cos(\lambda_m X_c)\sin(\frac{1}{2}\lambda_m c)}{\lambda_m c \delta_n d}.\end{aligned} \tag{2.54}$$

The solution for the flux channel with multiple heat sources was also implemented using the superposition method [16, 20].

2.2.4 Rectangular Flux Channel with Concentric Heat Source

One of the common geometries in the electronic devices is the rectangular flux channel with central heat source, Fig. 2.4. It is a special case of the solution for the rectangular flux channel that is presented in the previous section.

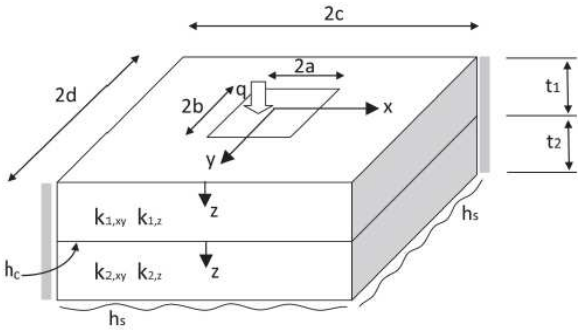

Figure 2.4: Compound flux channel with central heat source, interfacial contact resistance, h_c, and orthotropic properties.

For simplicity in using the symmetry properties, the length and width of the heat source and the flux channel are assumed as $2a$, $2b$, $2c$ and $2d$, respectively [23]. The eigenvalues of this problem are,

$$\lambda_m = \frac{m\pi}{c}, \qquad \delta_n = \frac{n\pi}{d}, \qquad \beta_{mn} = \sqrt{\lambda_m^2 + \delta_n^2}. \tag{2.55}$$

Total thermal resistance consists of one dimensional thermal resistance and thermal spreading resistance, Eq. (2.52). The one dimensional thermal resistance and thermal spreading resistance are as follows,

$$R_{1D} = \frac{1}{4cd}\left(\frac{\bar{t}_1}{k_1} + \frac{1}{h_s}\right), \tag{2.56}$$

$$R_s = \frac{1}{2a^2cdk_1}\sum_{m=1}^{\infty}\frac{\sin^2(a\lambda_m)}{\phi(\lambda_m)\lambda_m^3} + \frac{1}{2b^2cdk_1}\sum_{n=1}^{\infty}\frac{\sin^2(b\delta_n)}{\phi(\delta_n)\delta_n^3} + \frac{1}{a^2b^2cdk_1}\sum_{m=1}^{\infty}\sum_{n=1}^{\infty}\frac{\sin^2(a\lambda_m)\sin^2(b\delta_n)}{\phi(\beta_{mn})\lambda_m^2\delta_n^2\beta_{mn}}. \tag{2.57}$$

2.3 Extension the Solutions to Compound Systems

The presented solutions for the rectangular flux channel and cylindrical flux tube can be extended to the compound system with and without interfacial contact resistance. The only change to the solution is the definition of the spreading function. The spreading functions for the compound systems are presented in the following subsections. It is worth mentioning that area of the base, A_b, for each case is different and should be calculated as follows,

$$A_b = \pi b^2, \quad \text{Base area for the cylindrical flux tube,} \tag{2.58}$$

$$A_b = a\,.\,b, \quad \text{Base area for the general flux channel,} \tag{2.59}$$

$$A_b = 2c\,.\,2d, \quad \text{Base area for the flux channel with central source.} \tag{2.60}$$

To model the system with multiple layers, some extensions were done by Bagnall et al. [94]. The general procedure is the same and a recursion method was used to consider the effect of each layer in the spreading function of other layers.

2.3.1 Compound System with Interfacial Contact Resistance

For the case of compound flux channel or flux tube with interfacial contact resistance, the spreading function is,

$$\phi = \frac{C_1 + C_2 \tanh(\gamma_n \bar{t}_1)}{C_1 \tanh(\gamma_n \bar{t}_1) + C_2}, \tag{2.61}$$

where,

$$C_1 = \left[\gamma_n \tanh(\gamma_n \bar{t}_2) + \frac{h_s}{k_2} \right], \tag{2.62}$$

and,

$$C_2 = \frac{k_1}{k_2} \left[\gamma_n \left(1 + \frac{h_s}{h_c} \right) + \left(\frac{h_s}{k_2} + \frac{\gamma_n^2 k_2}{h_c} \right) \tanh(\gamma_n \bar{t}_2) \right]. \tag{2.63}$$

Further, the one dimensional thermal resistance, R_{1D}, is changed due to the different conductivities in different layers and existence of contact conductance,

$$R_{1D} = \frac{1}{A_b} \left(\frac{\bar{t}_1}{k_1} + \frac{1}{h_c} + \frac{\bar{t}_2}{k_2} + \frac{1}{h_s} \right). \tag{2.64}$$

2.3.2 Compound System with Interfacial Contact Resistance and Ideal Heat Sink

The spreading function for the compound flux channel or compound flux tube with ideal heat sink, $h_s \to \infty$, that represents the constant sink temperature is,

$$\phi = \frac{1 + \left(\frac{\gamma_n k_1}{h_c} \right) \tanh(\gamma_n \bar{t}_1) + \frac{k_1}{k_2} \tanh(\gamma_n \bar{t}_2) \tanh(\gamma_n \bar{t}_1)}{\gamma_n \frac{k_1}{h_c} + \frac{k_1}{k_2} \tanh(\gamma_n \bar{t}_2) + \tanh(\gamma_n \bar{t}_1)} \tag{2.65}$$

and the one dimensional thermal resistance is,

$$R_{1D} = \frac{1}{A_b}\left(\frac{\bar{t}_1}{k_1} + \frac{1}{h_c} + \frac{\bar{t}_2}{k_2}\right). \tag{2.66}$$

2.3.3 Compound System without Interfacial Contact Resistance

The spreading function for the compound flux channel or compound flux tube with perfect interfacial contact is,

$$\phi = \frac{\left[\gamma_n \tanh(\gamma_n \bar{t}_2) + \frac{h_s}{k_2}\right] + \frac{k_1}{k_2}\left[\gamma_n + \frac{h_s}{k_2}\tanh(\gamma_n \bar{t}_2)\right]\tanh(\gamma_n \bar{t}_1)}{\left[\gamma_n \tanh(\gamma_n \bar{t}_2) + \frac{h_s}{k_2}\right]\tanh(\gamma_n \bar{t}_1) + \frac{k_1}{k_2}\left[\gamma_n + \frac{h_s}{k_2}\tanh(\gamma_n \bar{t}_2)\right]}, \tag{2.67}$$

and the one dimensional thermal resistance is,

$$R_{1D} = \frac{1}{A_b}\left(\frac{\bar{t}_1}{k_1} + \frac{\bar{t}_2}{k_2} + \frac{1}{h_s}\right). \tag{2.68}$$

2.3.4 Compound System without Interfacial Contact Resistance and Ideal Heat Sink

The last case is the spreading function of the compound flux channel and compound flux tube with constant temperature heat sink, $h_s \to \infty$, and no interfacial resistance between the layers,

$$\phi = \frac{1 + \frac{k_1}{k_2}\tanh(\gamma_n \bar{t}_2)\tanh(\gamma_n \bar{t}_1)}{\tanh(\gamma_n \bar{t}_1) + \frac{k_1}{k_2}\tanh(\gamma_n \bar{t}_2)}, \tag{2.69}$$

and the one dimensional resistance is,

$$R_{1D} = \frac{1}{A_b}\left(\frac{\bar{t}_1}{k_1} + \frac{\bar{t}_2}{k_2}\right). \tag{2.70}$$

It is worth mentioning that the base area for all of the above cases should be substituted by the proper value based on Eqs. (2.58- 2.60).

2.4 Influence Coefficient Method

Muzychka [14] proposed the influence coefficient method for solving the spreading resistance problems in the flux channel. In this method, a matrix approach is used to solve the problems with more than five sources with less computation. Later, Muzychka et al. [16] extended the solution to the multi-layer system with and without interfacial contact resistance. Based on this method, for the mean temperature excess of the jth heat source,

$$\overline{\theta}_j = \overline{\theta}_{1j} + \overline{\theta}_{2j} + \cdots + \overline{\theta}_{N_s j} = Q_1 \overline{f}_{1j} + Q_2 \overline{f}_{2j} + \cdots + Q_{N_s} \overline{f}_{N_s j} = \sum_{i=1}^{N_s} Q_i \overline{f}_{i,j}, \quad (2.71)$$

where,

$$\begin{aligned} \overline{f}_{ij} = B_0^i &+ \sum_{m=1}^{\infty} B_m^i \frac{2\cos(\lambda_m X_{c,j})\sin(\tfrac{1}{2}\lambda_m c_j)}{\lambda_m c_j} \\ &+ \sum_{n=1}^{\infty} B_n^i \frac{2\cos(\delta_n Y_{c,j})\sin(\tfrac{1}{2}\delta_n d_j)}{\delta_n d_j} \\ &+ \sum_{m=1}^{\infty}\sum_{n=1}^{\infty} B_{mn}^i \frac{4\cos(\delta_n Y_{c,j})\sin(\tfrac{1}{2}\delta_n d_j)\cos(\lambda_m X_{c,j})\sin(\tfrac{1}{2}\lambda_m c_j)}{\lambda_m c_j \delta_n d_j}. \end{aligned} \quad (2.72)$$

The influence coefficients, f_{ij}, are affected by the location and size of the neighboring heat sources. The temperature excess may be written in the following form,

$$\begin{Bmatrix} \theta_1 \\ \theta_2 \\ \theta_3 \\ \vdots \\ \theta_{Ns} \end{Bmatrix} = \begin{bmatrix} f_{11} & f_{12} & \cdots & f_{1Ns} \\ f_{21} & f_{22} & \cdots & f_{2Ns} \\ f_{31} & f_{32} & \cdots & f_{3Ns} \\ \vdots & \vdots & \vdots & \vdots \\ f_{N_s1} & f_{N_s2} & \cdots & f_{N_sN_s} \end{bmatrix} \begin{bmatrix} Q_1 \\ Q_2 \\ Q_3 \\ \vdots \\ Q_{Ns} \end{bmatrix} \Rightarrow \Big\{\theta\Big\} = \Big[F_{ij}\Big] \Big[,Q\Big] \tag{2.73}$$

where F_{ij} is the matrix of influence coefficients. In this method, the reciprocity property exists when $i \neq j$,

$$f_{ij} = f_{ji}. \tag{2.74}$$

By using this property, the computation time reduces significantly when there are more than five heat sources. In general, for a system with N sources, the number of coefficient that should be calculated is $(N_s^2 + N_s)/2$.

2.5 Flux Channel with Arbitrarily Specified Inward and Outward Heat Fluxes and Different Thermal Conductivities in the x, y and z Directions

Gholami and Bahrami [93] studied the thermal spreading resistance in graphite-based materials which have different thermal conductivities in different directions, $k_x \neq k_y \neq k_z$. The considered geometry is a rectangular flux channel with discretely specified inward and outward heat fluxes along the source and sink plane, respectively. The outer surfaces of sources and sinks beside the edges of the channel are insulated, Fig. 2.5. Their solution for one source and one sink is briefly described which can be extended to system with multiple sources and sinks by using the superposition method.

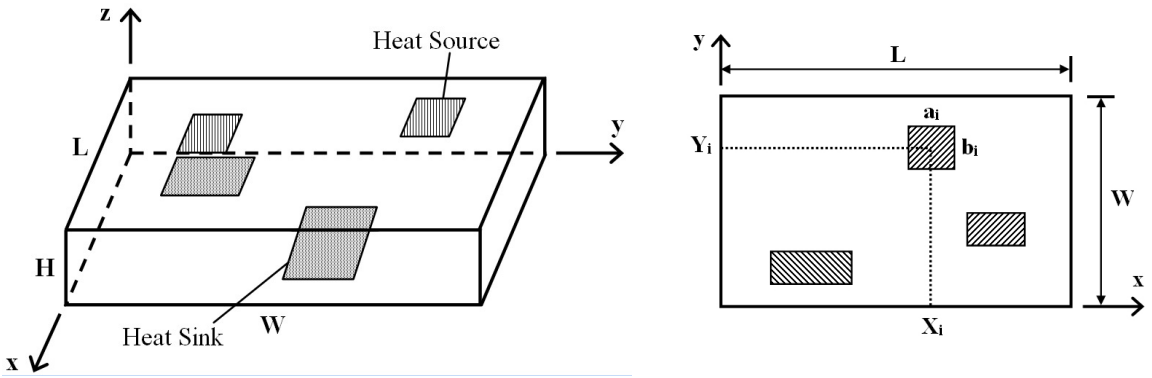

Figure 2.5: Schematic of anisotropic rectangular spreader with multiple hotspots on a) top and bottom surfaces size and b) location of hotspots [93].

The governing equation and boundary conditions are defined using the following dimensionless parameters,

$$\epsilon = \frac{W}{L}, \qquad \epsilon_H = \frac{H}{L}, \qquad x^* = \frac{x}{L}, \qquad y^* = \frac{y}{W}, \qquad z^* = \frac{z}{H}, \tag{2.75}$$

$$a_i^* = \frac{a_i}{L}, \qquad b_i^* = \frac{b_i}{W}, \qquad q_{i(x,y)}^* = \frac{LWq_{i(x,y)}}{Q_0}, \qquad \theta = \frac{Lk_0}{Q_0}(T - T_0),$$

$$\kappa_x = \sqrt{\frac{k_0}{k_x}}, \qquad \kappa_y = \sqrt{\frac{k_0}{k_y}}, \qquad \kappa_z = \sqrt{\frac{k_0}{k_z}}, \qquad R^* = Lk_zR, \tag{2.76}$$

where, Q_0 is the arbitrary reference heat flux and k_0 is the arbitrary reference thermal conductivity. The dimensionless form of the governing equation and boundary conditions are presented as follows,

$$\nabla^2\theta = \frac{1}{\kappa_x^2}\frac{\partial^2\theta}{\partial x^{*2}} + \frac{1}{\epsilon^2\kappa_y^2}\frac{\partial^2\theta}{\partial y^{*2}} + \frac{1}{\epsilon_H^2\kappa_z^2}\frac{\partial^2\theta}{\partial z^{*2}} = 0. \tag{2.77}$$

Due to the insulated edges, the boundary conditions along the edges are,

$$\begin{aligned} \frac{\partial \theta}{\partial x^*} &= 0 \qquad \text{at} \qquad x^* = 0, \qquad x^* = 1, \\ \frac{\partial \theta}{\partial y^*} &= 0 \qquad \text{at} \qquad y^* = 0, \qquad y^* = 1. \end{aligned} \tag{2.78}$$

Source and sink boundary conditions are defined using the Neumann boundary condition or prescribed heat flux. Along the source plane,

$$\text{at } \; z^* = 0 \rightarrow \begin{cases} \frac{\partial \theta}{\partial z^*} = \frac{\kappa_z^2 \epsilon_H}{\epsilon} q^*_{i(x,y)} & \text{at spot i domain,} \\ \frac{\partial \theta}{\partial z^*} = 0 & \text{at remainder ,} \end{cases} \tag{2.79}$$

and along the sink plane,

$$\text{at } \; z^* = 1 \rightarrow \begin{cases} \frac{\partial \theta}{\partial z^*} = \frac{\kappa_z^2 \epsilon_H}{\epsilon} q'^*_{i(x,y)} & \text{at spot i domain,} \\ \frac{\partial \theta}{\partial z^*} = 0 & \text{at remainder.} \end{cases} \tag{2.80}$$

The general form of the solution is obtained using the method of separation of variables,

$$\begin{aligned} \theta = A_0 z^* &+ \sum_{m=1}^{\infty} \cos(\lambda \kappa_x x^*)[A_m \cosh(\lambda \epsilon_H \kappa_z z^*) + B_m \sinh(\lambda \epsilon_H \kappa_z z^*)] \\ &+ \sum_{n=1}^{\infty} \cos(\delta \epsilon \kappa_y y^*)[A_n \cosh(\delta \epsilon_H \kappa_z z^*) + B_n \sinh(\delta \epsilon_H \kappa_z z^*)] \\ &+ \sum_{n=1}^{\infty} \sum_{m=1}^{\infty} \cos(\lambda \kappa_x x^*) \cos(\delta \epsilon \kappa_y y^*)[A_{mn} \cosh(\beta \epsilon_H \kappa_z z^*) + B_{mn} \sinh(\beta \epsilon_H \kappa_z z^*)], \end{aligned} \tag{2.81}$$

where the eigenvalues of the system are,

$$\lambda = \frac{m\pi}{\kappa_x}, \qquad \delta = \frac{n\pi}{\kappa_y \epsilon}, \qquad \beta = \sqrt{\lambda^2 + \delta^2}. \tag{2.82}$$

To apply the discretely specified Neumann boundary conditions along the source and sink plane in the general form of the solution, Eq. (2.81), a two dimensional Fourier expansion technique is used. For a system with one heat source along the top plane (superscript t) and one heat sink along the bottom plane (superscript b), the coefficients of the solution are,

$$\begin{aligned}
&A_0 = \frac{\kappa_z^2 \epsilon_H}{\epsilon} s_{00}^t = \frac{\kappa_z^2 \epsilon_H}{\epsilon} s_{00}^b, \qquad B_m = \frac{2\kappa_z s_{m0}^t}{\epsilon\lambda}, \qquad B_n = \frac{2\kappa_z s_{0n}^t}{\epsilon\delta}, \qquad B_{mn} = \frac{4\kappa_z s_{mn}^t}{\epsilon\beta}, \\
&A_m = \frac{2\kappa_z}{\epsilon\lambda}\left(S_{m0}^b \mathrm{csch}(\lambda\epsilon_H) - s_{m0}^t \coth(\lambda\epsilon_H)\right), \\
&A_n = \frac{2\kappa_z}{\epsilon\delta}\left(S_{0n}^b \mathrm{csch}(\delta\epsilon_H) - s_{0n}^t \coth(\delta\epsilon_H)\right), \\
&A_{mn} = \frac{4\kappa_z}{\epsilon\beta}\left(S_{mn}^b \mathrm{csch}(\beta\epsilon_H) - s_{mn}^t \coth(\beta\epsilon_H)\right),
\end{aligned} \tag{2.83}$$

where the auxiliary coefficients obtained from Fourier expansion are,

$$\begin{aligned}
s_{00}^{t/b} &= \iint_{t/b} q_{(x,y)}^* dx^* dy^*, \\
s_{m0}^{t/b} &= \iint_{t/b} q_{(x,y)}^* \cos(\lambda\kappa_x x^*) dx^* dy^*, \\
s_{0n}^{t/b} &= \iint_{t/b} q_{(x,y)}^* \cos(\delta\epsilon\kappa_y y^*) dy^* dx^*, \\
s_{mn}^{t/b} &= \iint_{t/b} q_{(x,y)}^* \cos(\lambda\kappa_x x^*) \cos(\delta\epsilon\kappa_y y^*) dx^* dy^*.
\end{aligned} \tag{2.84}$$

2.6 Temperature Dependent Thermal Conductivity

Thermal conductivity of some of the semiconductor materials are dependent on the working temperature. This temperature dependent thermal conductivity should be considered

in the solution of the thermal behavior of the system for having a proper thermal analysis. To solve the heat conduction problems with the temperature dependent thermal conductivity, the Kirchhoff transform is used. The general form of the non-linear steady-state heat conduction equation is,

$$\nabla . (k \nabla T) = 0, \tag{2.85}$$

where $k = k(T)$ is temperature dependent. To transform this equation to the Laplace's equation, a new variable is defined as,

$$\theta = T_0 + \frac{1}{k_0} \int_{T_0}^{T} k(\tau) d\tau, \tag{2.86}$$

where θ is the apparent temperature. Therefore, the non-linear heat conduction equation may be transformed to the Laplace's equation in terms of the apparent temperature, θ, as follows,

$$\nabla^2 \theta = 0. \tag{2.87}$$

All boundary conditions should also be transformed in form of the apparent temperature. The problem can be solved using the presented solutions in the previous sections. Finally, the obtained apparent temperature should be transformed back to the non-linear temperature by using the inverse Kirchhoff transform.

2.6.1 Boundary Condition of the First Kind

To consider the procedure for applying the Kirchhoff transform to the boundary condition of the first kind, a linear thermal conductivity in the form of $k(T) = A + BT$ is assumed. The apparent temperature for this case is,

$$\theta = T_0 + \frac{1}{k_0}\int_{T_0}^{T} k(\tau)d\tau = T_0 + \frac{1}{k_0}\int_{T_0}^{T}(A + B\tau)d\tau, \tag{2.88}$$
$$\theta = T_0 + \frac{1}{k_0}\left(AT + \frac{1}{2}BT^2 - AT_0 - \frac{1}{2}BT_0^2\right).$$

As can be seen, the constant temperature in the problem with temperature dependent thermal conductivity turned to a more complicated expression as an apparent temperature. Therefore, application of the Kirchhoff transform to the first kind of boundary condition adds some complexity to the solving process of the thermal spreading resistance problems.

2.6.2 Boundary Condition of the Second Kind

The second kind boundary condition or prescribed heat flux can be stated as,

$$\vec{q} = -\vec{n}\,.\,k\nabla T. \tag{2.89}$$

The temperature, T, should be transformed in terms of the apparent temperature, θ, as follows,

$$k\nabla T = k_0\nabla\theta \tag{2.90}$$

and as a result, the heat flux of the apparent temperature remains the same with the heat flux of the temperature, T,

$$\vec{q} = -\vec{n}\,.\,k\nabla T = -\vec{n}\,.\,k_0\nabla\theta. \tag{2.91}$$

2.6.3 Boundary Condition of the Third Kind

The boundary condition of the third kind can be expressed as,

$$-\vec{n}\,.\,k\nabla T = h(T - T_\infty). \tag{2.92}$$

As discussed, $-\vec{n}\,.\,k\nabla T = -\vec{n}\,.\,k_0\nabla\theta$ and $T = K^{-1}\{\theta\} \neq \theta$. Therefore, the convection boundary condition is not linear on θ,

$$-\vec{n}\,.\,k_0\nabla\theta = h\left(K^{-1}\{\theta\} - T_\infty\right) \neq h(\theta - T_\infty). \tag{2.93}$$

Due to the non-linear behavior, the Kirchhoff transform cannot be applied to the boundary condition of the third kind or Robin boundary condition. Recently, Bagnall et al. [10] proposed a solution to approximate the thermal spreading resistance problems with temperature dependent thermal conductivity and the third kind of boundary condition. For the flux channel and flux tube problems that are discussed in this paper, the temperature, T, and the apparent temperature, θ, are approximately equal at the sink plane. To obtain an appropriate reference temperature, T_0, the problem is assumed as a one dimensional problem with heat flux boundary condition in the source plane and convective cooling along the sink plane. Therefore, the reference temperature is assumed as,

$$\theta \approx T_0 = \overline{T}_{base} = \frac{Q}{A_b}\frac{1}{h_s} + T_\infty. \tag{2.94}$$

The common expression for the temperature dependent thermal conductivity of semiconductors is,

$$k(T) = k_{ref}\left(\frac{T_{ref}}{T}\right)^n. \tag{2.95}$$

For the compound system, the limitation for using the Kirchhoff transform is that the exponent in the dependence of the thermal conductivity, n, for all layers should be equal.

The temperature of the flux channel or the flux tube with temperature dependent thermal conductivity can be found by substituting the temperature dependent thermal conductivity, $k(T)$, into the Kirchhoff transform, Eq. (2.86), and solve to obtain the temperature. For the semiconductors with $n > 1$, the actual temperature is,

$$T = K\{\theta\}^{-1} = T_0 \left[1 + \frac{(\theta - T_0)(1-n)}{T_0}\right]^{\frac{1}{1-n}}. \tag{2.96}$$

2.7 2D Flux Channel with Variable Heat Transfer Coefficient Along the Sink Plane

The heat transfer coefficient along the sink plane in all previous research was assumed constant. However, the geometry of the heat sinks is designed to remove heat from the hot spots of the system. Therefore, the heat transfer coefficient along the sink plane is not constant in most of the electronic devices. Razavi et al. [6] considered the flux channel with variable conductance along the sink plane. A schematic 3D view of the studied system is shown in the Figs. 2.6- 2.7 and the 2D model of the system is shown in the Fig. 2.8.

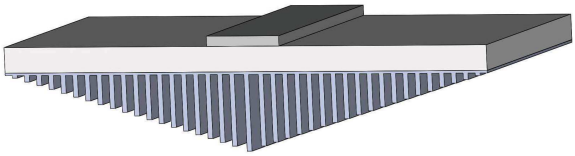

Figure 2.6: 3D view of symmetrical flux channel with variable conductance.

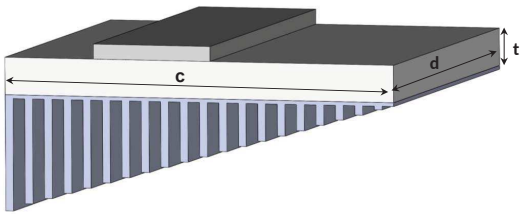

Figure 2.7: 3D view of non-symmetrical flux channel with variable conductance.

As mentioned, the sink boundary condition is convective cooling with variable heat transfer coefficient,

$$\left.\frac{\partial\theta}{\partial z}\right|_{z=t} = -\frac{h(x)}{k}\theta. \tag{2.97}$$

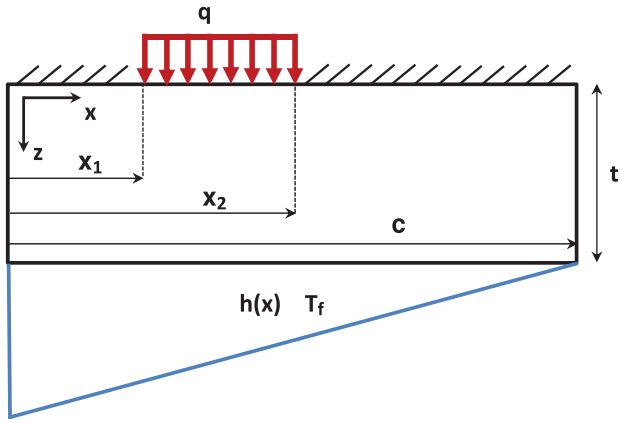

Figure 2.8: 2D flux channel with linear heat transfer coefficient along the sink plane.

The general form of the solution is,

$$\theta(x,z) = \sum_{n=1}^{\infty} \cos\left(\lambda_n x\right)\left(C_n \cosh\left(\lambda_n z\right) + D_n \sinh\left(\lambda_n z\right)\right), \tag{2.98}$$

where the eigenvalues of the system are obtained using the right edge boundary condition.

$$\lambda_n \sin(\lambda_n c) = \frac{h_e}{k}\cos(\lambda_n c). \tag{2.99}$$

By considering $Bi_e = \frac{h_e c}{k}$ and $\delta_n = \lambda_n c$, the eigenvalues are,

$$\delta_n \sin(\delta_n) = Bi_e \cos(\delta_n) \qquad n = 1, 2, 3, \cdots. \tag{2.100}$$

By using the boundary condition along the sink plane, the C_n and D_n become related based on the spreading function,

$$D_n = -\,C_n \left(\frac{\lambda_n \sinh(\lambda_n t) + \frac{h(x)}{k} \cosh(\lambda_n t)}{\lambda_n \cosh(\lambda_n t) + \frac{h(x)}{k} \sinh(\lambda_n t)} \right), \tag{2.101}$$

$$D_n = -\,C_n \phi_n(x),$$

Due to the dependence of heat transfer coefficient on x, the spreading function is a function of x. For the compound system, the spreading function would be more complex. Now, the only unknown coefficient is the general form of the solution is C_n,

$$\theta(x,z) = \sum_{n=1}^{\infty} C_n \cos\left(\delta_n \frac{x}{c}\right) \left(\cosh\left(\delta_n \frac{z}{c}\right) - \phi_n(x) \sinh\left(\delta_n \frac{z}{c}\right) \right), \tag{2.102}$$

To obtain the C_n, the orthogonality property cannot be used as the spreading function is dependent on x. The authors used the method of least squares to apply the boundary condition along the source plane,

$$\begin{aligned} I_N = &\int_0^{x_1} \left[-k \left. \frac{\partial \theta}{\partial z} \right|_{z=0} - f(x) \right]^2 dx \\ &+ \int_{x_1}^{x_2} \left[-k \left. \frac{\partial \theta}{\partial z} \right|_{z=0} - g(x) \right]^2 dx \\ &+ \int_{x_2}^{c} \left[-k \left. \frac{\partial \theta}{\partial z} \right|_{z=0} - p(x) \right]^2 dx, \end{aligned} \tag{2.103}$$

where,

$$f(x) = -k \left.\frac{\partial \theta}{\partial z}\right|_{z=0} = 0 \qquad (0 < x < x_1),$$
$$g(x) = -k \left.\frac{\partial \theta}{\partial z}\right|_{z=0} = q \qquad (x_1 < x < x_2), \tag{2.104}$$
$$p(x) = -k \left.\frac{\partial \theta}{\partial z}\right|_{z=0} = 0 \qquad (x_2 < x < c).$$

Substituting Eq. (2.104) in Eq. (2.103), results,

$$\begin{aligned} I_N = &\int_0^{x_1} \left[-k \sum_{n=1}^{\infty} -C_n \left(\frac{\delta_n}{c}\right) \phi_n(x) \cos\left(\frac{\delta_n x}{c}\right) - 0\right]^2 dx \\ &+ \int_{x_1}^{x_2} \left[-k \sum_{n=1}^{\infty} -C_n \left(\frac{\delta_n}{c}\right) \phi_n(x) \cos\left(\frac{\delta_n x}{c}\right) - q\right]^2 dx \\ &+ \int_{x_2}^{c} \left[-k \sum_{n=1}^{\infty} -C_n \left(\frac{\delta_n}{c}\right) \phi_n(x) \cos\left(\frac{\delta_n x}{c}\right) - 0\right]^2 dx. \end{aligned} \tag{2.105}$$

and the last unknown coefficients, C_n, can be calculated by a mathematical software package in order to minimize the I_N,

$$\frac{\partial I_N}{\partial C_n} = 0 \qquad\qquad n = 1, 2, ...N. \tag{2.106}$$

Finally, the thermal resistance is obtained using the mean source temperature,

$$R_t = \frac{\overline{\theta}_s}{Q} = \frac{c}{q\ (x_2 - x_1)^2\ d} \sum_{n=1}^{\infty} \frac{C_n \left(\sin\left(\frac{\delta_n x_2}{c}\right) - \sin\left(\frac{\delta_n x_1}{c}\right)\right)}{\delta_n}. \tag{2.107}$$

2.8 Comparing Analytical Method with Finite Element Analysis (FEA)

In this section, a case study is presented to compare infinite series analytical method and FEA results and their efficiencies [19]. The case study is a Gallium nitride (GaN) high electron mobility transistors (HEMTs) with geometry and specification that is shown in Fig. 2.9.

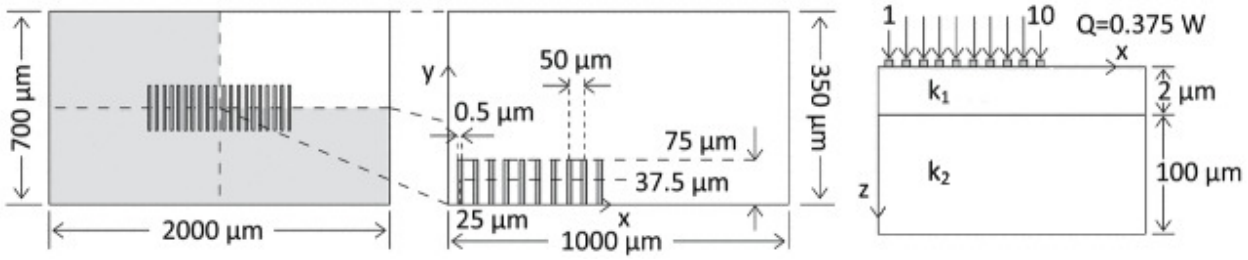

Figure 2.9: Layout of a two layer device with ten heat sources [19].

On the top of the device, there are 10 heat sources of $0.5\,\mu m$ length by $75\,\mu m$ width and their source-to-source spacing is $50\,\mu m$. Top layer of the device is isotropic with thermal conductivity of $k_1 = 150\,W/mK$ and the bottom layer is orthotropic with thermal conductivities of $k_{2,xy} = 490\,W/mK$ and $k_{2,z} = 390\,W/mK$. An interfacial conductance exists between the layers with the magnitude of $h_c = 9.28 \times 10^7\,W/m^2K$ and sink heat transfer coefficient and temperature are $h_s = 3.27 \times 10^5\,W/m^2K$ and $T_f = 20°C$. The average and centroidal temperatures of the heat sources that are obtained by analytical and FEA are shown in Table. 2.1, [19]. The results of two methods differ by $< 0.1\%$.

To compare the computation efficiency of both methods, the computation time required to calculate the mean temperature of the heat sources is considered. The computation time for the analytical model is ~ 22 s for all heat source numbers while the FEA model required from ~ 4 min to ~ 8 h for two to ten heat sources. The reason is that when the heat source dimensions are much smaller than the other characteristic lengths, an extremely fine mesh is

	Average temperature (°C)		Centroidal temperature (°C)	
Source no.	Analytical	FEA	Analytical	FEA
1	132.071	131.988	136.818	136.869
2	131.761	131.678	136.506	136.556
3	131.131	131.048	135.874	135.923
4	130.164	130.080	134.900	134.948
5	128.826	128.741	133.551	133.599
6	127.067	126.982	131.773	131.823
7	124.808	124.723	129.481	129.530
8	121.912	121.828	126.520	126.570
9	118.094	118.010	122.562	122.612
10	112.515	112.431	116.603	116.652

Table 2.1: Average and centroidal temperature.

required near the sources. Although FEA is more flexible, it is less efficient than analytical models especially for the heat conduction problems involving many discrete heat sources.

2.9 Recommendation for Further Studies

Many aspects of thermal spreading resistance problems were studied in the past six decades. Due to the complexity of the problems, each literature studied a special case with some simplifications in the geometry, property and boundary conditions. Although a wide variety of models were presented, there are still some gaps that should be addressed. The authors propose the following problems be studied:

- Systems with more flexible specification of conductance such as discretely specified heat transfer coefficient along the heat sink plane. It is a practical boundary condition in electronic devices such as systems with coolant channels along the heat sink plane or systems with fin heat sinks with varying fin heights and gaps between the fins.

- Systems with a combination of temperature, heat flux, and conductance along the heat source plane.

- Multi-layer systems with discretely specified inward and outward heat fluxes along

the heat source and heat sink plane.

- Extension of problems with variable and discretely specified heat conductance along the heat sink plane in compound systems.
- Examining the effect of orthotropic properties and temperature dependent thermal conductivity in compound systems with variable or discretely specified heat conductance.
- Additionally, studying the effect of different thermal conductivity in all three principal directions will further add value to all previously published papers.

Acknowledgments

The authors acknowledge the financial support of the Natural Sciences and Engineering Research Council of Canada.

2.10 References

[1] Yovanovich, M. M., "Recent Developments in Thermal Contact, Gap and Joint Conductance Theories and Experiment," *in Proc. Keynote Paper Int. Heat Transfer Conf.*, San Francisco, CA, Aug. 17-22, 1986.

[2] Yovanovich, M. M., and Marotta, E. E., "Thermal Spreading and Contact Resistances," in *Heat Transfer Handbook*, A. Bejan, and A. D. Kraus, Eds. New York: Wiley, ch. 4, pp. 261-393, 2003.

[3] Yovanovich, M. M., "Four Decades of Research on Thermal Contact, Gap and Joint Resistance in Microelectronics," *IEEE Transactions on Components and Packaging Technologies*, vol. 28, no. 2, pp. 182-206, 2005.

[4] Kennedy, D. P., "Spreading Resistance in Cylindrical Semiconductor devices," *Journal of Applied Physics*, vol. 31, pp. 1490-1497, 1960.

[5] Mikic, B. B., and Rohsenow, W. M., "Thermal Contact Resistance," *M.I.T. Heat Transfer Lab Report No. 4542-41*, Sep. 1966.

[6] Razavi, M., Muzychka, Y. S., and Kocabiyik, S., "Thermal Spreading Resistance in a Flux Channel with Arbitrary Heat Convection in the Sink Plane," *Proceedings of the ASME 2014 International Mechanical Engineering & Congress & Exposition IMECE 2014*, November 14-20, 2014, Montreal, Canada.

[7] Martin, K. A., Yovanovich, M. M., and Chow, Y. L., "Method of Moments Formulation of Thermal Constriction Resistance of Arbitrary Contacts," *in Proc. AIAA 19th Thermophysics Conf.*, Snowmass, CO, Jun. 25-28, 1984.

[8] Rozon, B. J., Galpin, P. F., Schneider, G. E., and Yovanovich, M. M., "The Effect of Geometry on the Contact Conductance of Contiguous Interfaces," *in Proc. AIAA 19th Thermophysics Conf.*, Snowmass, CO, Jun. 25-28, 1984.

[9] Wang, A. L. and Yan, C. P., "Influence of Heat Source Characteristics on Dimensionless Thermal Spreading Resistance," *IUPAP C20 Conf. on Computational Physics*, 2011.

[10] Bagnall, K., Muzychka, Y.S., and Wang, E., "Application of the Kirchhoff Transform to Thermal Spreading Problems with Convection Boundary Conditions", *IEEE Transactions on Components, Packaging and Manufacturing Technologies*, 2013.

[11] Ellison, G. N., "The Thermal Design of an LSI Single-Chip Package," *IEEE Transactions on Parts, Hybrids, and Packaging*, vol. PHP-12, no. 4, Dec. 1976.

[12] Fisher, N. J. and Yovanovich, M. M., "Thermal Constriction Resistance of Sphere/Layered Flat Contacts: Theory and Experiment," *ASME Journal of Heat Transfer*, vol. 111, pp. 249-256, May, 1989.

[13] Muzychka, Y. S., Yovanovich, M. M., and Culham, J. R., "Influence of Geometry and Edge Cooling on Thermal Spreading Resistance," *AIAA Journal of Thermophysics and Heat Transfer*, vol. 20. no. 2, pp. 247-255, April-June 2006.

[14] Muzychka, Y.S., "Influence Coefficient Method for Calculating Discrete Heat Source Temperature on Finite Convectively Cooled Substrates," *IEEE Transactions on Components and Packaging Technologies*, vol. 29, no. 3, pp. 636-643, Sep. 2006.

[15] Yovanovich, M. M., Tien, C. H., and Schneider, G. E., "General Solution of Constriction Resistance Within a Compound Disk," *Heat Transfer Thermal Control, Heat Pipes*, vol. 70, pp. 47-62, 1979.

[16] Muzychka, Y.S., Bagnall, K., and Wang, E., "Thermal Spreading Resistance and Heat Source Temperature in Compound Orthotropic Systems with Interfacial Resistance", *IEEE Transactions on Components, Packaging and Manufacturing Technologies*, vol. 3, no. 11, pp. 1826-1841, 2013.

[17] Dryden, J., Yovanovich, M. M., and Deakin, A. S., "The Effect of Coatings Upon the Steady-State and Short Time Constriction Resistance for an Arbitrary Axisymmetric Flux," *ASME J. Heat Transf.*, vol. 107, pp. 33-38, Feb. 1985.

[18] Yovanovich, M. M., "Thermal Resistances of Circular Source on Finite Circular Cylinder with Side and End cooling," *ASME J. Electron. Packag.*, vol. 125, no. 2, pp. 169-177, 2003.

[19] Guan, D., Marz, M., and Liang, J., "Analytical Solution of Thermal Spreading Resistance in Power Electronics," *IEEE Transactions on Components, Packaging and Manufacturing Technology*, pp. 278-285, 2012.

[20] Muzychka, Y. S., Culham, J. R., and Yovanovich, M. M., "Thermal Spreading Resistance of Eccentric Heat Sources on Rectangular Flux Channels," *Journal of Electronic Packaging*, vol. 125, pp. 178-185, June 2003.

[21] Kim, Y. H., Kim, S. Y., and Rhee, G. H., "Evaluation of Spreading Thermal Resistance for Heat Generating Multi-Electronic Components," *IEEE*, pp. 258-264, 2006.

[22] Karmalkar, S., Mohan, P. V., Nair, H. P., and Yeluri, R., "Compact Models of Spreading Resistances for Electrical/Thermal Design of Devices and ICs," *IEEE Transactions on Electron Devices*, vol. 54, no. 7, July 2007.

[23] Muzychka, Y. S., "Thermal Spreading Resistance in Compound Orthotropic Circular Disks and Rectangular Channels with Interfacial Resistance," *44th AIAA Thermophysics Conference*, June 24-27, 2013.

[24] Dong, S., Zhou, Q., Wang, M., Jiang, X., and Yang, J., "Analysis of Thermal Spreading Resistance in High Power LED Package and Its Design Optimization," *Int. Conf. on Electronic Packaging Technology and High Density Packaging*, pp. 1056-1060, 2011.

[25] Ellison, G. N., "Maximum Thermal Spreading Resistance for Rectangular Sources and Plates with Nonunity Aspect Ratios," *IEEE Trans. Comp. Packag. Tech.*, vol. 26, no. 2, pp. 439-454, Jun. 2003.

[26] Lam, T. T., and Fischer, W. D., "Thermal Resistance in Rectangular Orthotropic Heat Spreaders," *ASME Advances in Electronic Packaging*, vol. 26-1, American Society of Mechanical Engineers, Fairfield, NJ, pp. 891-898, 1999.

[27] Muzychka, Y. S., Yovanovich, M. M, and Culham, J. R., "Thermal Spreading Resistance in Compound and Orthotropic Systems," *Journal of Thermophysics and Heat Transfer*, vol. 18, no. 1, January-March 2004.

[28] Kokkas, A. G., "Thermal Analysis of Multiple-Layer Structures," *IEEE Transactions on Electron Devices*, vol. ED-21, no. 11, pp. 674-681, Nov. 1974.

[29] Joyce, W. B., "Thermal Resistance of Heat Sinks with Temperature-Dependent Thermal Conductivity," *Solid-state Electronics*, vol. 18, pp. 321-322, Sep. 1974.

[30] Bonani, F., and Ghione, G., "On the Application of the Kirchhoff Transformation to the Steady-State Thermal Analysis of Semiconductor Devices with Temperature-Dependent and Piecewise Inhomogeneous Thermal Conductivity," *Solid-State Electronics*, vol. 38, no. 7, pp. 1409-1412, Sep. 1994.

[31] Hui, P., and Tan, H. S., "On the Effect of Nonlinear Boundary Conditions for Heat Condition in Diamond Heat Spreaders with Temperature-Dependent Thermal Conductivity," *IEEE Trans. Components, Packaging, and Manufacturing Technol. - Part A*, vol. 20, no. 4, pp. 537-540, Dec. 1997.

[32] Lee, S., Song, S., Au., V., and Moran, K. P., "Constriction/Spreading Resistance Model for Electronics Packaging," *in Proc. 4th ASME/JSME Thermal Eng. Joint Conf.*, Maui, HI, pp. 199-206, Mar. 1995.

[33] Ellison, G., "Extensions of a Closed Form Method for Substrate Thermal Analyzers to Include Thermal Resistances From Source-to-Substrate and Source-to-Ambient," *Seventh IEEE Semi-Therm Symposium*, pp. 140-148, 1991.

[34] Muzychka, Y. S., Stevanovic, M., and Yovanovich, M. M., "Thermal Spreading Resistances in Compound Annular Sectors," *Journal of Thermophysics and Heat Transfer*, vol. 15, no. 3, pp. 354-359, 2001.

[35] Negus, K. J., and Yovanovich, M. M., "Constriction Resistance of Circular Flux Tubes with Mixed Boundary Conditions by Linear Superposition of Neumann Solutions," *in Proc. 22nd ASME/AIChE Nat. Heat Transfer Conf.*, Niagara Falls, NY, Aug. 6-8, 1984.

[36] Yovanovich, M. M., Culham, J. R. and Teertstra, P. M., "Modeling Thermal Resistances of Diamond Spreaders on Copper Heat Sinks," *Int. Electronics Packaging Conf.*, Austin, TX, September 29 - October 2, 1996.

[37] Lemczyk, T. F., and Yovanovich, M. M., "Thermal Constriction Resistance with Convective Boundary Conditions, Part 1: Half-Space Contacts," *Int. J. Heat Mass Transf.*, vol. 31, no. 9, pp. 1861-1872, 1988.

[38] Lemczyk, T. F., and Yovanovich, M. M., "Thermal Constriction Resistance with Convective Boundary Conditions, Part 2: Layered Half-Space Contacts," *Int. J. Heat Mass Transf.*, vol. 31, no. 9, pp. 1873-1883, 1988.

[39] Yovanovich, M. M., Culham, J. R., and Teertstra, P. M., "Analytical Modeling of Spreading Resistance in Flux Tubes, Half Spaces, and Compound Disks," *IEEE Transactions on Components, Packaging, and Manufacturing Technology-Part A*, vol. 21, no. 1, pp. 168-176, 1998.

[40] Mikic, B, B., "Thermal Contact Resistance," *SC.D. Thesis*, Department of Mechanical Engineering, MIT, Cambridge, Massachusetts, 1966.

[41] Cooper, M. G., Mikic, B. B., and Yovanovich, M. M., "Thermal Contact Conductance," *Int. J. Heat and Mass Transfer*, vol. 12, pp. 279-300, 1969.

[42] Yovanovich, M. M., "Overall Constriction Resistance Between Contacting Rough, Wavy Surfaces," *Int. J. Heat Mass Transf.*, vol. 12, pp. 1517-1520, 1969.

[43] Yovanovich, M. M., "A Correlation of Minimum Thermal Resistance of Soldered Joints," *J. Spacecrafts Rockets*, vol. 7, no. 8, pp. 1013-1014, 1970.

[44] Yovanovich, M. M., "Thermal Constriction Resistance of Contacts on a Half-Space: Integral Formulation," *AIAA Progress in Astronautics and Aeronautics, Radiative Transfer and Thermal Control*, vol. 49, edited by A. M. Smith, New York, pp. 397-418, 1976.

[45] Yovanovich, M. M., and Burde, S. S., "Centroidal and Area Average Resistances of Nonsymmetric, Singly Connected Contacts," *AIAA Journal*, vol. 15, no. 10, pp. 1523-1525, 1977.

[46] Yovanovich, M. M., Burde, S. S., and Thompson, J. C., "Thermal Constriction Resistance of Arbitrary Planar Contacts With Constant Flux," *AIAA Progress in Astronautics and Aeronautics, Thermophysics of Spacecraft and Outer Planet Entry Probes*, vol. 56, edited by A. M. Smith, New York, pp. 127-139, 1977.

[47] Strong, A. B., Schneider, G. E., and Yovanovich, M. M., "Thermal Constriction Resistance of a Disk with Arbitrary Heat Flux," *in Proc. AIAA/ASME Conf.*, Boston, MA, 1974.

[48] Schneider, G. E., Strong, A. B., and Yovanovich, M. M., "Transient Heat Flow From a Thin Circular Disk," *in Proc. AIAA 10th Thermophysics Conf.*, Denver, CO, May 27-29, 1975.

[49] Schneider, G. E., Strong, A. B., and Yovanovich, M. M., "Transient Heat Flow From a Thin Circular Disc," *Relative Transfer and Thermal Control*, vol. 49, pp. 419-426, 1976.

[50] Yovanovich, M. M., "General Thermal Constriction Parameter for Annular Contacts on Circular Flux Tubes," *AIAA J.*, vol. 14, no. 6, pp. 822-824, 1976.

[51] Yovanovich, M. M., "General Expression for Constriction Resistances Due to Arbitrary Flux Distribution at Non-symmetric, Coaxial Contacts", *AIAA 13th Aerospace Sciences Meeting*, Pasadena, California, 1975.

[52] Schneider, G. E., Strong,A. B., and Yovanovich, M. M., "Transient Thermal Response to Two Bodies Communicating Through a Small Circular Contact Area," *Int. J. Heat Mass Transfer*, vol. 20, pp. 301-308, 1977.

[53] Yovanovich, M. M., Martin, K. A., and Schneider, G. E., "Constriction Resistance of Doubly-Connected Contact Areas Under Uniform Flux," *AIAA 14th Thermophysics Conf.*, pp. 1-5, June 4-6, 1979.

[54] Yovanovich, M. M., "Thermal Constriction Resistance Between Contacting Metallic Paraboloids: Application to Instrument Bearings," *Progress in Astronautics and Aeronautics: Fundamentals of Spacecraft Thermal Design*, vol. 24, pp. 337-358, 1971.

[55] Yovanovich, M. M., and Schneider, G. E., "Thermal Constriction Resistance Due to a Circular Annular Contact," *AIAA Progress in Astronautics and Aeronautics, Thermophysics of Spacecraft and Outer Planet Entry Probes*, vol. 56, edited by A.M. Smith, New York, pp. 141-154, 1976.

[56] Burde, S. S., and Yovanovich, M. M., "Thermal Resistance at Smooth Sphere/ Rough Flat Contacts: Theoretical Analysis," *Thermophysics and Thermocontrol*, vol. 65, pp. 83-102, 1978.

[57] Yovanovich, M. M., Negus, K. J., and Thompson, J. C., "Transient Temperature Rise of Arbitrary Contacts with Uniform Flux by Surface Element Methods," *in Proc. AIAA 22nd Aerospace Sciences Meeting*, Reno, NV, Jan. 9-12, 1984.

[58] Turyk, P. J., and Yovanovich, M. M., "Transient Constriction Resistance for Elemental Flux Channels Heated by Uniform Flux Sources," *in Proc. ASME/AIChE National Heat Transfer Conf.*, Niagara Falls, NY, Aug. 6-8, 1984.

[59] Yovanovich, M. M., Thompson, J. C., and Negus, K. J., "Thermal Resistance of Arbitrarily Shaped Contacts," *in Proc. 3rd Int. Conf. Numerical Methods Thermal Problems*, R. W. Lewis, J. A. Johnson, and R. Smith, Eds., Seattle, WA, pp. 1072-1082, Aug. 2-5, 1983.

[60] Negus, K. J., and Yovanovich, M. M., "Application of the Method of Optimized Images to Steady Three-Dimensional Conduction Problems," *in Proc. ASME WAM Meeting*, New Orleans, LA, Dec. 9-13, 1984.

[61] Negus, K. J., Yovanovich, M. M., and DeVaal, J. W., "Development of Thermal Constriction Resistance for Anisotropic Rough Surfaces by the Method of Infinite Images," *in Proc. 23rd ASME-AIChE Nat. Heat Transfer Conf.*, Denver, CO, Aug. 4-7, 1985.

[62] Saabas, H. J., and Yovanovich, M. M., "Application of SEM and Superposition Techniques to Circular Microcontacts Distributed Over Elliptical Contours on Circular Flux Tubes and Half-Spaces," *in Proc. AIAA 20th Thermophysics Conf.*, Williamsburg, VA, Jun. 19-21, 1985.

[63] Negus, K. J., Yovanovich, M. M., and Beck, J. V., "On the Non-Dimensionalization of Constriction Resistance for Semi-Infinite Heat Flux Tubes," *J. Heat Transf.*, vol. 111, pp. 804-807, Aug. 1989.

[64] Yovanovich, M. M., McGee, G. R., and Schankula, M. H., "Ellipsoidal Thermal Constriction Model for Crowned-Cylinder/Flat Elastic Contacts," *in Proc. 22nd ASME/AIChE Nat. Heat Transfer Conf.*, Niagara Falls, NY, Aug. 6-8, 1984.

[65] Negus, K. J., Yovanovich, M. M. and Thompson, J. C., "Thermal Constriction Resistance of Circular Contacts on Coated Surfaces: Effect of Contact Boundary Conditions," *AIAA 20th Thermophysics Conf.*, AIAA Paper No. 85-1014, Williamsburg, VA, pp. 1-8, June 19-21, 1985.

[66] Muzychka, Y. S., Sridhar, M. S., Yovanovich M. M., and Antonetti, V. W., "Thermal Constriction Resistance in Multilayered Contacts: Applications in Thermal Contact Resistance," *AIAA National Heat Transfer Conf., Thermophysics and Thermophysical Properties Session*, Houston, Texas, Aug. 3-6, 1996.

[67] Muzychka, Y. S., Sridhar, M. R., Yovanovich, M. M. and Antonetti, V. W., "Thermal Constriction Resistance in Multilayered Contacts: Applications in Thermal Contact Resistance," *AIAA Journal of Thermophysics and Heat Transfer*, vol. 13, no. 4, pp. 489-494, 1999.

[68] Mantelli, M. B. H., and Yovanovich, M. M., "Compact Analytical Model for Overall Thermal Resistance of Bolted Joints," *Int. Journal of Heat and Mass Transfer*, vol. 41, no. 10, pp. 1255-1266, 1998.

[69] Yovanovich, M. M., Muzychka, Y. S., and Culham, J. R., "Spreading Resistance in Isoflux Rectangles and Strips on Compound Flux Channels," *J. Thermophys. Heat Transf.*, vol. 13, no. 4, pp. 495-500, 1999.

[70] Yovanovich, M. M., Muzychka, Y. S., and Culham, J. R., "Spreading Resistance of Isoflux Rectangles and Strips on Compound Flux Channels," *6th AIAA Aerospace Sciences Meeting and Exhibit*, Reno, NV, January 12-15, 1998.

[71] Lee, S., Yovanovich, M. M., Song, S., and Moran, K. P., "Analysis of Thermal Constriction Resistance in Bolted Joints," *Int. Journal of Microcircuits and Electronic Packaging*, vol. 16, no. 2, pp. 125, 1993.

[72] Song, S., Lee, S., and Au, V., "Closed-Form Equation for Thermal Constriction/Spreading Resistances with Variable Resistance Boundary Condition," *in Proc. IEPS Conf.*, Atlanta, GA, pp. 111-121, Sep. 1994.

[73] Das, A. K., and Sadhal, S. S., "Thermal Constriction Resistance Between Two Solids for Random Distribution of Contacts," *Heat Mass Transfer*, vol. 35, pp. 101-111, 1999.

[74] Ellison, G., "Thermal Analysis of Microelectric Packages and Printed Circuit Boards Using an Analytic Solution to the Heat Conduction Equation," *Advances in Engineering Software*, pp. 99-111, 1994.

[75] Ellison, G., "Thermal Analysis of Circuit Boards and Microelectronic Components Using an Analytical Solution to the Heat Conduction Equation," *Twelfth IEEE Semi-Therm Symposium*, pp. 144-150, 1996.

[76] Yovanovich, M. M., and Teertstra, P., "Thermal Constriction Resistance of Isothermal Circular Disks with Insulated Back Face and Extensions," *Fundamental problems in Conduction Heat Transfer, ASME 27th National Heat Transfer Conf. and Exhibit*, San Diego, CA, HTD-vol. 207, pp. 23-30, Aug. 9-12, 1992.

[77] Yovanovich, M. M., "Constriction Resistance of Planar Isoflux Heat Sources within Semi-Infinite Conductors: Image Method," *in Proc. 4th ASME/JSME Thermal Engineering Joint Conf.*, Maui, HI, Mar. 19-24, 1995.

[78] Yovanovich, M. M., "Transient Spreading Resistance of Arbitrary Isoflux Contact Areas: Development of a Universal Time Function," *in Proc. AIAA 32nd Thermophysics Conf.*, Atlanta, GA, Jun. 23-25, 1997.

[79] Muzychka, Y. S., Yovanovich, M. M., and Culham, J. R., "Thermal Spreading Resistance in Rectangular Flux Channels, Part I: Geometric Equivalences," *AIAA Paper 2003-4187*, June 2003.

[80] Muzychka, Y. S., Culham, J. R., and Yovanovich, M. M., "Thermal Spreading Resistance in Rectangular Flux Channels: Part II Edge Cooling," *AIAA Paper 2003-4188*, June 2003.

[81] Sadeghi, E., Bahrami, M., and Djilali, N., "Analytic Solution of Thermal Spreading Resistance: Generalization to Arbitrary-Shape Heat Sources on a Half-Space," *ASME 2008 Summer Heat Transfer Conf.*, Jacksonville, FL., USA, August 10-14, 2008.

[82] Muzychka, Y. S. and Yovanovich, M. M., "Thermal Resistance Models for Non-Circular Moving Heat Sources on a Half Space," *Journal of Heat Transfer*, vol. 123, pp. 624-632, August 2001.

[83] Bhullar, S. K., and Wegner, J. L., "Thermal Spreading Resistance of Isoflux Hyperellipse on a Half-space," *Proc. of the Int. MultiConf. of Engineers and Computer Scientists*, vol II, IMECS, Hong Kong, March 18-20, 2009.

[84] Rahmani, Y., and Shokouhmand, H., "A Numerical Study of Thermal Spreading/-Constriction Resistance of Silicon," *13th IEEE ITHERM Conf.*, pp. 482-486, 2012.

[85] Sadeghi, E., Bahrami, M., and Djilali, N., "Thermal Spreading Resistance of Arbitrary-Shape Heat Sources on a Half-Space: A Unified Approach," *IEEE Transactions on Components and Packaging Technologies*, vol. 33, no. 2, pp. 267-277, June 2010.

[86] Ying, T. M., and Toh, K. C., "A Heat Spreading Resistance Model for Anisotropic Thermal Conductivity Materials in Electronic Packaging," *Proceedings of the Sev-*

enth Intersociety Conf. on Thermal and Thermomechanical Phenomena in Electronic Systems, edited by G. B. Kromann, J. R. Culham, and K. Ramakrishna, Inst. of Electrical and Electronics Engineers, Piscataway, NJ, pp. 314-321, 2000.

[87] Muzychka, Y. S., Yovanovich, M. M., and Culham, J. R., "Applications of Thermal Spreading Resistance in Compound and Orthotropic Systems," *in Proc. 39th Aerospace Sciences Meeting Exhibit*, Reno, NV, Jan. 8-11, 2001.

[88] Culham, J. R., Teertstra, P., and Yovanovich, M. M., "The Role of Spreading Resistance on Effective Conductivity in Laminated Substrates," *Future Circuits*, vol. 6., pp. 73-78, 2000.

[89] Vermeersch, B. and De Mey, G., "Dependency of thermal spreading resistance on convective heat transfer coefficient," *Microelectronics Reliability*, vol. 48, pp. 734-738, 2008.

[90] Culham, J. R., Khan, W., Yovanovich, M. M., and Muzychka, Y. S., "The Influence of Material Properties and Spreading Resistance in the Thermal Design of Plate Fin Heat Sinks," *ASME Journal of Electronic Packaging*, vol. 129, pp. 76-81, March, 2007.

[91] Lasance, C. J. M., "How to Estimate Heat Spreading Effects in Practice," *Journal of Electronic Packaging*, vol. 132, September 2010.

[92] Lasance, C. J. M., "Two-layer Heat spreading Approximations Revisited," *28th IEEE Semi-Therm symposium*, pp. 269-274, 2012.

[93] Gholami, and Bahrami, M., "Thermal Spreading Resistance Inside Anisotropic Plates with Arbitrarily Located Hotspots", *Journal of Thermophysics and Heat Transfer*, vol. 28, no. 4, pp. 679-686, 2014.

[94] Bagnall, K., Muzychka, Y.S., and Wang, E., "Analytical Solution for Temperature Rise in Complex Multilayer Structures with Discrete Heat Sources", *IEEE Transactions on Components, Packaging and Manufacturing Technologies*, vol. 4, no. 5, pp. 817-830, 2014.

Chapter 3

Thermal Resistance in a Rectangular Flux Channel with Non-Uniform Heat Convection in the Sink Plane

M. Razavi
Y.S. Muzychka

Department of Mechanical Engineering, Memorial University of Newfoundland, St. John's, NL, Canada, A1B 3X5

S. Kocabiyik

Department of Mathematics and Statistics, Memorial University of Newfoundland, St. John's, NL, Canada, A1C 5S7

Abstract

In this paper, thermal resistance of a 2D flux channel with non-uniform convection coefficient in the heat sink plane is studied using the method of separation of variables and the least squares technique. For this purpose, a two dimensional flux channel with discretely specified heat flux is assumed. The heat transfer coefficient at the sink boundary is defined symmetrically using a hyperellipse function which can model a wide variety of different distributions of heat transfer coefficient from uniform cooling to the most intense cooling in the central region. The boundary condition along the edges is defined with convective cooling. As a special case, the heat transfer coefficient along the edges can be made negligible to simulate a flux channel with adiabatic edges. To obtain the temperature profile and

[1]Published in the Journal of Heat Transfer

the thermal resistance, the Laplace equation is solved by the method of separation of variables considering the applied boundary conditions. The temperature along the flux channel is presented in the form of a series solution. Due to the complexity of the sink plane boundary condition, there is a need to calculate the Fourier coefficients using the least squares method. Finally, the dimensionless thermal resistance for a number of different systems is presented. Results are validated using data obtained from the finite element method. It is shown that the thick flux channels with variable heat transfer coefficient can be simplified to a flux channel with the same uniform heat transfer coefficient.

Keywords: Electronics Cooling, Heat Conduction, Thermal Resistance, Variable Heat Transfer Coefficient, Least Squares Method, Spreading Resistance

3.1 Introduction

Thermal resistance calculations are one of the most important challenges for designing microelectronic devices. In these devices, heat enters through a portion of the semi-conductor area and flows by conduction. Semi-conductors can often be modelled as flux channels. In a flux channel with adiabatic edges and uniform cooling over the sink region, the total thermal resistance is composed of one dimensional resistance and thermal spreading resistance. However, when the cooling over the sink region is not uniform and/or the edges are not adiabatic, the total thermal resistance cannot be simply divided into one dimensional and spreading resistances. Therefore, the total thermal resistance should be calculated. Due to the different geometries and boundary conditions of each device, this aspect becomes more complicated and as a result, some thermal engineers prefer to use more time consuming software packages to model devices.

Significant research has been done on different aspects of thermal spreading resistance during the previous five decades. Lee et al. [1] and Song et al. [2] developed an analytical

solution for constriction/spreading resistance for electronic components with different types of heat sinks. Das and Sadhal [3] modeled the thermal constriction resistance between two solids for random distribution of contacts by using a square region containing randomly placed contacts. Lam and Fischer [4] presented a solution for the thermal resistance of rectangular orthotropic heat spreaders. They demonstrated the result for several values of the vertical-to-horizontal thermal conductivity ratio, the Biot number, and the full range of the nondimensional width of the applied heat flux.

Ellison [5-7] analytically modeled the thermal behavior of printed circuit boards and microelectronic packages as a rectangular, multi-layer structure with discrete heat sources. Muzychka et al. [8-17] solved thermal spreading resistance problems for different systems with different geometries, boundary conditions and properties. The most important models for thermal spreading resistance are summarized by Yovanovich and Marotta [18]. Also, Yovanovich [19] reviewed forty years of research on thermal spreading resistance.

Although, different aspects of thermal spreading resistance were considered by different researchers, no research has been done on non-uniform convective heat transfer coefficients in the sink plane and its influence on the total thermal resistance. The non-uniform heat transfer coefficient can be caused by the heat sink's configuration to make it more practical in the thermal management systems. In Fig. 3.1, a symmetrical heat sink which causes variable heat transfer coefficient (conductance) is shown.

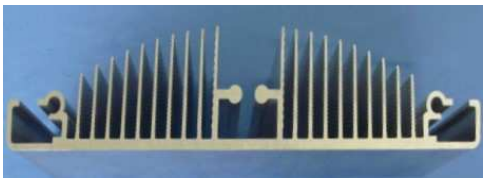

Figure 3.1: A sample of heat sink with variable heat transfer coefficient.

The non-uniform heat sink is widely used in the industry. It helps to reduce the material, distribute convection cooling exactly at the place that is needed and effective passive cool-

ing systems. For example, ASUS released NVIDIA GeForce GT 520 silent low profile graphics card, Fig. 3.2a, and ASUS R.O.G. Rampage Formula that is part of the Republic of Gamers (ROG) line of motherboards, Fig. 3.2b. Both systems are equipped with an efficiently designed heat sink.

(a) ASUS NVIDIA GeForce GT 520 silent low profile graphics card [20].

(b) ASUS R.O.G. Rampage Formula motherboard [21].

Figure 3.2: Example of systems with non-uniform heat sink.

The main goal of this research is modeling thermal resistance of 2-D heat flux channels with a finite and uniform heat source on the source plane and non-uniform convection coefficient in the sink plane. The heat sink plane conductance models both the combined effect of fins and prime surface through an effective conductance. The proposed approach is useful for thermal engineers who want to define the heat sink plane convection as a distributed function by considering a specific configuration of cooling channels or fins on the sink plane.

3.2 Problem Statement

Long semi-conductor devices can be assumed as a 2-D flux channel. In this paper, a flux channel is studied considering a discrete strip heat source in the source plane and a non-uniform convection coefficient in the sink plane, Fig. 3.3. Due to the non-uniform cooling

over the sink plane, the thermal resistance of the system is multi-dimensional even when the heat source covers the source plane of the flux channel with adiabatic edges. Therefore, the total thermal resistance of the system should be considered. For this purpose, the total thermal resistance, R_t, is calculated using the mean source temperature, $\overline{T}_s$, film temperature, T_f, and total heat transfer rate from the source:

$$R_t = \frac{\overline{T}_s - T_f}{Q}. \tag{3.1}$$

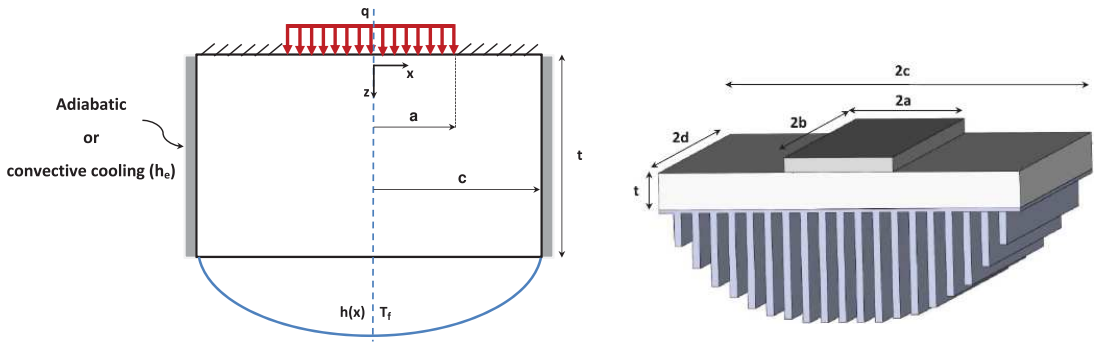

Figure 3.3: 2D flux channel with a central heat source and a variable heat transfer coefficient.

The temperature distribution in the flux channel can be obtained by solving the Laplace equation:

$$\frac{\partial^2 T}{\partial x^2} + \frac{\partial^2 T}{\partial z^2} = 0 \tag{3.2}$$

and, by defining $\theta = T - T_f$:

$$\frac{\partial^2 \theta}{\partial x^2} + \frac{\partial^2 \theta}{\partial z^2} = 0. \tag{3.3}$$

Boundary conditions of the system are as follows. Over the source plane of the flux channel:

$$\left.\frac{\partial \theta}{\partial z}\right|_{z=0} = -\frac{q}{k}, \qquad 0 < x < a, \tag{3.4}$$

$$\left.\frac{\partial\theta}{\partial z}\right|_{z=0} = 0, \qquad a < x < c, \tag{3.5}$$

and along the center line:

$$\left.\frac{\partial\theta}{\partial x}\right|_{x=0} = 0. \tag{3.6}$$

The boundary condition along the edges is convective cooling. The convective cooling boundary condition turns to adiabatic when $h_e \to 0$ where h_e is the heat transfer coefficient along the edge. Therefore, the edge boundary condition is defined as follows:

$$\left.\frac{\partial\theta}{\partial x}\right|_{x=c} = -\frac{h_e}{k}\theta. \tag{3.7}$$

Over the heat sink plane, a variable heat transfer coefficient is applied. For modeling the heat transfer coefficient, the following function is proposed which can model a wide variety of heat transfer coefficient distributions:

$$h(x) = h_o\left[1 - \left(\frac{x}{c}\right)^m\right]. \tag{3.8}$$

It is clear that by changing the power of the function, m, the distribution of the heat transfer coefficient changes over the sink plane. The dependency of the non-uniform heat transfer coefficient using the power of the function, m, for half of the slab is shown in Fig. 3.4. However, the total conductance is changed for different m values. For instance, a system with $m = 1$ has almost half of the heat sink ability in comparison with a system with $m \to \infty$. To specify a model with different distributions of the heat transfer coefficient of a system with the same constant overall conductance, the heat transfer coefficient is integrated over half of the slab and h_o is redefined based on $\overline{h}$,

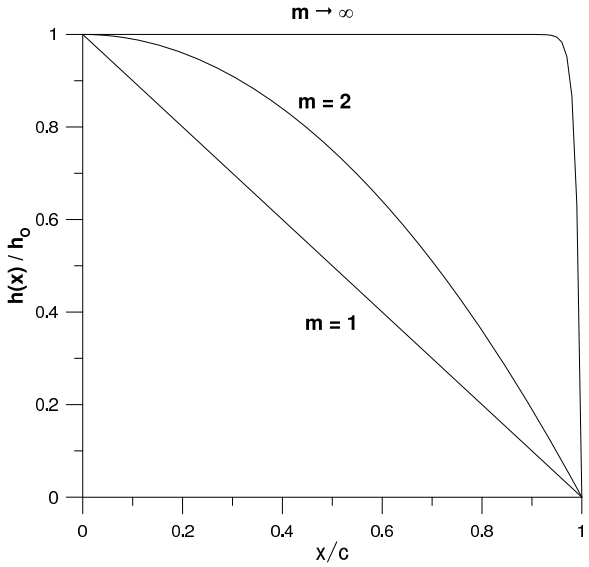

Figure 3.4: Variable heat transfer coefficient for half of the slab by considering the conductance as the function of: $\frac{h(x)}{h_o} = 1 - (\frac{x}{c})^m$.

$$\overline{h} = \frac{1}{c}\int_0^c h(x)dx = \frac{mh_o}{m+1} \qquad \Rightarrow \qquad h_o = \frac{\overline{h}\,(m+1)}{m}, \tag{3.9}$$

$$h(x) = \frac{\overline{h}\,(m+1)}{m}\left[1 - \left(\frac{x}{c}\right)^m\right]. \tag{3.10}$$

The dependency of the non-uniform heat transfer coefficient using the exponent of the function, m, for Eq. (3.10) is shown in Fig. 3.5. This approach can be used to compare different distributions of heat transfer coefficient for a system with constant overall mean heat transfer coefficient or conductance.

By considering the functions for variable heat transfer coefficient, the boundary condition along the sink plane is:

$$\left.\frac{\partial\theta}{\partial z}\right|_{z=t} = -\frac{h(x)}{k}\theta. \tag{3.11}$$

By applying the mentioned boundary conditions, Laplace's equation, Eq. (3.3), can be

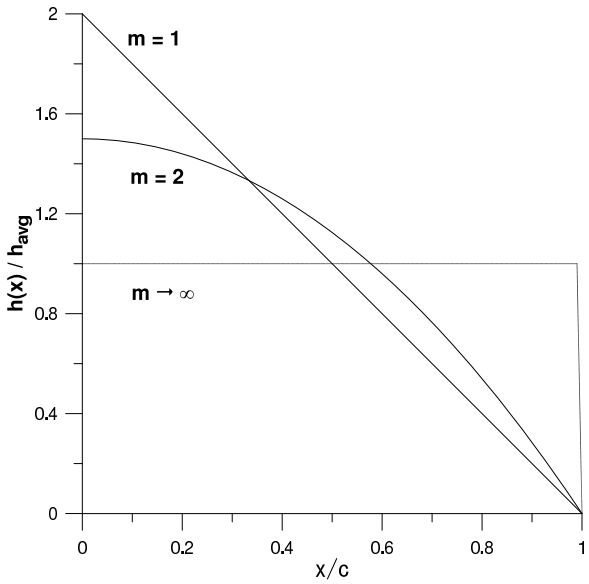

Figure 3.5: Variable heat transfer coefficient for half of the slab by considering the conductance as the function of: $\frac{h(x)}{\bar{h}} = \frac{(m+1)}{m}[1 - \left(\frac{x}{c}\right)^m]$.

solved using the separation of variables technique. The solution which satisfies the symmetry condition can be stated as:

$$\theta(x,z) = \sum_{n=1}^{\infty} \cos(\lambda_n x)\left(C_n \cosh(\lambda_n z) + D_n \sinh(\lambda_n z)\right). \tag{3.12}$$

The eigenvalues of the system, λ_n, are obtained using Eq. (3.7) as follows:

$$\lambda_n \sin(\lambda_n c) = \frac{h_e}{k}\cos(\lambda_n c) \qquad n = 1, 2, 3, \cdots . \tag{3.13}$$

For simplicity, $\delta_n = \lambda_n c$ and $Bi_e = \frac{h_e c}{k}$ are used. The characteristic length that was employed to determine the Biot number is half length of the flux channel, c. Therefore, the eigenvalues are:

$$\delta_n \sin(\delta_n) = Bi_e \cos(\delta_n) \qquad n = 1, 2, 3, \cdots . \tag{3.14}$$

This equation can be solved numerically to obtain the eigenvalues of the system.

Applying the sink boundary condition to the solution, Eq. (3.12), gives:

$$D_n = - C_n \left(\frac{\lambda_n \sinh(\lambda_n t) + \frac{h(x)}{k} \cosh(\lambda_n t)}{\lambda_n \cosh(\lambda_n t) + \frac{h(x)}{k} \sinh(\lambda_n t)} \right), \tag{3.15}$$

$$D_n = -C_n \phi_n(x), \tag{3.16}$$

where $\phi_n(x)$ is the spreading function. This function can be written as follows:

$$\phi_n(x) = \frac{\delta_n \tanh(\delta_n \tau) + Bi(x)}{\delta_n + Bi(x) \tanh(\delta_n \tau)}, \tag{3.17}$$

where $Bi(x) = \frac{h(x)c}{k}$ and $\tau = \frac{t}{c}$. Therefore,

$$\theta(x,z) = \sum_{n=1}^{\infty} C_n \cos\left(\delta_n \frac{x}{c}\right) \left[\cosh\left(\delta_n \frac{z}{c}\right) - \phi_n(x) \sinh\left(\delta_n \frac{z}{c}\right) \right]. \tag{3.18}$$

Now the application of the final boundary condition which is the source plane boundary condition is considered. Due to the dependency of spreading function on x, $\phi_n(x)$, the orthogonality property is not easily satisfied. For the flux channel with constant heat transfer coefficient, the last unknown coefficient can be obtained by using an orthogonal function expansion [10]. However, for the flux channel with variable heat transfer coefficient, the method of least squares is used to obtain the unknown coefficients, C_n [22]. For this purpose, the following integral is defined in different regions of the heat source plane,

$$I_N = \int_0^a \left[-k \left. \frac{\partial \theta}{\partial z} \right|_{z=0} - f(x) \right]^2 dx + \int_a^c \left[-k \left. \frac{\partial \theta}{\partial z} \right|_{z=0} - g(x) \right]^2 dx, \tag{3.19}$$

where $f(x)$ and $g(x)$ are the exact value of the source plane flux distributions,

$$\left.\frac{\partial\theta}{\partial z}\right|_{z=0} = \sum_{n=1}^{\infty} -C_n \left(\frac{\delta_n}{c}\right) \phi_n(x) \cos\left(\frac{\delta_n x}{c}\right) \tag{3.20}$$

$$f(x) = -k \left.\frac{\partial\theta}{\partial z}\right|_{z=0} = q \qquad (0 < x < a) \tag{3.21}$$

$$g(x) = -k \left.\frac{\partial\theta}{\partial z}\right|_{z=0} = 0 \qquad (a < x < c).$$

Therefore,

$$I_N = \int_0^a \left[-k \sum_{n=1}^{\infty} -C_n \left(\frac{\delta_n}{c}\right) \phi_n(x) \cos\left(\frac{\delta_n x}{c}\right) - q\right]^2 dx + \int_a^c \left[-k \sum_{n=1}^{\infty} -C_n \left(\frac{\delta_n}{c}\right) \phi_n(x) \cos\left(\frac{\delta_n x}{c}\right) - 0\right]^2 dx. \tag{3.22}$$

The coefficients C_n should be calculated in order to minimize the above function,

$$\frac{\partial I_N}{\partial C_n} = 0 \qquad n = 1, 2, \cdots N. \tag{3.23}$$

This equation can be solved numerically by using the symbolic computation program Maple [23] in order to obtain the constants, C_n. As a result, the temperature distribution over the channel is known by substituting the calculated constants, C_n, in the Eq. (3.18).

For calculating the total thermal resistance, the mean temperature over the source region is calculated, $\overline{\theta}_s = \overline{T}_s - T_f$, and divided by the total heat flow rate over the source area, $Q = 4ab \times q$. Then,

$$R_t = \frac{\overline{\theta}_s}{Q}, \tag{3.24}$$

$$\overline{\theta}_s = \frac{1}{2a}\int_{-a}^{a}\theta(x,0)dx = \frac{1}{\epsilon}\sum_{n=1}^{\infty}\frac{C_n \sin(\delta_n \epsilon)}{\delta_n}, \tag{3.25}$$

$$R_t = \frac{1}{Q\epsilon}\sum_{n=1}^{\infty}\frac{C_n \sin(\delta_n \epsilon)}{\delta_n}. \tag{3.26}$$

Finally, the total thermal resistance is non-dimensionalized as follows:

$$R_t^* = kaR_t, \tag{3.27}$$

using the half source width. In the next section, the dimensionless thermal resistance for flux channels with different geometries and properties are calculated.

3.3 Results and Discussion

In this part, dimensionless thermal resistance of a flux channel versus dimensionless source aspect ratio are calculated analytically and compared to FEM computations for different variable heat transfer coefficients over the sink plane including linear, $m = 1$; quadratic, $m = 2$; and uniform heat transfer coefficient, $m \to \infty$. To consider the effect of variable heat transfer coefficient along the sink plane, the edges of the channel are assumed adiabatic, $h_e \to 0$. Different Biot numbers for the sink conductance, $Bi = 0.1, 1, 10, 100$, and different dimensionless thicknesses, $\tau = 0.1, 0.5$, are considered.

The FEM results are obtained using a commercial finite element software package [24]. The convergence of the FEM was checked by increasing the number of elements as shown in Table 3.1. The system with a triangular mesh consisting of 2606 elements is converged.

Number of triangular mesh	Mean source temperature	R_t	R^*_t
15	0.000375331	9.3833	0.01876653
44	0.000379293	9.4823	0.01896467
87	0.000381965	9.5491	0.01909825
223	0.000382807	9.5702	0.01914033
608	0.000383168	9.5792	0.01915838
2606	0.000383338	9.5834	**0.01916689**
3120	0.000383338	9.5834	**0.01916689**

Table 3.1: The convergence of the FEM by refining the mesh.

Both FEM and analytical results are presented on the same plot. The variable heat transfer coefficient is calculated for both of the proposed approaches by considering $m = 1, 2$ and ∞. The analytical solution based on the least squares technique is used for modelling the variable heat transfer coefficient with $m = 1$ and 2. The analytical results for the case of uniform convective cooling, $m \to \infty$, are based on another paper of one of the authors [10].

As mentioned before, there are two approaches to specify the variable heat transfer coefficient. The first approach is using the maximum conductance, $h(x) = h_0[1 - (x/c)^m]$, which results in a variable conductance with the same peak but not the same average for different values of m, Fig. 3.4. The second approach is using the mean conductance, $h(x) = \frac{\overline{h}(m+1)}{m}[1 - \left(\frac{x}{c}\right)^m]$, which results in the same effective cooling but distributed non-uniformly over the heat sink plane, Fig. 3.5.

At first, the dimensionless thermal resistance is calculated based on the first approach. It is worth mentioning that in this approach, the total heat transfer coefficient in the sink plane is changed by changing m and as shown in Fig. 3.4, the area below of the curves is expanding by increasing m. Therefore, in this approach the total convective cooling is not the same for different values of m. Figures 3.6-3.8 demonstrate the dimensionless thermal resistance of the flux channels with different geometries, properties and variable heat transfer coefficient.

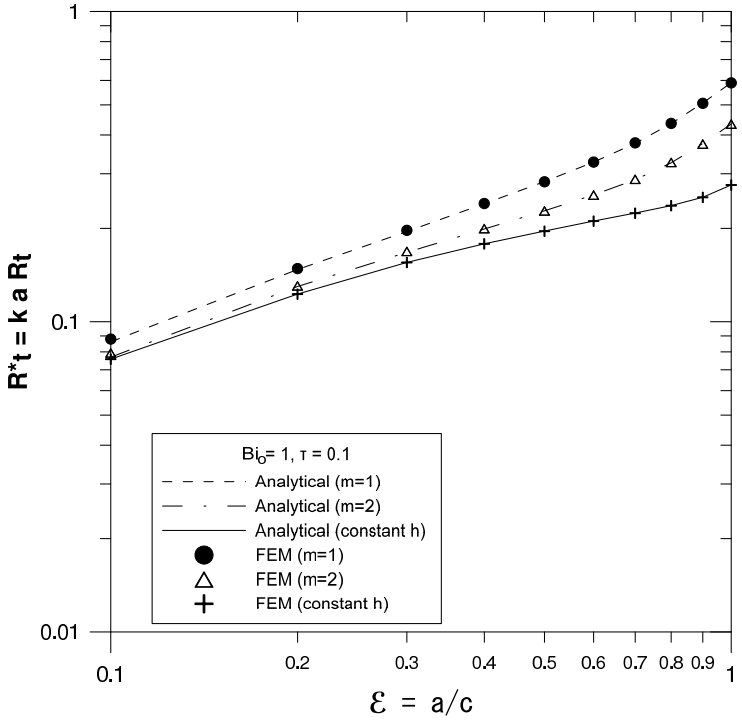

Figure 3.6: Dimensionless thermal resistance for $Bi_o = 1$ and $\tau = t/c = 0.1$.

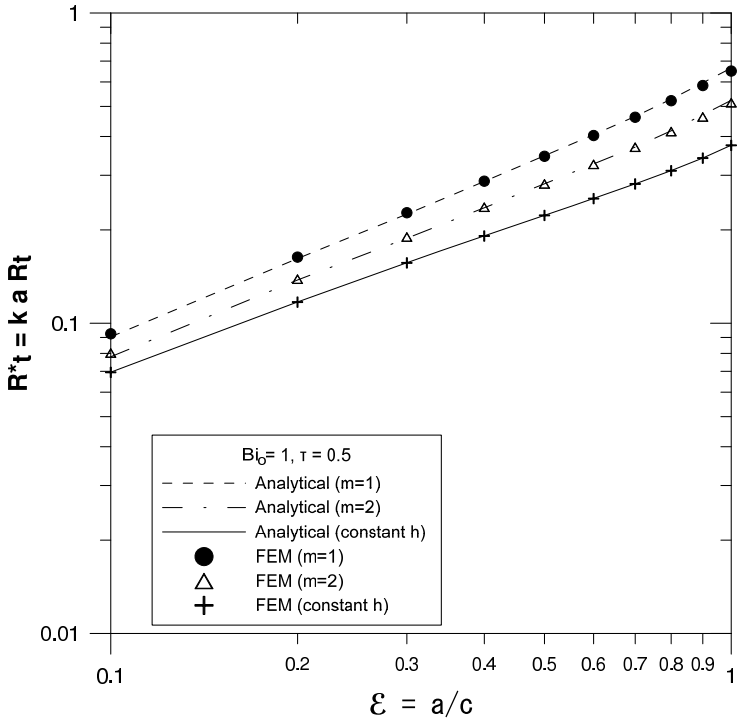

Figure 3.7: Dimensionless thermal resistance for $Bi_o = 1$ and $\tau = t/c = 0.5$.

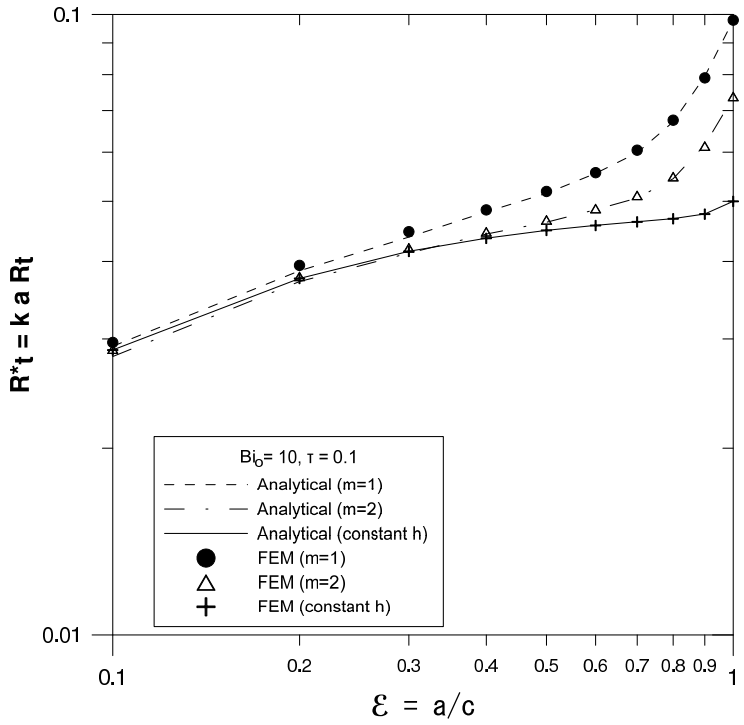

Figure 3.8: Dimensionless thermal resistance for $Bi_o = 10$ and $\tau = t/c = 0.1$.

As shown, the analytical and FEM results are in excellent agreement. In the analytical solution based on the least squares technique, 5 and 9 terms are used in the series to ensure the series expansion is sufficiently well approximated. If the Biot number is greater than 10, $Bi_o > 10$, and contact ratio is less than 0.1, $\epsilon = a/c < 0.1$, more terms are needed to have a more precise answer.

Now, the dimensionless thermal resistance is calculated based on the second approach. Due to the constant overall mean heat transfer coefficient over the sink plane for different values of m, this approach is much more meaningful for comparison of different flux channels with different geometries, properties and boundary conditions. In other words, the integrals of the plots over the sink are constant as shown in the Fig. 3.5. Hence, the system has the same overall mean conductance for different distributions over the sink region, $m = 1$, $m = 2$ and $m \to \infty$. Figures 3.9-3.13 show dimensionless thermal resistance versus dimensionless source size based on analytical and FEM results for a variety of flux channels.

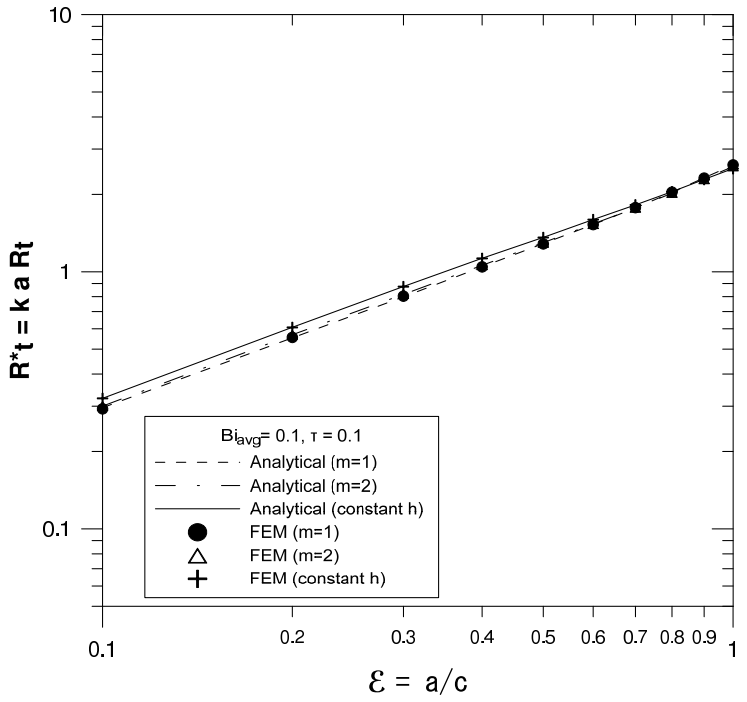

Figure 3.9: Dimensionless thermal resistance for $Bi_{avg} = 0.1$ and $\tau = t/c = 0.1$.

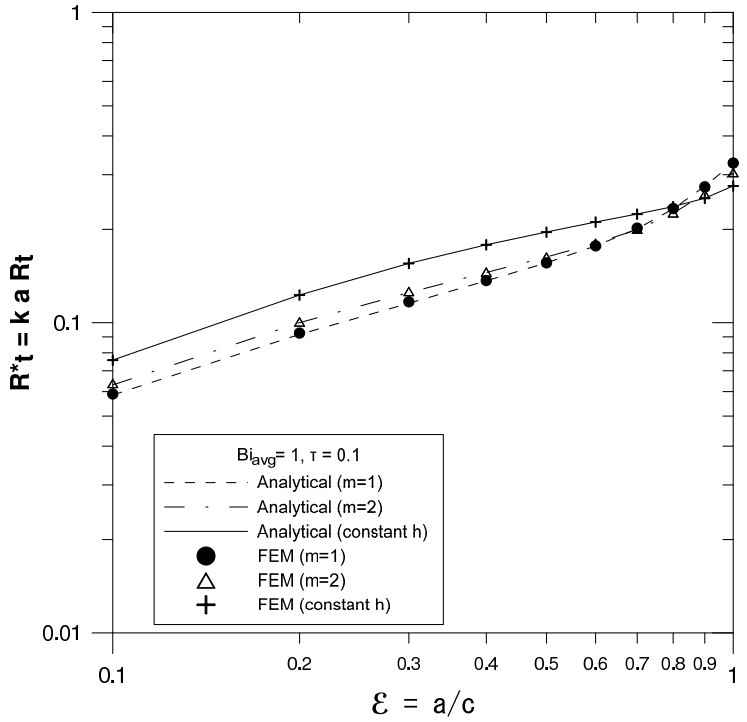

Figure 3.10: Dimensionless thermal resistance for $Bi_{avg} = 1$ and $\tau = t/c = 0.1$.

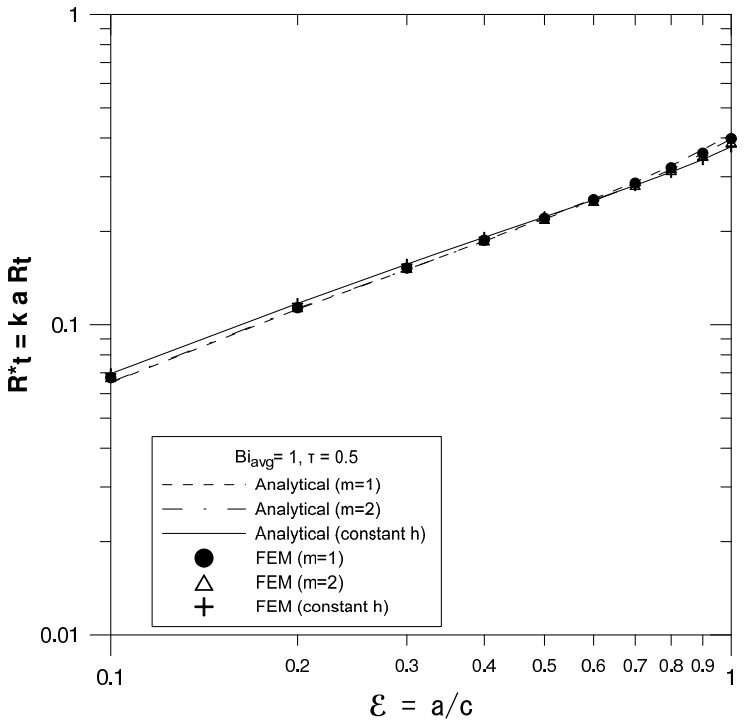

Figure 3.11: Dimensionless thermal resistance for $Bi_{avg} = 1$ and $\tau = t/c = 0.5$.

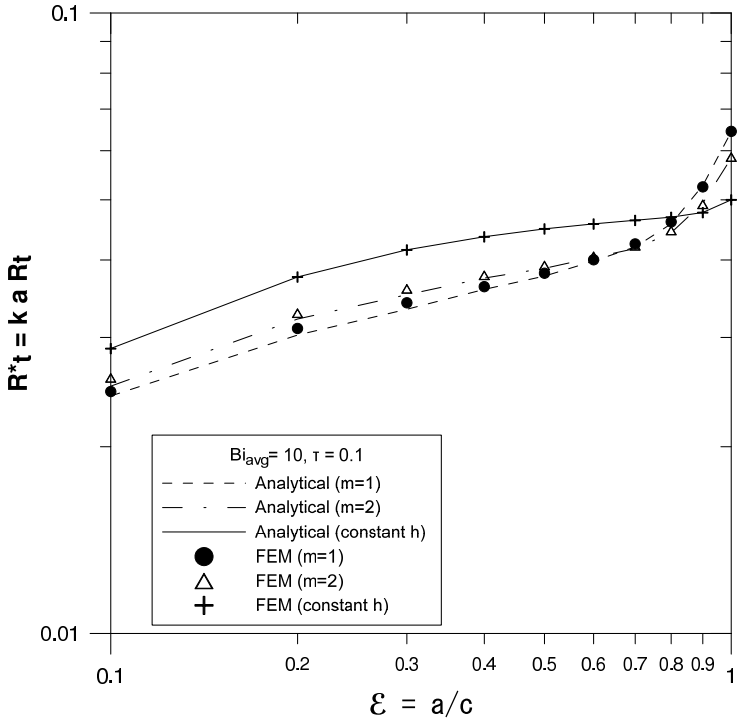

Figure 3.12: Dimensionless thermal resistance for $Bi_{avg} = 10$ and $\tau = t/c = 0.1$.

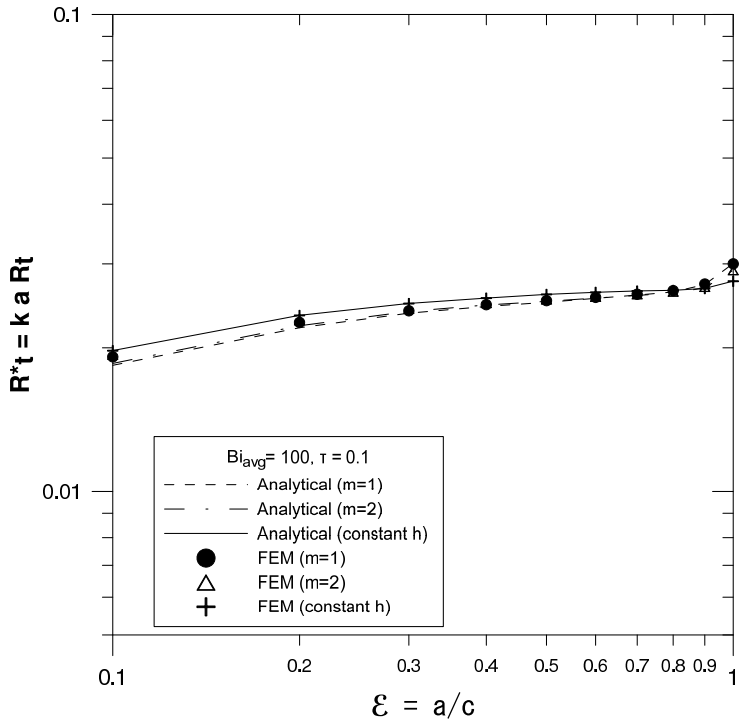

Figure 3.13: Dimensionless thermal resistance for $Bi_{avg} = 100$ and $\tau = t/c = 0.1$.

Results show the least squares technique works efficiently by using less than 10 terms in the series. The percent error of the dimensionless thermal resistance based on the second approach for the case of $Bi_{avg} = 100$ and $\tau = t/c = 0.1$ in a channel with linear heat transfer coefficient, $m = 1$, is shown in Table 3.2 . The percent error is measured based on a comparison between FEM and analytical results with 5 and 9 terms in the series.

ε=a/c	R^*_t -Analytical (5 terms)	R^*_t-Analytical (9 terms)	R^*_t -FEM	Percentage Error (5 terms)	Percentage Error (9 terms)
0.1	0.0165	0.0187	0.0191	13.5%	1.9%
0.2	0.0219	0.0223	0.0226	3.1%	1.0%
0.3	0.0231	0.0237	0.0239	3.2%	0.7%
0.4	0.0242	0.0244	0.0246	1.5%	0.6%
0.5	0.0246	0.0250	0.0251	1.8%	0.5%
0.6	0.0252	0.0254	0.0255	0.9%	0.4%
0.7	0.0255	0.0258	0.0259	1.3%	0.3%
0.8	0.0261	0.0263	0.0263	0.9%	0.2%
0.9	0.0271	0.0271	0.0272	0.5%	0.4%
1	0.0298	0.0301	0.0300	0.5%	0.4%

Table 3.2: Percent error of dimensionless thermal resistance for a flux channel with linear heat transfer coefficient, $m = 1$, and $Bi_{avg} = 100$ and $\tau = t/c = 0.1$.

Results given in Table 3.2 indicate that the percent error for $Bi_{avg} = 100$, $\tau = t/c = 0.1$ and $m = 1$ is decreased from 13.5% to 1.9% by increasing the number of terms in the series, Eq. (3.26), from 5 to 9 terms. Moreover, the percent error is less than 1% if 9 terms is used in the series for most of the cases.

Some important characteristic of thermal resistance of the flux channel with variable heat transfer coefficient can be concluded from the Figs. 3.9-3.13. These figures show that the order of magnitude for dimensionless thermal resistance decreases by increasing the Biot number from 0.1 to 100. It is worth mentioning that for increasing the Biot number, the thermal conductivity of the flux channel is constant and the value of the heat transfer coefficient increases. Therefore, the one dimensional thermal resistance of the system decreases and more heat can be removed from the system. The other interesting point for the systems with the dimensionless thickness of $\tau = 0.1$, is that the lines for different conductance are so close in the Fig. 3.9 and Fig. 3.13 in comparison to the Fig. 3.10 and Fig. 3.12. The reason for this behavior is that the total thermal resistance consists of both spreading resistance and one dimensional resistance. For the case of $Bi_{avg} = 0.1$, the spreading resistance is much smaller than the effect of one dimensional resistance and for the $Bi_{avg} = 100$, the spreading resistance is much greater than the one dimensional resistance. Therefore, the slope of the thermal spreading resistance is not so dependent on the variable heat transfer coefficient in Fig. 3.9 and Fig. 3.13 and a uniform conductance can be assumed without too much loss in accuracy. Further, due to the strength of the conductance in the system with $Bi_{avg} = 100$, the heat easily flows through the channel and the lines overlap and the variable heat transfer coefficient can be assumed as a uniform conductance. For the Biot numbers greater than 0.1 and less than 100, $0.1 < Bi_{avg} < 100$, the effect of both spreading resistance and one dimensional resistance should be considered. As shown in Fig. 3.10 and Fig. 3.12, the shape of the variable heat transfer coefficient has significant impact on the thermal resistance and the variable conductance can not be simplified to a uniform conductance.

Another important physical characteristic is the effect of the source size on the thermal resistance of the systems with variable heat transfer coefficient. In Table 3.3, the thermal resistance of flux channels with different distributions of heat transfer coefficient is shown. It can be seen that for the systems with linear heat transfer coefficient, $m = 1$, thermal resistance decreases when the source aspect ratio increases from 0.1 to 0.7 and then it increases again from 0.7 to 1. The reason is that the heat flow should spread over the channel for the small source aspect ratios and when the source aspect ratio is greater than 0.7, the heat should constrict to go through the heat sink. Therefore, less effort is needed for transferring the heat through the heat sink when the source aspect ratio is almost 0.7. The same trend can be seen for the quadratic distribution, $m = 2$, of heat transfer coefficient. The thermal resistance of the system with uniform heat transfer coefficient, $m \to \infty$, continuously decreases by increasing the source aspect ratio and reaches its minimum when $\epsilon = 1$ because of disappearing of the thermal spreading resistance.

ε=a/c	R_t for System with Linear Heat Transfer Coefficient (m=1)	R_t for System with Quadratic Heat Transfer Coefficient (m=2)	R_t for System with Uniform Heat Transfer Coefficient (m→∞)
0.1	29.48	31.89	37.9
0.2	23.16	25.18	30.7
0.3	19.47	21.03	25.9
0.4	17.11	18.22	22.3
0.5	15.61	16.29	19.6
0.6	14.74	15.04	17.6
0.7	14.42	14.33	16
0.8	14.59	14.14	14.8
0.9	15.24	14.44	14
1	16.36	15.25	13.8

Table 3.3: Thermal resistance for flux channels with $Bi_{avg} = 1$, $\tau = t/c = 0.1$, and different distributions of heat transfer coefficient.

Another interesting comparison which can be done is considering the effect of different configuration of heat transfer coefficient in the flux channels with different thicknesses. In other words, the accuracy of simplifying a flux channel with variable heat transfer coefficient to a flux channel with the same overall mean heat transfer coefficient over the sink

plane. As mentioned, the mean convective cooling of the system remains constant in the second approach, $h(x) = \frac{\overline{h}(m+1)}{m}[1 - \left(\frac{x}{c}\right)^m]$, and the dimensionless thermal resistance for different variable heat transfer coefficient can be easily compared. For this purpose, the uniform and quadratic heat transfer coefficient, $m = 2$, are compared for different Biot numbers, $Bi_{avg} = 0.1, 1, 10, 100$, and dimensionless thicknesses, $\tau = t/c = 0.1, 0.5$. Figure 3.14 shows two systems with different dimensionless thicknesses, $\tau = t/c = 0.1, 0.5$, to give a better insight of the geometry aspect ratio of the system.

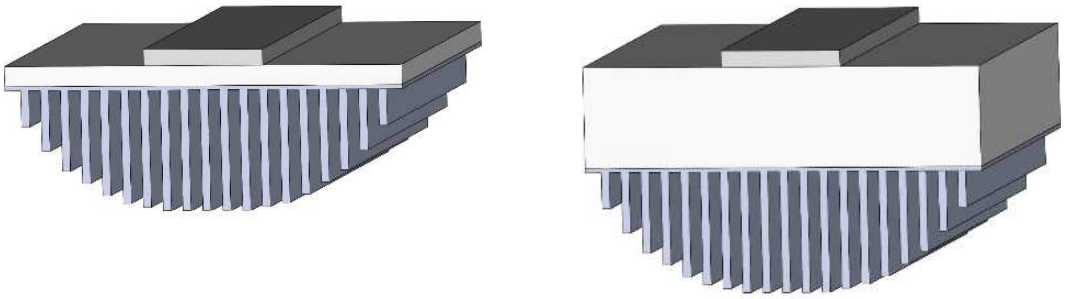

Figure 3.14: Left) 2D flux channel with dimensionless thickness of $\tau = 0.1$ Right) 2D flux channel with dimensionless thickness of $\tau = 0.5$.

$\varepsilon = a/c$	Bi_{avg}=0.1, τ=0.1 Percentage Error	Bi_{avg} =1, τ =0.1 Percentage Error	Bi_{avg} =10, τ =0.1 Percentage Error	Bi_{avg} =100, τ =0.1 Percentage Error
0.1	6.6%	15.8%	10.2%	2.0%
0.2	6.3%	17.9%	12.5%	2.4%
0.3	6.2%	18.7%	13.4%	2.6%
0.4	5.9%	18.2%	13.3%	2.4%
0.5	4.6%	16.8%	12.6%	2.5%
0.6	3.8%	15.5%	11.2%	2.2%
0.7	2.4%	10.4%	8.9%	1.6%
0.8	0.9%	4.4%	4.7%	0.6%
0.9	0.2%	3.1%	3.1%	0.7%
1	2.0%	10.5%	17.2%	5.3%
Mean Percentage Error	**3.9%**	**13.0%**	**10.7%**	**2.2%**

Table 3.4: Mean percent error for assuming uniform heat transfer coefficient instead of equivalent quadratic distribution heat transfer coefficient, $m = 2$, for different Biot numbers in a flux channel with dimensionless thickness of $\tau = 0.1$.

ε=a/c	Bi_{avg} =0.1, τ =0.5 Percentage Error	Bi_{avg} =1, τ =0.5 Percentage Error	Bi_{avg} =10, τ =0.5 Percentage Error	Bi_{avg} =100, τ =0.5 Percentage Error
0.1	0.7%	2.5%	1.1%	0.1%
0.2	0.7%	2.7%	1.3%	0.1%
0.3	0.6%	2.6%	1.4%	0.1%
0.4	0.5%	2.2%	1.2%	0.1%
0.5	0.3%	1.6%	0.8%	0.0%
0.6	0.1%	0.7%	0.2%	0.0%
0.7	0.0%	0.2%	0.6%	0.2%
0.8	0.2%	1.4%	1.7%	0.5%
0.9	0.4%	2.6%	2.9%	0.8%
1	0.6%	3.6%	4.1%	1.1%
Mean Percentage Error	**0.4%**	**2.0%**	**1.5%**	**0.3%**

Table 3.5: Mean percent error for assuming uniform heat transfer coefficient instead of equivalent quadratic distribution heat transfer coefficient, $m = 2$, for different Biot numbers in a flux channel with dimensionless thickness of $\tau = 0.5$.

The percent error for assuming a uniform heat transfer coefficient instead of quadratic conductance for a channel with $\tau = 0.1$ is shown in Table 3.4. As shown, the mean percent error for different cases is always less than 13% and even in most of the cases, it is less than 5%.

The effects of different Biot numbers, $0.1 < Bi_{avg} < 100$, that are already discussed are also shown in the Table 3.4 that quantified the mean percent error for assuming uniform heat transfer coefficient instead of equivalent quadratic distribution heat transfer coefficient. As shown in Table 3.4, the mean percent error for assuming a uniform heat transfer coefficient shows a peak for Biot number between 1 and 10.

Furthermore, the percent error for the channel with $\tau = 0.5$ is shown in Table 3.5 and it shows the mean percent error is less than 2% in all cases. The same manner can be seen in Fig. 3.11 that the values of dimensionless thermal resistance for different configurations of conductance are almost the same and the lines are very close. Therefore, it can be concluded that for flux channels with $\tau = t/c > 0.5$, the variable heat transfer coefficient can be simplified to a uniform heat transfer coefficient with the same mean coefficient. The

cases which need more attention are thin flux channels with the dimensionless thickness less than 0.5, $\tau < 0.5$. Hence, for the thick channels, a uniform distribution of mean overall conductance can be assumed without too much loss in accuracy and the proposed approach in paper [10] which is more computationally efficient can be used.

3.4 Conclusion

In this paper, general expressions for temperature distribution and thermal resistance of a two dimensional flux channel with central strap heat source and variable heat transfer coefficient are investigated using the separation of variables method. A novel solution for temperature distribution is obtained using the least squares technique. For modeling the variable heat transfer coefficient, two functions are proposed to simulate a wide variety of different heat sink configurations. Different factors including the size of the heat source, thickness of the channel and the variable heat transfer coefficient are considered in both methods. Finally, the trend of dimensionless thermal resistance versus dimensionless source size is presented considering variable heat transfer coefficient, dimensionless thickness, and different Biot numbers. The presented results show a good agreement between the analytical solution and the FEM method. Also, based on the mean percent error for different flux channels with different geometries, properties and variable heat transfer coefficient, it can be concluded that the simplification of using a uniform heat transfer coefficient instead of variable coefficient can be applied without too much loss in accuracy.

Acknowledgments

The authors acknowledge the financial support of the Natural Sciences and Engineering Research Council of Canada.

3.5 References

[1] Lee, S., Song, S., Au, V., and Moran, K. P., 1995, "Constriction/Spreading Resistance Model for Electronics Packaging," *in Proc. 4th ASME/JSME Thermal Eng. Joint Conf.*, Maui, HI, pp. 199-206, March.

[2] Song, S., Lee, S., and Au, V., 1994, "Closed-Form Equation for Thermal Constriction/Spreading Resistances with Variable Resistance Boundary Condition," *in Proc. IEPS Conf.*, Atlanta, GA, pp. 111-121, September.

[3] Das, A. K., and Sadhal, S.S., 1999, "Thermal Constriction Resistance Between Two Solids for Random Distribution of Contacts," *Heat Mass Transfer*, 35, pp. 101-111. DOI: 10.1007/s002310050303

[4] Lam, T. T., and Fischer, W. D., 1999, "Thermal Resistance in Rectangular Orthotropic Heat Spreaders," *ASME Advances in Electronic Packaging*, Vol. 26-1, American Society of Mechanical Engineers, Fairfield, NJ, pp. 891-898.

[5] Ellison, G., 1991, "Extensions of a Closed Form Method for Substrate Thermal Analyzers to Include Thermal Resistances From Source-to-Substrate and Source-to-Ambient," *Seventh IEEE Semi-Therm Symposium*, pp. 140-148. DOI: 10.1109/33.180028

[6] Ellison, G., 1994, "Thermal Analysis of Microelectric Packages and Printed Circuit Boards Using an Analytic Solution to the Heat Conduction Equation," *Advances in Engineering Software*, pp. 99-111. DOI: 10.1016/0965-9978(94)00032-E

[7] Ellison, G., 1996, "Thermal Analysis of Circuit Boards and Microelectronic Components Using an Analytical Solution to the Heat Conduction Equation," *Twelfth IEEE Semi-Therm Symposium*, pp. 144-150. DOI: 10.1109/STHERM.1996.545104

[8] Muzychka, Y. S., Yovanovich, M. M, and Culham, J. R., 2004, "Thermal Spreading Resistance in Compound and Orthotropic Systems," *Journal of Thermophysics and Heat Transfer*, vol. 18, no. 1, January-March. DOI: 10.2514/1.1267

[9] Muzychka, Y.S. and Yovanovich, M.M., 2001, "Thermal Resistance Models for Non-Circular Moving Heat Sources on a Half Space," *Journal of Heat Transfer*, vol. 123, pp. 624-632, August. DOI: 10.1115/1.1370516

[10] Muzychka, Y. S., Culham, J. R., and Yovanovich, M. M., 2003, "Thermal Spreading Resistance of Eccentric Heat Sources on Rectangular Flux Channels," *Journal of Electronic Packaging*, vol. 125, pp. 178-185, June. DOI: 10.1115/1.1568125

[11] Muzychka, Y. S., Stevanovic, M., and Yovanovich, M. M., 2001, "Thermal Spreading Resistances in Compound Annular Sectors," *Journal of Thermophysics and Heat Transfer*, vol. 15, no. 3, pp. 354-359. DOI: 10.2514/2.6615

[12] Muzychka, Y.S., 2006, "Influence Coefficient Method for Calculating Discrete Heat Source Temperature on Finite Convectively Cooled Substrates," *IEEE Transactions on Components and Packaging Technologies*, vol. 29, no. 3, pp. 636-643, September. DOI: 10.1109/ITHERM.2004.1319202

[13] Muzychka, Y. S., Yovanovich, M. M., and Culham, J. R., 2006, "Influence of Geometry and Edge Cooling on Thermal Spreading Resistance," *AIAA Journal of Thermophysics and Heat Transfer*, vol. 20. no. 2, pp. 247-255, April-June. DOI: 10.2514/1.14807

[14] Muzychka, Y.S., Bagnall, K., and Wang, E., 2013, "Thermal Spreading Resistance and Heat Source Temperature in Compound Orthotropic Systems with Interfacial Resistance", *IEEE Transactions on Components, Packaging and Manufacturing Technologies*, vol. 3, no. 11, pp. 1826-1841. DOI: 10.1109/TCPMT.2013.2269273

[15] Bagnall, K., Muzychka, Y.S., and Wang, E., 2013, "Application of the Kirchhoff Transform to Thermal Spreading Problems with Convection Boundary Conditions", *IEEE Transactions on Components, Packaging and Manufacturing Technologies*. DOI: 10.1109/TCPMT.2013.2292584

[16] Bagnall, K., Muzychka, Y.S., and Wang, E., 2014, "Analytical Solution for Temperature Rise in Complex, Multi-layer Structures with Discrete Heat Sources", *IEEE Transactions on Components, Packaging and Manufacturing Technologies*. DOI: 10.1109/TCPMT.2014.2299766

[17] Muzychka, Y.S., 2014, "Spreading Resistance in Compound Orthotropic Flux Tubes and Channels with Interfacial Resistance", *AIAA Journal of Thermophysics and Heat Transfer*. DOI: 10.2514/1.T4203

[18] Yovanovich, M. M., and Marotta, E. E., 2003, "Thermal Spreading and Contact Resistances," in *Heat Transfer Handbook*, A. Bejan, and A. D. Kraus, Eds. New York: Wiley, ch. 4, pp. 261-393.

[19] Yovanovich, M. M., 2005, "Four Decades of Research on Thermal Contact, Gap and Joint Resistance in Microelectronics," *IEEE Transactions on Components and Packaging Technologies*, vol. 28, no. 2, pp. 182-206. DOI: 10.1109/TCAPT.2005.848483

[20] http://www.legitreviews.com

[21] http://www.techreport.com

[22] Kelman, R. B., 1979, "Least Squares Fourier Series Solutions To Boundary Value Problems," *Society for Industrial and Applied Mathematics*, vol. 21, no. 3, pp. 329-338, July. DOI: 10.1137/1021051

[23] Maple 10, Waterloo Maple Software, Waterloo, ON, Canada.

[24] COMSOL Multiphysics® Version 4.2a.

Chapter 4

Thermal Spreading Resistance in a Asymmetric Flux Channel with Arbitrary Heat Convection in the Sink Plane

M. Razavi
Y.S. Muzychka

Department of Mechanical Engineering, Memorial University of Newfoundland, St. John's, NL, Canada, A1B 3X5

S. Kocabiyik

Department of Mathematics and Statistics, Memorial University of Newfoundland, St. John's, NL, Canada, A1C 5S7

Abstract

Thermal spreading resistance is one of the key factors for designing the thermal management systems in microelectronic devices. This type of thermal resistance occurs in most of the microelectronic devices and causes some difficulties for thermal engineers to model the system. One of the common geometries in these devices is the flux channel. Different boundary conditions can be applied on the flux channel based on the designing criteria of the system including the arbitrary distribution of heat sinks over the sink plane. This boundary condition is usually simplified as a constant heat transfer coefficient to facilitate the modeling of the system. In this paper, a flux channel with an arbitrary distributed heat

[1]IMECE 2014, the ASME 2014 International Mechanical Engineering Congress & Exposition, Montreal, Canada.

transfer coefficient over the sink plane is studied without simplification of the sink boundary condition. Both adiabatic and convective cooling over the edges of the flux channel are considered. Due to the complexity of the sink boundary condition, the conventional analytical solutions are not applicable and the method of least squares is used. By employing this approach, the effect of a non-uniform heat transfer coefficient on thermal spreading resistance is investigated. The solution is presented in form of a Fourier series expansion which can be used to obtain the temperature all over the channel. Results are validated with Finite Element Models, FEM. This approach is useful for thermal engineers who have some difficulty for modeling complex boundary conditions and presents an effective solution for thermal resistance in the flux channels.

Keywords: Thermal analysis, Thermal spreading resistance, Variable heat transfer coefficient, Least squares method

4.1 Introduction

Design of effective thermal management systems for micro-electronic devices is one of the most important factors for capability, life and safety of the product. Due to different configurations and boundary conditions, thermal resistance of each device should be studied. The thermal resistance of micro-electronic devices consist of one dimensional resistance and/or spreading resistance. The thermal spreading resistance occurs whenever heat flows in the regions with different cross sections.

Different researchers have worked on different aspects of thermal spreading resistance for more than five decades. The primers in this field are Kennedy [1] and Mikic [2, 3] who considered the spreading and contact resistance in cylindrical semiconductor devices. Yovanovich [4] comprehensively studied the thermal spreading/constriction resistance and reviewed all of his fourty years research on thermal spreading, constriction and gap resis-

tance. Yovanovich and Marrota [5] wrote a chapter on thermal spreading and constriction resistance in a heat transfer handbook. Lemczyk and Yovanovich [6, 7] used the least squares method to solve the thermal constriction resistance problems with convective boundary conditions. Yovanovich et al. [8] studied the spreading resistance of isoflux strips and rectangles on compound flux channel. Muzychka et al. [9-15] studied the thermal spreading resistance for different systems. They considered different geometries including single and multi-layer flux channels and flux tubes with different boundary conditions. The edges of both mentioned geometries can be adiabatic or have convective cooling condition. The sink boundary condition assumed as a constant temperature or a constant heat transfer coefficient. Bagnall et al. [16, 17] studied the spreading resistance problem in single and multi-layer structures with discrete heat sources and considered the effect of temperature dependent thermal conductivity of the channel.

Although, a comprehensive research has been done on different aspects of thermal spreading resistance, no research conducted on variable heat transfer coefficient along the sink plane. This boundary condition always simplified and assumed as a constant heat transfer coefficient along the sink. In this paper, a 2D flux channel with variable convective cooling along the sink plane is considered. Both adiabatic and convective cooling along the edge are considered. All results are validated with COMSOL multiphysics commercial software package [18] that is based on Finite Element Method (FEM). The presented models are useful for thermal engineers who want to analytically model the systems with variable heat transfer coefficient.

4.2 Problem Statement

In this research, a 2D flux channel with variable heat transfer coefficient along the sink plane is considered. The flux channels that are usually used in the real engineering sys-

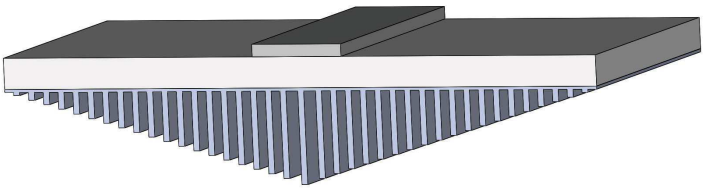

Figure 4.1: 3D view of symmetrical flux channel with linear heat transfer coefficient along the sink plane.

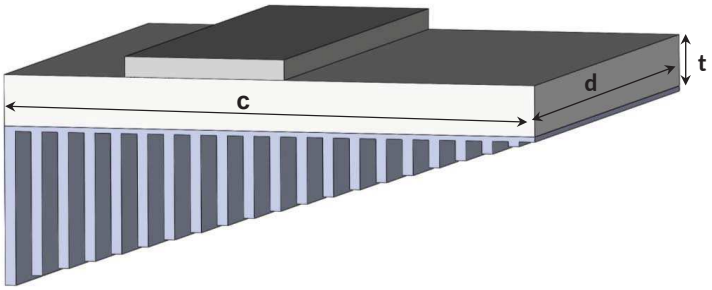

Figure 4.2: 3D view of non-symmetrical flux channel with linear heat transfer coefficient along the sink plane.

tems are symmetric with the most intense cooling along the center line of the heat sink plane, Fig. 4.1. As it is a specific case, a more general model for non-symmetrical systems are studied that can be simplified as half of the channel in the symmetrical systems. A schematic 3D view of the flux channel is shown in the Fig. 4.2 and the 2D model of the system is shown in the Fig. 4.3. The temperature profile over the flux channel is obtained and the total thermal resistance is calculated. The total thermal resistance can be calculated using the mean source temperature, $\overline{T}_s$; film temperature, T_f; and the total heat flow rate of the system, Q;

$$R_t = R_{1D} + R_s = \frac{\overline{T}_s - T_f}{Q}. \tag{4.1}$$

In the symmetrical system, half of the channel is investigated and the total thermal resistance of the system is equal to the total thermal resistance of half of the channel divided by

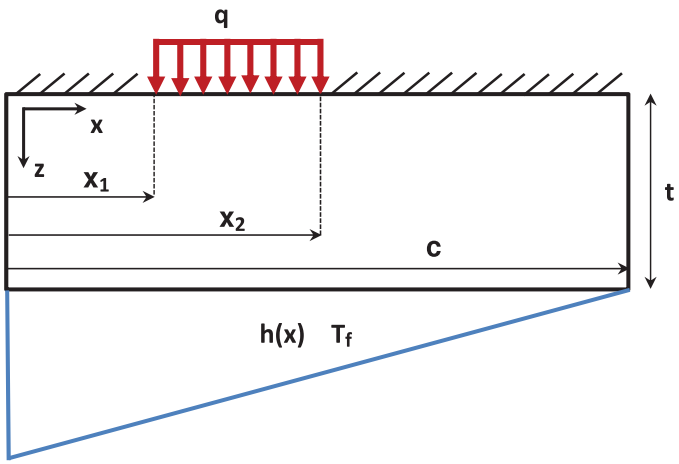

Figure 4.3: 2D non-symmetrical flux channel with linear heat transfer coefficient along the sink plane.

two.

The governing equation of the system is the Laplace equation,

$$\frac{\partial^2 T}{\partial x^2} + \frac{\partial^2 T}{\partial z^2} = 0. \tag{4.2}$$

For solving this equation and homogenized the boundary conditions, the variable θ is defined as $\theta = T - T_f$.

$$\frac{\partial^2 \theta}{\partial x^2} + \frac{\partial^2 \theta}{\partial z^2} = 0. \tag{4.3}$$

The source plane boundary conditions are,

$$\begin{aligned} \left.\frac{\partial \theta}{\partial z}\right|_{z=0} &= -\frac{q}{k}, && \text{over the source region} \\ \left.\frac{\partial \theta}{\partial z}\right|_{z=0} &= 0, && \text{out of the source region} \end{aligned} \tag{4.4}$$

The left edge of the system is adiabatic,

$$\left.\frac{\partial\theta}{\partial x}\right|_{x=0} = 0, \tag{4.5}$$

and the boundary condition along the right edges is,

$$\left.\frac{\partial\theta}{\partial x}\right|_{x=c} = -\frac{h_e}{k}\theta. \tag{4.6}$$

Although, the convective cooling along the right edge is considered, the adiabatic boundary condition can be produced using a small number for heat transfer coefficient along the right edge, h_e.

The sink boundary condition is convective cooling with variable heat transfer coefficient,

$$\left.\frac{\partial\theta}{\partial z}\right|_{z=t} = -\frac{h(x)}{k}\theta. \tag{4.7}$$

The variable heat transfer coefficient assumed as a linear profile along the sink plane,

$$h(x) = h_o\left[1 - \left(\frac{x}{c}\right)\right]. \tag{4.8}$$

The Laplace equation can be solved using the separation of variables method with the mentioned boundary conditions. The general form of the solution after applying the boundary conditions along the edges of the system is,

$$\theta(x,z) = \sum_{n=1}^{\infty} \cos\left(\lambda_n x\right)\left(C_n \cosh\left(\lambda_n z\right) + D_n \sinh\left(\lambda_n z\right)\right), \tag{4.9}$$

where λ_n are the eigenvalues of the system and obtained using the right edge boundary condition, Eq. (4.6).

$$\lambda_n \sin(\lambda_n c) = \frac{h_e}{k}\cos(\lambda_n c). \tag{4.10}$$

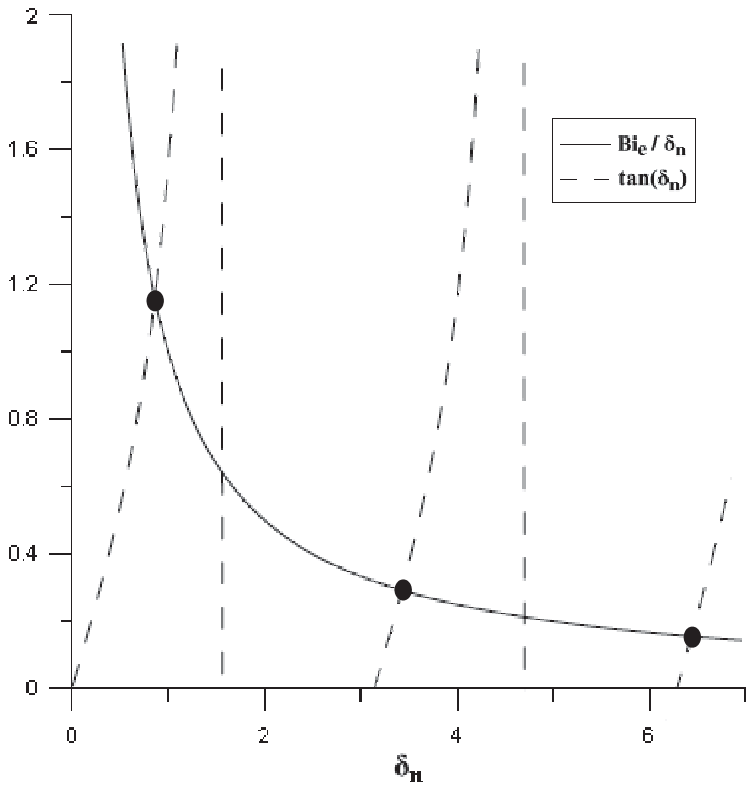

Figure 4.4: Eigenvalues of a flux channel with $Bi_e = 1$.

By considering $Bi_e = \frac{h_e c}{k}$ and $\delta_n = \lambda_n c$, the eigenvalues of the flux channel are,

$$\delta_n \sin(\delta_n) = Bi_e \cos(\delta_n) \qquad n = 1, 2, 3, \cdots . \tag{4.11}$$

This equation can be solved numerically to obtain the eigenvalues of the system. For example, the eigenvalues of a flux channel with $Bi_e = 1$ is shown in the Fig. 4.4 and are as follows:

$$\delta_1 = 0.86,\ \delta_2 = 3.426,\ \delta_3 = 6.437,\ \delta_4 = 9.529, \cdots . \tag{4.12}$$

More eigenvalues can be calculated using $\delta_n = \pi + \delta_{n-1}$. Applying the boundary condition along the sink plane,

$$D_n = -C_n \left(\frac{\lambda_n \sinh(\lambda_n t) + \frac{h(x)}{k} \cosh(\lambda_n t)}{\lambda_n \cosh(\lambda_n t) + \frac{h(x)}{k} \sinh(\lambda_n t)} \right), \tag{4.13}$$

$$D_n = -C_n \phi_n(x),$$

where $\phi_n(x)$ is the spreading function. As the heat transfer coefficient is a function of x, the spreading function is also a function of x. For the flux channels that consists of several layers, the spreading function is much more complex. Therefore, the variable conductance along the sink plane is simplified to a constant conductance in the multi-layer systems to reduce the complexity of the spreading function. In this case study, the spreading function can be written in terms of $Bi(x) = \frac{h(x)c}{k}$, $\delta_n = \lambda_n c$, and $\tau = \frac{t}{c}$ as follows,

$$\phi_n(x) = \frac{\delta_n \tanh(\delta_n \tau) + Bi(x)}{\delta_n + Bi(x) \tanh(\delta_n \tau)}. \tag{4.14}$$

Substituting the defined variables, the general form of the solution is,

$$\theta(x, z) = \sum_{n=1}^{\infty} C_n \cos\left(\delta_n \frac{x}{c}\right) \left(\cosh\left(\delta_n \frac{z}{c}\right) - \phi_n(x) \sinh\left(\delta_n \frac{z}{c}\right) \right). \tag{4.15}$$

Due to the dependency of the spreading function on x, i.e. $\phi_n(x)$, the orthogonality property is not easily satisfied and can not be applied for obtaining the last unknown constant, C_n. Therefore, the least squares method is used for solving the problem [19]. The least square method along the source plane can be defined as follows,

$$
\begin{aligned}
I_N = &\int_0^{x_1} \left[-k \left. \frac{\partial \theta}{\partial z} \right|_{z=0} - f(x) \right]^2 dx \\
&+ \int_{x_1}^{x_2} \left[-k \left. \frac{\partial \theta}{\partial z} \right|_{z=0} - g(x) \right]^2 dx \\
&+ \int_{x_2}^{c} \left[-k \left. \frac{\partial \theta}{\partial z} \right|_{z=0} - p(x) \right]^2 dx
\end{aligned}
\tag{4.16}
$$

where $f(x)$, $g(x)$, and $p(x)$ are the known values of heat flux along the source plane. Implementing this concept to the general form of the solution, Eq. (4.15), and the boundary condition along the source plane, Eq. (4.4):

$$
\begin{aligned}
\left. \frac{\partial \theta}{\partial z} \right|_{z=0} &= \sum_{n=1}^{\infty} -C_n \left(\frac{\delta_n}{c} \right) \phi_n(x) \cos \left(\frac{\delta_n x}{c} \right), \\
f(x) = -k \left. \frac{\partial \theta}{\partial z} \right|_{z=0} &= 0 \qquad (0 < x < x_1), \\
g(x) = -k \left. \frac{\partial \theta}{\partial z} \right|_{z=0} &= q \qquad (x_1 < x < x_2), \\
p(x) = -k \left. \frac{\partial \theta}{\partial z} \right|_{z=0} &= 0 \qquad (x_2 < x < c).
\end{aligned}
\tag{4.17}
$$

By substituting the values of Eq. (4.17) in the Eq. (4.16),

$$
\begin{aligned}
I_N = &\int_0^{x_1} \left[-k \sum_{n=1}^{\infty} -C_n \left(\frac{\delta_n}{c} \right) \phi_n(x) \cos \left(\frac{\delta_n x}{c} \right) - 0 \right]^2 dx \\
&+ \int_{x_1}^{x_2} \left[-k \sum_{n=1}^{\infty} -C_n \left(\frac{\delta_n}{c} \right) \phi_n(x) \cos \left(\frac{\delta_n x}{c} \right) - q \right]^2 dx \\
&+ \int_{x_2}^{c} \left[-k \sum_{n=1}^{\infty} -C_n \left(\frac{\delta_n}{c} \right) \phi_n(x) \cos \left(\frac{\delta_n x}{c} \right) - 0 \right]^2 dx.
\end{aligned}
\tag{4.18}
$$

The coefficients C_n are calculated in order to minimize the I_N,

$$\frac{\partial I_N}{\partial C_n} = 0 \qquad\qquad n = 1, 2, ...N. \tag{4.19}$$

This equation can be solved numerically in order to obtain the coefficients, C_n, using the Maple mathematical package [20]. As a result, the temperature profile over the flux channel is known. The thermal resistance can be calculated using the mean source temperature, $\overline{\theta}_s = \overline{T_s} - T_f$, and the total heat flux, Q.

$$\begin{aligned} R_t &= \frac{\overline{\theta}_s}{Q}, \\ \overline{\theta}_s &= \frac{1}{(x_2 - x_1)} \int_{x_1}^{x_2} \theta(x, 0) dx = \sum_{n=1}^{\infty} \frac{C_n \, c \left(\sin\left(\frac{\delta_n x_2}{c}\right) - \sin\left(\frac{\delta_n x_1}{c}\right) \right)}{\delta_n \, (x_2 - x_1)}, \\ Q &= q \, (x_2 - x_1) \, d. \end{aligned} \tag{4.20}$$

$$R_t = \frac{\overline{\theta}_s}{Q} = \frac{c}{q \, (x_2 - x_1)^2 \, d} \sum_{n=1}^{\infty} \frac{C_n \left(\sin\left(\frac{\delta_n x_2}{c}\right) - \sin\left(\frac{\delta_n x_1}{c}\right) \right)}{\delta_n}. \tag{4.21}$$

Dimensionless thermal resistance can be calculated using the thermal conductivity, k, length of the source, $x_2 - x_1$, and total thermal resistance, R_t, as follows:

$$R_t^* = k \, (x_2 - x_1) \, R_t. \tag{4.22}$$

Using the above mentioned solution, temperature profile and thermal resistance in a 2D flux channel with variable heat transfer coefficient is known. In the next section, the solution is compared with the result of COMSOL commercial software package based on FEM.

Number of free tetrahedral element	Mean source temperature	Rt
952	0.002907	48.46
2779	0.002910	48.51
4909	0.002912	48.53
13824	0.002913	48.55
95981	0.002914	48.57
224528	0.002914	48.57

Table 4.1: Checking the convergency of FEM.

4.3 Results and Discussion

In this section, the thermal resistance of a flux channel with variable heat transfer coefficient along the sink plane is calculated using analytical method and FEM. Both adiabatic edges and convective cooling along the right edge are considered. The geometry and property of the flux channel are $k = 2W/mK$, $h_o = 200W/m^2K$, $c = d = 0.02m$, and $t = 0.001m$. For the case of adiabatic edges, the convective cooling along the right edge is assumed a small number such as $h_e = 0.01W/m^2K$. For the case of convective cooling along the right edge, the heat transfer coefficient along the right edge is $h_e = 1000W/m^2K$ to show the effect of the edge cooling.

Also, for testing the convergency in the FEM, a flux channel with mentioned geometry and properties and adiabatic edges is considered. The heat source position is defined by $x_1 = 0.007m$ and $x_2 = 0.01m$. The temperature distribution of the flux channel modelled with FEM is shown in Fig. 4.5. The convergency of the FEM is checked using finer mesh in the system. In the Table 4.1, the converegency of the thermal resistance for different number of elements in the mesh is shown. It shows that the result of the thermal resistance in a flux channel with a mesh consist of 95981 free tetrahedral elements is converged with 2 digits of precision and there is no change in the thermal resistance of the system by increasing the number of elements in the mesh.

The results of the thermal resistance of a flux channel with adiabatic edges is shown in

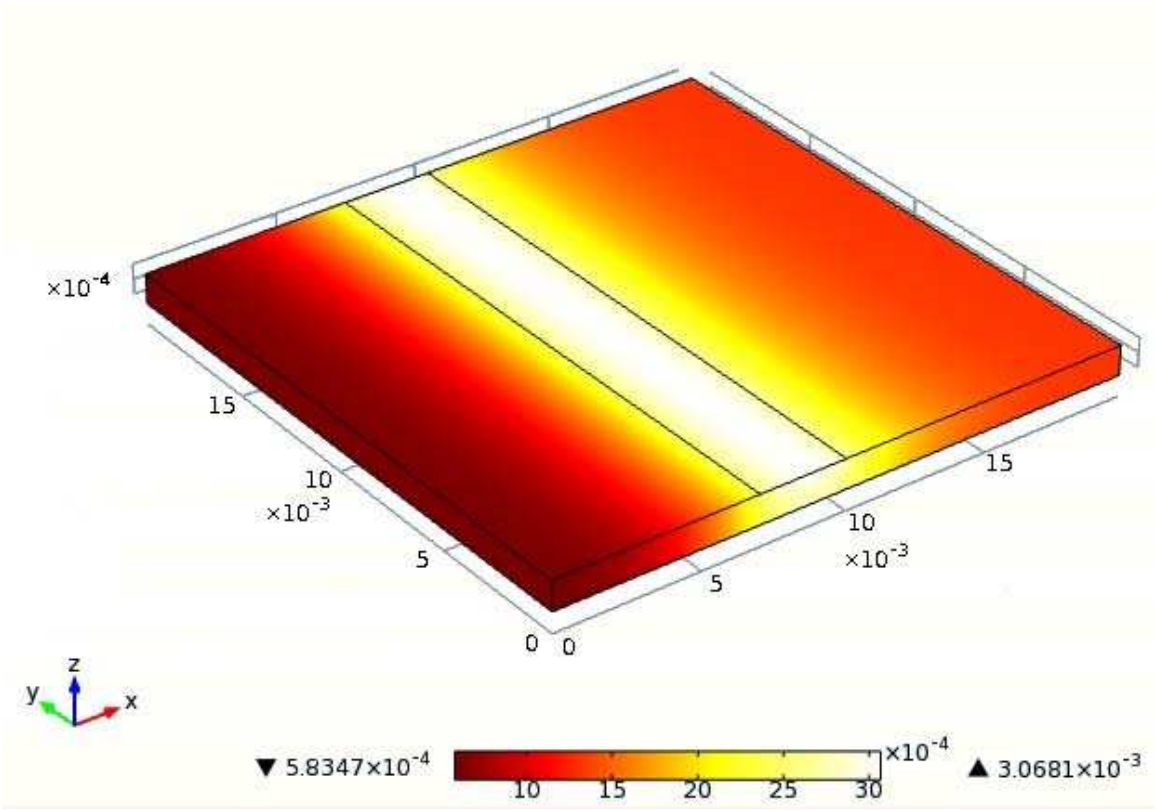

Figure 4.5: Thermal modeling of a flux channel with linear heat conductance and adiabatic edges by Comsol (FEM).

Table 4.2. As mentioned, for modeling the channel with adiabatic edges, the heat transfer coefficient along the right edge, h_e, is assumed a small number to calculate the eigenvalues of the system, Eq. (4.4). Different source sizes and different heat source positions are considered. In the analytical method, less than 10 terms is used in the series. Table 4.2 demonstrate the percent error between the analytical method and FEM and it shows less than 1% error.

Also, the flux channel with convective cooling along the right edge is considered in Table 4.3. The heat transfer coefficient along the right edge is assumed $h_e = 1000W/m^2K$ to show the effect of edge cooling. As expected, the thermal resistance decreases in comparison of the flux channel with adiabatic edges. For the analytical results, the number of terms

Source position	R_t-Analytical	R_t-FEM	Percent Error
x_1=0.001, x_2=0.004	47.72	48.00	0.5%
x_1=0.001, x_2=0.007	36.03	36.31	0.7%
x_1=0.001, x_2=0.010	30.46	30.73	0.8%
x_1=0.001, x_2=0.013	28.53	28.59	0.2%
x_1=0.001, x_2=0.016	29.22	29.39	0.5%
x_1=0.001, x_2=0.019	33.66	33.55	0.3%

Table 4.2: Percent error for thermal resistance of flux channels with adiabatic edges.

Source position	R_t-Analytical	R_t-FEM	Percent Error
x_1=0.001, x_2=0.004	47.63	47.89	0.5%
x_1=0.001, x_2=0.007	35.80	36.08	0.7%
x_1=0.001, x_2=0.010	29.85	30.12	0.8%
x_1=0.001, x_2=0.013	26.81	26.91	0.3%
x_1=0.001, x_2=0.016	24.92	25.01	0.3%
x_1=0.001, x_2=0.019	23.04	23.08	0.2%

Table 4.3: Percent error for thermal resistance of flux channels with convective cooling along the right edge.

in the series is less than 10 terms. For the FEM, the mesh consists of 95981 free tetrahedral elements. The percent error between the analytical results and FEM is less than 1%.

Based on the presented results, it can be seen that the presented analytical method with less than 10 terms in the series can model the system accurately.

4.4 Conclusion

In this paper, an analytical solution for modelling the temperature profile and thermal resistance of a 2D flux channel with variable heat transfer coefficient along the sink plane is studied. The governing equation of the system is the Laplace equation and solved using separation of variables method and least squares technique. Both adiabatic edges and convective cooling along the right edge of the system are considered. All results are compared with COMSOL commercial software package that is based on FEM. A perfect agreement

exist between the analytical models and FEM results. This method is really useful for thermal engineers who want to model the flux channels in micro electronic devices with variable heat transfer coefficient along the sink plane.

4.5 References

[1] Kennedy, D. P., "Spreading Resistance in Cylindrical Semiconductor devices," *Journal of Applied Physics*, vol. 31, pp. 490-1497, 1960.

[2] Mikic, B, B., "Thermal Contact Resistance," *SC.D. Thesis*, Department of Mechanical Engineering, MIT, Cambridge, Massachusetts, 1966.

[3] Mikic, B. B., and Rohsenow, W. M., "Thermal Contact Resistance," *M.I.T. Heat Transfer Lab Report No. 4542-41*, Sep. 1966.

[4] Yovanovich, M. M., "Four Decades of Research on Thermal Contact, Gap and Joint Resistance in Microelectronics," *IEEE Transactions on Components and Packaging Technologies*, vol. 28, no. 2, pp. 182-206, 2005.

[5] Yovanovich, M. M., and Marotta, E. E., "Thermal Spreading and Contact Resistances," in *Heat Transfer Handbook*, A. Bejan, and A. D. Kraus, Eds. New York: Wiley, ch. 4, pp. 261-393, 2003.

[6] Lemczyk, T. F., and Yovanovich, M. M., "Thermal Constriction Resistance with Convective Boundary Conditions, Part 1: Half-Space Contacts," *Int. J. Heat Mass Transf.*, vol. 31, no. 9, pp. 1861-1872, 1988.

[7] Lemczyk, T. F., and Yovanovich, M. M., "Thermal Constriction Resistance with Convective Boundary Conditions, Part 2: Layered Half-Space Contacts," *Int. J. Heat Mass Transf.*, vol. 31, no. 9, pp. 1873-1883, 1988.

[8] Yovanovich, M. M., Muzychka, Y. S., and Culham, J. R., "Spreading Resistance in Isoflux Rectangles and Strips on Compound Flux Channels," *J. Thermophys. Heat Transf.*, vol. 13, no. 4, pp. 495-500, 1999.

[9] Muzychka, Y. S., Sridhar, M. R., Yovanovich, M. M., and Antonetti, V. W., "Thermal Constriction Resistance in Multilayered Contacts: Applications in Thermal Contact Resistance," *AIAA Journal of Thermophysics and Heat Transfer*, vol. 13, no. 4, pp. 489-494, 1999.

[10] Muzychka, Y. S., Culham, J. R., and Yovanovich, M. M., "Thermal Spreading Resistance of Eccentric Heat Sources on Rectangular Flux Channels," *Journal of Electronic Packaging*, vol. 125, pp. 178-185, June 2003.

[11] Muzychka, Y. S., Yovanovich, M. M, and Culham, J. R., "Thermal Spreading Resistance in Compound and Orthotropic Systems," *Journal of Thermophysics and Heat Transfer*, vol. 18, no. 1, January-March 2004.

[12] Muzychka, Y. S., "Influence Coefficient Method for Calculating Discrete Heat Source Temperature on Finite Convectively Cooled Substrates," *IEEE Transactions on Components and Packaging Technologies*, vol. 29, no. 3, pp. 636-643, Sep. 2006.

[13] Muzychka, Y. S., Yovanovich, M. M., and Culham, J. R., "Influence of Geometry and Edge Cooling on Thermal Spreading Resistance," *AIAA Journal of Thermophysics and Heat Transfer*, vol. 20. no. 2, pp. 247-255, April-June 2006.

[14] Muzychka, Y. S., Bagnall, K., and Wang, E., "Thermal Spreading Resistance and Heat Source Temperature in Compound Orthotropic Systems with Interfacial Re-

sistance", *IEEE Transactions on Components, Packaging and Manufacturing Technologies*, vol. 3, no. 11, pp. 1826-1841, 2013.

[15] Muzychka, Y. S., "Spreading Resistance in Compound Orthotropic Flux Tubes and Channels with Interfacial Resistance", *AIAA Journal of Thermophysics and Heat Transfer*, 2014.

[16] Bagnall, K., Muzychka, Y. S., and Wang, E., "Application of the Kirchhoff Transform to Thermal Spreading Problems with Convection Boundary Conditions", *IEEE Transactions on Components, Packaging and Manufacturing Technologies*, 2013.

[17] Bagnall, K., Muzychka, Y. S., and Wang, E., "Analytical Solution for Temperature Rise in Complex, Multi-layer Structures with Discrete Heat Sources", *IEEE Transactions on Components, Packaging and Manufacturing Technologies*, 2014.

[18] COMSOL Multiphysics® Version 4.2a.

[19] Kelman, R. B., "Least Squares Fourier Series Solutions To Boundary Value Problems," *Society for Industrial and Applied mathematics*, vol. 21, no. 3, pp. 329-338, July 1979.

[20] Maple 10, Waterloo Maple Software, Waterloo, ON, Canada.

Chapter 5

Thermal Resistance of a Two Dimensional Flux Channel with Eccentric Heat Source and Edge Cooling

M. Razavi
Y.S. Muzychka

Department of Mechanical Engineering, Memorial University of Newfoundland, St. John's, NL, Canada, A1B 3X5

S. Kocabiyik

Department of Mathematics and Statistics, Memorial University of Newfoundland, St. John's, NL, Canada, A1C 5S7

Abstract

In this paper, an analytical solution is presented for the temperature profile and thermal resistance of a non-symmetrical flux channel with convective cooling along the sink plane and edges. The heat transfer coefficients along the right and left edges of the channel are defined separately and both are independent from the heat transfer coefficient applied over the sink plane. The system is solved using the method of separation of variables. Due to the edge cooling and non-symmetry, the eigenvalues should be calculated using the heat transfer coefficient on both edges. For satisfying the orthogonality condition, a normalized function is defined. The temperature distribution over the channel is presented in the form of a Fourier series expansion and some expressions are presented to calculate

[1]Submitted to the Journal of Advances in Applied Mathematics and Mechanics

the thermal resistance and dimensionless thermal resistance. Application of the method to the orthotropic channels is also discussed. Some case studies are considered and the results are compared with other literature and the Finite Element Method (FEM) using COMSOL commercial software package [1]. The proposed model is useful for thermal engineers who wish to model micro-electronic devices with different conductance and heat sink configurations.

Keywords: Electronics Cooling, Heat Conduction, Thermal Resistance, Separation of Variables, Eccentric System

5.1 Introduction

Thermal analysis of electronic devices is crucial for designing a proper thermal management system. For analytical modeling of the temperature profile over the electronic device, the geometry of the device is usually simplified as a flux channel (cubical geometry) or a flux tube (cylinder). Rectangular flux channels are one of the common geometries of different electronic devices. Different boundary conditions are applied on the channels based on the design and configuration of the system. Several analytical solutions are available for analyzing the thermal spreading resistance in the flux channels. Due to different properties and boundary conditions of the system, there is no general analytical solution for modeling the temperature profile and thermal resistance.

Many studies have been done on different aspects of thermal spreading resistance [2-4]. Different industrial applications were studied in [5-12]. Ying and Toh [7] studied the thermal resistance in electronic packaging. Kim et al. [8] presented a correlation for modeling the thermal spreading resistance of multi electronic components with several sources. Culham et al. [9, 10] modeled the thermal resistance in circuit boards. Lasance [11, 12] studied the thermal resistance in LEDs.

Muzychka et al. [13-19] studied the thermal spreading resistance of flux channels with different geometries and boundary conditions, and considered isotropic and orthotropic properties. They [19] modeled the rectangular flux channel using an equivalent system in a circular flux tube. Furthermore, the effect of edge cooling in a symmetrical flux channel is considered. These researchers considered the effect of interfacial resistance on thermal resistance of compound, orthotropic systems [18]. Bagnall et al. [20] presented an approximate solution for the spreading resistance in compound orthotropic systems with interfacial resistance and convection in the sink plane using Kirchhoff transform. Yovanovich and Marrota [21] summarized the most important models of thermal spreading and contact resistance. Yovanovich [22] also reviewed forty years research on thermal spreading resistance.

Although different aspects of thermal spreading resistance problems are considered, no research has been done on the effect of edge cooling and different wall conductance for the non-symmetrical flux channels. In most of the analytical models, the convective cooling condition along the edges of the channel is simplified as an adiabatic boundary condition. This is usually a proper assumption due to the small surface area along the edges that is exposed to natural convection. However; in some cases, the heat sinks are designed to install along the edges. For these systems, an analytical solution was proposed for the case of symmetrical flux channel with a concentric heat source [19]. In the symmetrical channel, the heat source is concentric and the heat transfer coefficient is the same for all edges of the channel. In this paper, a more general model for non- symmetrical channel with an eccentric heat source and different convective cooling along each edge is proposed. For solving the problem, the method of separation of variables is used. In this analysis, the most challenging problem is satisfying the orthogonality condition by defining a weight function. It is worth mentioning that heat transfer coefficient along each edge is defined independently from each other and both are different from the heat transfer coefficient along

the sink plane.

5.2 Problem Statement

In this paper, a non-symmetrical flux channel is studied using the method of separation of variables. Convective cooling exists along the edges and bottom surface. As shown in the Fig. 5.1, the heat transfer coefficient along the left edge is shown as h_1, along the right edge as h_2, and along the sink plane is shown as h_s. An eccentric heat source as a constant heat flux is applied along the source plane.

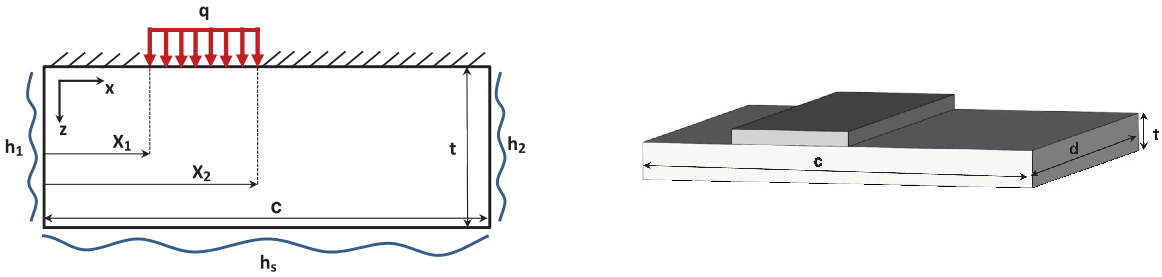

Figure 5.1: 2D flux channel with eccentric heat source and edge cooling.

5.2.1 Isotropic Systems

The governing equation for the system is the Laplace equation and for the isotropic system can be written as follows,

$$\frac{\partial^2 T}{\partial x^2} + \frac{\partial^2 T}{\partial z^2} = 0. \tag{5.1}$$

The parameter $\theta = T - T_f$ is defined and the Laplace equation takes the form,

$$\frac{\partial^2 \theta}{\partial x^2} + \frac{\partial^2 \theta}{\partial z^2} = 0. \tag{5.2}$$

The boundary condition along the source plane, $z = 0$, is,

$$\begin{aligned} \left.\frac{\partial\theta}{\partial z}\right|_{z=0} &= 0, & 0 < x < x_1, \\ -k \left.\frac{\partial\theta}{\partial z}\right|_{z=0} &= q, & x_1 < x < x_2, \\ \left.\frac{\partial\theta}{\partial z}\right|_{z=0} &= 0, & x_2 < x < c. \end{aligned} \tag{5.3}$$

A different heat transfer coefficient is assumed for the left, right, and bottom of the flux channel. The boundary condition along the left edge, $x = 0$, is,

$$k \left.\frac{\partial\theta}{\partial x}\right|_{x=0} = h_1\theta, \tag{5.4}$$

and along the right edge, $x = c$, is,

$$-k \left.\frac{\partial\theta}{\partial x}\right|_{x=c} = h_2\theta. \tag{5.5}$$

The boundary condition along the bottom of the flux channel, $z = t$, is defined as,

$$-k \left.\frac{\partial\theta}{\partial z}\right|_{z=t} = h_s\theta. \tag{5.6}$$

The method of separation of variables is used for solving the Laplace equation, Eq. (5.2), by considering the mentioned boundary conditions. The general form of the solution is,

$$\theta(x, z) = [A\cos(\lambda x) + B\sin(\lambda x)][C\cosh(\lambda z) + D\sinh(\lambda z)]. \tag{5.7}$$

Applying the boundary condition along the left edge, Eq. (5.4), results,

$$B = \frac{h_1 A}{k\lambda}. \tag{5.8}$$

Using the boundary condition along the right edge of the system, Eq. (5.5), gives,

$$k\left(-A\lambda\sin(\lambda c)+\frac{h_1A}{k\lambda}\lambda\cos(\lambda c)\right)=-h_2\left(A\cos(\lambda c)+\frac{h_1A}{k\lambda}\sin(\lambda c)\right) \tag{5.9}$$

which results in eigenvalues of the system [23],

$$\tan(\lambda_n c)=\frac{\lambda_n\left(\frac{h_1}{k}+\frac{h_2}{k}\right)}{\lambda_n^2-\frac{h_1h_2}{k^2}} \qquad n=1,2,3,\cdots. \tag{5.10}$$

The general solution can be written in the following form:

$$\theta(x,z)=\sum_{n=1}^{\infty}\left(\cos\left(\lambda_n x\right)+\frac{h_1}{k\lambda_n}\sin\left(\lambda_n x\right)\right)\left(C_n\cosh\left(\lambda_n z\right)+D_n\sinh\left(\lambda_n z\right)\right). \tag{5.11}$$

Applying the boundary condition along the bottom of the channel, Eq. (5.6), results,

$$C_n=-D_n\left(\frac{\lambda_n\cosh(\lambda_n t)+\frac{h_s}{k}\sinh(\lambda_n t)}{\lambda_n\sinh(\lambda_n t)+\frac{h_s}{k}\cosh(\lambda_n t)}\right)=-D_n\phi_n \tag{5.12}$$

and the spreading function, ϕ_n, is defined as follows:

$$\phi_n=\frac{\lambda_n+\frac{h_s}{k}\tanh(\lambda_n t)}{\lambda_n\tanh(\lambda_n t)+\frac{h_s}{k}}. \tag{5.13}$$

Now, the general solution can be written as,

$$\theta(x,z)=\sum_{n=1}^{\infty}D_n\left(\cos(\lambda_n x)+\frac{h_1}{k\lambda_n}\sin(\lambda_n x)\right)\left(\sinh(\lambda_n z)-\phi_n\cosh(\lambda_n z)\right). \tag{5.14}$$

The boundary condition along the source plane, Eq. (5.3), is the last boundary condition that is applied,

$$\left.\frac{\partial\theta}{\partial z}\right|_{z=0} = \sum_{n=1}^{\infty} D_n\left(\lambda_n\cos\left(\lambda_n x\right)+\frac{h_1}{k}\sin\left(\lambda_n x\right)\right)=0, \qquad 0<x<x_1, \tag{5.15}$$
$$\left.\frac{\partial\theta}{\partial z}\right|_{z=0} = \sum_{n=1}^{\infty} D_n\left(\lambda_n\cos\left(\lambda_n x\right)+\frac{h_1}{k}\sin\left(\lambda_n x\right)\right)=-\frac{q}{k}, \qquad x_1<x<x_2,$$
$$\left.\frac{\partial\theta}{\partial z}\right|_{z=0} = \sum_{n=1}^{\infty} D_n\left(\lambda_n\cos\left(\lambda_n x\right)+\frac{h_1}{k}\sin\left(\lambda_n x\right)\right)=0, \qquad x_2<x<c.$$

The eigenfunction is defined as,

$$X=\lambda_n\cos\left(\lambda_n x\right)+\frac{h_1}{k}\sin\left(\lambda_n x\right). \tag{5.16}$$

This function is not orthogonal and as a result the orthogonality property cannot be used without using a weight function, $N(\lambda_n)$. The weight function is defined as,

$$N(\lambda_n)=\int_0^c X_n^2 dx. \tag{5.17}$$

By considering the method of separation of variables, the differential equation for X is,

$$X''+\lambda_n^2 X=0, \qquad 0<x<c. \tag{5.18}$$

where primes denote differentiation with respect to x. Therefore,

$$X=A\cos(\lambda_n x)+B\sin(\lambda_n x), \tag{5.19}$$
$$X''=-A\lambda_n^2\cos(\lambda_n x)-B\lambda_n^2\sin(\lambda_n x). \tag{5.20}$$

and,

$$X = -\frac{1}{\lambda_n^2} X''. \tag{5.21}$$

As discussed, the weight function is defined as,

$$N(\lambda_n) = \int_0^c X_n^2 dx = -\frac{1}{\lambda_n^2}\int_0^c X_n X_n'' dx = -\frac{1}{\lambda_n^2}\left[X_n X_n'\right]_0^c + \frac{1}{\lambda_n^2}\int_0^c X_n'^2 dx. \tag{5.22}$$

Further, by differentiating the eigenfunction, Eq. (5.16),

$$\frac{1}{\lambda_n} X_n' = -\lambda_n \sin(\lambda_n x) + \frac{h_1}{k}\cos(\lambda_n x). \tag{5.23}$$

Squaring the Eq. (5.16) and Eq. (5.23) and then adding the resulting equations gives,

$$\begin{aligned}(X_n)^2 + (\frac{1}{\lambda_n} X_n')^2 =& \left(\lambda_n \cos(\lambda_n x) + \frac{h_1}{k}\sin(\lambda_n x)\right)^2 + \left(-\lambda_n \sin(\lambda_n x) + \frac{h_1}{k}\cos(\lambda_n x)\right)^2 \\ =& \lambda_n^2 + \left(\frac{h_1}{k}\right)^2.\end{aligned} \tag{5.24}$$

which can be rewritten as,

$$X_n^2 = \lambda_n^2 + \left(\frac{h_1}{k}\right)^2 - \left(\frac{X_n'}{\lambda_n}\right)^2, \tag{5.25}$$

and the weight function takes the form,

$$N(\lambda_n) = \int_0^c X_n^2 dx = \lambda_n^2 c + \left(\frac{h_1}{k}\right)^2 c - \frac{1}{\lambda_n^2}\int_0^c X_n'^2 dx. \tag{5.26}$$

By adding Eq. (5.22) and Eq. (5.26), we obtain,

$$2\,N(\lambda_n) = \lambda_n^2 c + \left(\frac{h_1}{k}\right)^2 c - \frac{1}{\lambda_n^2}\left[X_n X_n'\right]_0^c, \tag{5.27}$$

and after the following substitutions for the eigenfunction and its derivative,

$$X_n\Big|_{x=0} = \lambda_n \qquad\qquad X_n'\Big|_{x=0} = \frac{h_1}{k}\lambda_n. \tag{5.28}$$

Further, in the right edge of the channel, $x = c$,

$$\frac{\partial X}{\partial x} = -\frac{h_2}{k}X \qquad \rightarrow \qquad X_n X_n'\Big|_{x=c} = -\frac{h_2}{k}X_n^2\Big|_{x=c} \tag{5.29}$$

The results of Eq. (5.28) and Eq. (5.29) are used to evaluate $\left[X_n X_n'\right]_0^c$ as follows,

$$\left[X_n X_n'\right]_0^c = -\frac{h_2}{k}X_n^2\Big|_{x=c} - \lambda_n^2\frac{h_1}{k}. \tag{5.30}$$

Using the boundary condition at the right edge, $x = c$, and Eq. (5.24), gives,

$$X_n' = -\frac{h_2}{k}X_n \qquad \text{and} \qquad X_n^2 = \frac{\lambda_n^2 + \left(\frac{h_1}{k}\right)^2}{1 + \frac{h_2^2}{\lambda_n^2 k^2}}. \tag{5.31}$$

This equation is substituted in the Eq. (5.30),

$$\left[X_n X_n'\right]_0^c = -\frac{h_2\left(\lambda_n^2 + \left(\frac{h_1}{k}\right)^2\right)}{k\left(1 + \frac{h_2^2}{\lambda_n^2 k^2}\right)} - \lambda_n^2\frac{h_1}{k} \tag{5.32}$$

and the result is used in Eq. (5.27). Therefore, the weight function can be defined as follows:

$$N(\lambda_n) = \frac{1}{2}\left[\left(\lambda_n^2 + \left(\frac{h_1}{k}\right)^2\right)\left(c + \frac{\left(\frac{h_2}{k}\right)}{\lambda_n^2 + \left(\frac{h_2}{k}\right)^2}\right) + \frac{h_1}{k}\right]. \tag{5.33}$$

By using the above weight function, the orthogonality condition is now satisfied,

$$\int_0^c D_n \left(\lambda_n \cos(\lambda_n x) + \frac{h_1}{k}\sin(\lambda_n x)\right)^2 N(\lambda_n)dx = -\frac{q}{k}\int_{x_1}^{x_2} N(\lambda_n)\left(\lambda_n \cos(\lambda_n x) + \frac{h_1}{k}\sin(\lambda_n x)\right)dx. \tag{5.34}$$

Then, D_n can be calculated as,

$$D_n = \frac{4q\left[-h_1\cos(x_1\lambda_n) + h_1\cos(x_2\lambda_n) + k\lambda_n(\sin(x_1\lambda_n) - \sin(x_2\lambda_n))\right]}{2\lambda_n(ch_1^2 + h_1k + ck^2\lambda_n^2) - 2h_1k\lambda_n\cos(2c\lambda_n) + (k^2\lambda_n^2 - h_1^2)\sin(2c\lambda_n)}. \tag{5.35}$$

Now, the Eq. (5.14) can be written as follows:

$$\theta(x,z) = \sum_{n=1}^{\infty}\left(\frac{4q\left[-h_1\cos(x_1\lambda_n) + h_1\cos(x_2\lambda_n) + k\lambda_n(\sin(x_1\lambda_n) - \sin(x_2\lambda_n))\right]}{2\lambda_n(ch_1^2 + h_1k + ck^2\lambda_n^2) - 2h_1k\lambda_n\cos(2c\lambda_n) + (k^2\lambda_n^2 - h_1^2)\sin(2c\lambda_n)}\right) \left(\cos(\lambda_n x) + \frac{h_1}{k\lambda_n}\sin(\lambda_n x)\right)\left(\sinh(\lambda_n z) - \phi_n\cosh(\lambda_n z)\right). \tag{5.36}$$

The thermal resistance can be calculated as follows:

$$R_t = \frac{\overline{\theta}_{source}}{Q}, \tag{5.37}$$

$$\overline{\theta}_{source} = \frac{\int_{x_1}^{x_2}\theta(x,0)dx}{(x_2 - x_1)}, \tag{5.38}$$

$$Q = q(x_2 - x_1)d. \tag{5.39}$$

$\overline{\theta}_{source}$ is calculated to be,

$$\overline{\theta}_{source} = \sum_{n=1}^{\infty} \frac{4q(k\lambda_n + h_s \tanh(\lambda_n t))}{k(x_2 - x_1)\lambda_n^2 (h_s + k\lambda_n \tanh(\lambda_n t))} \times \frac{\left[h_1 \cos(x_1\lambda_n) - h_1 \cos(x_2\lambda_n) + k\lambda_n (\sin(x_2\lambda_n) - \sin(x_1\lambda_n))\right]^2}{\left[2\lambda_n(ch_1^2 + h_1 k + ck^2\lambda_n^2) - 2h_1 k\lambda_n \cos(2c\lambda_n) + (k^2\lambda_n^2 - h_1^2)\sin(2c\lambda_n)\right]}. \tag{5.40}$$

Finally, the total thermal resistance is defined as,

$$R_t = \sum_{n=1}^{\infty} \frac{4(k\lambda_n + h_s \tanh(\lambda_n t))}{kd\lambda_n^2 (x_1 - x_2)^2 (h_s + k\lambda_n \tanh(\lambda_n t))} \times \frac{\left[h_1 \cos(x_1\lambda_n) - h_1 \cos(x_2\lambda_n) + k\lambda_n (\sin(x_2\lambda_n) - \sin(x_1\lambda_n))\right]^2}{\left[2\lambda_n(ch_1^2 + h_1 k + ck^2\lambda_n^2) - 2h_1 k\lambda_n \cos(2c\lambda_n) + (k^2\lambda_n^2 - h_1^2)\sin(2c\lambda_n)\right]}. \tag{5.41}$$

The dimensionless thermal resistance can be defined as,

$$R_t^* = k(x_2 - x_1)R_t. \tag{5.42}$$

This new solution is general and can model the non-symmetrical flux channel with different heat transfer coefficient along each edge and sink plane. Further, the solution can model the adiabatic boundary condition in each edge or even along the bottom plane. The only required change is that the value of the heat transfer coefficient should set to a small number for the adiabatic boundary condition, i.e. $h \to 0$, and not $h = 0$.

5.2.2 Orthotropic Systems

For an orthotropic system with different in-plane and through plane thermal conductivity, $k_x = k_y = k_{xy} \neq k_z$, the Laplace equation, Eq. (5.1), has the following form:

$$k_{xy}\frac{\partial^2 T}{\partial x^2} + k_z \frac{\partial^2 T}{\partial z^2} = 0 \qquad 0 < z < t. \tag{5.43}$$

This equation and associated boundary conditions can be transformed to the discussed isotropic system using the method of stretched coordinates [13, 18]. The schematic view of the transformation from an orthotropic system to an isotropic system is shown in Fig. 5.2.

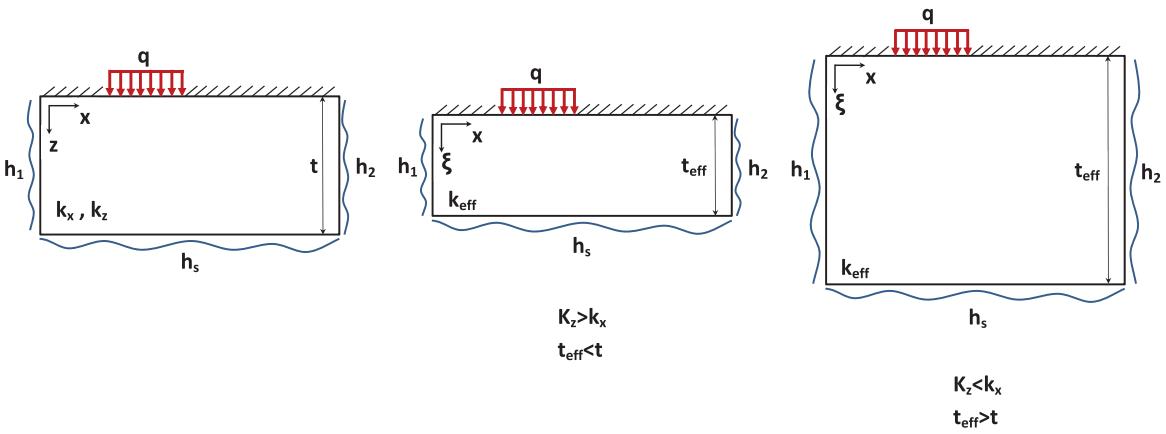

Figure 5.2: Transformation of an orthotropic system to an isotropic system.

The method of stretched coordinates is applied to the system. Application of the following transformation simplifies the Laplace equation,

$$\xi = \frac{z}{\sqrt{\frac{k_z}{k_{xy}}}}. \tag{5.44}$$

The effective isotropic properties are as follows:

$$k_{eff} = \sqrt{k_{xy} k_z}, \qquad t_{eff} = \frac{t}{\sqrt{\frac{k_z}{k_{xy}}}}. \tag{5.45}$$

By using the effective isotropic properties and defining $\theta = T - T_f$, Eq. (5.43) becomes,

$$\frac{\partial^2 \theta}{\partial x^2} + \frac{\partial^2 \theta}{\partial \xi^2} = 0 \qquad 0 < \xi < t_{eff}. \tag{5.46}$$

The boundary conditions are also transformed. The boundary condition along the source plane is,

$$\left.\frac{\partial\theta}{\partial\xi}\right|_{\xi=0} = 0, \qquad 0 < x < x_1, \tag{5.47}$$

$$-k_{eff}\left.\frac{\partial\theta}{\partial\xi}\right|_{\xi=0} = q, \qquad x_1 < x < x_2,$$

$$\left.\frac{\partial\theta}{\partial\xi}\right|_{\xi=0} = 0, \qquad x_2 < x < c.$$

Along the edges of the system,

$$k_{eff}\left.\frac{\partial\theta}{\partial x}\right|_{x=0} = h_1\theta, \tag{5.48}$$

$$-keff\left.\frac{\partial\theta}{\partial x}\right|_{x=c} = h_2\theta. \tag{5.49}$$

The boundary condition along the bottom of the flux channel, $\xi = t_{eff}$, is defined as,

$$-k_{eff}\left.\frac{\partial\theta}{\partial\xi}\right|_{\xi=t_{eff}} = h_s\theta. \tag{5.50}$$

The transformed governing equation and boundary conditions have the same form as the governing equation and boundary conditions of the isotropic system. Therefore, the same procedure can be used for solving the orthotropic system. The only differences are the thermal conductivity, k, and the thickness, t, should be transformed to the effective thermal conductivity, k_{eff}, and the effective thickness, t_{eff}. The total thermal resistance for the orthotropic system can be written as follows:

$$R_t = \sum_{n=1}^{\infty} \frac{4(k_{eff}\lambda_n + h_s \tanh(\lambda_n t_{eff}))}{k_{eff}\, d\, \lambda_n^2\, (x_1 - x_2)^2\, (h_s + k_{eff}\, \lambda_n\, \tanh(\lambda_n t_{eff}))} \times \frac{[h_1 \cos(x_1\lambda_n) - h_1 \cos(x_2\lambda_n) + k_{eff}\, \lambda_n\, (\sin(x_2\lambda_n) - \sin(x_1\lambda_n))]^2}{[2\lambda_n(c\, h_1^2 + h_1\, k_{eff} + c\, k_{eff}^2\, \lambda_n^2) - 2\, h_1\, k_{eff}\, \lambda_n\, \cos(2c\lambda_n) + (k_{eff}^2\, \lambda_n^2 - h_1^2)\, \sin(2c\lambda_n)]}. \tag{5.51}$$

The dimensionless thermal resistance can be calculated using Eq. (5.42) by substituting the equivalent thermal resistance in the orthotropic systems.

5.3 Results and Discussion

This section considers the thermal resistance of a non-symmetrical flux channel with different conductance along the edges. Three different cases are investigated including: different heat transfer coefficients along the left and right edges and the heat sink plane, an adiabatic boundary condition along the right edge of the channel, and an adiabatic boundary condition along the bottom surface of the channel. For these three cases, the source dimension increases to investigate its effect on dimensionless thermal resistance. All results are compared with FEM using COMSOL commercial software package.

The geometry of the flux channel are $c = d = 0.02\,m$ and $t = 0.001\,m$. Some arbitrary properties are used for modeling the three case studies. The properties of the channel for the first case study are $k = 2\ W/mK$, $h_1 = 100\ W/m^2K$, $h_2 = 200\ W/m^2K$ and $h_s = 300\ W/m^2K$. The position of the left edge of the source is assumed $x_1 = 0.002\,m$ and the position of the right edge of the source varies from $x_2 = 0.004\,m$ to $x_2 = 0.018\,m$ with an increment of $0.002\,m$. The dimensionless thermal resistance for different source dimensions is shown in Fig. 5.3.

The flexibility of the proposed approach is shown by considering some other case studies. For the second case study, the right edge of the channel is assumed adiabatic. For mod-

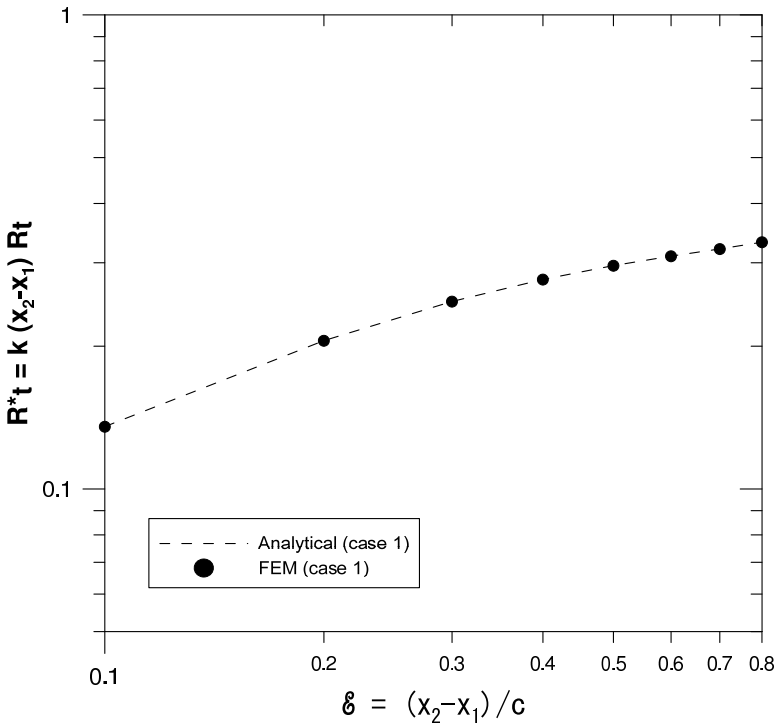

Figure 5.3: Dimensionless thermal resistance for the 1^{st} case study ($h_1 = 100\ W/m^2K$, $h_2 = 200\ W/m^2K$ and $h_s = 300\ W/m^2K$).

eling the adiabatic boundary condition, the heat transfer coefficient along the right edge is assumed $h_2 = 0.01\ W/m^2K$. Dimensionless thermal resistance of the channel is shown in Fig. 5.4.

The third case study is for a flux channel with an adiabatic boundary condition along the bottom plane. The heat transfer coefficients are $h_1 = 100\ W/m^2K$, $h_2 = 200\ W/m^2K$ and $h_s = 0.01\ W/m^2K$. The dimensionless thermal resistance for this case study is shown in Fig. 5.5.

By considering the dimensionless thermal resistance for case 1 and case 2, it can be concluded that the convective cooling along the edges almost has no effect in total thermal resistance of thin flux channels if the conductance along the bottom surface is greater than conductance along the edges. However, if the heat transfer coefficient along the bottom plane is small in comparison to the heat transfer coefficient along the edges, the cooling

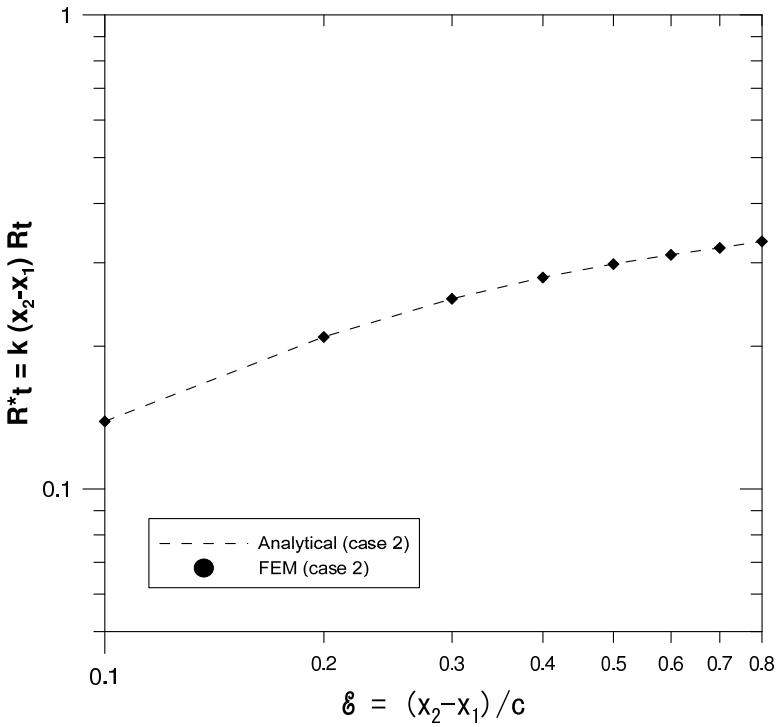

Figure 5.4: Dimensionless thermal resistance for the 2^{nd} case study ($h_1 = 100\ W/m^2K$, $h_2 = 0.01\ W/m^2K$ and $h_s = 300\ W/m^2K$).

along the edges has a significant effect on the thermal resistance of the system even for the thin systems, Fig. 5.5.

The presented analytical solution is in the form of a Fourier series. The convergence of the Fourier series can be checked by increasing the number of terms. A similar approach should be used to check the convergence of the FEM by refining the mesh and increasing the number of free tetrahedral elements. Table 5.1 shows the convergence of both methods for the first case study when $x_2 = 0.004$. For testing the convergence of the Fourier series representation of the solution, six partial sums of the series are used, $\sum_{n=1}^{5}$, $\sum_{n=1}^{10}$, $\sum_{n=1}^{20}$, $\sum_{n=1}^{50}$, $\sum_{n=1}^{90}$, $\sum_{n=1}^{100}$. As can be seen, 90 terms in the series can model the dimensionless thermal resistance of the system with four digits of precision. Further, it shows that even 10 terms can model the dimensionless thermal resistance with two digits of precision. The execution time for 100 terms is 0.16 seconds. Furthermore, the convergence checking of

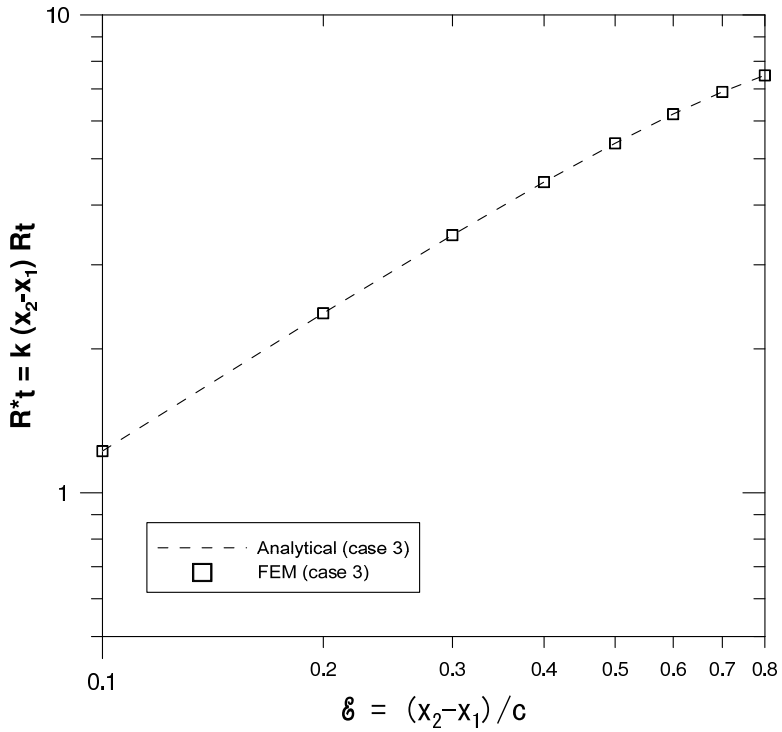

Figure 5.5: Dimensionless thermal resistance for the 3^{rd} case study ($h_1 = 100\ W/m^2K$, $h_2 = 200\ W/m^2K$ and $h_s = 0.01\ W/m^2K$).

FEM shows 95851 elements can model the dimensionless resistance with four digits of precision. The execution time for 226061 elements is 22 seconds. Based on a comparison of the execution time for each method in a converged solution, it is clear that the analytical method is much faster than FEM.

Partial sums of the Fourier series	R_t	R^*_t	Number of tetrahedral elements	R_t	R^*_t
N = 5	26.4967	0.105987	**84**	30.64117	0.122565
N = 10	32.9216	0.131686	**842**	33.60173	0.134407
N = 20	33.6721	0.134689	**1373**	33.642	0.134568
N = 50	33.8178	0.135271	**23294**	33.80308	0.135212
N = 90	**33.8405**	**0.135362**	**95851**	**33.83185**	**0.135327**
N = 100	**33.8425**	**0.13537**	**226061**	**33.83789**	**0.135351**

Table 5.1: Checking the convergence of the Fourier series and FEM.

For comparing both analytical and FEM results, the percent difference and mean percent difference for all aspect ratios are presented in Table 5.2. The results of both methods are in

good agreement and the mean percentage difference is less than 0.01% for all three cases.

X_2	h_1=100, h_2=200, h_s=300 Percentage Difference	h_1=0.01, h_2=200, h_s=300 Percentage Difference	h_1=100, h_2=200, h_s=0.01 Percentage Difference
0.004 m	0.031%	0.031%	0.003%
0.006 m	0.012%	0.012%	0.001%
0.008 m	0.008%	0.008%	0.001%
0.01 m	0.006%	0.006%	0.000%
0.012 m	0.006%	0.006%	0.000%
0.014 m	0.005%	0.005%	0.000%
0.016 m	0.004%	0.004%	0.000%
0.018 m	0.004%	0.004%	0.000%
Mean Percentage Difference	**0.01%**	**0.009%**	**0.001%**

Table 5.2: Percent difference for analytical and FEM for three case studies.

For a better understanding of the thermal resistance trend in these three cases, the total thermal resistance for different source sizes is presented in Table 5.3. By increasing the dimensionless source aspect ratio, $\epsilon = (x_2 - x_1)/c$, the total thermal resistance decreases as a result of decreasing the thermal spreading resistance.

Position of x_2		0.004 m	0.006 m	0.008 m	0.01 m	0.012 m	0.014 m	0.016 m	0.018 m
Case 1	Analytical	33.8425	25.6934	20.7127	17.2894	14.7962	12.9112	11.457	10.3595
	FEM	33.8318	25.69	20.7109	17.2882	14.7952	12.9105	11.4564	10.359
Case 2	Analytical	34.7229	26.1688	20.9922	17.4665	14.9157	12.9963	11.5202	10.4082
	FEM	34.7122	26.1654	20.9904	17.4653	14.9148	12.9956	11.5196	10.4077
Case 3	Analytical	305.627	297.071	288.608	279.45	269.421	258.459	246.538	233.643
	FEM	305.6165	297.0681	288.6057	279.4484	269.4199	258.4588	246.5377	233.6426

Table 5.3: Total thermal resistance for different source sizes.

The last validation test is done with published literature about thermal spreading resistance in a flux channel with adiabatic edges [15]. For this purpose, a symmetrical flux channel with different dimensionless source aspect ratios is investigated. The adiabatic condition along the edges of the system is modeled using a small number for the heat transfer coefficient, $h_1 = h_2 = 10^{-10}$. All other geometries and properties are the same as other

presented case studies. The dimensionless thermal resistance versus dimensionless source aspect ratio is shown in Fig. 5.6. A good agreement is observed between both models.

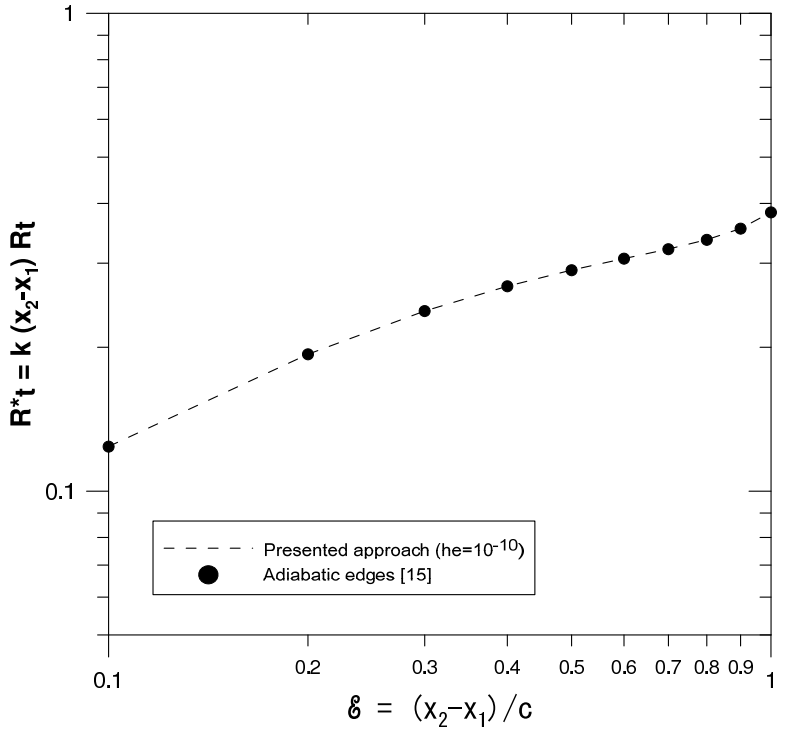

Figure 5.6: Comparison of proposed analytical model with published literature [15] for modeling a symmetrical flux channel with adiabatic edges.

Based on the presented results, the validation for the proposed model is done and it shows this model can solve the thermal resistance problems faster than FEM. Furthermore, this method is more general than previously published literature and can model different conductance along the edges in non-symmetrical flux channels. The proposed approach can even model the flux channels with an adiabatic boundary condition along any of the edges and/or the bottom plane.

5.4 Summary and Conclusions

In this paper, an analytical model is presented for modeling the temperature distribution and thermal resistance of non-symmetrical flux channels with different heat transfer coefficients along each edge and convective cooling along the sink plane. For solving the governing equation, the method of separation of variables is used. Due to different heat transfer coefficients along the edges of the channel, the orthogonality property is not satisfied without a weight function. After some algebra, a weight function is proposed for satisfying the orthogonality property. The temperature distribution in the flux channel is presented in the form of a Fourier series, Eq. (5.36). The proposed method is a general solution for modeling different conductance along the edges and the bottom plane including the adiabatic boundary condition. Different case studies are investigated and results are compared with FEM and other literature. The dimensionless thermal resistance, Eq. (5.42), for four different case studies is illustrated for different source aspect ratios. Based on the results, it can be concluded that the common adiabatic assumption along the edges is valid for thin flux channels with an effective heat sinking along the sink plane. The proposed model is much faster than FEM and can be used as a practical tool for modeling the thermal behavior of flux channels. Thermal engineers just need the Eqs. (5.10, 5.36, 5.40, 5.41) to model the system.

Acknowledgments

The authors acknowledge the financial support of the Natural Sciences and Engineering Research Council of Canada.

5.5 References

[1] COMSOL Multiphysics® Version 4.2a.

[2] Yovanovich, M. M., Muzychka, Y. S., and Culham, J. R., "Spreading Resistance in Isoflux Rectangles and Strips on Compound Flux Channels," *J. Thermophys. Heat Transf.*, vol. 13, no. 4, pp. 495-500, 1999.

[3] Ellison, G. N., "The Thermal Design of an LSI Single-Chip Package," *IEEE Transactions on Parts, Hybrids, and Packaging*, vol. PHP-12, no. 4, Dec. 1976.

[4] Ellison, G. N., "Maximum Thermal Spreading Resistance for Rectangular Sources and Plates with Nonunity Aspect Ratios," *IEEE Trans. Comp. Packag. Tech.*, vol. 26, no. 2, pp. 439-454, Jun. 2003.

[5] Guan, D., Marz, M., and Liang, J., "Analytical Solution of Thermal Spreading Resistance in Power Electronics," *IEEE Transactions on Components, Packaging and Manufacturing Technology*, pp. 278-285, 2012.

[6] Karmalkar, S., Mohan, P. V., Nair, H. P., and Yeluri, R., "Compact Models of Spreading Resistances for Electrical/Thermal Design of Devices and ICs," *IEEE Transactions on Electron Devices*, vol. 54, no. 7, July 2007.

[7] Ying, T. M., and Toh, K. C., "A Heat Spreading Resistance Model for Anisotropic Thermal Conductivity Materials in Electronic Packaging," *Proceedings of the Seventh Intersociety Conf. on Thermal and Thermomechanical Phenomena in Electronic Systems*, edited by G. B. Kromann, J. R. Culham, and K. Ramakrishna, Inst. of Electrical and Electronics Engineers, Piscataway, NJ, pp. 314-321, 2000.

[8] Kim, Y. H., Kim, S. Y., and Rhee, G. H., "Evaluation of Spreading Thermal Resistance for Heat Generating Multi-Electronic Components," *IEEE*, pp. 258-264, 2006.

[9] Culham, J. R., Teertstra, P., and Yovanovich, M. M., "The Role of Spreading Resistance on Effective Conductivity in Laminated Substrates," *Future Circuits*, vol. 6., pp. 73-78, 2000.

[10] Culham, J. R., Khan, W., Yovanovich, M. M., and Muzychka, Y. S., "The Influence of Material Properties and Spreading Resistance in the Thermal Design of Plate Fin Heat Sinks," *ASME Journal of Electronic Packaging*, vol. 129, pp. 76-81, March, 2007.

[11] Lasance, C. J. M., "How to Estimate Heat Spreading Effects in Practice," *Journal of Electronic Packaging*, vol. 132, September 2010.

[12] Lasance, C. J. M., "Two-layer Heat spreading Approximations Revisited," *28th IEEE Semi-Therm symposium*, pp. 269-274, 2012.

[13] Muzychka, Y. S., Yovanovich, M. M, and Culham, J. R., "Thermal Spreading Resistance in Compound and Orthotropic Systems," *Journal of Thermophysics and Heat Transfer*, vol. 18, no. 1, January-March 2004.

[14] Muzychka, Y. S. and Yovanovich, M. M., "Thermal Resistance Models for Non-Circular Moving Heat Sources on a Half Space," *Journal of Heat Transfer*, vol. 123, pp. 624-632, August 2001.

[15] Muzychka, Y. S., Culham, J. R., and Yovanovich, M. M., "Thermal Spreading Resistance of Eccentric Heat Sources on Rectangular Flux Channels," *Journal of Electronic Packaging*, vol. 125, pp. 178-185, June 2003.

[16] Muzychka, Y. S., Stevanovic, M., and Yovanovich, M. M., "Thermal Spreading Resistances in Compound Annular Sectors," *Journal of Thermophysics and Heat Transfer*, vol. 15, no. 3, pp. 354-359, 2001.

[17] Muzychka, Y. S., "Influence Coefficient Method for Calculating Discrete Heat Source Temperature on Finite Convectively Cooled Substrates," *IEEE Transactions on Components and Packaging Technologies*, vol. 29, no. 3, pp. 636-643, Sep. 2006.

[18] Muzychka, Y. S., Bagnall, K. R., and Wang, E. N., "Thermal Spreading Resistance and Heat Source Temperature in Compound Orthotropic Systems With Interfacial resistance," *IEEE Transactions on Components, Packaging, and Manufacturing Technology*, vol. 3. no. 11, pp. 1826-1841, November, 2013.

[19] Muzychka, Y. S., Yovanovich, M. M., and Culham, J. R., "Influence of Geometry and Edge Cooling on Thermal Spreading Resistance," *AIAA Journal of Thermophysics and Heat Transfer*, vol. 20. no. 2, pp. 247-255, April-June, 2006.

[20] Bagnall, K., Muzychka, Y.S., and Wang, E., "Application of the Kirchhoff Transform to Thermal Spreading Problems with Convection Boundary Conditions", *IEEE Transactions on Components, Packaging and Manufacturing Technologies*, 2013.

[21] Yovanovich, M. M., and Marotta, E. E., "Thermal Spreading and Contact Resistances," in *Heat Transfer Handbook*, A. Bejan, and A. D. Kraus, Eds. New York: Wiley, ch. 4, pp. 261-393, 2003.

[22] Yovanovich, M. M., "Four Decades of Research on Thermal Contact, Gap and Joint Resistance in Microelectronics," *IEEE Transactions on Components and Packaging Technologies*, vol. 28, no. 2, pp. 182-206, 2005.

[23] Necati Ozisik , M., "Heat Conduction-2nd ed.," A Wiley-Interscience Publication, 1993.

[24] Matlab, The Language of Technical Computing, R2012a.

Chapter 6

Thermal Behavior of Rectangular Flux Channels with Discretely Specified Contact Flux and Temperature

M. Razavi
Y.S. Muzychka

Department of Mechanical Engineering, Memorial University of Newfoundland, St. John's, NL, Canada, A1B 3X5

S. Kocabiyik

Department of Mathematics and Statistics, Memorial University of Newfoundland, St. John's, NL, Canada, A1C 5S7

Abstract

An analytical approach for the thermal behavior of two dimensional rectangular flux channels with arbitrary boundary conditions on the source plane is presented. The boundary condition along the source plane can be a combination of the first kind boundary condition (Dirichlet or prescribed temperature) and the second kind boundary condition (Neumann or prescribed heat flux). For modeling the boundary conditions along the source plane, the method of least squares is used. The proposed solution is in the form of Fourier series expansion and can be applied to both symmetrical and non-symmetrical channels. This method is more general than other approaches and there is no need to use equivalent heat

[1]InterPACKICNMM2015, the ASME 2015 International Technical Conference and Exhibition on Packaging and Integration of Electronic and Photonic Microsystems and ASME 2015 12th International Conference on Nanochannels, Microchannels, and Minichannels, San Francisco, California.

flux distributions to model isothermal heat sources. The general approach for obtaining the multidimensional temperature profile in flux channels and the advantages of the least squares method is discussed. The proposed solution can be used to calculate the temperature at any specified point in the flux channel. Two case studies are presented. The first case study is a flux channel with five discretely specified contact temperature along the source plane. The second case study has both the first kind and second kind boundary conditions on the source plane. The analytical results for both systems are compared with FEM results using COMSOL multiphysics commercial software package [1]. It is shown that the proposed approach can precisely model the temperature profile over the flux channel. The proposed model can be used to model the electronic devices with different heat contact boundary condition on the surface.

Keywords: Heat Conduction, Temperature Profile, Thermal Resistance, Least Squares Method

6.1 Introduction

Temperature profile and thermal resistance in electronic devices are of interest to thermal engineers for designing an effective thermal management system. Thermal resistance consists of one dimensional resistance and thermal spreading resistance. Thermal spreading resistance is the main source of thermal resistance in some electronic devices and occurs when heat flows from a portion of a surface and flows by conduction. If there is just one source in the source plane, the thermal spreading resistance can be exactly calculated using the difference between the total thermal resistance and one dimensional thermal resistance. However, the exact value for thermal spreading resistance cannot be calculated when there is more than one heat source since the resistance of anyone source will depend on the proximity and strength of a neighboring source. For the flux channels with multiple heat sources,

the temperature profile along the system is useful for designing the proper thermal management system. For modeling the temperature profile along the system, the electronic devices usually assumed as some common geometries such as flux channels (cubical geometries) or flux tubes (cylinders). Due to the variety of applied boundary conditions in the flux channels and tubes, different analytical and numerical models were proposed according to the specified boundary conditions, geometries, and properties.

Research on thermal spreading resistance starts with Kennedy [2] who worked on spreading resistance in semiconductor devices. Lee et al. [3] and Song et al. [4] proposed an analytical model for spreading resistance in electronic devices with different heat sinking. Ellison [5] used theoretical and empirical methods for obtaining thermal characteristics of a forced-convection cooled ceramic package with an extruded aluminum heat sink. Also, Ellsion [6-8] analytically studied the thermal modeling of printed circuit boards and microelectronic packages such as discrete patches of heat flux on rectangular multi-layer devices. Kokkas [9] analytically studied the thermal behavior of multi-layer structures and the insulated semiconductor chip. Lemczyk et al. [10-13] studied the thermal constriction resistance with convective boundary condition for half-space contacts and thermal analysis of three-dimensional conjugate heat transfer problems.

Muzychka et al. [14-21] worked on different aspects of thermal spreading resistance. They presented a solution for the thermal constriction resistance of an isoflux or isothermal planar heat source in contact with multilayered semi-infinite flux tube with application in conductive coatings [14, 15]. Also, they obtained thermal spreading resistance of circular flux tubes and rectangular flux channels for isotropic and compound systems and modeled the rectangular flux channel using the circular flux tube's solution using suitable geometric equivalence. They also considered the effect of edge cooling on the thermal spreading resistance in circular flux tubes and rectangular flux channels [16]. Further, they proposed a solution for the thermal spreading resistance of eccentric isoflux rectangular heat sources

on finite rectangular compound flux channels [17, 18]. Muzychka [19] presented an influence coefficient method for calculating the mean and centroidal temperature of discrete heat sources on a finite convectively cooled substrate by considering isotropic, orthotropic, and compound systems. The convection in the source plane which causes heat dissipation through the source plane was considered. Muzychka et al. [20, 21] modeled the thermal spreading resistance in compound orthotropic systems with interfacial resistance. Bagnall et al. [22, 23] modeled the systems with temperature dependent thermal conductivity and multi-layer structures. Recently, Razavi et al. [24-26] studied the thermal spreading resistance problems in two dimensional flux channels and modeled the thermal behavior of channels with a non-uniform heat convection along the sink plane. Yovanovich [27] has researched over four decades on solutions of thermal spreading resistance problems.

Although numerous researches have been done on different aspects of thermal spreading resistance problems, there are still some gaps in this subject. For example, some of the boundary conditions were simplified in order to be easily solved by analytical methods. One of these boundary conditions is the specified heat source temperature that was modeled as a general expression equivalent to the isothermal flux distribution [28, 29]. This model has some limitations including the contact ratio of the heat source and the channel. Also, it can just model one source over the channel. In this paper, a more general model for thermal bahaviour of convective cooled flux channel with different boundary conditions along the source plane is presented. The source plane boundary conditions can be a combination of discrete heat fluxes, specified temperatures, and adiabatic conditions. Also, no equivalent flux distribution is used for modeling the isothermal sources. For solving the problem and modeling the thermal behavior of the system, the method of separation of variables and the least squares technique are used.

6.2 Problem Statement

Two common geometries in semi-conductor devices are flux tubes and flux channels. In this article, a rectangular flux channel with discrete boundary conditions that are arbitrarily specified along the source plane is studied. Convective cooling exist in the sink plane. The edges of the channel are adiabatic. The proposed method can solve both symmetrical and non-symmetrical channels with the mentioned boundary conditions, Fig. 6.1 and Fig. 6.2. Two case studies are considered. The first case study is a channel with discretely specified contact temperatures along the source plane, Fig. 6.1a and Fig. 6.2a, and the second case study has a combination of arbitrary specified flux, temperature, and adiabatic conditions along the source plane, Fig. 6.1b and Fig. 6.2b.

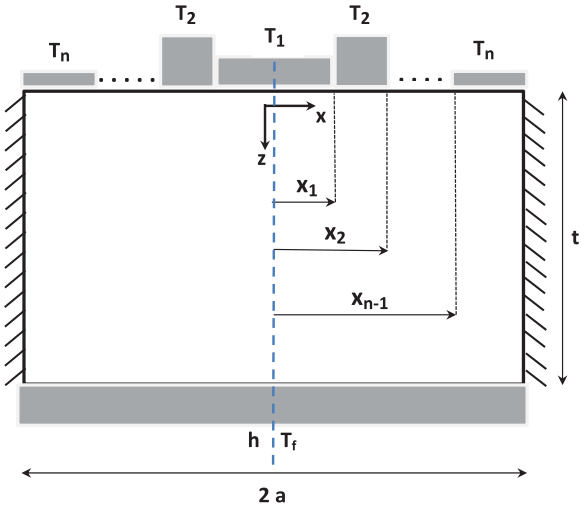

(a) Discretely specified contact temperatures along the source plane.

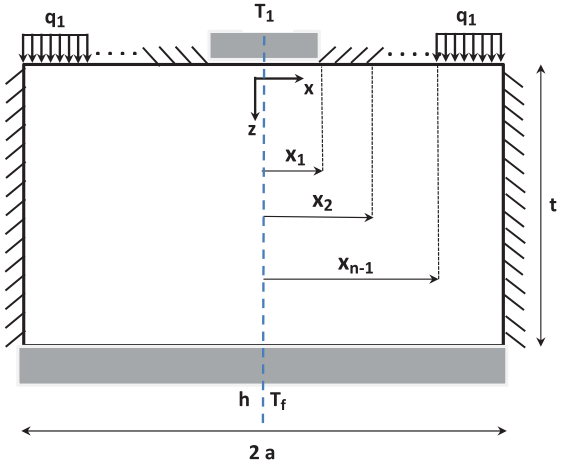

(b) Discretely specified temperature, heat flux, and adiabatic conditions along the source plane.

Figure 6.1: 2D symmetrical flux channel.

Temperature profile is obtained by solving the Laplace equation:

$$\frac{\partial^2 T}{\partial x^2} + \frac{\partial^2 T}{\partial z^2} = 0, \tag{6.1}$$

or, by defining $\theta = T - T_f$:

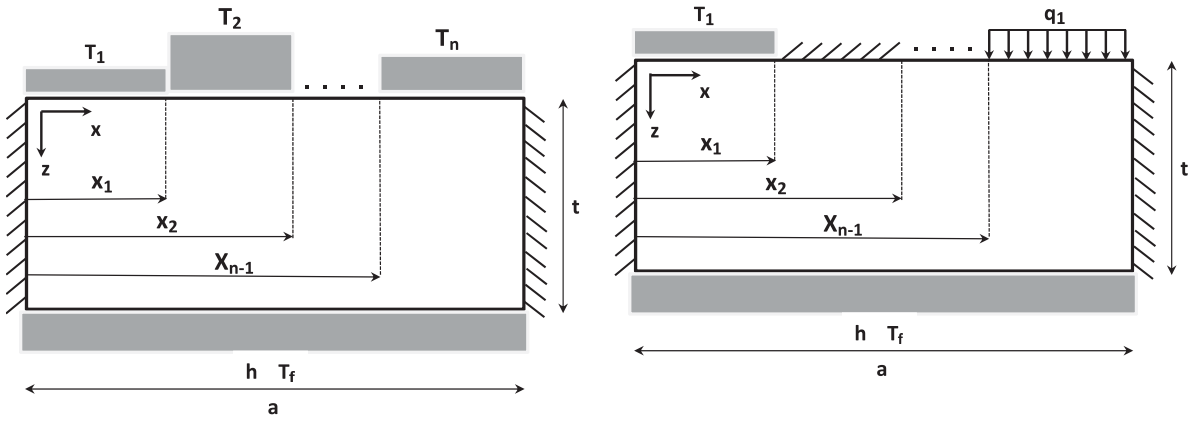

(a) Discretely specified contact temperatures along the source plane.

(b) Discretely specified temperature, heat flux, and adiabatic conditions along the source plane.

Figure 6.2: 2D non-symmetrical flux channel.

$$\frac{\partial^2\theta}{\partial x^2} + \frac{\partial^2\theta}{\partial z^2} = 0. \tag{6.2}$$

Along the source plane, the boundary condition for the first case study, Fig 6.1a and Fig 6.2a, is as follows:

$$\theta = \theta_1 \qquad 0 < x < x_1, \qquad \theta = \theta_2 \qquad x_1 < x < x_2 \qquad ... \qquad \theta = \theta_n \qquad x_{n-1} < x < a. \tag{6.3}$$

and for the second case study, Fig. 6.1b and Fig 6.2b:

$$\begin{aligned} \theta &= \theta_1 \qquad 0 < x < x_1, \\ -k\frac{\partial\theta}{\partial z} &= 0 \qquad x_1 < x < x_2, \\ &\vdots \\ -k\frac{\partial\theta}{\partial z} &= q_1 \qquad x_{n-1} < x < a. \end{aligned} \tag{6.4}$$

The boundary conditions along the center line in Fig. 6.1 and first edge in Fig. 6.2 are:

$$\left.\frac{\partial\theta}{\partial x}\right|_{x=0} = 0. \tag{6.5}$$

Also, the edges of the channels, $x = a$, for both cases are adiabatic,

$$\left.\frac{\partial\theta}{\partial x}\right|_{x=a} = 0. \tag{6.6}$$

In the sink plane, $z = t$, the constant heat transfer coefficient represents the convective cooling condition,

$$\left.\frac{\partial\theta}{\partial z}\right|_{z=t} = -\frac{h}{k}\theta. \tag{6.7}$$

The Laplace equation, Eq. (6.2), is solved using separation of variables method and prescribed boundary conditions. The general solution of the Laplace equation has the following form:

$$\theta(x,z) = A_0 + B_0 z + \sum_{n=1}^{\infty} \cos(\lambda_n x)[C_n \cosh(\lambda_n z) + D_n \sinh(\lambda_n z)]. \tag{6.8}$$

By applying the boundary condition at $x = a$ and by defining $\delta_n = \lambda_n a$, the eigenvalues of the system are stated as follows:

$$\lambda_n = \frac{n\pi}{a} \qquad \Rightarrow \qquad \delta_n = n\pi \qquad\qquad n = 1, 2, 3, \cdots . \tag{6.9}$$

Now, the sink boundary condition is applied and deduced:

$$A_0 = -B_0 \left(t + \frac{k}{h}\right), \tag{6.10}$$

$$C_n = -D_n \left(\frac{\lambda_n \cosh(\lambda_n t) + \frac{h}{k} \sinh(\lambda_n t)}{\lambda_n \sinh(\lambda_n t) + \frac{h}{k} \cosh(\lambda_n t)} \right) = -D_n \phi_n. \tag{6.11}$$

The spreading function, ϕ_n, is defined as follows:

$$\phi_n = \frac{\delta_n + Bi \tanh(\delta_n \tau)}{\delta_n \tanh(\delta_n \tau) + Bi}, \tag{6.12}$$

where $Bi = \frac{ha}{k}$ and $\tau = \frac{t}{a}$. Therefore,

$$\theta(x,z) = -B_0 \left(t + \frac{k}{h} - z \right) + \sum_{n=1}^{\infty} D_n \cos(\lambda_n x) \Big(\sinh(\lambda_n z) - \phi_n \cosh(\lambda_n z) \Big). \tag{6.13}$$

To obtain the unknown constants, B_0 and D_n, the source plane boundary condition is used. For the case of arbitrarily specified contact temperatures in the different regions of the source plane, Fig. 6.1a and Fig. 6.2a, source plane boundary condition, Eq. (6.3), is applied to the general form of solution, Eq. (6.13).

$$\begin{aligned}
-B_0 \left(t + \frac{k}{h} \right) - \sum_{n=1}^{\infty} D_n \phi_n \cos(\lambda_n x) &= \theta_1 \qquad 0 < x < x_1, \\
-B_0 \left(t + \frac{k}{h} \right) - \sum_{n=1}^{\infty} D_n \phi_n \cos(\lambda_n x) &= \theta_2 \qquad x_1 < x < x_2, \\
&\vdots \\
-B_0 \left(t + \frac{k}{h} \right) - \sum_{n=1}^{\infty} D_n \phi_n \cos(\lambda_n x) &= \theta_n \qquad x_{n-1} < x < a.
\end{aligned} \tag{6.14}$$

For the case of arbitrary specified heat flux, temperature, and adiabatic boundary conditions, Fig. 6.1b and Fig. 6.2b, Eq. (6.4) is applied to the general form of solution, Eq. (6.13) and results:

$$\theta = -B_0\left(t+\frac{k}{h}\right) - \sum_{n=1}^{\infty} D_n\phi_n\cos(\lambda_n x) = \theta_1 \qquad 0<x<x_1, \tag{6.15}$$
$$-k\frac{\partial\theta}{\partial z} = -k\left(B_0 + \sum_{n=1}^{\infty} D_n\lambda_n\cos(\lambda_n x)\right) = 0 \qquad x_1<x<x_2,$$
$$\vdots$$
$$-k\frac{\partial\theta}{\partial z} = -k\left(B_0 + \sum_{n=1}^{\infty} D_n\lambda_n\cos(\lambda_n x)\right) = q_1 \qquad x_{n-1}<x<a.$$

For more simplicity, the naming of the coefficients D_n in Eqs. (6.13- 6.15) can be changed to B_n . Therefore, Eq. (6.14) can be written as follows, [30],

$$\sum_{m=0}^{\infty} B_m\rho_m\psi_m(x) = \theta_1 \qquad 0<x<x_1, \tag{6.16}$$
$$\sum_{m=0}^{\infty} B_m\varphi_m\psi_m(x) = \theta_2 \qquad x_1<x<x_2,$$
$$\vdots$$
$$\sum_{m=0}^{\infty} B_m\vartheta_m\psi_m(x) = \theta_n \qquad x_{n-1}<x<a,$$

where,

$$0<x<x_1 \rightarrow \quad \begin{cases} \rho_m = \begin{cases} -(t+\frac{k}{h}), & m=0 \\ -\phi_m, & m=1,2,... \end{cases} \\ \psi_m(x) = \cos(\lambda_m x) \end{cases}, \tag{6.17}$$

$$x_1 < x < x_2 \rightarrow \quad \begin{cases} \varphi_m = \begin{cases} -(t+\frac{k}{h}), & m=0 \\ -\phi_m, & m=1,2,... \end{cases} \\ \psi_m(x) = \cos(\lambda_m x) \end{cases} , \tag{6.18}$$

$$\vdots$$

$$x_{n-1} < x < a \rightarrow \quad \begin{cases} \vartheta_m = \begin{cases} -(t+\frac{k}{h}), & m=0 \\ -\phi_m, & m=1,2,... \end{cases} \\ \psi_m(x) = \cos(\lambda_m x) \end{cases} . \tag{6.19}$$

and Eq. (6.15) can be written as follows,

$$\begin{aligned} \sum_{m=0}^{\infty} B_m \rho_m \psi_m(x) &= \theta_1 && 0 < x < x_1, \\ \sum_{m=0}^{\infty} B_m \varphi_m \psi_m(x) &= 0 && x_1 < x < x_2, \\ &\vdots \\ \sum_{m=0}^{\infty} B_m \vartheta_m \psi_m(x) &= q_1 && x_{n-1} < x < a, \end{aligned} \tag{6.20}$$

where,

$$0 < x < x_1 \rightarrow \quad \begin{cases} \rho_m = \begin{cases} -(t + \frac{k}{h}), & m = 0 \\ -\phi_m, & m = 1, 2, ... \end{cases} \\ \psi_m(x) = \cos(\lambda_m x) \end{cases}, \tag{6.21}$$

$$x_1 < x < x_2 \rightarrow \quad \begin{cases} \varphi_m = \begin{cases} -k, & m = 0 \\ -k\lambda_m, & m = 1, 2, ... \end{cases} \\ \psi_m(x) = \cos(\lambda_m x) \end{cases}, \tag{6.22}$$

$$\vdots$$

$$x_{n-1} < x < a \rightarrow \quad \begin{cases} \vartheta_m = \begin{cases} -k, & m = 0 \\ -k\lambda_m, & m = 1, 2, ... \end{cases} \\ \psi_m(x) = \cos(\lambda_m x) \end{cases}. \tag{6.23}$$

Applying the least squares method, the following integrals are defined in different regions of the heat source plane. For the first case study, Fig. 6.1a and Fig. 6.2a,

$$
\begin{aligned}
I_N = &\int_0^{x_1} \left[\sum_{m=0}^{N} B_m \rho_m \psi_m(x) - \theta_1\right]^2 dx \\
&+ \int_{x_1}^{x_2} \left[\sum_{m=0}^{N} B_m \varphi_m \psi_m(x) - \theta_2\right]^2 dx \\
&\vdots \\
&+ \int_{x_{n-1}}^{a} \left[\sum_{m=0}^{N} B_m \vartheta_m \psi_m(x) - \theta_n\right]^2 dx,
\end{aligned} \tag{6.24}
$$

and for the second case study, Fig. 6.1b and Fig. 6.2b,

$$
\begin{aligned}
I_N = &\int_0^{x_1} \left[\sum_{m=0}^{N} B_m \rho_m \psi_m(x) - \theta_1\right]^2 dx \\
&+ \int_{x_1}^{x_2} \left[\sum_{m=0}^{N} B_m \varphi_m \psi_m(x) - 0\right]^2 dx \\
&\vdots \\
&+ \int_{x_{n-1}}^{a} \left[\sum_{m=0}^{N} B_m \vartheta_m \psi_m(x) - q_1\right]^2 dx.
\end{aligned} \tag{6.25}
$$

The coefficients, B_m, should be calculated in order to minimize the above integrals,

$$
\frac{\partial I_N}{\partial B_m} = 0 \qquad\qquad m = 0, 1, 2, ..., N. \tag{6.26}
$$

For having a more computationally efficient method, the following $N + 1$ algebraic equations can be defined,

$$\begin{aligned} A_{jm} =& \rho_j \rho_m \int_0^{x_1} \psi_j(x)\psi_m(x)\,dx \\ &+\varphi_j \varphi_m \int_{x_1}^{x_2} \psi_j(x)\psi_m(x)\,dx \\ &\vdots \\ &+\vartheta_j \vartheta_m \int_{x_{n-1}}^{a} \psi_j(x)\psi_m(x)\,dx, \end{aligned} \tag{6.27}$$

$$b_j = \rho_j \theta_1 \int_0^{x_1} \psi_j(x)\,dx + \varphi_j \theta_2 \int_{x_1}^{x_2} \psi_j(x)\,dx + ... + \vartheta_j \theta_n \int_{x_{n-1}}^{a} \psi_j(x)\,dx. \tag{6.28}$$

Then ρ_j, ρ_m, φ_j, φ_m, ϑ_j, ϑ_m and $\psi_j(x)$, $\psi_m(x)$ are substituted into Eq. (6.27) and Eq. (6.28) using Eqs. (6.17- 6.19) for the first case, Fig. 6.1a and Fig. 6.2a, or by using Eqs. (6.21-6.23) for the second case, Fig. 6.1b and Fig. 6.2b.

$$\begin{aligned} A_{jm} =& \rho_j \rho_m \int_0^{x_1} \cos(\lambda_j x)\cos(\lambda_m x)\,dx \\ &+\varphi_j \varphi_m \int_{x_1}^{x_2} \cos(\lambda_j x)\cos(\lambda_m x)\,dx \\ &\vdots \\ &+\vartheta_j \vartheta_m \int_{x_{n-1}}^{a} \cos(\lambda_j x)\cos(\lambda_m x)\,dx, \end{aligned} \tag{6.29}$$

$$b_j = \rho_j \theta_1 \int_0^{x_1} \cos(\lambda_j x)\,dx + \varphi_j \theta_2 \int_{x_1}^{x_2} \cos(\lambda_j x)\,dx + ... + \vartheta_j \theta_n \int_{x_{n-1}}^{a} \cos(\lambda_j x)\,dx. \tag{6.30}$$

As a result, a matrix system, $AB = b$, can be easily solved in a mathematical package in order to obtain B_m constants. As mentioned, the coefficients D_n was changed to B_n in Eq. (6.13). Thus, the temperature over the channel is known by substituting obtained B_m coefficients in Eq. (6.13) and the temperature profile along the flux channel can be obtained. In the next sections, the temperature profile of flux channels representing both discussed case studies are presented. The first system has five discretely specified contact temperatures along the source plane and the second system has specified contact temperature, heat flux, and adiabatic conditions.

6.2.1 First Case Study Example

A symmetrical flux channel is assumed with arbitrary specified contact temperatures in the source plane, Fig. 6.3.

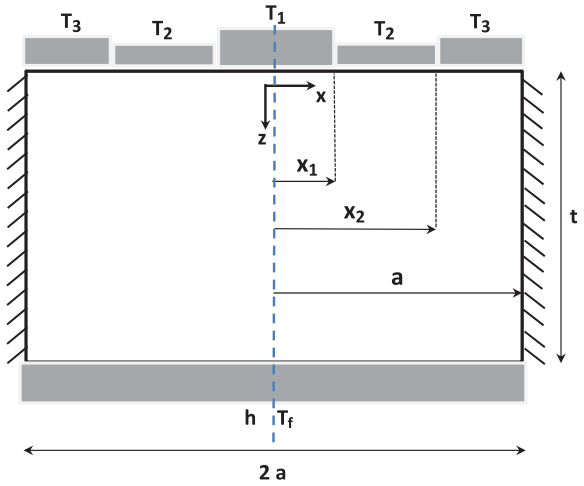

Figure 6.3: Symmetrical flux channel with specified contact temperatures in five regions.

In this example, dimensions of the channel are assumed $a = 10\,cm$, $t = 1\,cm$ and the positions of the sources are $x_1 = 3\,cm$ and $x_2 = 7\,cm$. The temperatures of the sources are $T_1 = 100°C$, $T_2 = 50°C$ and $T_3 = 70°C$. Also, the sink plane properties are $h = 1000\,\frac{W}{m^2K}$ and $T_f = 25°C$ and the thermal conductivity of the channel is assumed $k = 20\,\frac{W}{mK}$. The

temperature profile of the channel is modeled analytically and the results are compared with the FEM results.

The proposed analytical solution is applied and temperature profiles in different cross-sections of the channel, $z = 0.2, 0.4, 0.6, 0.8, 1\, cm$, are shown in Fig. 6.4. The calculations are done in Matlab [31].

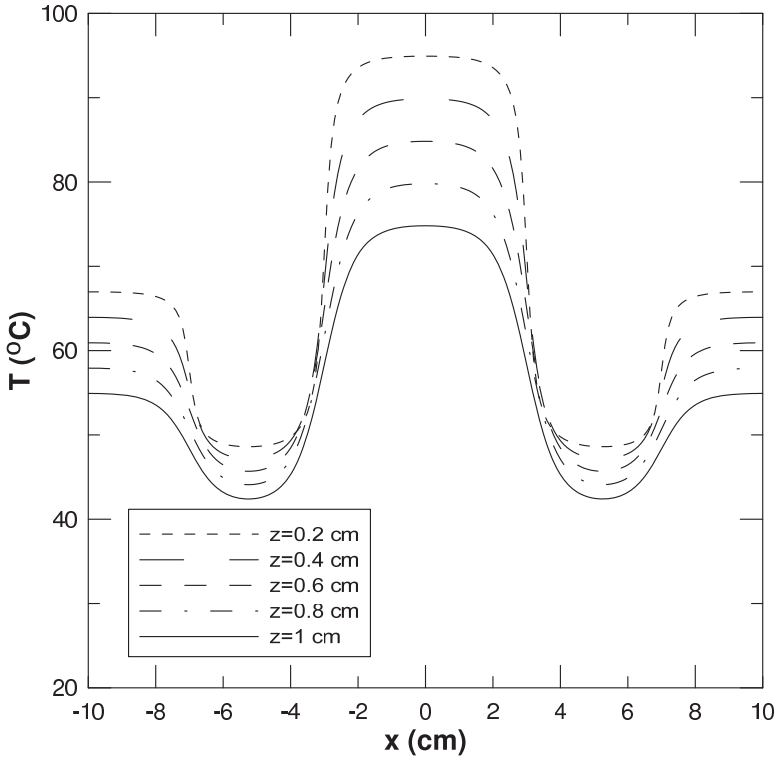

Figure 6.4: Temperature profile based on analytical model for the first case study example.

The convergence of analytical model is evaluated using different number of terms in the Fourier series expansion. In Table 6.1, the temperature over the convective cooling sink plane is shown for different number of terms in the series, $n = 1, 5, 10, 100, 150$. It shows that the analytical solution is completely converged after using 100 terms in the series. Also, it shows even 5 terms in the series can model the system precise enough for most designing applications. The other interesting point is the execution time. It shows that the execution time for modeling the system with 100 terms in the series is done in less than 2 seconds in

a laptop with 4 GB RAM and Intel Core i5-2410M CPU. It is worth mentioning that this execution time can be reached by defining a separate function in the Matlab for calculating the integral of $\int_{x_1}^{x_2} \cos(\lambda_j x) \cos(\lambda_m x)\, dx$.

Number of terms in series	Execution Time (s)	Temperature (°C) x=0 cm z=1 cm	Temperature (°C) x=2 cm z=1 cm	Temperature (°C) x=4 cm z=1 cm	Temperature (°C) x=6 cm z=1 cm	Temperature (°C) x=8 cm z=1 cm	Temperature (°C) x=10 cm z=1 cm
n=1	0.24	65.58379	63.68979	58.73123	52.60211	47.64354	45.74954
n=5	0.34	74.98216	70.42567	46.11547	43.89163	52.61435	55.59026
n=10	0.43	74.98434	71.57498	45.15025	43.06462	53.57848	54.94566
n=100	1.90	74.81325	71.39984	45.3027	43.19953	53.56193	54.9254
n=150	2.19	74.81325	71.39984	45.3027	43.19953	53.56193	54.9254

Table 6.1: Checking the convergence of partial sums in the Fourier series representing the analytical solution for the first case study example.

Moreover, FEM results are obtained using the commercial COMSOL multiphysics software package for comparison purposes. A triangular mesh is used in the FEM and the convergence of the FEM was checked by increasing the number of elements and producing finer mesh in the system. As can be seen in Table 6.2, the accuracy of the results and the computation time are increased by increasing the number of elements. For having an accurate result with five digits of precision, 20230 elements are required. These results are shown in the last row of Table 6.2 and are as same as the analytical results with n = 100 in Table 6.1. However, 1332 elements can model the system accurately enough. In Fig. 6.5, the temperature plot of the FEM is shown.

Number of elements	Execution Time (s)	Temperature (°C) x=0 cm z=1 cm	Temperature (°C) x=2 cm z=1 cm	Temperature (°C) x=4 cm z=1 cm	Temperature (°C) x=6 cm z=1 cm	Temperature (°C) x=8 cm z=1 cm	Temperature (°C) x=10 cm z=1 cm
279	3	74.81053	71.21659	45.38134	43.26974	53.5363	54.92383
439	3	74.81232	71.30147	45.33143	43.22685	53.55121	54.92468
1332	4	74.81321	71.39964	45.30331	43.19964	53.56169	54.92539
5310	5	74.81323	71.39979	45.30275	43.19956	53.56188	54.9254
20230	6	74.81325	71.39984	45.3027	43.19953	53.56193	54.9254

Table 6.2: Checking the convergence of the FEM by increasing the number of elements.

For comparing analytical and FEM results, temperature at specified points in the x and z directions, $x = 0, 2, 4, 6, 8, 10\, cm$ and $z = 0.2, 0.4, 0.6, 0.8, 1\, cm$, is shown in Table 6.3. For modeling the system using FEM, 1332 elements are used. It shows that both models agree with 4 decimal digits of precision in most of the points.

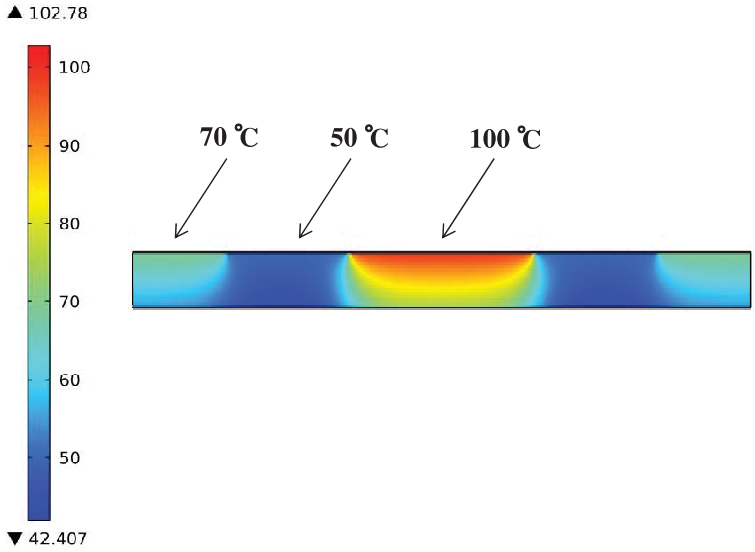

Figure 6.5: Temperature profile over the channel based on FEM for the first case study example.

Temperature		x=0 cm	x=2 cm	x=4 cm	x=6 cm	x=8 cm	x=10 cm
Analytical	z=0.2 cm	94.93047	93.56046	49.78623	48.9437	66.42492	66.97222
FEM		94.93047	93.5604	49.78591	48.94372	66.42505	66.97223
Analytical	z=0.4 cm	89.87024	87.36647	49.32512	47.78457	62.94797	63.94817
FEM		89.87023	87.36643	49.32523	47.78458	62.94793	63.94816
Analytical	z=0.6 cm	84.82729	81.57946	48.45372	46.45405	59.63363	60.93101
FEM		84.8273	81.57931	48.45377	46.4541	59.63361	60.93102
Analytical	z=0.8 cm	79.80742	76.25944	47.1109	44.92526	56.50584	57.92305
FEM		79.80743	76.25963	47.11111	44.92518	56.50574	57.92308
Analytical	z=1 cm	74.81325	71.39984	45.3027	43.19953	53.56193	54.9254
FEM		74.81321	71.39964	45.30331	43.19964	53.56169	54.92539

Table 6.3: Comparison of analytical and FEM results for the first case study example.

6.2.2 Second Case Study Example

A system with different source boundary conditions including heat flux, constant temperature, and adiabatic conditions is shown in Fig. 6.6, [26]. The geometry and properties of the flux channel are assumed as same as the first case study example. For calculation purposes, temperature and heat flux on the source plane are assumed as $T_1 = 50°C$ and $q_1 = 10000\ \frac{W}{m^2}$. Also, adiabatic regions exist between T_1 and q_1. Temperature profile that is calculated by the analytical method is presented in Fig. 6.7.

The convergence of the Fourier series expansion is shown in Table 6.4. Based on this table,

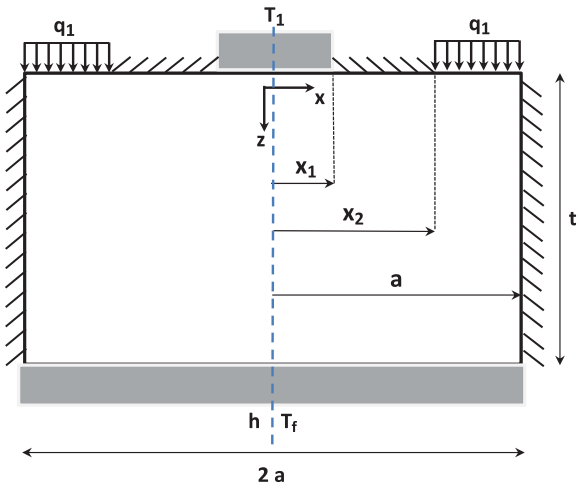

Figure 6.6: Symmetrical flux channel with temperature, heat flux, and adiabatic boundary conditions along the source plane.

it is clear that the good results can be achieved by using 20 terms in the series and the computation time for 20 terms is just 0.17 seconds.

Number of terms in series	Execution Time (s)	Temperature (°C) x=0 cm z=1 cm	Temperature (°C) x=2 cm z=1 cm	Temperature (°C) x=4 cm z=1 cm	Temperature (°C) x=6 cm z=1 cm	Temperature (°C) x=8 cm z=1 cm	Temperature (°C) x=10 cm z=1 cm
n=20	0.17	41.05	56.94	35.68	30.41	32.80	33.88
n=100	0.41	41.59	41.11	34.55	30.15	32.73	33.84
n=200	1.18	41.62	40.79	32.24	29.48	32.54	33.75
n=500	14.06	41.62	40.92	32.96	29.69	32.60	33.78
n=1000	70.78	41.63	40.95	33.12	29.74	32.61	33.78
n=2000	318.70	41.63	40.95	33.12	29.74	32.61	33.78

Table 6.4: Checking the convergence of partial sums in the Fourier series representing the analytical solution for the second case study example.

Figure 6.8 shows the temperature potential lines obtained by FEM. To compare the analytical and FEM results, the calculated temperatures of both methods are shown at 30 specified points in the channel, Table 6.5. Also, Table 6.6 shows the mean average difference of both methods along different planes, $z = 0.2\,cm \cdots 1\,cm$. According to the presented results in Table 6.6, the mean average difference is less than 0.5%.

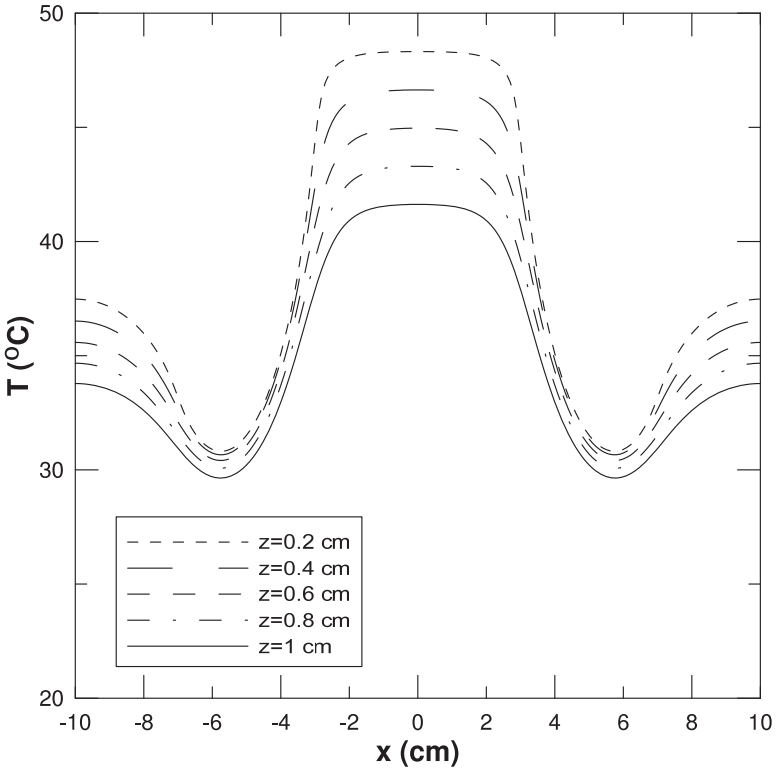

Figure 6.7: Temperature profile based on analytical model for the second case study example.

6.3 Results and Discussion

These examples shows that the proposed analytical method can precisely calculate the temperature profile for a channel with discretely specified boundary conditions along the source plane. The proposed analytical model has some advantages in comparison with other existing heat transfer spreading tools. The heat transfer tools discretize the domain to solve the governing equations. As a result, the temperature is obtained for the nodes and the final result is not continuous over the domain. In the analytical model, domain griding is not needed and the obtained temperature profile is continuous over the system. Also, there is no need to do the regridding for modeling a system with different parameters and as shown in another paper of one of the authors, the regridding time is conserved [20]. In the numerical commercial packages, different meshing systems should be used to ensure

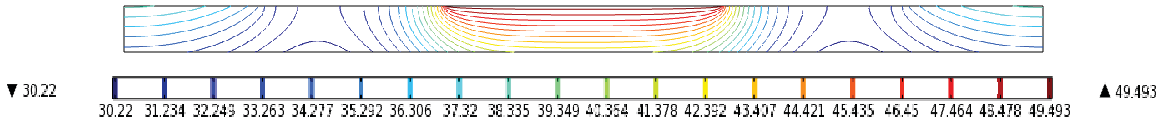

Figure 6.8: Temperature potential lines over the channel based on FEM for the second case study example.

Temperature		x=0 cm	x=2 cm	x=4 cm	x=6 cm	x=8 cm	x=10 cm
Analytical	z=0.2 cm	48.31979	48.05739	35.3138	30.9576	35.98937	37.48761
FEM		48.31999	48.06188	35.37181	30.97281	35.99376	37.48982
Analytical	z=0.4 cm	46.64137	46.15809	35.00431	30.79601	35.07533	36.52641
FEM		46.64176	46.16648	35.05934	30.81083	35.07961	36.52857
Analytical	z=0.6 cm	44.96633	44.33386	34.51759	30.53421	34.21254	35.59034
FEM		44.96686	44.34471	34.56854	30.54838	34.21664	35.59241
Analytical	z=0.8 cm	43.29578	42.60001	33.8833	30.1809	33.39446	34.67829
FEM		43.29637	42.6118	33.92982	30.19419	33.3983	34.68023
Analytical	z=1 cm	41.63025	40.95904	33.12611	29.74496	32.61516	33.78876
FEM		41.63082	40.97035	33.1683	29.75713	32.61868	33.79053

Table 6.5: Comparison of analytical and FEM results for the second case study example.

a good convergency in the result. The other advantage is the accessibility of the proposed approach. This method can be easily implemented in most of the mathematical softwares. Therefore, if there is no access to the heat transfer tools, the system can be modeled easily in a mathematical package. Moreover, thermal engineers can have a better understanding of the system using the analytical models.

6.4 Summary and Conclusions

An analytical method for modeling the temperature profile in a flux channel with discretely specified source plane boundary conditions is presented. Both symmetrical and non-symmetrical channels are studied. The Laplace equation is solved using the separation of variables method and least squares technique. The proposed solution is in the form of Fourier series expansion which can be easily modeled in computational software packages. Two case studies are presented and the temperature profiles over the channel for both cases are calculated. The effect of using different number of terms in the series is considered.

	z=0.2 cm	z=0.4 cm	z=0.6 cm	z=0.8 cm	z=1 cm
Mean Percent Error	0.0402%	0.0404%	0.0395%	0.0379%	0.0355%

Table 6.6: Mean average difference between the analytical and FEM results along different planes of the flux channel for the second case study example.

Also, the results are compared with FEM and an excellent agreement is obtained between analytical and FEM results. The proposed analytical solution can be used for modeling the flux channels with numerous different source plane boundary conditions without any limitations in the number and position of heat sources. Different temperatures and fluxes can be specified for each source. All sources are modeled at the same time and there is no need to use the superposition method to consider the effect of each individual heat source. The proposed method can be efficiently used by thermal engineers for designing electronic devices.

Acknowledgments

The authors acknowledge the financial support of the Natural Sciences and Engineering Research Council of Canada.

6.5 References

[1] COMSOL Multiphysics® Version 4.2a.

[2] Kennedy, D. P., "Spreading Resistance in Cylindrical Semiconductor devices," *Journal of Applied Physics*, vol. 31, pp. 490-1497, 1960.

[3] Lee, S., Song, S., Au, V., and Moran, K. P., "Constriction/Spreading Resistance Model for Electronics Packaging," *in Proc. 4th ASME/JSME Thermal Eng. Joint Conf.*, Maui, HI, pp. 199-206, Mar. 1995.

[4] Song, S., Lee, S., and Au, V., "Closed-Form Equation for Thermal Constriction/Spreading Resistances with Variable Resistance Boundary Condition," *in Proc. IEPS Conf.*, Atlanta, GA, pp. 111-121, Sep. 1994.

[5] Ellison, G. N., "The Thermal Design of an LSI Single-Chip Package," *IEEE Transactions on Parts, Hybrids, and Packaging*, vol. PHP-12, no. 4, Dec. 1976.

[6] Ellison, G., "Extensions of a Closed Form Method for Substrate Thermal Analyzers to Include Thermal Resistances From Source-to-Substrate and Source-to-Ambient," *Seventh IEEE Semi-Therm Symposium*, pp. 140-148, 1991.

[7] Ellison, G., "Thermal Analysis of Microelectric Packages and Printed Circuit Boards Using an Analytic Solution to the Heat Conduction Equation," *Advances in Engineering Software*, pp. 99-111, 1994.

[8] Ellison, G., "Thermal Analysis of Circuit Boards and Microelectronic Components Using an Analytical Solution to the Heat Conduction Equation," *Twelfth IEEE Semi-Therm Symposium*, pp. 144-150, 1996.

[9] Kokkas, A., "Thermal Analysis of Multiple-Layer Structures," *IEEE Trans. Electron Devices*, vol. ED-21, no. 11, pp. 674-680, 1974.

[10] Lemczyk, T. F. and Yovanovich, M. M., "Thermal Constriction Resistance with Convection Boundary Conditions: 1. Half-space Contacts," *Int. J. Heat Mass Transfer*, vol. 31, no. 9, pp. 1861-1872, 1988.

[11] Lemczyk, T. F. and Yovanovich, M. M., "Thermal Constriction Resistance with Convection Boundary Conditions: 2. Layered Half-space Contacts," *Int. J. Heat Mass Transfer*, vol. 31, no. 9, pp. 1873-1883, 1988.

[12] Lemczyk, T. F., Culham, J. R. and Yovanovich, M. M., "Analysis of Three-Dimensional Conjugate Heat Transfer Problems in Microelectronics," *Sixth International Conference on Numerical Methods in Thermal Problems*, Swansea, Wales, United Kingdom, pp. 1346-1356, July 3-7, 1989.

[13] Lemczyk, T. F., Mack, B. L., Culham, J. R. and Yovanovich, M. M., "Printed Circuit Board Trace Thermal Analysis and Effective Conductivity," *ASME Journal of Electronic Packaging*, vol. 114, pp. 413-419, December, 1992.

[14] Muzychka, Y. S., Sridhar, M. S., Yovanovich M. M., and Antonetti, V. W., "Thermal Constriction Resistance in Multilayered Contacts: Applications in Thermal Contact Resistance," *AIAA National Heat Transfer Conf., Thermophysics and Thermophysical Properties Session*, Houston, Texas, Aug. 3-6, 1996.

[15] Muzychka, Y. S., Sridhar, M. R., Yovanovich, M. M., and Antonetti, V. W., "Thermal Constriction Resistance in Multilayered Contacts: Applications in Thermal Contact Resistance," *AIAA Journal of Thermophysics and Heat Transfer*, vol. 13, no. 4, pp. 489-494, 1999.

[16] Muzychka, Y. S., Yovanovich, M. M., and Culham, J. R., "Influence of Geometry and Edge Cooling on Thermal Spreading Resistance," *AIAA Journal of Thermophysics and Heat Transfer*, vol. 20. no. 2, pp. 247-255, April-June 2006.

[17] Muzychka, Y. S., Culham, J. R., and Yovanovich, M. M., "Thermal Spreading Resistance of Eccentric Heat Sources on Rectangular Flux Channels," *Journal of Electronic Packaging*, vol. 125, pp. 178-185, June 2003.

[18] Muzychka, Y. S., Yovanovich, M. M, and Culham, J. R., "Thermal Spreading Resistance in Compound and Orthotropic Systems," *Journal of Thermophysics and Heat Transfer*, vol. 18, no. 1, January-March 2004.

[19] Muzychka, Y. S., "Influence Coefficient Method for Calculating Discrete Heat Source Temperature on Finite Convectively Cooled Substrates," *IEEE Transactions on Components and Packaging Technologies*, vol. 29, no. 3, pp. 636-643, Sep. 2006.

[20] Muzychka, Y. S., Bagnall, K. R., and Wang, E. N., "Thermal Spreading Resistance and Heat Source Temperature in Compound Orthotropic Systems With Interfacial resistance," *IEEE Transactions on Components, Packaging, and Manufacturing Technology*, vol. 3, no. 11, pp. 1826-1841, November 2013.

[21] Muzychka, Y. S., "Spreading Resistance in Compound Orthotropic Flux Tubes and Channels with Interfacial Resistance", *AIAA Journal of Thermophysics and Heat Transfer*, 2014.

[22] Bagnall, K., Muzychka, Y. S., and Wang, E., "Application of the Kirchhoff Transform to Thermal Spreading Problems with Convection Boundary Conditions", *IEEE Transactions on Components, Packaging and Manufacturing Technologies*, 2013.

[23] Bagnall, K., Muzychka, Y. S., and Wang, E., "Analytical Solution for Temperature Rise in Complex, Multi-layer Structures with Discrete Heat Sources", *IEEE Transactions on Components, Packaging and Manufacturing Technologies*, 2014.

[24] Razavi, M., Muzychka, Y. S., and Kocabiyik, S., "Thermal Resistance in a Rectangular Flux Channel with Non-Uniform Heat Convection in the Sink Plane", *Journal of Heat Transfer*, Paper No: HT-14-1786, 2015.

[25] Razavi, M., Dehghani-sanij, A., and Muzychka, Y. S., "Numerical Investigation of Thermal Resistance in a Rectangular Flux Channel with Non-Uniform Heat Convection in the Sink Plane", *Proceedings of the ASME InterPACKICNMM*, San Francisco, California, USA, 2015.

[26] Razavi, M., Muzychka, Y. S., and Kocabiyik, S., "Thermal Behavior of Rectangular Flux Channels with Discretely Specified Contact Flux and Temperature", *Proceedings of the ASME InterPACKICNMM*, San Francisco, California, USA, 2015.

[27] Yovanovich, M. M., "Four Decades of Research on Thermal Contact, Gap and Joint Resistance in Microelectronics," *IEEE Transactions on Components and Packaging Technologies*, vol. 28, no. 2, pp. 182-206, 2005.

[28] Yovanovich, M. M., "General Expression for Constriction Resistances Due to Arbitrary Flux Distribution at non-symmetric, coaxial contacts", *AIAA 13th Aerospace Sciences Meeting*, Pasadena, California, 1975.

[29] Yovanovich, M. M., Muzychka, Y. S., and Culham, J. R., "Spreading Resistance in Isoflux Rectangles and Strips on Compound Flux Channels," *J. Thermophys. Heat Transf.*, vol. 13, no. 4, pp. 495-500, 1999.

[30] Kelman, R. B., "Least Squares Fourier Series Solutions to Boundary Value Problems," *Society for Industrial and Applied mathematics*, vol. 21, no. 3, pp. 329-338, July 1979.

[31] Matlab, The Language of Technical Computing, R2012a.

Chapter 7

Temperature Distribution in a Circular Flux Tube with Arbitrary Specified Contact Temperature and Heat Flux

M. Razavi
Y.S. Muzychka

Department of Mechanical Engineering, Memorial University of Newfoundland, St. John's, NL, Canada, A1B 3X5

S. Kocabiyik

Department of Mathematics and Statistics, Memorial University of Newfoundland, St. John's, NL, Canada, A1C 5S7

Abstract

Temperature profile and thermal resistance of the electronic devices are the key factors for designing the thermal management system. In this paper, an analytical solution for temperature distribution and thermal resistance of a circular flux tube with discretely specified source boundary conditions is presented. The boundary condition along the source plane can be specified as constant temperature, heat flux, adiabatic condition or a combination of all mentioned conditions. The boundary condition along the sink plane is convective cooling and the boundary condition along the walls is adiabatic. For solving the governing equation, the method of separation of variables and the least squares method are used by considering the mentioned boundary conditions. Three different case studies are presented

[1]Submitted to ITHERM 2016, The Intersociety Conference on Thermal and Thermomechanical Phenomena in Electronic Systems, Las Vegas, NV, USA.

and the results are compared with the Finite Element Method (FEM). Further, the effect of orthotropic properties is considered. These analytical solutions help thermal engineers to have a better understanding of the thermal behavior of electronic devices.

Keywords: Electronic Cooling, Heat Conduction, Temperature Profile, Thermal Resistance, Orthotropic Properties, Separation of Variables, Lease Squares Method

7.1 Introduction

Thermal management is one of the most important issues for designing modern microelectronic devices. One of the key factors for choosing the best thermal management system is the accurate prediction of temperature profile and thermal resistance of the system. Due to the heat flow through different layers with different areas in electronic devices, thermal spreading resistance is important and in some cases is the main source of thermal resistance. Thermal spreading resistance is a known parameter needed when designing electronic devices. Many researchers work on different aspects of spreading resistance by considering different shapes, materials, configuration, boundary conditions and other properties. Research on thermal spreading resistance began with Kennedy [1] who worked on spreading resistance in semiconductor devices. Yovanovich et al. [2] considered the thermal spreading resistance between contacting paraboloids. They developed a general expression for thermal spreading resistance of circular contact flux on right circular cylinders [3] and on a half-space [4]. Single arbitrary shape with constant flux on insulated half-spaces [5], annular contacts on circular flux tubes [6], and constriction resistance due to a circular annular contact [4] were investigated. Negus et al. [7] considered square root of the heat source to non-dimensionalize thermal constriction resistance.

Muzychka et al. [8-15] solved the thermal spreading resistance problem for different systems with different geometries, boundaries and properties. They analyzed the circular and

rectangular systems with isotropic and orthotropic properties and concentric and eccentric arbitrary heat sources [9, 10, 11, 15, 16, 17]. Furthermore, they considered thermal spreading resistance of circular flux tubes and rectangular flux channels for isotropic and compound system [9, 17]. Orthotropic and compound systems were investigated and a simple transformation for orthotropic and isotropic systems were proposed [15, 18]. Moreover, the effect of edge cooling on thermal spreading resistance in circular flux tubes and rectangular flux channels was considered [10]. The solution for thermal spreading resistance for flux tubes and channels by considering compound and orthotropic systems with or without edge cooling was considered and the effect of eccentric heat sources and different heat flux distributions was investigated [8]. Recently, Muzychka et al. [19] analyzed the compound orthotropic systems with interfacial resistance. Bagnall et al. [20] studied the thermal spreading resistance for a system with temperature dependent thermal conductivity.

Yovanovich and Marrota [21] summarized most of the important models for spreading resistance problems. Furthermore, Yovanovich [22] reviewed all of his forty years of research on steady-state and transient thermal constriction and spreading resistances.

The main goal of this research is modeling the temperature profile and thermal resistance of a circular flux tube (cylinder) with discretely specified source plane boundary conditions. The boundary conditions along the source plane can be specified as constant temperature, heat flux, adiabatic condition and a combination of them. The only limitation is that the specified boundary condition should be concentric on the flux tube. Furthermore, systems with orthotropic properties are analyzed and a general model for the orthotropic systems is presented. The proposed models are useful for modeling the thermal behavior of electronic devices such as LEDs.

7.2 Thermal Spreading Resistance

Thermal spreading resistance exists in microelectronic devices where heat enters a material through a finite region. Some microelectronic devices can be modeled as a heat source on a flux tube which is cooled by a heat transfer coefficient in the sink plane. In the case of a flux tube with adiabatic edges, the total thermal resistance is composed of the one dimensional thermal resistance and thermal spreading resistance as follows:

$$R_T = R_{1D} + R_s. \tag{7.1}$$

The total thermal resistance for steady heat transfer can be calculated using mean source temperature $(\overline{T}_s)$, film temperature (T_f), and total heat flow rate from the source into the flux (Q),

$$R_T = \frac{\overline{T}_s - T_f}{Q}. \tag{7.2}$$

The one dimensional thermal resistance can be obtained as follows:

$$R_{1D} = \frac{\overline{T}_{z=0} - T_f}{Q}. \tag{7.3}$$

For a single discrete source, Mikic and Rohsenow [23] proposed,

$$R_s = R_T - R_{1D} = \frac{\overline{T}_s - T_f}{Q} - \frac{\overline{T}_{z=0} - T_f}{Q}, \tag{7.4}$$

$$R_s = \frac{\overline{T}_s - \overline{T}_{z=0}}{Q}. \tag{7.5}$$

The thermal spreading resistance disappears when the source completely covers the top of the flux tube. The thermal spreading resistance is the major part of the thermal resistance

for thin electronic devices and should be considered for designing the thermal management system [24].

In some flux tubes, combinations of different sources such as discretely specified contact temperature and heat flux exist along the source plane. For these cases, the thermal spreading resistance cannot be exactly calculated as the thermal resistance of each source depends on the strength of other sources. Therefore, the temperature distribution can be used to have a better understanding of the uniformity of the temperature along the system and recognize the hot spots. Also, if the heat fluxes of all the heat sources are known, the total resistance can be calculated by using the mean source contact plane temperature to the sink plane temperature and total heat flow. The total heat flow can be calculated if the prescribed heat flux in different regions of the source plane is known.

$$\overline{T}_{cp} = \frac{1}{A} \int \int_A T dA, \tag{7.6}$$

$$Q_T = \int \int_A q dA, \tag{7.7}$$

$$R_T = \frac{\overline{T}_{cp} - T_f}{Q_T}. \tag{7.8}$$

In this paper, the temperature profile along the flux tube is calculated. The obtained temperature profile shows the thermal spreading along the flux tube and can be used to identify the uniformity of the temperature and recognize the hot spots of the system.

7.3 Problem Statement

The semi-conductor of micro-electronic devices can be assumed as a finite region such as flux tubes or flux channels that are in contact with heat sources and heat sink. To obtain

the temperature distribution along the flux tube, the Laplace equation should be solved by considering specified boundary conditions. In this paper, a flux tube is considered as a model of a micro-electronic device with discretely specified concentric heat sources. The sources can be defined as specified temperature and heat flux and there is no limitation on their quantity. A sample of the flux tube with three discrete regions along the source plane is shown in Fig. 7.1. The surfaces between the specified sources and along the walls of the tube are assumed to be adiabatic. Furthermore, the convective cooling condition is applied along the sink plane.

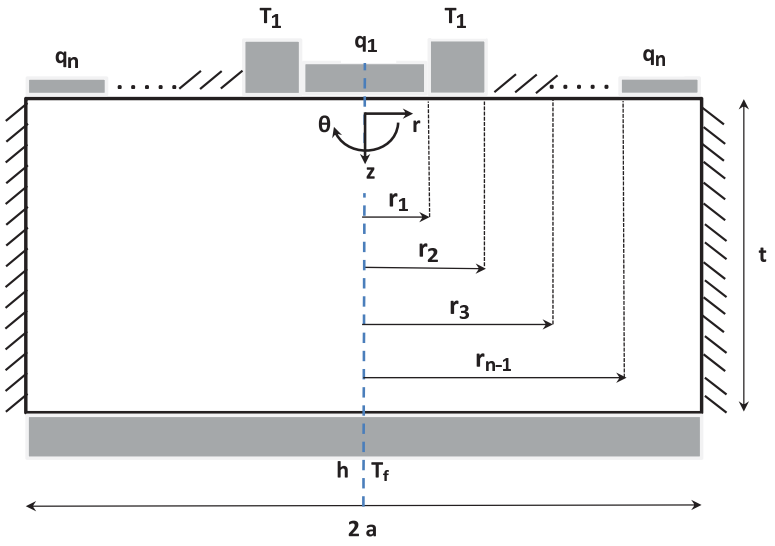

Figure 7.1: Flux tube with arbitrary boundary condition along the source plane.

For the isotropic system, thermal conductivity is constant in all directions and the Laplace equation has the following form:

$$\nabla^2 T = 0. \tag{7.9}$$

For cylindrical co-ordinates, the Laplace equation is defined as follows:

$$\frac{\partial^2 \theta}{\partial r^2} + \frac{1}{r}\frac{\partial \theta}{\partial r} + \frac{\partial^2 \theta}{\partial z^2} = 0 \qquad 0 < z < t. \tag{7.10}$$

where $\theta = T - T_f$ is the temperature excess that is defined relative to the sink temperature. The following boundary conditions are imposed on the system. Along the source plane, discretely contact temperature and heat flux are arbitrary specified. All of the sources are concentric and the adiabatic condition exists between them. There is no limitation for the number and position of the sources. In this paper, a sample of the source plane boundary conditions is presented, Fig. 7.1. The system has the following boundary condition along the source plane,

$$\begin{aligned}
-k \left.\frac{\partial\theta}{\partial z}\right|_{z=0} &= q_1 && 0 < r < r_1, \\
\left.\theta\right|_{\xi=0} &= \theta_1 && r_1 < r < r_2, \\
-k \left.\frac{\partial\theta}{\partial z}\right|_{z=0} &= 0 && r_2 < r < r_3, \\
&\vdots \\
-k \left.\frac{\partial\theta}{\partial z}\right|_{z=0} &= q_n && r_{n-1} < r < a.
\end{aligned} \tag{7.11}$$

The boundary conditions along the center-line and edge of the flux tube are,

$$\left.\frac{\partial\theta}{\partial r}\right|_{r=0} = 0, \tag{7.12}$$

$$\left.\frac{\partial\theta}{\partial r}\right|_{r=a} = 0. \tag{7.13}$$

The boundary condition along the sink plane can be defined as follows:

$$-k \left.\frac{\partial\theta}{\partial z}\right|_{z=t} = h\theta. \tag{7.14}$$

7.3.1 Solution for Isotropic Circular Disk

In this section, a short summary of the solving procedure is introduced. A solution may be found using the method of separation of variables and the least squares technique. The general solution to the Laplace equation is,

$$\theta(r,z) = A_0 + B_0 z + [AJ_0(\lambda r) + BY_0(\lambda r)][C\cosh(\lambda z) + D\sinh(\lambda z)]. \tag{7.15}$$

The first two terms of the above equation stand for uniform heat flow.

Applying the condition along the center-line of the flux tube, Eq. (7.12), results in $B = 0$. Further, the eigenvalues of the system can be determined using the edge boundary condition, Eq. (7.13) as follows:

$$\frac{d}{dr}(J_0(\lambda r))\bigg|_{r=a} = -\lambda J_1(\lambda r)\bigg|_{r=a} = J_1(\lambda a) = 0 \tag{7.16}$$

and the eigenvalues are,

$$\delta_n = \lambda_n a = 3.8317, 7.0156, 10.1735.13.2327, \cdots . \tag{7.17}$$

It is worth mentioning that each eigenvalue can be determined by adding π to the previous eigenvalue ($\delta_n - \delta_{n-1} \to \pi$) when $n > 5$. Hence, the general solution is,

$$\theta(r,z) = A_0 + B_0 z + \sum_{n=1}^{\infty} J_0(\lambda_n r)\Big(C_n \cosh(\lambda_n z) + D_n \sinh(\lambda_n z)\Big). \tag{7.18}$$

Applying the boundary condition along the sink plane, Eq. (7.14), results,

$$A_0 = -B_0\left(t + \frac{k}{h}\right), \tag{7.19}$$

$$C_n = -D_n \left(\frac{\lambda_n \cosh(\lambda_n t) + \frac{h}{k} \sinh(\lambda_n t)}{\lambda_n \sinh(\lambda_n t) + \frac{h}{k} \cosh(\lambda_n t)} \right) = -D_n \phi_n. \tag{7.20}$$

The spreading function, ϕ_n, is defined as follows:

$$\phi_n = \frac{\delta_n + Bi \tanh(\delta_n \tau)}{\delta_n \tanh(\delta_n \tau) + Bi}, \tag{7.21}$$

where the Biot number is defined as , $Bi = ha/k$, and dimensionless thickness is defined as, $\tau = t/a$.

The solution at this point can be stated as,

$$\theta(r,z) = -B_0 \left(t + \frac{k}{h} - z \right) + \sum_{n=1}^{\infty} D_n J_0(\lambda_n r) \Big(\sinh(\lambda_n z) - \phi_n \cosh(\lambda_n z) \Big). \tag{7.22}$$

To obtain the unknown coefficients, D_n, the boundary condition along the source plane should be used. As mentioned, the source plane boundary condition is arbitrarily specified as a combination of heat flux, contact temperatures and adiabatic condition. Applying the general form of the solution, Eq. (7.22), to the source-plane boundary condition, Eq. (7.11), results,

$$\begin{aligned}
-k \left. \frac{\partial \theta}{\partial z} \right|_{z=0} &= -k \left(B_0 + \sum_{n=1}^{\infty} D_n \lambda_n J_0(\lambda_n r) \right) = q_1 && 0 < r < r_1, \\
\theta(r,0) &= -B_0 \left(t + \frac{k}{h} \right) - \sum_{n=1}^{\infty} D_n \phi_n J_0(\lambda_n r) = \theta_1 && r_1 < r < r_2, \\
-k \left. \frac{\partial \theta}{\partial z} \right|_{z=0} &= -k \left(B_0 + \sum_{n=1}^{\infty} D_n \lambda_n J_0(\lambda_n r) \right) = 0 && r_2 < r < r_3, \\
&\vdots \\
-k \left. \frac{\partial \theta}{\partial z} \right|_{z=0} &= -k \left(B_0 + \sum_{n=1}^{\infty} D_n \lambda_n J_0(\lambda_n r) \right) = q_n && r_{n-1} < r < a.
\end{aligned} \tag{7.23}$$

The coefficients D_n are renamed to B_n in Eqs. (7.22- 7.23), and as a result, Eq. (7.23) becomes [25],

$$\begin{aligned}
-k\left.\frac{\partial\theta}{\partial z}\right|_{z=0} &= \sum_{m=0}^{\infty} B_m\rho_m\psi_m(r) = q_1 && 0<r<r_1, \\
\theta(r,0) &= \sum_{m=0}^{\infty} B_m\varphi_m\psi_m(r) = \theta_1 && r_1<r<r_2, \\
-k\left.\frac{\partial\theta}{\partial z}\right|_{z=0} &= \sum_{m=0}^{\infty} B_m\vartheta_m\psi_m(r) = 0 && r_2<r<r_3, \\
&\vdots \\
-k\left.\frac{\partial\theta}{\partial z}\right|_{z=0} &= \sum_{m=0}^{\infty} B_m\kappa_m\psi_m(r) = q_n && r_{n-1}<r<a.
\end{aligned} \tag{7.24}$$

where,

$$0<r<r_1 \rightarrow \quad \begin{cases} \rho_m = \begin{cases} -k, & m=0 \\ -k\lambda_m, & m=1,2,... \end{cases} \\ \psi_m(r) = J_0\left(\lambda_m r\right) \end{cases}, \tag{7.25}$$

$$r_1<r<r_2 \rightarrow \quad \begin{cases} \varphi_m = \begin{cases} -(t+\frac{k}{h}), & m=0 \\ -\phi_m, & m=1,2,... \end{cases} \\ \psi_m(r) = J_0\left(\lambda_m r\right) \end{cases}, \tag{7.26}$$

$$r_2 < r < r_3 \rightarrow \quad \begin{cases} \vartheta_m = \begin{cases} -k, & m = 0 \\ -k\lambda_m, & m = 1, 2, ... \end{cases} \\ \psi_m(r) = J_0\left(\lambda_m r\right) \end{cases}, \tag{7.27}$$

$$\vdots$$

$$r_{n-1} < r < a \rightarrow \quad \begin{cases} \kappa_m = \begin{cases} -k, & m = 0 \\ -k\lambda_m, & m = 1, 2, ... \end{cases} \\ \psi_m(r) = J_0\left(\lambda_m r\right) \end{cases}. \tag{7.28}$$

For obtaining B_m coefficients, the method of least squares is used and the following integrals are defined in different regions of the heat source plane,

$$\begin{aligned} I_N = & \int_0^{r_1} \left[\sum_{m=0}^{N} B_m \rho_m \psi_m(x) - q_1 \right]^2 dr \\ & + \int_{r_1}^{r_2} \left[\sum_{m=0}^{N} B_m \varphi_m \psi_m(x) - \theta_1 \right]^2 dr \\ & + \int_{r_2}^{r_3} \left[\sum_{m=0}^{N} B_m \vartheta_m \psi_m(x) - 0 \right]^2 dr \\ & \vdots \\ & + \int_{r_{n-1}}^{a} \left[\sum_{m=0}^{N} B_m \kappa_m \psi_m(x) - q_n \right]^2 dr. \end{aligned} \tag{7.29}$$

The coefficients, B_m, are calculated in order to minimize the above integrals,

$$\frac{\partial I_N}{\partial B_m} = 0 \qquad\qquad m = 0, 1, 2, ..., N. \tag{7.30}$$

A more computationally efficient method can be obtained using the following $N + 1$ algebraic equations,

$$\begin{aligned} A_{jm} =& \rho_j \rho_m \int_0^{r_1} r\psi_j(r)\psi_m(r)\, dr \\ &+ \varphi_j \varphi_m \int_{r_1}^{r_2} r\psi_j(r)\psi_m(r)\, dr \\ &+ \vartheta_j \vartheta_m \int_{r_2}^{r_3} r\psi_j(r)\psi_m(r)\, dr \\ &\vdots \\ &+ \kappa_j \kappa_m \int_{r_{n-1}}^{a} r\psi_j(r)\psi_m(r)\, dr, \end{aligned} \tag{7.31}$$

$$\begin{aligned} b_j =& \rho_j q_1 \int_0^{r_1} r\psi_j(r)\, dr \\ &+ \varphi_j \theta_1 \int_{r_1}^{r_2} r\psi_j(r)\, dr \\ &+ \vartheta_j 0 \int_{r_2}^{r_3} r\psi_j(r)\, dr \\ &\vdots \\ &+ \kappa_j q_n \int_{r_{n-1}}^{a} r\psi_j(r)\, dr. \end{aligned} \tag{7.32}$$

The variables ρ_j, ρ_m, φ_j, φ_m, ϑ_j, ϑ_m,κ_j, κ_m and $\psi_j(r)$, $\psi_m(r)$ are defined based on Eqs. (7.25- 7.28) and substituted into Eq. (7.31) and Eq. (7.32),

$$
\begin{aligned}
A_{jm} =& \rho_j \rho_m \int_0^{r_1} r J_0(\lambda_j r)\, J_0(\lambda_m r)\, dr \\
&+ \varphi_j \varphi_m \int_{r_1}^{r_2} r J_0(\lambda_j r)\, J_0(\lambda_m r)\, dr \\
&+ \vartheta_j \vartheta_m \int_{r_2}^{r_3} r J_0(\lambda_j r)\, J_0(\lambda_m r)\, dr \\
&\vdots \\
&+ \kappa_j \kappa_m \int_{r_{n-1}}^{a} r J_0(\lambda_j r)\, J_0(\lambda_m r)\, dr,
\end{aligned}
\tag{7.33}
$$

$$
\begin{aligned}
b_j =& \rho_j q_1 \int_0^{r_1} r J_0(\lambda_j r)\, dr \\
&+ \varphi_j \theta_1 \int_{r_1}^{r_2} r J_0(\lambda_j r)\, dr \\
&+ \vartheta_j 0 \int_{r_2}^{r_3} r J_0(\lambda_j r)\, dr \\
&\vdots \\
&+ \kappa_j q_n \int_{r_{n-1}}^{a} r J_0(\lambda_j r)\, dr.
\end{aligned}
\tag{7.34}
$$

The matrix system of $AB = b$ is defined in order to obtain the B_m constants. This matrix can be solved in a mathematical package. Therefore, the temperature profile in the disk is known by substituting the obtained B_m coefficients in Eq. (7.22) by considering that the coefficients D_n were changed to B_m. This equation can be used to obtain temperature at each specified point of the flux tube.

7.3.2 Solution for Orthotropic Circular Disk

The Laplace equation for a circular disk with different thermal conductivity ($k_r \neq k_z$) can be written as follows:

$$k_r\left(\frac{\partial^2 T}{\partial r^2}+\frac{1}{r}\frac{\partial T}{\partial r}\right)+k_z\frac{\partial^2 T}{\partial z^2}=0 \qquad 0<z<t. \tag{7.35}$$

To convert the orthotropic system to the isotropic system, the method of stretched coordinates is used. By using $\xi=\frac{z}{\sqrt{\frac{k_z}{k_r}}}$ and $\theta=T-T_\infty$, the orthotropic system is converted to the following isotropic system with effective isotropic properties ($k_e=\sqrt{k_r k_z}$, $t_e=\frac{t}{\sqrt{\frac{k_z}{k_r}}}$),

$$\frac{\partial^2\theta}{\partial r^2}+\frac{1}{r}\frac{\partial\theta}{\partial r}+\frac{\partial^2\theta}{\partial\xi^2}=0 \qquad 0<\xi<t_e. \tag{7.36}$$

Further, the boundary conditions of the system are transformed. Along the source plane, the boundary conditions are,

$$\begin{aligned}
-k_e\left.\frac{\partial\theta}{\partial\xi}\right|_{\xi=0} &= q_1 && 0<r<r_1, \\
\left.\theta\right|_{\xi=0} &= \theta_1 && r_1<r<r_2, \\
-k_e\left.\frac{\partial\theta}{\partial\xi}\right|_{\xi=0} &= 0 && r_2<r<r_3, \\
&\vdots \\
-k_e\left.\frac{\partial\theta}{\partial\xi}\right|_{\xi=0} &= q_n && r_{n-1}<r<a.
\end{aligned} \tag{7.37}$$

Along the center and edge of the flux tube, the following conditions are required,

$$\left.\frac{\partial\theta}{\partial r}\right|_{r=0}=0, \tag{7.38}$$

$$\left.\frac{\partial\theta}{\partial r}\right|_{r=a}=0. \tag{7.39}$$

The boundary conditions along the sink plane can be defined as follows:

$$-k_e \left.\frac{\partial \theta}{\partial \xi}\right|_{z=t_e} = h\theta. \tag{7.40}$$

All of the above boundary conditions have the same form of the boundary conditions for the isotropic system; however, k, t and z were replaced by $k_e = \sqrt{k_r k_z}$, $t_e = \frac{t}{\sqrt{\frac{k_z}{k_r}}}$ and $\xi = \frac{z}{\sqrt{\frac{k_z}{k_r}}}$. Hence, the temperature profile for the orthotropic system can be obtained by substituting the effective properties:

$$\theta(r,z) = -B_0\left(t_e + \frac{k_e}{h} - \xi\right) + \sum_{n=1}^{\infty} B_n J_0(\lambda_n r)\Big(\sinh(\lambda_n \xi) - \phi_n \cosh(\lambda_n \xi)\Big), \tag{7.41}$$

where,

$$\phi_n = \frac{\lambda_n \cosh(\lambda_n t_e) + \frac{h}{k_e}\sinh(\lambda_n t_e)}{\lambda_n \sinh(\lambda_n t_e) + \frac{h}{k_e}\cosh(\lambda_n t_e)}. \tag{7.42}$$

To obtain the unknown constants, the least squares method is used. The only difference from the isotropic system is the following redefined variables based on the effective property,

$$0 < r < r_1 \rightarrow \quad \begin{cases} \rho_m = \begin{cases} -k_e, & m = 0 \\ -k_e \lambda_m, & m = 1, 2, \ldots \end{cases} \\ \psi_m(r) = J_0(\lambda_m r) \end{cases}, \tag{7.43}$$

$$r_1 < r < r_2 \rightarrow \quad \begin{cases} \varphi_m = \begin{cases} -(t_e + \frac{k_e}{h}), & m = 0 \\ -\phi_m, & m = 1, 2, ... \end{cases} \\ \psi_m(r) = J_0(\lambda_m r) \end{cases} , \tag{7.44}$$

$$r_2 < r < r_3 \rightarrow \quad \begin{cases} \vartheta_m = \begin{cases} -k_e, & m = 0 \\ -k_e \lambda_m, & m = 1, 2, ... \end{cases} \\ \psi_m(r) = J_0(\lambda_m r) \end{cases} , \tag{7.45}$$

$$\vdots$$

$$r_{n-1} < r < a \rightarrow \quad \begin{cases} \kappa_m = \begin{cases} -k_e, & m = 0 \\ -k_e \lambda_m, & m = 1, 2, ... \end{cases} \\ \psi_m(r) = J_0(\lambda_m r) \end{cases} . \tag{7.46}$$

Using the above variables in Eq. (7.33) and Eq. (7.34), the matrix system of $AB = b$ can be defined to obtain the B_m constants.

7.4 Results and Discussion

In this section, three different case studies for a symmetrical flux tube are investigated. In the first case study, the boundary condition along the source plane consists of one central heat flux and adiabatic condition, Fig. 7.2a. The second case study consists of one central

heat source with constant temperature and adiabatic condition, Fig. 7.2b. The third case study consists of the constant contact temperature, heat flux and adiabatic condition along the source plane, Fig. 7.2c.

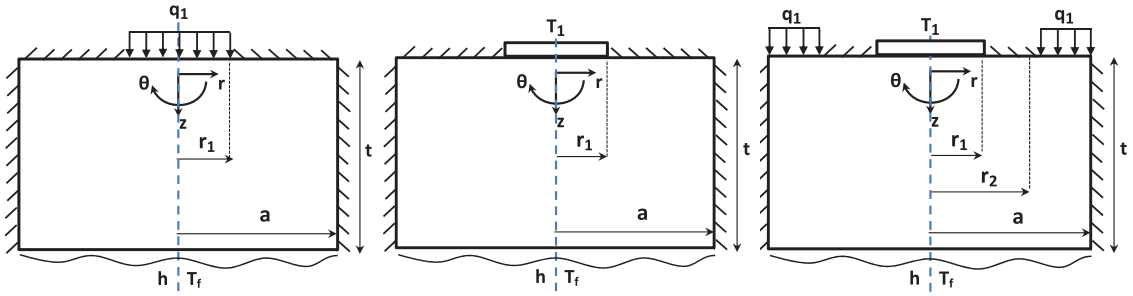

(a) Case A (b) Case B (c) Case C

Figure 7.2: Case studies.

The boundary condition along the source plane for the first case study is,

$$\begin{aligned} -k \left.\frac{\partial \theta}{\partial z}\right|_{z=0} &= q_1 && 0 < r < r_1, \\ -k \left.\frac{\partial \theta}{\partial z}\right|_{z=0} &= 0 && r_1 < r < a. \end{aligned} \tag{7.47}$$

The boundary conditions for the second case study are constant contact temperature and adiabatic condition as follows:

$$\begin{aligned} \left.\theta\right|_{z=0} &= \theta_1 && 0 < r < r_1, \\ -k \left.\frac{\partial \theta}{\partial z}\right|_{z=0} &= 0 && r_1 < r < a. \end{aligned} \tag{7.48}$$

The boundary condition along the source plane for the third case study includes the constant contact temperature, heat flux and adiabatic condition,

$$\begin{aligned} \theta\Big|_{z=0} &= \theta_1 && 0 < r < r_1, \\ -k\,\frac{\partial\theta}{\partial z}\Big|_{z=0} &= 0 && r_1 < r < r_2, \\ -k\,\frac{\partial\theta}{\partial z}\Big|_{z=0} &= q_1 && r_2 < r < a. \end{aligned} \tag{7.49}$$

The geometry and property are assumed as follows: $a = 0.1\,m$, $r_1 = 0.03\,m$, $r_2 = 0.07\,m$, $t = 0.01\,m$, $q_1 = 10^4\,\frac{W}{m^2}$, $T_1 = 45\,^\circ C$, $T_f = 20\,^\circ C$, $k = 20\,\frac{W}{mK}$ and $h = 1000\,\frac{W}{m^2K}$. Temperature distribution of the flux tube is modeled using the computation program Matlab [26]. The temperature profile for all three cases is shown in Figs. 7.3- 7.5. Different cross-sections, $z = 0, 0.2, 0.4, 0.6, 0.8, 1\,cm$, are considered. Further, all case studies are compared with the Finite Element Method (FEM) using a commercial software package [27]. The temperature of the flux tube in 36 points is compared. As can be seen in Tables 7.1- 7.3, the obtained temperatures for both methods are in good agreement.

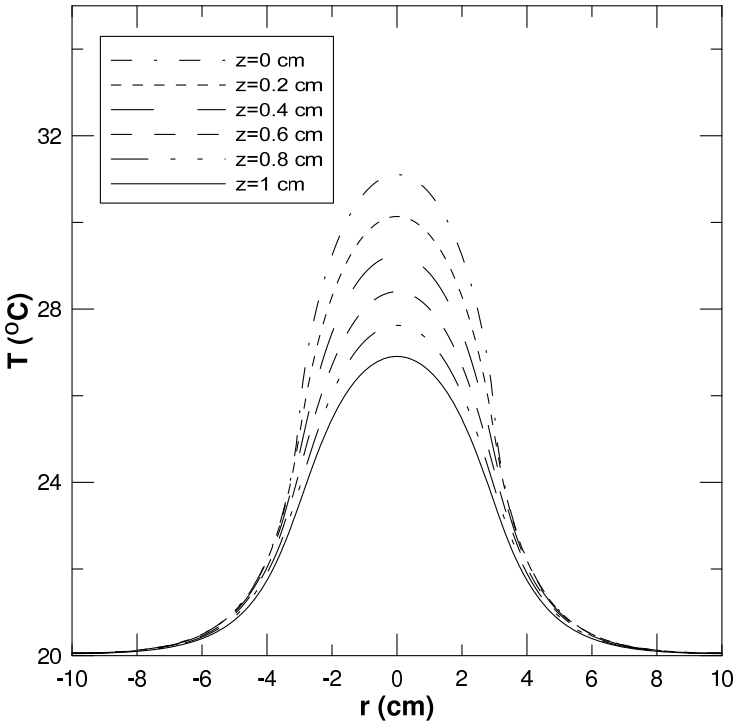

Figure 7.3: Temperature profile for the case A.

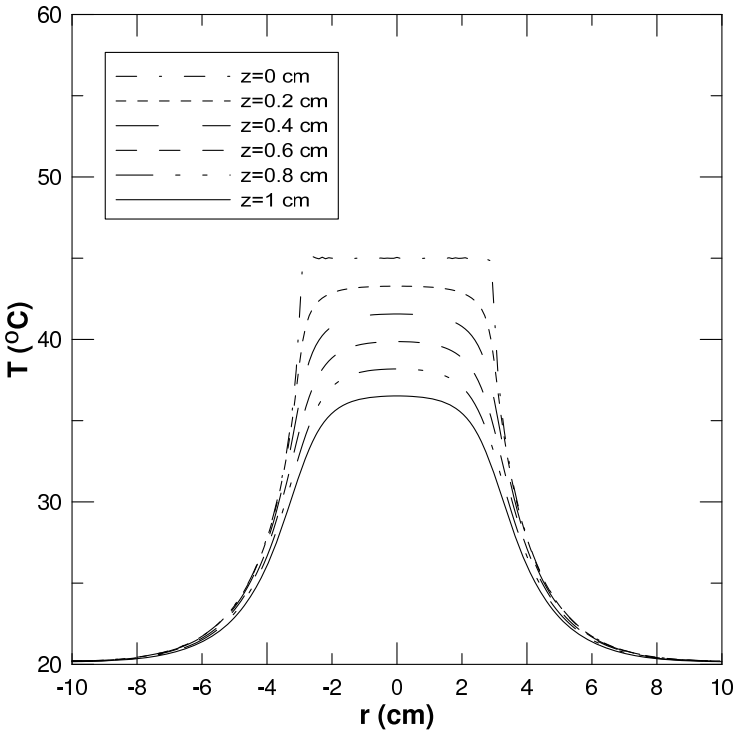

Figure 7.4: Temperature profile for the case B.

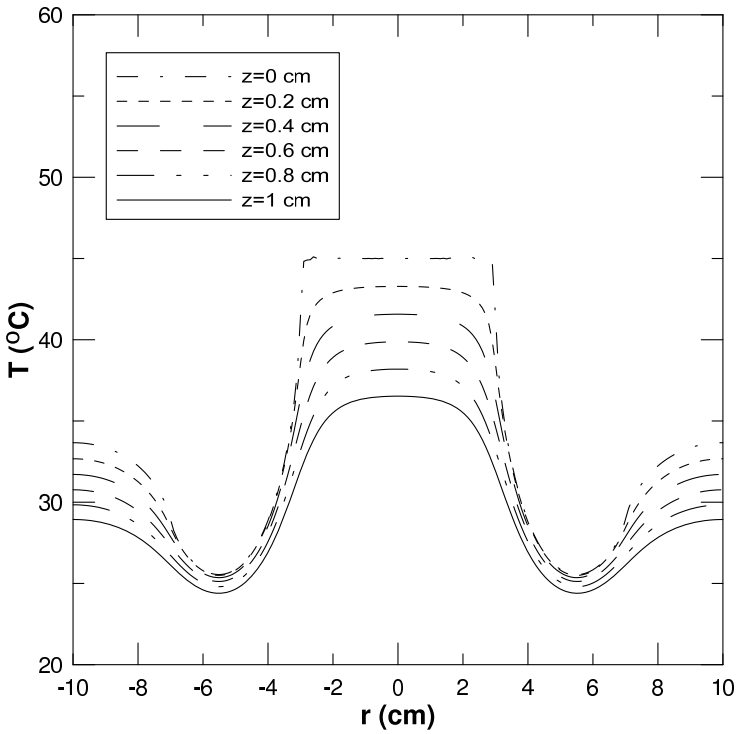

Figure 7.5: Temperature profile for the case C.

Case A		r=0 m	r=0.02 m	r=0.04 m	r=0.06 m	r=0.08 m	r=0.1 m
z=0	Analytical	31.10407	29.23582	22.22198	20.49725	20.1267	20.06146
	FEM	31.10527	29.23595	22.22185	20.49724	20.12669	20.06146
z=0.002 m	Analytical	30.13851	28.2895	22.20016	20.49301	20.12562	20.06094
	FEM	30.1385	28.28945	22.20006	20.49302	20.12562	20.06094
z=0.004 m	Analytical	29.23763	27.44728	22.13652	20.48036	20.1224	20.05938
	FEM	29.23762	27.44724	22.13661	20.48036	20.12239	20.05938
z=0.006 m	Analytical	28.40089	26.70154	22.0353	20.45952	20.11709	20.0568
	FEM	28.40091	26.70144	22.03536	20.45955	20.11709	20.0568
z=0.008 m	Analytical	27.62548	26.04248	21.90172	20.43085	20.10978	20.05326
	FEM	27.62549	26.04249	21.90164	20.43084	20.10979	20.05326
z=0.01 m	Analytical	26.90753	25.46062	21.74036	20.39484	20.10061	20.04881
	FEM	26.9073	25.4604	21.74047	20.39485	20.10062	20.04881

Table 7.1: Comparing the results of analytical and FEM for the case A.

Case B		r=0 m	r=0.02 m	r=0.04 m	r=0.06 m	r=0.08 m	r=0.1 m
z=0	Analytical	45.05465	45.00332	27.8342	21.74621	20.44492	20.21584
	FEM	45	45	28.23495	21.83239	20.46686	20.22649
z=0.002 m	Analytical	43.2807	42.86685	27.75081	21.73131	20.44113	20.214
	FEM	43.28514	42.90775	28.14434	21.81682	20.4629	20.22456
z=0.004 m	Analytical	41.56789	40.80166	27.50996	21.68687	20.42981	20.20851
	FEM	41.57631	40.88101	27.88485	21.77016	20.45102	20.2188
z=0.006 m	Analytical	39.8683	38.86424	27.13471	21.61366	20.41117	20.19947
	FEM	39.87952	38.96798	27.48189	21.69343	20.43146	20.20932
z=0.008 m	Analytical	38.18636	37.08151	26.65152	21.51297	20.38553	20.18703
	FEM	38.19885	37.19414	26.96827	21.58761	20.40456	20.19626
z=0.01 m	Analytical	36.52406	35.45824	26.08173	21.38651	20.35331	20.1714
	FEM	36.53615	35.56637	26.36964	21.45498	20.37077	20.17986

Table 7.2: Comparing the results of analytical and FEM for the case B.

Case C		r=0 m	r=0.02 m	r=0.04 m	r=0.06 m	r=0.08 m	r=0.1 m
z=0	Analytical	45.85465	45.62033	28.88071	25.84125	32.23476	33.66591
	FEM	45	45	29.39016	25.95056	32.26286	33.67942
z=0.002 m	Analytical	43.28411	42.89312	28.79035	25.78763	31.26151	32.67725
	FEM	43.28855	42.93712	29.29055	25.89606	31.28906	32.69067
z=0.004 m	Analytical	41.5735	40.84304	28.52776	25.62951	30.33976	31.71119
	FEM	41.58263	40.93531	29.00376	25.73528	30.36681	31.72426
z=0.006 m	Analytical	39.87541	38.91585	28.11402	25.37386	29.46463	30.7671
	FEM	39.88792	39.03948	28.5548	25.47522	29.4904	30.77958
z=0.008 m	Analytical	38.19411	37.13743	27.57399	25.02973	28.63015	29.84402
	FEM	38.20822	37.27324	27.97617	25.12453	28.65435	29.85573
z=0.01 m	Analytical	36.53155	35.512	26.92863	24.60611	27.83089	28.94064
	FEM	36.54523	35.64283	27.29405	24.69327	27.85291	28.95135

Table 7.3: Comparing the results of analytical and FEM for the case C.

For a better understanding of the accuracy of the results, the mean percentage difference between the analytical and FEM results for all three cases are calculated, Table 7.4. All 36 points in the flux tube are considered. The results show the mean percentage difference in all three cases is less than 0.5%.

	Case A	Case B	Case C
Mean Percent Error	0.0002 %	0.3388 %	0.4813 %

Table 7.4: Mean percentage difference between the analytical and FEM results.

The proposed method can be easily programmed in most of the mathematical software

packages.

7.5 Summary and Conclusions

In this paper, the temperature distribution of a cylindrical flux tube with arbitrary boundary conditions along the source plane is analytically studied using the method of separation of variables and least square method. A combination of different boundary conditions along the source plane including the contact temperature, heat flux and adiabatic condition is investigated. Further, three different case studies are considered and their temperature profiles are presented. All results are compared with the FEM using a commercial software package. Based on the comparison between the analytical and FEM results, it can be concluded that the proposed analytical method can accurately solve the thermal distribution problems along the flux tube. The mean percent error for all three cases is less than 0.5%. The proposed model is really useful for thermal engineers who want to have a better understanding of thermal distribution of cylindrical flux tubes with complex boundary conditions along the source plane. It is a popular geometry in electronic industry.

Acknowledgments

The authors acknowledge the financial support of the Natural Sciences and Engineering Research Council of Canada.

7.6 References

[1] Kennedy, D. P., Spreading Resistance in Cylindrical Semiconductor Devices, *Journal of Applied Physics*, vol. 31, pp. 490-1497, 1960.

[2] Yovanovich, M. M., Thermal Constriction Resistance Between Contacting Metallic Paraboloids: Application to Instrument Bearings, *Progress in Astronautics and Aeronautics: Fundamentals of Spacecraft Thermal Design*, vol. 24, pp. 337-358, 1971.

[3] Yovanovich, M. M., General Expression for Constriction Resistances Due to Arbitrary Flux Distribution at non-symmetric, coaxial contacts, *AIAA 13th Aerospace Sciences Meeting*, Pasadena, California, 1975.

[4] Yovanovich, M. M., and Schneider, G. E., Thermal Constriction Resistance Due to a Circular Annular Contact, *AIAA Progress in Astronautics and Aeronautics, Thermophysics of Spacecraft and Outer Planet Entry Probes*, vol. 56, edited by A.M. Smith, New York, pp. 141-154, 1976.

[5] Yovanovich, M. M., Burde, S. S., and Thompson, J. C., Thermal Constriction Resistance of Arbitrary Planar Contacts With Constant Flux, *AIAA Progress in Astronautics and Aeronautics, Thermophysics of Spacecraft and Outer Planet Entry Probes*, vol. 56, edited by A.M. Smith, New York, pp. 127-139, 1977.

[6] Yovanovich, M. M., General Thermal Constriction Parameter for Annular Contacts on Circular Flux Tubes, *AIAA J.*, vol. 14, no. 6, pp. 822–824, 1976.

[7] Negus, K. J., Yovanovich, M. M., and Beck, J. V., On the Non-Dimensionalization of Constriction Resistance for Semi-Infinite Heat Flux Tubes, *J. Heat Transf.*, vol. 111, pp. 804–807, Aug. 1989.

[8] Muzychka, Y. S., Yovanovich, M. M., and Culham, J. R., Thermal Spreading Resistance in Compound and Orthotropic Systems, *Journal of Thermophysics and Heat Transfer*, vol. 18, No. 1, January-March 2004.

[9] Muzychka, Y. S., Yovanovich, M. M., and Culham, J. R., Thermal Spreading Resistance in Rectangular Flux Channels, Part I: Geometric Equivalences, *AIAA Paper 2003-4187*, June 2003.

[10] Muzychka, Y. S., Culham, J. R., and Yovanovich, M. M., Thermal Spreading Resistance in Rectangular Flux Channels: Part II Edge Cooling, *AIAA Paper 2003-4188*, June 2003.

[11] Muzychka, Y. S., Culham, J. R., and Yovanovich, M. M., Thermal Spreading Resistance of Eccentric Heat Sources on Rectangular Flux Channels, *Journal of Electronic Packaging*, vol. 125, pp. 178–185, June 2003.

[12] Muzychka, Y. S., Stevanovic, M., and Yovanovich, M. M., Thermal Spreading Resistances in Compound Annular Sectors, *Journal of Thermophysics and Heat Transfer*, vol. 15, No. 3, pp. 354–359, 2001.

[13] Muzychka, Y.S. and Yovanovich, M.M., Thermal Resistance Models for Non-Circular Moving Heat Sources on a Half Space, *Journal of Heat Transfer*, vol. 123, pp. 624-632, August 2001.

[14] Muzychka, Y.S., Influence Coefficient Method for Calculating Discrete Heat Source Temperature on Finite Convectively Cooled Substrates, *IEEE Transactions on Components and Packaging Technologies*, vol. 29, no. 3, pp. 636-643, Sep. 2006.

[15] Muzychka, Y. S., Yovanovich, M. M., and Culham, J. R., Applications of Thermal Spreading Resistance in Compound and Orthotropic Systems, *in Proc. 39th Aerospace Sciences Meeting Exhibit*, Reno, NV, Jan. 8–11, 2001.

[16] Yovanovich, M. M., Thermal Resistances of Circular Source on Finite Circular Cylinder with Side and End cooling, *ASME J. Electron. Packag.*, vol. 125, no. 2, pp. 169–177, 2003.

[17] Muzychka, Y. S., Yovanovich, M.M., and Culham, J. R., Influence of Geometry and Edge Cooling on Thermal Spreading Resistance, *AIAA Journal of Thermophysics and Heat Transfer*, vol. 20. no. 2, pp. 247-255. April-June, 2006.

[18] Carslaw, H. S., and Jaeger, J. C., Conduction of Heat in Solids, London, UK: *Oxford University Press*, second ed., 1959.

[19] Muzychka, Y. S., Bagnall, K. R., and Wang, E. N., Thermal Spreading Resistance and Heat Source Temperature in Compound Orthotropic Systems With Interfacial resistance, *IEEE Transactions on Components, Packaging, and Manufacturing Technology*, vol. 3. no. 11, pp. 1826-1841, November, 2013.

[20] Bagnall, K., Muzychka, Y.S., and Wang, E., Application of the Kirchhoff Transform to Thermal Spreading Problems with Convection Boundary Conditions, *IEEE Transactions on Components, Packaging and Manufacturing Technologies*, 2013.

[21] Yovanovich, M. M., and Marotta, E. E., Thermal Spreading and Contact Resistances, in *Heat Transfer Handbook*, A. Bejan, and A. D. Kraus, Eds. New York: Wiley, ch. 4, pp. 261–393, 2003.

[22] Yovanovich, M. M., Four Decades of Research on Thermal Contact, Gap and Joint Resistance in Microelectrics, *IEEE Transactions on Components and Packaging Technologies*, vol. 28, no. 2, pp. 182-206, 2005.

[23] Mikic, B. B., and Rohsenow, W. M., Thermal Contact Resistance, *M.I.T. Heat Transfer Lab Report No. 4542-41*, Sep. 1966.

[24] Lee, S., Song, S., Au., V., and Moran, K. P., Constriction/Spreading Resistance Model for Electronics Packaging, *in Proc. 4th ASME/JSME Thermal Eng. Joint Conf.*, Maui, HI, pp. 199–206, Mar. 1995.

[25] Kelman, R. B., Least Squares Fourier Series Solutions to Boundary Value Problems, *Society for Industrial and Applied mathematics*, vol. 21, no. 3, pp. 329-338, July 1979.

[26] Matlab, The Language of Technical Computing, R2012a.

[27] COMSOL Multiphysics® Version 4.2a.

Chapter 8

Thermal Resistance of a Three Dimensional Flux Channel with Non-Uniform Heat Convection in the Sink Plane

M. Razavi
Y.S. Muzychka

Department of Mechanical Engineering, Memorial University of Newfoundland, St. John's, NL, Canada, A1B 3X5

S. Kocabiyik

Department of Mathematics and Statistics, Memorial University of Newfoundland, St. John's, NL, Canada, A1C 5S7

Abstract

In this paper, the temperature profile and thermal resistance of a three dimensional flux channel with non-uniform heat convection in the sink plane is modeled analytically using the method of separation of variables. The heat source on the flux channel is concentric and the conductance along the sink plane is defined symmetrically using a hyperellipse function. This function is used to define different conductance distributions along the sink plane from the most intense cooling in the central region to uniform conductance along the sink plane. Further, the convective cooling condition is assumed along the edges of the system. This boundary condition can even model the system with adiabatic edges by assuming a negligible heat transfer coefficient along the edges. Due to the three dimensional

[1]Submitted to the Journal of Thermophysics and Heat Transfer

geometry of the flux channel, the thermal resistance consists of thermal spreading resistance in the x and y directions and three dimensional spreading resistance on the xy plane. The governing equation of each part is solved individually and the final answer is obtained using the superposition method. The final solutions for temperature profile and thermal resistance are presented in form of Fourier series expansions. All results are compared with the Finite Element Method (FEM) using COMSOL commercial software package [1].

Keywords: Electronics Cooling, Heat Conduction, Thermal Resistance, Variable Heat Transfer Coefficient

8.1 Introduction

A proper analysis of temperature profile and thermal resistance of electronic systems is essential for designing a durable device. For this purpose, different analytical, experimental and numerical methods are used to obtain a precise thermal behavior of the system. For the analytical methods, the geometry of the device is usually simplified to rectangular flux channels (cubical geometries) or cylindrical flux tubes (cylindrical geometries). Another important factor for thermal behavior and thermal resistance calculation is the effect of thermal spreading resistance. Thermal spreading resistance occurs when heat enters the channel through a small region and flows by conduction. Thermal spreading resistance is a major part of thermal resistance in some electronic devices.

Kennedy [2] started the research on thermal spreading resistance. Ellison [3-5] analytically studied the thermal spreading resistance in electronic devices. Yovanovich [6-10] studied different spreading resistance problems for more than forty years. Lemczyk and Yovanovich [11, 12] studied the thermal spreading/constriction resistance in systems with convective boundary conditions. Yovanovich [13] summarized the most important models of thermal spreading resistance in a review paper about contact, gap and joint resis-

tance. Yovanovich and Marotta [14] wrote a chapter about thermal spreading resistance in a heat transfer handbook. Muzychka et al. [15-19] have done comprehensive research on different aspects of thermal spreading resistance problems including different geometries, boundaries and properties. They modeled the spreading resistance of rectangular flux channels with eccentric heat sources, adiabatic edges and a uniform heat transfer coefficient along the sink plane [15]. Further, they studied the effect of the geometry and edge cooling on thermal spreading resistance [16]. He developed a computationally efficient method for calculating the temperature of flux channels with discrete heat sources and uniform conductance along the sink plane [17]. Recently, Muzychka et al. [18] analytically modeled the thermal spreading resistance for compound orthotropic systems with interfacial resistance between layers of the channel. He developed the same model for the cylindrical flux tubes [19]. Bagnall et al. [20] studied the effect of temperature dependent thermal conductivity on thermal spreading resistance of the system with a uniform heat transfer coefficient along the sink plane using the Kirchhoff transform. Furthermore, they modeled the spreading resistance in multi-layered flux channels [21].

Although a comprehensive study has been done on different aspects of thermal spreading resistance, no research has been conducted on the effect of non-uniform conductance along the sink plane. The heat transfer coefficient along the sink always simplifies as a uniform conductance. However, in the most of the electronic devices, the sink configuration is not uniform, Fig. 8.1.

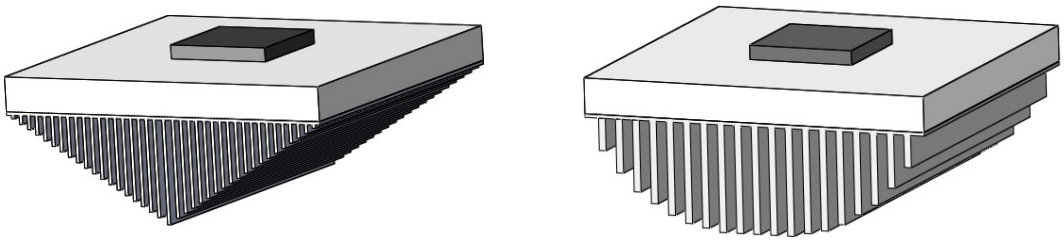

Figure 8.1: Flux channel with non-uniform conductance.

In this study, the effect of non-uniform heat transfer coefficient on the sink plane of a three dimensional flux channel is investigated.

8.2 Problem Statement and Solving Procedure

Rectangular flux channels are one of the main geometries that are used in the electronic devices. Based on the configuration and boundary conditions of the system, the heat transfer analysis of the flux channels is done in two or three dimensions. In this paper, a three dimensional flux channel is assumed with a central heat source, convective cooling along the edges and variable heat transfer coefficient along the sink plane. The top view of the system is shown in Fig. 8.2.

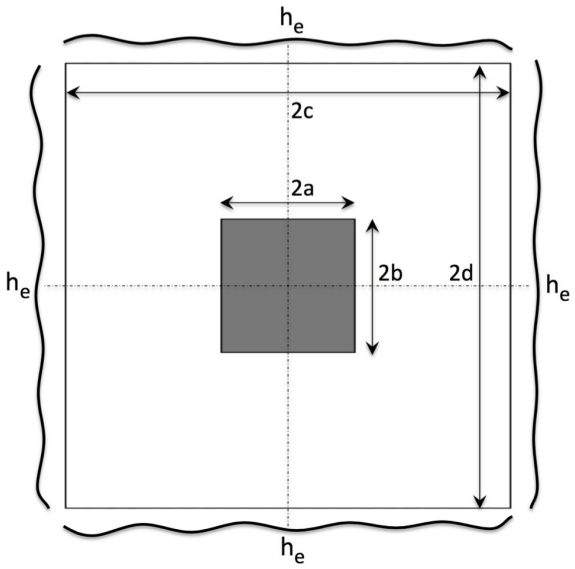

Figure 8.2: Top view of a 3D flux channel with a central heat source and convective edge cooling.

The thermal behavior of the flux channel can be obtained by solving the Laplace equation,

$$\frac{\partial^2 T}{\partial x^2} + \frac{\partial^2 T}{\partial y^2} + \frac{\partial^2 T}{\partial z^2} = 0, \tag{8.1}$$

or,

$$\frac{\partial^2\theta}{\partial x^2}+\frac{\partial^2\theta}{\partial y^2}+\frac{\partial^2\theta}{\partial z^2}=0, \tag{8.2}$$

where $\theta = T - T_f$. Based on the Fig. 8.2, boundary conditions of the system along the source plane stated as follows:

$$\left.\frac{\partial\theta}{\partial z}\right|_{z=0} = -\frac{q}{k}, \text{Over the source region,} \tag{8.3}$$

$$\left.\frac{\partial\theta}{\partial z}\right|_{z=0} = 0, \text{Out of the source region.} \tag{8.4}$$

The boundary conditions along the edges of the system are as follows:

$$\left.\frac{\partial\theta}{\partial x}\right|_{x=c} = -\frac{h_e}{k}\theta, \tag{8.5}$$

$$\left.\frac{\partial\theta}{\partial y}\right|_{y=d} = -\frac{h_e}{k}\theta. \tag{8.6}$$

The side views of the system are shown in Fig. 8.3 and Fig. 8.4. The convective cooling boundary condition along the edges of the system can be turned to the adiabatic condition when $h_e \to 0$.

The boundary conditions along the centerline of the system are as follows:

$$\left.\frac{\partial\theta}{\partial x}\right|_{x=0} = 0, \tag{8.7}$$

$$\left.\frac{\partial\theta}{\partial y}\right|_{y=0} = 0. \tag{8.8}$$

Along the sink plane, a variable heat transfer coefficient exists. The boundary condition along the sink plane is stated as follows:

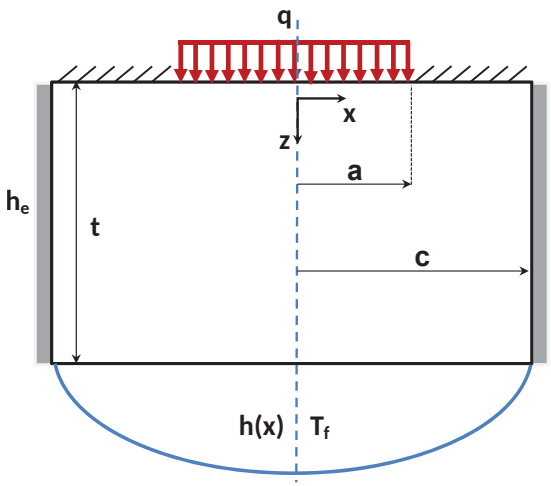

Figure 8.3: xz view of a 3D flux channel.

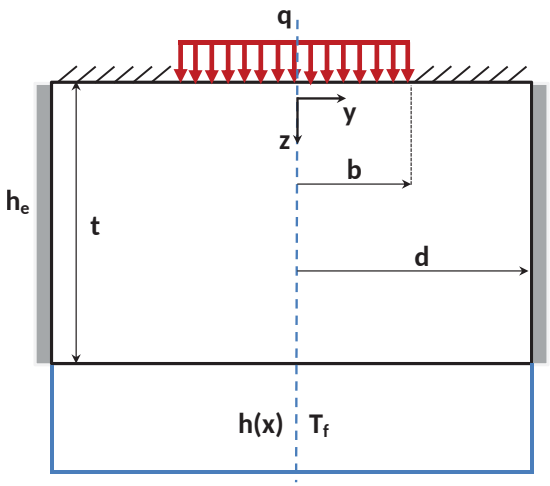

Figure 8.4: yz view of a 3D flux channel.

$$\left.\frac{\partial\theta}{\partial z}\right|_{z=t} = -\frac{h(x)}{k}\theta. \tag{8.9}$$

To define the variable heat transfer coefficient, $h(x)$, a hyperellipse function in the x direction is used to define a wide variety of different conductance distribution along the sink plane,

$$h(x) = h_o\left[1 - \left(\frac{x}{c}\right)^m\right]. \tag{8.10}$$

To change the configuration of the conductance along the sink plane, the power of the hyperellipse function, m, should be changed. Different distributions of conductance for half of the flux channel in the x direction for different values of m is shown in Fig. 8.5.

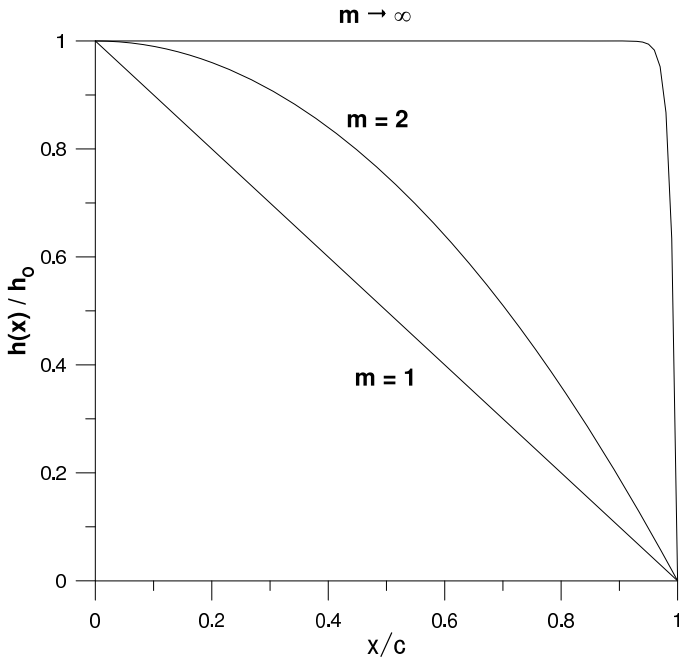

Figure 8.5: Variable heat transfer coefficient for half of the slab by considering $\frac{h(x)}{h_o} = 1 - (\frac{x}{c})^m$.

It is clear that the total conductance is dependent to the value of m. For instance, the total conductance for $m = 1$ is half of the conductance for $m \to \infty$. To represent a system with constant conductance for different values of m, the conductance is integrated over half of the flux channel and h_o is reevaluated according to the $\overline{h}$,

$$\overline{h} = \frac{1}{c}\int_0^c h(x)\,dx = \frac{m\,h_o}{m+1} \Rightarrow h_o = \frac{\overline{h}\,(m+1)}{m},$$

$$h(x) = \frac{\overline{h}\,(m+1)}{m}\left[1 - \left(\frac{x}{c}\right)^m\right]. \tag{8.11}$$

Eq. (8.11) can be used to compare flux channels with different distributions of the heat transfer coefficient and the same total conductance. Different distribution of heat transfer coefficient based on Eq. (8.11) for half of the flux channel is shown in Fig. 8.6.

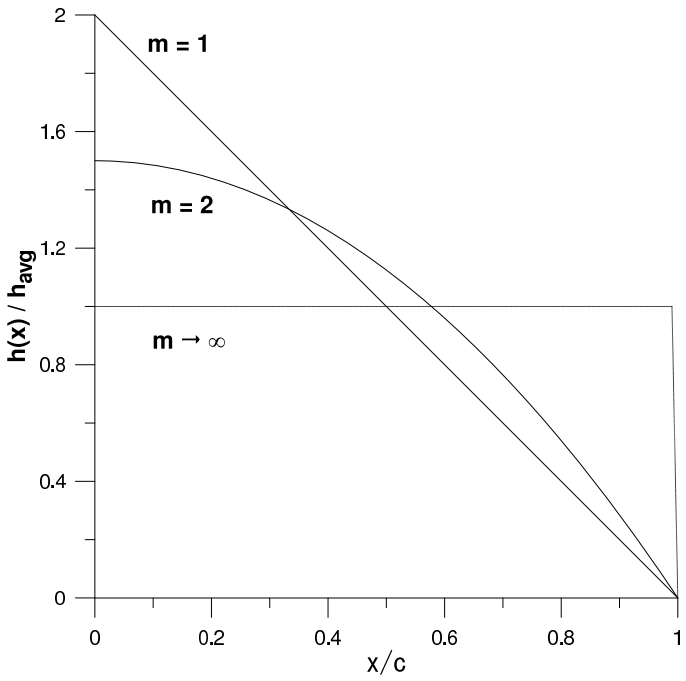

Figure 8.6: Variable heat transfer coefficient for half of the slab by considering $\frac{h(x)}{\bar{h}} = \frac{(m+1)}{m}[1 - \left(\frac{x}{c}\right)^m]$.

To obtain the thermal behavior of the $3D$ flux channel with non-uniform conductance along the sink plane, Fig. 8.1, the governing equation, Eq. (8.2) is solved with the method of separation of variables and using the mentioned boundary conditions. The solution is obtained by superposing the solution of temperature distributions for $2D$ flux channels in the xz and yz planes and the effect of the three dimensional solution.

8.2.1 Temperature Distribution of 2D Flux Channel in xz Plane

The two dimensional flux channel in the xz plane is shown in Fig. 8.3. As mentioned, the method of separation of variables is used to solve the Laplace equation. By considering the boundary condition along the centerline, Eq. (8.7), and edge of the channel, Eq. (8.5), the solution for the $2D$ flux channel in the xz plane can be stated as follows:

$$\theta(x,z) = \sum_{n=1}^{\infty} \cos\left(\lambda_n x\right)\left(C_n \cosh\left(\lambda_n z\right) + D_n \sinh\left(\lambda_n z\right)\right). \tag{8.12}$$

The edge boundary condition, Eq. (8.5), is used to define the eigenvalues of the system,

$$\lambda_n \sin(\lambda_n c) = \frac{h_e}{k}\cos(\lambda_n c) n = 1, 2, 3, \cdots . \tag{8.13}$$

To obtain the eigenvalues of the system, this equation can be solved numerically by a mathematical software package. The first eigenvalue, $n = 1$, represents the effect of one dimensional solution. However, due to the non-uniform heat conductance along the sink plane and edge cooling, there is no one dimensional resistance.

The next boundary condition that is applied to Eq. (8.12) is the sink boundary condition, Eq. (8.9). Therefore,

$$D_n = -\,C_n \left(\frac{\lambda_n \sinh(\lambda_n t) + \frac{h(x)}{k}\cosh(\lambda_n t)}{\lambda_n \cosh(\lambda_n t) + \frac{h(x)}{k}\sinh(\lambda_n t)}\right), \tag{8.14}$$

$$D_n = -C_n \phi_n(x). \tag{8.15}$$

where $\phi_n(x)$ is the spreading function. The general solution can be rewritten as follows:

$$\theta(x,z) = \sum_{n=1}^{\infty} C_n \cos\left(\lambda_n x\right)\left(\cosh\left(\lambda_n z\right) - \phi_n(x)\sinh\left(\lambda_n z\right)\right). \tag{8.16}$$

The final boundary condition is along the source plane for the $2D$ flux channel in the xz plane. According to Eq. (8.3) and Eq. (8.4), the boundary condition along the source plane can be defined as follows:

$$\left.\frac{\partial\theta}{\partial z}\right|_{z=0} = -\frac{q}{k}, \qquad 0 < x < a, \tag{8.17}$$
$$\left.\frac{\partial\theta}{\partial z}\right|_{z=0} = 0, \qquad a < x < c.$$

Due to the dependence of the spreading function, $\phi_n(x)$, on x, the orthogonality property cannot be used and the method of least squares [22] is applied to obtain the last unknown coefficient, C_n, of the Fourier series in the xz plane. By considering the source plane boundary condition in the xz plane, Eq. (8.17), the following integrals are defined for use in the least squares method,

$$I_N = \int_0^a \left[-k \left.\frac{\partial\theta}{\partial z}\right|_{z=0} - f(x)\right]^2 dx + \int_a^c \left[-k \left.\frac{\partial\theta}{\partial z}\right|_{z=0} - g(x)\right]^2 dx \tag{8.18}$$

where $f(x)$ and $g(x)$ are the known source plane flux distributions in different regions,

$$\left.\frac{\partial\theta}{\partial z}\right|_{z=0} = \sum_{n=1}^{\infty} -C_n\lambda_n\phi_n(x)\cos(\lambda_n x), \tag{8.19}$$
$$f(x) = -k \left.\frac{\partial\theta}{\partial z}\right|_{z=0} = q, \qquad (0 < x < a), \tag{8.20}$$
$$g(x) = -k \left.\frac{\partial\theta}{\partial z}\right|_{z=0} = 0, \qquad (a < x < c). \tag{8.21}$$

Therefore, Eq. (8.18) can be rewritten as:

$$I_N = \int_0^a \left[-k\sum_{n=1}^{\infty} -C_n\lambda_n\phi_n(x)\cos(\lambda_n x) - q\right]^2 dx + \int_a^c \left[-k\sum_{n=1}^{\infty} -C_n\lambda_n\phi_n(x)\cos(\lambda_n x) - 0\right]^2 dx. \tag{8.22}$$

The above Eq. (8.22) should be minimized in order to obtain the unknown coefficients, C_n,

$$\frac{\partial I_N}{\partial C_n} = 0 n = 1, 2, \cdots, N. \tag{8.23}$$

This equation can be easily solved to obtain the unknown coefficient, C_n, using the symbolic computation program Maple [23]. Therefore, the temperature distribution of the $2D$ flux channel is found by substituting the values of C_n in Eq. (8.16).

Thermal resistance for the $2D$ flux channel in the xz plane can be obtained as follows:

$$\overline{\theta}_{s,xz} = \overline{T}_s - T_f = \frac{1}{2a}\int_{-a}^{a} \theta(x,0)dx = \frac{1}{a}\sum_{n=1}^{\infty} \frac{C_n \sin(\lambda_n a)}{\lambda_n}, \tag{8.24}$$

$$R_{t,xz} = \frac{\overline{\theta}_{s,xz}}{Q} = \frac{1}{4\,a^2\,b\,q}\sum_{n=1}^{\infty} \frac{C_n \sin(\lambda_n a)}{\lambda_n}. \tag{8.25}$$

This definition describes the total thermal resistance of a $2D$ flux channel in the xz plane with variable heat transfer coefficient along the sink plane.

8.2.2 Temperature Distribution of 2D Flux Channel in yz Plane

In this section, the thermal behavior of the $2D$ flux channels in the yz plane, Fig. 8.4, is solved using the method of separation of variables. The main difference between the $2D$ flux channel in the xz and yz planes is the sink boundary condition. As the heat transfer coefficient along the sink plane is a function of x and it is not dependent on y and z directions, conductance is assumed constant and considered as the average of $h(x)$ over the sink plane. The general solving procedure is similar to the solving procedure for the $2D$ flux channel in the xz plane except for the method that is used for obtaining the last unknown

coefficients. The general solution for the $2D$ flux channel in the yz plane can be written as follows:

$$\theta(y,z) = \sum_{m=2}^{\infty} \cos\left(\delta_m y\right) \Big(C_m \cosh\left(\delta_m z\right) + D_m \sinh\left(\delta_m z\right) \Big). \tag{8.26}$$

The first term in the series, $m = 1$, was discarded as it represents the one dimensional solution and was considered in the solution in the xz plane. Therefore, all summations started from $m = 2$ for the solution in the flux channel in yz plane. The eigenvalues of the channel in the yz plane, δ_m, are,

$$\delta_m \sin(\delta_m d) = \frac{h_e}{k} \cos(\delta_m d) m = 2, 3, 4, \cdots . \tag{8.27}$$

By using the sink boundary condition,

$$D_m = - C_m \left(\frac{\delta_m \sinh(\delta_m t) + \frac{h(x)}{k} \cosh(\delta_m t)}{\delta_m \cosh(\delta_m t) + \frac{h(x)}{k} \sinh(\delta_m t)} \right) = -C_m \phi_m(x), \tag{8.28}$$

and the spreading function in the yz plane is defined as,

$$\phi_m = \frac{\delta_m \sinh(\delta_m t) + \frac{h(x)}{k} \cosh(\delta_m t)}{\delta_m \cosh(\delta_m t) + \frac{h(x)}{k} \sinh(\delta_m t)}. \tag{8.29}$$

Therefore, the general form of the solution has the following form:

$$\theta(y,z) = \sum_{m=2}^{\infty} C_m \cos\left(\delta_m y\right) \Big(\cosh\left(\delta_m z\right) - \phi_m(x) \sinh\left(\delta_m z\right) \Big). \tag{8.30}$$

To obtain the last unknown coefficients, C_m, the source plane boundary condition is used. This boundary condition can be written as follows:

$$\left.\frac{\partial\theta}{\partial z}\right|_{z=0} = -\frac{q}{k}, \qquad 0 < y < b, \tag{8.31}$$
$$\left.\frac{\partial\theta}{\partial z}\right|_{z=0} = 0, \qquad b < y < d.$$

Due to the non-dependence of the heat transfer coefficient, $h(x)$, on the y and z directions, we assume that it is constant on the sink plane and consider its average along the sink plane. Therefore, the orthogonality property is satisfied. Applying the source boundary condition, Eq. (8.31), to Eq. (8.30) gives,

$$\sum_{m=2}^{\infty} -C_m\phi_m(x)\delta_m\cos(\delta_m y) = -\frac{q}{k}, \qquad 0 < y < b, \tag{8.32}$$
$$\sum_{m=2}^{\infty} -C_m\phi_m(x)\delta_m\cos(\delta_m y) = 0, \qquad b < y < d.$$

To use the orthogonality property, both sides of Eq. (8.32) are integrated over the flux channel and multiplied by $\cos(\delta_m y)$,

$$C_m\int_0^d \phi_m\delta_m\cos^2(\delta_m y)dy = \int_0^b \frac{q}{k}\cos(\delta_m y)dy. \tag{8.33}$$

As a result, the last unknown coefficient for the solution of $2D$ flux channel in the yz plane, C_m, is,

$$C_m = \frac{2\,q\,\sin(b\,\delta_m)}{k\,\delta_m^2\,d\,\phi_m}, \tag{8.34}$$

and the final solution for the $2D$ flux channel in the yz plane is,

$$\theta(y,z) = \frac{2\,q}{k\,d}\sum_{m=2}^{\infty}\left(\frac{\sin(\delta_m\,b)\cos\left(\delta_m y\right)}{\delta_m^2\,\phi_m}\right)\Big(\cosh\left(\delta_m z\right) - \phi_m \sinh\left(\delta_m z\right)\Big), \tag{8.35}$$

where ϕ_m is obtained by Eq. (8.29). Thermal spreading resistance in the yz direction is calculated using the mean temperature of the source in the yz direction,

$$R_{s,yz} = \sum_{m=2}^{\infty}\left(\frac{\sin^2(\delta_m b)}{2\,c\,k\,b^2\,d\,\delta_m^3}\right)\left(\frac{\delta_m\cosh(\delta_m t) + \frac{h(x)}{k}\sinh(\delta_m t)}{\delta_m\sinh(\delta_m t) + \frac{h(x)}{k}\cosh(\delta_m t)}\right). \tag{8.36}$$

As mentioned, the first term in the series was discarded as the effect of the first eigenvalue was considered in the $R_{t,xz}$ in Eq. (8.25).

8.2.3 Effect of 3D Spreading on Temperature Distribution

The last component of the solution for the temperature distribution along the $3D$ flux channel is the effect of $3D$ spreading. For this purpose, the method of separation of variables is used for solving the Laplace equation, Eq. (8.2), as follows [24]:

$$\theta(x,y,z)_{3D} = \sum_{m=2}^{\infty}\sum_{n=2}^{\infty}\cos\left(\lambda_n x\right)\cos\left(\delta_m y\right)\Big(C_{nm}\cosh\left(\beta_{nm} z\right) + D_{nm}\sinh\left(\beta_{nm} z\right)\Big), \tag{8.37}$$

where $\beta_{nm} = \sqrt{\lambda_n^2 + \delta_m^2}$.

The heat transfer coefficient along the sink plane is assumed to be the average of the variable heat transfer coefficient,

$$\overline{h} = \int_0^c\int_0^d h(x)\,dxdy. \tag{8.38}$$

By using the boundary condition along the sink plane, Eq. (8.9), and the assumption of

average conductance instead of variable heat transfer coefficient, Eq. (8.38), the spreading function, ϕ_{nm}, can be defined as follows:

$$D_{nm} = - C_{nm}\phi_{nm}, \tag{8.39}$$

$$\phi_{nm} = \frac{\beta_{nm}\sinh(\beta_{nm}t) + \frac{\overline{h}}{k}\cosh(\beta_{nm}t)}{\beta_{nm}\cosh(\beta_{nm}t) + \frac{\overline{h}}{k}\sinh(\beta_{nm}t)}. \tag{8.40}$$

The final boundary condition is along the source plane,

$$\left.\frac{\partial\theta}{\partial z}\right|_{z=0} = -\frac{q}{k}, \qquad 0 < x < a \text{and} 0 < y < b, \tag{8.41}$$

$$\left.\frac{\partial\theta}{\partial z}\right|_{z=0} = 0, \qquad a < x < c \text{or} b < y < d.$$

By applying the source plane boundary condition and using the orthogonality property, the last unknown coefficients are obtained,

$$D_{nm} = \frac{-q\int_0^a\int_0^b\cos(\lambda_n x)\cos(\delta_m y)dxdy}{\beta_{nm}k\int_0^c\int_0^d\cos^2(\lambda_n x)\cos^2(\delta_m y)dxdy}, \tag{8.42}$$

and after some algebra,

$$D_{nm} = \frac{-16\,q\,\delta_m\lambda_n\sin(a\delta_m)\sin(b\lambda_n)}{\delta_m\,\lambda_n\,\beta_{nm}\,k\,(2c\delta_m + \sin(2c\delta_m)\,(2d\lambda_n + \sin(2d\lambda_n))}, \tag{8.43}$$

$$C_{nm} = -\frac{D_{nm}}{\phi_{nm}} = -\frac{\frac{-16\,q\,\delta_m\,\lambda_n\,\sin(a\delta_m)\sin(b\lambda_n)}{\delta_m\,\lambda_n\,\beta_{nm}\,k\,(2c\delta_m+\sin(2c\delta_m)(2d\lambda_n+\sin(2d\lambda_n))}}{\frac{\beta_{nm}\sinh(\beta_{nm}t)+\frac{\overline{h}}{k}\cosh(\beta_{nm}t)}{\beta_{nm}\cosh(\beta_{nm}t)+\frac{\overline{h}}{k}\sinh(\beta_{nm}t)}}. \tag{8.44}$$

All coefficients are known and the temperature distribution based on the $3D$ effect is calculated using Eq. (8.37),

$$\theta(x,y,z)_{3d} = \sum_{m=2}^{\infty}\sum_{n=2}^{\infty} \cos(\lambda_n x)\cos(\delta_m y) \left(-\frac{\frac{-16q\delta_m\lambda_n \sin(a\delta_m)\sin(b\lambda_n)}{\delta_m\lambda_n\beta_{nm}k(2c\delta_m+\sin(2c\delta_m)(2d\lambda_n+\sin(2d\lambda_n))}}{\frac{\beta_{nm}\sinh(\beta_{nm}t)+\frac{\overline{h}}{k}\cosh(\beta_{nm}t)}{\beta_{nm}\cosh(\beta_{nm}t)+\frac{\overline{h}}{k}\sinh(\beta_{nm}t)}} \cosh(\beta_{nm}z) + \frac{-16q\delta_m\lambda_n \sin(a\delta_m)\sin(b\lambda_n)}{\delta_m\lambda_n\beta_{nm}k\left(2c\delta_m+\sin(2c\delta_m)\left(2d\lambda_n+\sin(2d\lambda_n)\right)\right)} \sinh(\beta_{nm}z) \right). \tag{8.45}$$

The thermal spreading resistance for $3D$ effect is obtained as follows [10]:

$$R_{s,3D} = \frac{1}{a^2\,b^2\,c\,d\,k}\sum_{m=2}^{\infty}\sum_{n=2}^{\infty}\left(\frac{\sin(a\,\delta_m)^2\sin(b\,\lambda_n)^2}{\delta_m^2\,\lambda_n^2\,\beta_{nm}}\right)\left(\frac{\beta_{nm}\sinh(\beta_{nm}t)+\frac{\overline{h}}{k}\cosh(\beta_{nm}t)}{\beta_{nm}\cosh(\beta_{nm}t)+\frac{\overline{h}}{k}\sinh(\beta_{nm}t)}\right). \tag{8.46}$$

Both series started at two, $m = 2$ and $n = 2$, to discarded the first eigenvalues.

8.2.4 Superposition of Solutions

The temperature profile along the three dimensional flux channel is calculated by superposition of the solution in the xz plane, Eq. (8.16); solution in the yz plane, Eq. (8.35); and $3D$ effects, Eq. (8.45),

$$T(x,y,z) = T_f + \theta(x,z) + \theta(y,z) + \theta(x,y,z)_{3d}. \tag{8.47}$$

The thermal resistance of the three dimensional flux channel can be calculated by superposing $R_{t,xz}$, Eq. (8.25); $R_{s,yz}$, Eq. (8.36); and $R_{s,3D}$, Eq. (8.46),

$$R_t = R_{t,xz} + R_{s,yz} + R_{s,3D}. \tag{8.48}$$

The total thermal resistance is non-dimensionalized as follows:

$$R_t^* = k\sqrt{ab}R_t. \tag{8.49}$$

In the next section, the dimensionless thermal resistance for a three dimensional flux channel with different source aspect ratios will be analyzed.

8.3 Results and Discussion

In this part, the dimensionless thermal resistance of a three dimensional flux channel for different source size aspect ratios is calculated. The obtained results are compared with the Finite Element Method (FEM) using COMSOL Commercial Software Package [1]. The flux channel has the following geometry and properties: $c = 0.01\,m$, $d = 0.01\,m$, $t = 0.001\,m$, $k = 2\,W/mK$, $h_e = 100\,W/m^2K$, $\overline{h} = 200\,W/m^2K$.

The convergence of the FEM was checked by refining the mesh in the system. Different numbers of tetrahedral elements is used. As a sample, the convergence of the FEM for a three dimensional flux channel with the aforementioned geometry and properties, a source size of $a = 0.002\,m$ and $b = 0.002\,m$ and a variable heat transfer coefficient along the sink plane based on Eq. (8.11) for $m = 1$ is analyzed. The system with a tetrahedral mesh consisting of 7338 elements converged with two digits of precision for dimensionless thermal resistance, Table 8.1.

	R_t	R^*_t
27	55.98292	0.223932
98	64.56095	0.258244
270	66.97987	0.267919
728	67.46619	0.269865
7338	67.74133	0.270965
226061	67.82096	0.271284

Table 8.1: The convergence of the FEM by refining the mesh.

To specify the variable heat transfer coefficient, two approaches may be used, Eq. (8.10) and Eq. (8.11). Based on the first approach, the variable heat transfer coefficient for different values of m have the same pick and different averages, Fig.8.5. For the second approach, variable heat transfer coefficients for different values of m have the same average and different picks, Fig.8.6. The second approach is more appropriate for comparing different configurations of heat sinks with the same overall conductance. In this case study, the variable heat transfer coefficient over the sink plane is based on Eq. (8.11) and assumed to be linear with $m = 1$ and quadratic with $m = 2$.

As discussed, the total thermal resistance of a three dimensional flux channel consists of three parts as follows: $R_{t,xz}$, $R_{s,yz}$ and $R_{s,3D}$. Tables 8.2 and 8.3 show the effects of each part and their influence on the total thermal resistance of a three dimensional flux channel with linear and quadratic variable heat transfer coefficient along the sink plane. Further, the effect of different source aspect ratios is shown. The number of terms that are used in each series is equal to 10. The first column represents the source aspect ratios, $\epsilon = \sqrt{ab}/\sqrt{cd} = 0.1 \cdots 1$; the second column represents the total thermal resistance in xz plane, $R_{t,xz}$ that is obtained by Eq. (8.25); the third column shows the spreading resistance in yz plane, $R_{s,yz}$, using Eq. (8.36); the fourth column represents the effect of three dimensional spreading resistance, $R_{s,3D}$, Eq. (8.46); and the last column is the total thermal resistance of the flux channel, R_t, Eq. (8.48). As can be seen in Table 8.2, the effect of three dimensional spreading resistance is negligible for source size aspect ratios greater than 0.8, $\epsilon > 0.8$.

a = b	$R_{t,xz}$	$R_{s,yz}$	$R_{s,3D}$	R_t
0.001 m	29.17593	23.1377	85.2511	137.5647
0.002 m	23.02743	16.01986	31.64875	70.69604
0.003 m	19.33197	11.23251	13.95992	44.5244
0.004 m	16.94692	7.729689	6.293872	30.97048
0.005 m	15.37624	5.107946	2.714778	23.19897
0.006 m	14.41453	3.146214	1.052148	18.61289
0.007 m	13.91698	1.71123	0.333119	15.96132
0.008 m	13.84085	0.725911	0.070812	14.63757
0.009 m	14.1117	0.158456	0.005739	14.2759
0.01 m	14.72442	0.028902	8.59E-05	14.75341

Table 8.2: Thermal resistance of a flux channel with linear heat transfer coefficient, $m = 1$, and different source aspect ratios.

a = b	$R_{t,xz}$	$R_{s,yz}$	$R_{s,3D}$	R_t
0.001 m	31.64031	23.1377	85.2511	140.0291
0.002 m	25.05398	16.01986	31.64875	72.72259
0.003 m	20.91325	11.23251	13.95992	46.10568
0.004 m	18.08441	7.729689	6.293872	32.10797
0.005 m	16.10977	5.107946	2.714778	23.93249
0.006 m	14.77572	3.146214	1.052148	18.97408
0.007 m	13.9376	1.71123	0.333119	15.98194
0.008 m	13.55425	0.725911	0.070812	14.35097
0.009 m	13.70501	0.005739	0.005739	13.71648
0.01 m	13.94196	0.028902	8.59E-05	13.97095

Table 8.3: Thermal resistance of a flux channel with quadratic heat transfer coefficient, $m = 2$, and different source aspect ratios.

The dimensionless thermal resistance for different source size aspect ratios, $\epsilon = a/c = b/d$, for both the analytical method and the FEM is shown in Figures 8.7 and 8.8. The dimensionless thermal resistance in both methods is calculated using $R_t^* = k\sqrt{ab}\,R_t$.

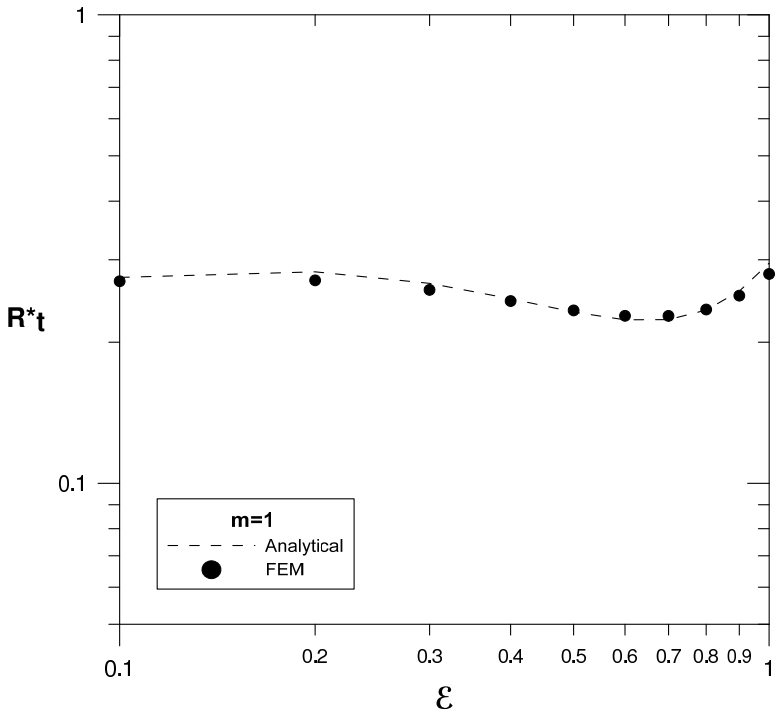

Figure 8.7: Dimensionless thermal resistance for $m = 1$.

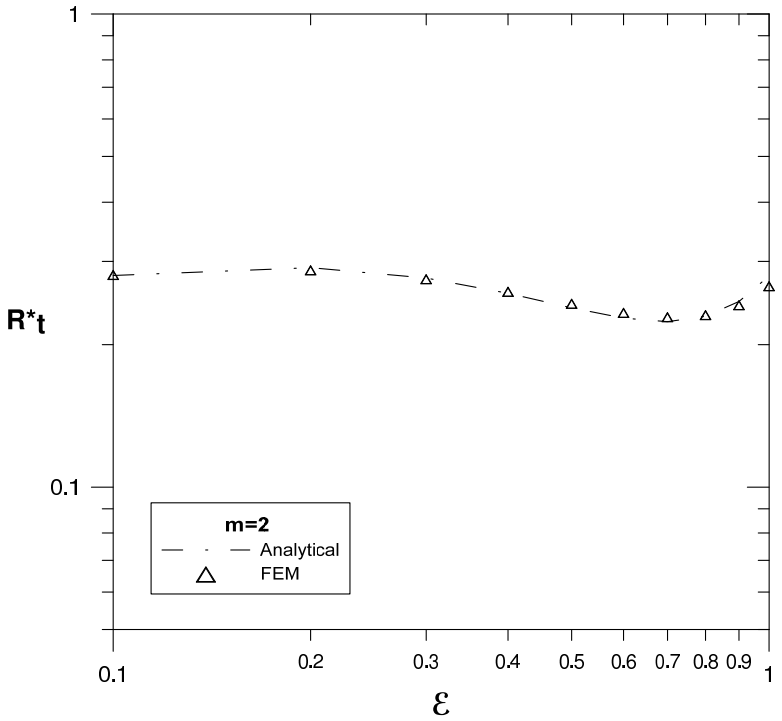

Figure 8.8: Dimensionless thermal resistance for $m = 2$.

Figures 8.7 and 8.8 show that the results of the dimensionless thermal resistance for both methods are in agreement. As an approximation technique is used in the analytical solution, the percent error is evaluated by comparing the results with the FEM. Table 8.4 shows the mean percent error of all aspect ratios for both linear and quadratic variable heat transfer coefficient.

	m=1	m=2
Mean Percent Error	2.3 %	1.7 %

Table 8.4: Mean percent error of different source size aspect ratios for linear, $m = 1$, and quadratic, $m = 2$, variable heat transfer coefficient.

As shown in Table 8.4, the mean percent error for both cases is less than 2.5%. The main source of error is the assumption of constant heat transfer coefficient, Eq. (8.38), for the third part of the solution. Furthermore, the mean percent error decreases by increasing m in the variable heat transfer coefficient. The reason is that by increasing m, a more uniform conductance occurs along the sink plane and the assumption of uniform conductance in the third part of the solution, Eq. (8.38), becomes more reasonable.

The proposed solution is useful for thermal engineers who want to have a better understanding of different factors contributing to the total thermal resistance of the three dimensional flux channels. Although, this method is able to calculate the total thermal resistance of the system with high accuracy, the dimensions of the flux channels should be analyzed precisely to consider the effect of the first term in the series.

8.4 Conclusion

In this paper, a general expression for the thermal resistance of a three dimensional flux channel with variable heat transfer coefficient along the sink plane is obtained. The method of separation of variables is used and the unknown Fourier coefficients are obtained using the least squares method and the orthogonality property. A hyperellipse function is used to

simulate a variable conductance along the sink plane. Furthermore, a dimensionless thermal resistance for different variable heat sink distributions is presented and compared with the Finite Element Method (FEM). The results are in agreement and the mean percent error for different source aspect ratios is less than 2.5%. The proposed models are useful for thermal engineers who want to have a better understanding of thermal resistance in three dimensional geometries to be able to analyze the effect of each dimension of the system.

Acknowledgments

The authors acknowledge the financial support of the Natural Sciences and Engineering Research Council of Canada.

8.5 References

[1] COMSOL Multiphysics® Version 4.2a.

[2] Kennedy, D. P., "Spreading Resistance in Cylindrical Semiconductor devices," *Journal of Applied Physics*, vol. 31, pp. 1490-1497, 1960.

[3] Ellison, G., "Extensions of a Closed Form Method for Substrate Thermal Analyzers to Include Thermal Resistances From Source-to-Substrate and Source-to-Ambient," *Seventh IEEE Semi-Therm Symposium*, pp. 140-148, 1991.

[4] Ellison, G., "Thermal Analysis of Microelectric Packages and Printed Circuit Boards Using an Analytic Solution to the Heat Conduction Equation," *Advances in Engineering Software*, pp. 99-111, 1994.

[5] Ellison, G., "Thermal Analysis of Circuit Boards and Microelectronic Components Using an Analytical Solution to the Heat Conduction Equation," *Twelfth IEEE Semi-Therm Symposium*, pp. 144-150, 1996.

[6] Yovanovich, M. M., "General Expression for Constriction Resistances Due to Arbitrary Flux Distribution at non-symmetric, coaxial contacts", *AIAA 13th Aerospace Sciences Meeting*, Pasadena, California, 1975.

[7] Yovanovich, M. M., "Thermal Constriction Resistance of Contacts on a Half-Space: Integral Formulation," *AIAA Progress in Astronautics and Aeronautics, Radiative Transfer and Thermal Control*, vol. 49, edited by A. M. Smith, New York, pp. 397-418, 1976.

[8] Yovanovich, M. M., Muzychka, Y. S., and Culham, J. R., "Spreading Resistance in Isoflux Rectangles and Strips on Compound Flux Channels," *J. Thermophys. Heat Transf.*, vol. 13, no. 4, pp. 495-500, 1999.

[9] Yovanovich, M. M., "Constriction Resistance of Planar Isoflux Heat Sources within Semi-Infinite Conductors: Image Method," *in Proc. 4th ASME/JSME Thermal Engineering Joint Conf.*, Maui, HI, Mar. 19-24, 1995.

[10] Yovanovich, M. M., Muzychka, Y. S., and Culham, J. R., "Spreading Resistance of Isoflux Rectangles and Strips on Compound Flux Channels," *6th AIAA Aerospace Sciences Meeting and Exhibit*, Reno, NV, January 12-15, 1998.

[11] Lemczyk, T. F., and Yovanovich, M. M., "Thermal Constriction Resistance with Convective Boundary Conditions, Part 1: Half-Space Contacts," *Int. J. Heat Mass Transf.*, vol. 31, no. 9, pp. 1861-1872, 1988.

[12] Lemczyk, T. F., and Yovanovich, M. M., "Thermal Constriction Resistance with Convective Boundary Conditions, Part 2: Layered Half-Space Contacts," *Int. J. Heat Mass Transf.*, vol. 31, no. 9, pp. 1873-1883, 1988.

[13] Yovanovich, M. M., "Four Decades of Research on Thermal Contact, Gap and Joint Resistance in Microelectronics," *IEEE Transactions on Components and Packaging Technologies*, vol. 28, no. 2, pp. 182-206, 2005.

[14] Yovanovich, M. M., and Marotta, E. E., "Thermal Spreading and Contact Resistances," in *Heat Transfer Handbook*, A. Bejan, and A. D. Kraus, Eds. New York: Wiley, ch. 4, pp. 261-393, 2003.

[15] Muzychka, Y. S., Culham, J. R., and Yovanovich, M. M., "Thermal Spreading Resistance of Eccentric Heat Sources on Rectangular Flux Channels," *Journal of Electronic Packaging*, vol. 125, pp. 178-185, June 2003.

[16] Muzychka, Y. S., Yovanovich, M. M., and Culham, J. R., "Influence of Geometry and Edge Cooling on Thermal Spreading Resistance," *AIAA Journal of Thermophysics and Heat Transfer*, vol. 20. no. 2, pp. 247-255, April-June 2006.

[17] Muzychka, Y.S., "Influence Coefficient Method for Calculating Discrete Heat Source Temperature on Finite Convectively Cooled Substrates," *IEEE Transactions on Components and Packaging Technologies*, vol. 29, no. 3, pp. 636-643, Sep. 2006.

[18] Muzychka, Y.S., Bagnall, K., and Wang, E., "Thermal Spreading Resistance and Heat Source Temperature in Compound Orthotropic Systems with Interfacial Resistance", *IEEE Transactions on Components, Packaging and Manufacturing Technologies*, vol. 3, no. 11, pp. 1826-1841, 2013.

[19] Muzychka, Y.S., "Spreading Resistance in Compound Orthotropic Flux Tubes and Channels with Interfacial Resistance", *AIAA Journal of Thermophysics and Heat Transfer*, 2014.

[20] Bagnall, K., Muzychka, Y.S., and Wang, E., "Application of the Kirchhoff Transform to Thermal Spreading Problems with Convection Boundary Conditions", *IEEE Transactions on Components, Packaging and Manufacturing Technologies*, 2013.

[21] Bagnall, K., Muzychka, Y.S., and Wang, E., "Analytical Solution for Temperature Rise in Complex, Multi-layer Structures with Discrete Heat Sources", *IEEE Transactions on Components, Packaging and Manufacturing Technologies*, 2014.

[22] Kelman, R. B., "Least Squares Fourier Series Solutions To Boundary Value Problems," *Society for Industrial and Applied mathematics*, vol. 21, no. 3, pp. 329-338, July 1979.

[23] Maple 10, Waterloo Maple Software, Waterloo, ON, Canada.

[24] Kakac, S., and Yener, Y., Heat conduction, 3rd ed, Washington, DC : Taylor & Francis, 1993.

Chapter 9

Summary, Conclusions, and Recommendations for Future Studies

Thermal analysis is an essential factor for designing the electronic devices. Thermal analysis of electronic devices was investigated by different researchers in the past fifty years. However, each model is applicable to a specific system with different limitation such as specific kind of geometry, property, and boundary conditions. Although a wide variety of models were presented, there are still some systems with specific boundary conditions that were not modeled. In this thesis, some of these systems are analytically studied and some models are presented for the thermal analysis of two common geometries in the electronic devices. The proposed models can be effectively used by thermal engineers for modeling the system.

The systems that are presented in this thesis can be categorized based on the geometry, boundary condition, and properties. The geometry of the system usually is simplified to circular flux tube or rectangular flux channel. Both of these geometries are analytically studied in this research. Also, symmetrical and non-symmetrical systems are modeled. Different boundary conditions along the source plane are discussed. Various configurations are studied and the trend of dimensionless thermal resistance versus dimensionless source size is presented. Furthermore, the effects of the following factors in the thermal resistance problems are examined in different chapters:

- Size of the heat source,
- Thickness of the channel,
- Variable conductance,
- Different Biot numbers.

The governing equation of the discussed problems through the thesis is the Laplace equation and solved by using the method of separation of variables. Also, a novel solution is obtained by using the least squares technique for temperature distribution in flux channels and tubes with variable conductance along the sink plane or combined heat sources along the source plane. Furthermore, a method for defining the appropriate weight function to satisfy the orthogonality property is discussed. The proposed method can be used to define the weight function for non-symmetrical flux channels with different conductance along the left edge, right edges, and sink plane. This is a useful model for analyzing the devices with wall-mounted heat sinks. The proposed solution is in the form of Fourier series expansion which can be easily modeled in computational software packages.

In chapter one, the general aspects of thermal spreading resistance problems are discussed. Also, some of the industrial applications are presented. In chapter two, past decades literatures are categorized and some of the most important models are summarized. In chapter three and four, a novel solution is presented for flux channels with variable heat transfer coefficient along the sink plane. In chapter five, a computational efficient model is presented for modeling a non-symmetrical flux channel with three different heat transfer coefficients along the edges. In chapter six, a system with numerous discretely specified source plane boundary conditions is modeled. This model has no limitation in the number and position of heat sources. Also, different temperatures and heat fluxes can be specified for each region along the source plane. All sources are modeled at the same time and there is no need to use the superposition method to consider the effect of each individual heat source.

In chapter seven, a circular flux tube with different boundary conditions along the source plane is modeled. The source plane boundary condition can be defined as a combinations of heat fluxes, adiabatic conditions, and contact temperatures. Both isotropic and orthotropic properties are discussed. In chapter eight, a general expression for the thermal resistance of a three-dimensional flux channel with variable heat transfer coefficient along the sink plane is obtained. A hyperellipse function is used along the heat sink plane to simulate a variable conductance.

The source plane boundary conditions in the presented models can be a combination of prescribed temperature, prescribed heat flux, and the adiabatic condition. In the proposed models, the prescribed temperature along the source plane is applied directly to the solutions. In the previous literature, this boundary condition was converted to an equivalent heat flux distribution and then applied to the solution. This conversion has some limitations for the contact size of the system. In the proposed models, there is no need for this conversion and different specified contact temperatures along the source plane can be modeled directly. The other big advantage versus the previous literature is that there is no need to model the system for each specific heat source and then apply the superposition method to consider the effect of each specific heat sources. The effect of all heat sources can be considered at the same time as discussed in the chapters five and seven.

Furthermore, the boundary condition along the edges of the system mostly assumed as convective cooling through the thesis. This boundary condition is general and even can model the adiabatic boundary condition along the edges by assuming $h_e \to 0$.

The boundary condition along the sink plane is assumed as constant or variable conductance. The variable conductance is a practical boundary condition in the industrial systems and never had been studied analytically. All the previous literature are assumed that the uniform heat transfer coefficient exists along the sink plane to simplify the solution procedure. Different configuration of heat sink conductance is presented and the effect of this

boundary condition in the thermal resistance of the system is discussed. Two functions are proposed to simulate a wide variety of different heat sink configurations. Due to the variable conductance, the orthogonality property is not satisfied and the least squares method is used to solve the problem.

The main contribution of this thesis for modeling the thermal behavior of the systems can be summarized as follows:

- In this thesis, a model for analyzing systems with variable heat transfer coefficient along the sink plane is proposed. Although it is a common heat sink configuration in the electronic industry, it was never addressed in the previous literature. This boundary condition was usually simplified as a uniform heat conductance. Through this thesis, it is shown that this simplification causes some errors for flux channels with dimensionless thickness less than 0.5, $\tau < 0.5$. However, if the dimensionless thickness is greater than 0.5, $\tau > 0.5$, a uniform heat transfer coefficient can be applied without too much loss in accuracy.

- Rectangular flux channels and circular flux tubes with combined heat source boundary conditions are modeled. The source plane boundary condition can be a combination of different heat fluxes, contact temperatures, and adiabatic conditions. All boundary conditions along the source plane are modeled simultaneously and there is no need to do the superposition method. In the previous literatures, the superposition method was used to capture the effect of each individual heat source on the source plane. The proposed model is faster and can be easily used to model complex systems.

- The contact temperature along the source plane is modeled without using the equivalent flux distributions. In previous literatures, contact temperatures were converted to the equivalent flux distribution to model the thermal behavior of the system. By using

the actual temperature instead of equivalent flux distribution, the proposed model is simpler and more accurate and there is no limitation on the geometry of the system.

- Rectangular flux channel with different heat conductance along the edges is modeled. Although it is a practical boundary condition for electronic devices with different wall-mounted heat sinks along the edges of the system, it was never addressed in the previous literature. Due to the non-similarity of the heat transfer coefficient along the edges, a weight-function is proposed to satisfy the orthogonality property and a computational efficient model is presented. Also, based on the results that are presented through the thesis, it can be concluded that the common adiabatic assumption along the edges is only valid for thin flux channels with an effective heat sinking along the sink plane.

- Through the thesis, it is shown that the proposed analytical methods are faster than commercial software. Therefore, the time of design phase of electronic products can be significantly reduced that results less expensive production cycle. Also, analytical methods produce more accurate results and thermal engineers can have a better insight about the thermal behavior of the system. Furthermore, commercial software usually does not provide enough information about the solving algorithms. Therefore, software works as a blackbox and thermal engineers usually cannot have enough insights about the accuracy of their result. Moreover, the results of analytical models are continuous through the models and there is no need to do gridding and the regridding time is conserved in case of any changes in the specification of the system.

Although different aspects of thermal spreading resistance problems are studied, there are still some gaps that should be addressed. The author proposes the following problems be studied:

- Systems with more flexible specification of conductance such as discretely specified

heat transfer coefficient along the heat sink plane. It is a practical boundary condition in the electronic devices such as systems with coolant channels along the heat sink plane or systems with fin heat sinks with varying fin heights and gaps between the fins.

- Systems with a combination of temperature, heat flux, and conductance along the heat source plane.
- Multi-layer systems with discretely specified inward and outward heat fluxes along the heat source and heat sink plane.
- Extension of problems with variable and discretely specified heat conductance along the heat sink plane in compound systems.
- Considering the effect of orthotropic properties and temperature dependent thermal conductivity in compound systems with variable or discretely specified heat conductance.
- Studying the effect of different thermal conductivity in all three principal directions will add value to all previously published papers.

It is worth to emphasize that the main advantage of the proposed models through the thesis is that thermal engineers can have a better understanding of the system by using these analytical models.